

**Massachusetts Institute of Technology  
Woods Hole Oceanographic Institution**



**Joint Program  
in Oceanography/  
Applied Ocean Science  
and Engineering**



---

**DOCTORAL DISSERTATION**

*High Molecular Weight (HMW)  
Dissolved Organic Matter (DOM) in Seawater:  
Chemical Structure, Sources and Cycling*

by

Lihini I. Aluwihare

June 1999

DTIC QUALITY INSPECTED 4

19991020 014

**MIT/WHOI**

**99-08**

**High Molecular Weight (HMW) Dissolved Organic Matter (DOM) in Seawater:  
Chemical Structure, Sources and Cycling**

by

Lihini I. Aluwihare

Massachusetts Institute of Technology  
Cambridge, Massachusetts 02139

and

Woods Hole Oceanographic Institution  
Woods Hole, Massachusetts 02543

June 1999

**DOCTORAL DISSERTATION**

Funding was provided by a grant from the US Department of Energy  
(Ocean Margins Program #DE-FG02-92ER61428) and the Woods Hole Oceanographic Institution.

Reproduction in whole or in part is permitted for any purpose of the United States Government. This thesis should be cited as: Lihini I. Aluwihare, 1999. High Molecular Weight (HMW) Dissolved Organic Matter (DOM) in Seawater: Chemical Structure, Sources and Cycling. Ph.D. Thesis. MIT/WHOI, 99-08.

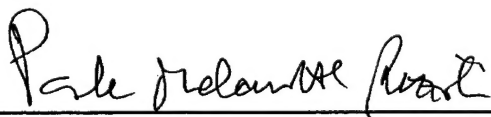
Approved for publication; distribution unlimited.

**Approved for Distribution:**

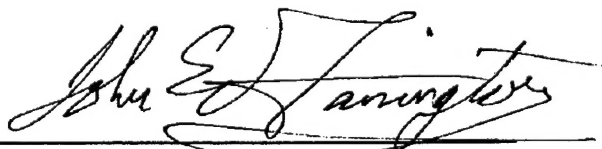


**Mark D. Kurz**

Department of Marine Chemistry and Geochemistry



**Paola Malanotte-Rizzoli**  
MIT Director of Joint Program



**John W. Farrington**  
WHOI Dean of Graduate Studies

**High Molecular Weight (HMW) Dissolved Organic Matter (DOM)  
In Seawater: Chemical Structure, Sources and Cycling**

by

Lihini I. Aluwihare

B.A., Mount Holyoke College  
(1993)

SUBMITTED IN PARTIAL FULFILLMENT OF THE  
REQUIREMENTS FOR THE DEGREE OF DOCTOR  
OF PHILOSOPHY

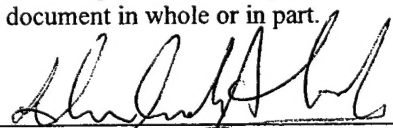
at the

MASSACHUSETTS INSTITUTE OF TECHNOLOGY  
and the  
WOODS HOLE OCEANOGRAPHIC INSTITUTION

April, 1999

© Lihini I. Aluwihare, 1999. All rights reserved.

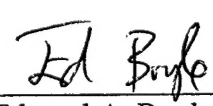
The author hereby grants to MIT and WHOI the permission to reproduce and to distribute copies of this  
thesis document in whole or in part.

Signature of Author: 

Department of Earth, Atmospheric and Planetary Sciences,  
Massachusetts Institute of Technology and the Joint Program  
in Oceanography, Massachusetts Institute of Technology/Woods  
Hole Oceanographic Institution, April 30, 1999.

Certified by 

Daniel J. Repeta  
Thesis Supervisor

Accepted by 

Edward A. Boyle  
Chairman, Joint Committee for Chemical Oceanography,  
Massachusetts Institute of Technology/Woods Hole  
Oceanographic Institution





# High Molecular Weight (HMW) Dissolved Organic Matter (DOM) in Seawater: Chemical Structure, Sources and Cycling.

Lihini I. Aluwihare

## Abstract

The goal of this thesis was to use high resolution analytical techniques coupled with molecular level analyses to chemically characterize high molecular weight ( $> 1$  k Da (HMW)) dissolved organic matter (DOM) isolated from seawater in an attempt to provide new insights in to the cycling of DOM in the ocean.

While a variety of sites spanning different environments (fluvial, coastal and oceanic) and ocean basins were examined, the chemical structure of the isolated HMW DOM varied little at both the polymer and monomer levels. All samples show similar ratios of carbohydrate:acetate:lipid carbon ( $80 \pm 4:10 \pm 2:9 \pm 4$ ) indicating that these biochemicals are present within a family of related polymers. The carbohydrate fraction shows a characteristic distribution of seven major neutral monosaccharides: rhamnose, fucose, arabinose, xylose, mannose, glucose and galactose; and additionally contains N-acetylated amino sugars as seen by Nuclear Magnetic Resonance Spectroscopy (NMR). This family of compounds, consisting of a specifically linked polysaccharide backbone that is acylated at several positions, has been termed acylated polysaccharides (APS) by our laboratory. APS accounts for 50% of the carbon in HMW DOM isolated from the surface ocean and 20% of the carbon in HMW DOM isolated from the deep ocean.

In order to identify a possible source for APS three species of phytoplankton, *Thalassiosira weissflogii*, *Emiliania huxleyi* and *Phaeocystis*, were cultured in seawater and their HMW DOM exudates examined by variety of analytical techniques. Both the *T. weissflogii* and *E. huxleyi* exudates contain compounds that resemble APS indicating that phytoplankton are indeed a source of APS to the marine environment. Furthermore, the degradation of the *T. weissflogii* exudate by a natural assemblage of microorganisms indicates that the component resembling APS is more resistant to microbial degradation compared to other polysaccharides present in the culture.

Molecular level analyses show the distribution of monosaccharides to be conservative in surface and deep waters suggesting that APS is present throughout the water column. In order to determine the mechanism by which APS is delivered to the deep ocean the  $\Delta^{14}\text{C}$  value of APS in the deep ocean was compared to the  $\Delta^{14}\text{C}$  value of the dissolved inorganic carbon (DIC) at the same depth. If the formation of deep water is the dominant mode of transport then both the DIC and APS will have similar  $\Delta^{14}\text{C}$  values. However, if APS is injected into the deep ocean from particles or marine snow then the  $\Delta^{14}\text{C}$  value of APS will be higher than the DIC at the same depth. Our results indicate that APS in the deep Pacific Ocean carries a modern  $\Delta^{14}\text{C}$  value and is substantially enriched in  $^{14}\text{C}$  relative to the total HMW DOM and the DIC at that depth. Thus, particle dissolution appears to be the most important pathway for the delivery of APS to the deep ocean.

Thesis Supervisor: Daniel J. Repeta

## ACKNOWLEDGEMENTS

I would like to thank my advisor, Dan Repeta, for his extraordinary commitment to this thesis. I have benefited greatly from his high expectations and his high scientific standards. I would also like to thank my thesis committee, Phil Gschwend, Charles Hopkinson and Cindy Lee who have all made invaluable contributions to this work. Tim Eglinton and Jim Moffet have both been instrumental to my survival in the joint program, offering fresh perspectives and a welcome sense of humour. I would also like to thank Tim for being a wonderful role model. Thanks also to Carl Johnson, Big "Bob" Nelson, Nelson Frew, Ollie Zafiriou, Jeff Seewald and Lorraine Eglinton, all of whom have left their marks on this thesis. I would like to thank the members of Fye Lab in general, for their sense of humour and compassion throughout my six eventful years here.

Many thanks to my friends here in Woods Hole: Kathy Barbeau, Liz Koodge, Mak D. S. Saito, Lil' Ann Pearson, the "24 Millfield bunch" (Danny Sigman, Garret Ito, Ellen Ito, Jon Woodruff, Joe Warren, Monica Relle, Kira Lawrence, Peter Sauer, Kitty, Zorro and Patches), Kirsten Laarkamp, Dana Stuart, CHRIS REDDY, Silvio Pantoja, Steve Jayne, Jess Adkins and Mike Atkins, for all the good times, support and encouragement.

Finally to my extended family: I made it because of you. I cannot find the words to thank my beloved parents who invested everything in me: ammi, I am everything I am because you loved me; apuchi, your incredible insight and dedication to education inspired me to reach this goal. To ayia, thank you for being my guardian angel. To Phyllis and Peter, your love and quiet support have carried me throughout the last six years. To my family in Sri-Lanka, I am lucky to be so loved. To Bill Shaw, our time together has been paradise, thank you for all your patience and support. To Emily Norton, the closest thing I have to a sister, Dianne Keller, Monica Chander and Laura Termini, thanks for still putting up with me after ten years. To the Arvons, the family of strong women, especially little Dr. Regina, thank you for your inspiration.

This thesis is dedicated to all the mothers who inspired their daughters to move mountains.

This thesis was funded by a grant from the US Department of Energy, Ocean Margins Program.

## TABLE OF CONTENTS

TABLE OF FIGURES .....	7
TABLE OF TABLES .....	11
<b>1. INTRODUCTION .....</b>	<b>13</b>
1.1 THE ROLE OF DOM IN THE CARBON CYCLE .....	13
1.2 SOURCES OF DOM .....	14
1.3 CYCLE OF DOM IN THE OCEAN.....	16
1.5 CHEMICAL STRUCTURE OF DOM .....	19
1.5 ORGANIZATION OF THIS THESIS.....	20
1.6 GOALS OF THIS THESIS .....	23
1.7 REFERENCES.....	24
<b>2. STRUCTURAL CHARACTERIZATION OF MARINE DISSOLVED HIGH MOLECULAR WEIGHT ORGANIC MATTER .....</b>	<b>31</b>
2.1 INTRODUCTION.....	31
2.2 MATERIALS AND METHODS.....	33
2.2.1 <i>Sampling Site</i> .....	33
2.2.2 <i>Sample Collection and Isolation</i> .....	33
2.2.2.1 Ultrafiltration .....	35
2.2.2.1.1 Cleaning The Membranes.....	38
2.2.2.2 Diafiltration.....	38
2.2.2.3 Desalting .....	39
2.2.3 <i>Dissolved Organic Carbon (DOC) Analysis</i> .....	40
2.2.4 <i>Elemental Analysis</i> .....	40
2.2.5 <i>Nuclear Magnetic Resonance Spectroscopy</i> .....	41
2.2.5.1 General Principles.....	41
2.2.5.2 Experimental Conditions for Proton NMR ( <sup>1</sup> HNMR).....	42
2.2.5.3 <sup>13</sup> C and <sup>15</sup> NNMR.....	44
2.2.6 <i>Carbohydrate Analysis</i> .....	45
2.2.6.1 Monosaccharide Analysis .....	45
2.2.6.2 Linkage Analysis .....	46
2.2.7 <i>Lipid Analysis</i> .....	49
2.2.8 <i>Amino Acid Analysis</i> .....	50
2.3 RESULTS.....	51
2.3.1 <i>Ancillary Data</i> .....	51
2.3.2 <i>Nuclear Magnetic Resonance Data</i> .....	53
2.3.2.1 Proton NMR.....	53
2.3.2.3 Nitrogen NMR .....	63
2.3.3 <i>Lipid Results</i> .....	67
2.3.4 <i>Monosaccharide Analyses</i> .....	69
2.3.5 <i>Methylation Analysis</i> .....	77
2.3.6 <i>Linkage Analysis</i> .....	80
2.3.7 <i>Amino Acid Analysis</i> .....	87
2.4 DISCUSSION.....	89
2.5 CONCLUSIONS .....	96
2.6 REFERENCES.....	98
2.7 APPENDIX.....	105
2.7.1 <i>Nuclear Magnetic Resonance Spectroscopy Conditions</i> .....	105
2.7.2 <i>Linkage Data for Seawater</i> .....	106
2.7.3 <i>Retention Times for Partially Methylated Alditol Acetates</i> .....	108

<b>3. A COMPARISON OF THE CHEMICAL CHARACTERISTICS OF OCEANIC HMW DOM AND EXTRACELLULAR DOM PRODUCED BY MARINE ALGAE.</b>	<b>111</b>
3.1 INTRODUCTION.....	111
3.2 MATERIALS AND METHODS.....	113
3.2.1 <i>Phytoplankton Cultures</i> .....	113
3.2.2 <i>Ultrafiltration</i> .....	117
3.2.3 <i>Analyses</i> .....	117
3.2.4 <i>Dissolved Oxygen Measurements</i> .....	117
3.3 RESULTS.....	118
3.3.1 <i>Phytoplankton Cultures</i> .....	118
3.3.1.1 POC, DOC, and HMW DOC.....	118
3.3.1.2 <sup>1</sup> HNMR Data.....	122
3.3.1.3 Monosaccharide Data.....	124
3.3.2 <i>Bacterial Degradation of the T. weissflogii Exudate</i> .....	126
3.3.2.1 Changes in DOC.....	126
3.3.2.2 <sup>1</sup> HNMR Data.....	128
3.3.2.3 Monosaccharide Data.....	130
3.3.2.4 Amino Acid Data.....	132
3.4 DISCUSSION.....	134
3.4.1 <i>Phytoplankton Cultures</i> .....	134
3.4.2 <i>Degradation of the T. weissflogii exudate</i> .....	143
3.5 CONCLUSIONS.....	150
3.6 REFERENCES.....	152
3.7 APPENDIX.....	160
3.7.1 <i>Linkage data for the Cultures</i> .....	160
<b>4. RADIOCARBON VALUES OF INDIVIDUAL MONOSACCHARIDES ISOLATED FROM OCEANIC HMW DOM.....</b>	<b>163</b>
4.1 INTRODUCTION.....	163
4.2 MATERIALS AND METHODS.....	166
4.2.1 <i>Sampling</i> .....	166
4.2.2 <i>Chemical Analyses</i> .....	168
4.2.3 <i>High-Performance Liquid Chromatography (HPLC)</i> .....	170
4.2.3.1 Ion Exchange.....	170
4.2.3.2 Normal Phase Chromatography.....	173
4.2.4 <i>Sample Preparation for Accelerator Mass Spectrometry (AMS)</i> .....	177
4.3 RESULTS.....	181
4.3.1 <i>Radiocarbon Analyses</i> .....	191
4.4 DISCUSSION.....	195
4.4.1 <i>Radiocarbon Results</i> .....	195
4.4.2 <i>Analytical Methods</i> .....	201
4.5 CONCLUSIONS.....	204
4.6 REFERENCES.....	206
<b>5. CONCLUSIONS.....</b>	<b>211</b>
5.1 GENERAL CONCLUSIONS.....	211
5.2 FUTURE RESEARCH DIRECTIONS.....	219
5.3 REFERENCES FOR CHAPTER 5.....	223

## TABLE OF FIGURES

### Chapter 1

Figure 1.1 Depth profiles of dissolved organic carbon (DOC) in the Sargasso Sea (filled diamonds) and the North Pacific Ocean (open squares) (data from Druffel et al. 1992). ..... 15

Figure 1.2 The  $\Delta^{14}\text{C}$  values of DOC and DIC (in parentheses) in different parts of the Worlds Ocean. Arrows depict the direction of ocean circulation. .... 18

Figure 1.3 Hypothetical structure for dissolved marine humic substances (Gagosian and Stuermer, 1977) 19

Figure 1.4 Monosaccharide structure: carbon and protons are labeled 1-6 as shown (a),  $\beta$  anomer (b) and  $\alpha$  anomer (c). .... 21

Figure 1.5 Eight neutral monosaccharides identified in HMW DOM: hexoses (A); deoxy hexoses (B); pentoses (C). Glucosamine in its acetylated and non-acetylated form (D) is also shown. .... 22

### Chapter 2

Figure 2.1 Map showing the locations of the different samples analyzed for this thesis ..... 34

Figure 2.2 Schematic representation of the procedure for the isolation of HMW DOM ..... 36

Figure 2.3 Synthesis of alditol acetates from monosaccharides ..... 46

Figure 2.4 The reaction scheme for the preparation of partially methylated alditol acetates for linkage analysis of polysaccharides. .... 48

Figure 2.5 The major  $^1\text{H}$ NMR resonances identified in HMW DOM. The baseline for each of the major peaks and the whole spectrum are shown on the figure as dashed lines. .... 54

Figure 2.6 Two  $^1\text{H}$ NMR spectra for surface HMW DOM isolated from the North Atlantic (MAB943) (A) and North Pacific (B) (P961). Note the similarities in the resonances present and the relative proportion of each resonance. .... 56

Figure 2.7 The figure shows  $^1\text{H}$ NMR spectra for a typical surface ocean sample (A) (CRL), a typical deep ocean sample (B) (P962) and a spectrum seen for two of the eight deep samples analyzed (C) (MAB944). Dashed lines in Spectrum B show the baseline for each of the identified peaks. .... 57

Figure 2.8  $^1\text{H}$ NMR spectra of MAB948, a HMW DOM sample from a depth of 750 m before desalting (A), after desalting with a cation exchange resin (B) and after hydrolysis (C). .... 59

Figure 2.9 Proton NMR spectrum of a 5:1 mixture of maltoheptose and Gramicidin S, in  $\text{D}_2\text{O}$ . Resonances enclosed in brackets arise from proteins. .... 60

Figure 2.10  $^{13}\text{C}$ NMR spectrum of HMW DOM in  $\text{D}_2\text{O}$  ..... 62

Figure 2.11 Solid state  $^{15}\text{N}$ NMR spectra of HMW DOM, before (A) and after (B) 1 M HCl hydrolysis for 11 h at  $105^\circ\text{C}$ . Resonances are reported relative to  $\text{NH}_3$ . Pyridine was added as an external standard to quantify the total nitrogen detected by  $^{15}\text{N}$  NMR. .... 64

Figure 2.12  $^1\text{H}$  NMR spectra of HMW DOM, before (A) 1 N HCl hydrolysis for 11 h at  $105^\circ\text{C}$  and after hydrolysis and freeze drying to remove acetic acid (B). .... 65

Figure 2.13 $^1\text{H}$ NMR of HMW DOM prior to 4 N HCl hydrolysis (A), following hydrolysis (B), the aqueous layer (pH = 3) after extraction with ethyl ether (C) and the ethyl ether layer (D).	68
Figure 2.14 Raw gas chromatograms of alditol acetates.	70
Figure 2.15 The mole percent distribution of the seven neutral monosaccharides identified in HMW DOM.	72
Figure 2.16 Correlation coefficient data for the mole percent monosaccharide distribution of each HMW DOM sample. All correlations are reported relative to MAB941.	75
Figure 2.17 A schematic representation of the flow of water in the MAB constructed using the correlation coefficient data for the mole percent monosaccharide distributions.	76
Figure 2.18 The $^1\text{H}$ NMR spectrum of a standard mixture of monosaccharides (A) and a hydrolyzed HMW DOM sample (B).	78
Figure 2.19 $^1\text{H}$ NMR spectra of HMW DOM prior to methylation (A) and following methylation and extraction into an organic solvent (B).	79
Figure 2.20: The total ion current of partially methylated alditol acetates from a HMW DOM sample. Each peak was identified using mass spectral data and retention time data.	81
Figure 2.21 Mass spectra of terminally linked rhamnose (A), terminally linked mannose (B), 1,4-linked galactose (C).	84
Figure 2.22 The relative distribution of different types of linkages per sugar for three different HMW DOM samples.	86
Figure 2.23 The total amount of carbon in surface water HMW DOM derived from refractory deep ocean HMW DOM, and HMW DOM newly added at the surface (A) and the relative amount of carbon accounted for by the hydrolysis products (B), assumed to be derived from new HMW DOM only.	91
Figure 2.24 The total carbon in surface water HMW DOM accounted for by the biochemicals identified in this study. Also refer to Figure 2.23	95
Figure 2.25 Hypothetical structure for APS, containing neutral monosaccharides and N-acetylated sugars.	95

### Chapter 3

Figure 3.1 Experimental set up for the culture experiments. Seawater was pre-filtered through 0.2 $\mu\text{m}$ and 1 nm membranes. Both the <i>Emiliania huxleyi</i> and <i>Phaeocystis</i> experiments were terminated after the algae were removed without further degradation of the exudate. TW3, TW4, TW5 and TW6 refer to samples taken during the degradation of the <i>Thalassiosira weissflogii</i> exudate (dates are given in Figure 3.3).	115
Figure 3.2 Growth curve for the <i>E. huxleyi</i> culture expressed in cell numbers/ml.	118
Figure 3.3 Ancillary data from the <i>Thalassiosira weissflogii</i> culture. (A) Changes in chl-a (filled squares) and POC (filled triangles). (B) Changes in the DOC (filled squares) concentration and C/N ratios of the POC (open triangles). Algae were removed on day 8. TW1, refers to the ultrafiltration sample taken during early log phase, TW2 was taken during late log phase, and TW3, 4, 5 and 6 were taken during the course of the degradation experiment after the algae had been removed. After day 9, changes in DOC concentration result from the action of microorganisms present in the incubation, or from physical removal mechanisms.	121

Figure 3.4  $^1\text{H}$ NMR spectra for HMW DOM isolated from seawater (Woods Hole) (A), and the exudates of *Thalassiosira weissflogii* (B), *Emiliania huxleyi* (C), and *Phaeocystis* (D). Carbohydrate resonances are between 3.2- 4.7 p.p.m (CHOH), 5-5.8 p.p.m (anomerics) and 1.3 p.p.m ( $\text{CH}_3$  from deoxy sugars). Spectra also show proton resonances for acetate (2.0 p.p.m) and lipids (1.3 and 0.9 p.p.m). The ratios of carbohydrate:acetate:lipid reported in the text are based on the areas under the peaks denoted C (for carbohydrates), Ac (for acetate) and Alkyl (lipids). To convert from hydrogen to carbon we use a C/H ratio of 1 for carbohydrates, 0.67 for acetate and 0.5 for lipids. .... 123

Figure 3.5 The relative distribution of monosaccharides in HMW DOM isolated from seawater, and the exudates of *Thalassiosira weissflogii*, *Emiliania huxleyi*, and *Phaeocystis*. R is rhamnose, F is fucose, A is arabinose, X is xylose, M is mannose, GL is glucose, GA is galactose, and RI is ribose. The seawater sample represents the average distribution of monosaccharides in ten seawater samples (the standard deviation is less than  $\pm 3\%$  for each monosaccharide). .... 126

Figure 3.6  $^1\text{H}$ NMR spectra of two HMW DOM samples isolated during the degradation of the *Thalassiosira weissflogii* exudate, TW3 (A) and TW4 (B). Resonances between 1.9-3.1 p.p.m are thought to arise from proteins which can be removed by passage through a cation exchange column (insets). .... 129

Figure 3.7 The relative distribution of amino acids in HMW DOM isolated during the degradation of the *Thalassiosira weissflogii* exudate, expressed as the percentage of each amino acid accounted for by the culture sample. Amino acid are: aspartic acid, glutamic acid, serine and histidine, glycine, threonine and arginine, alanine, tyrosine, methionine, valine, phenylalanine, isoleucine, leucine and lysine..... 133

Figure 3.8 Carbohydrate linkage data for the exudates. TW2, *E. huxleyi* and *Phaeocystis* samples were taken when the cultures were harvested. TW4 was isolated during the *Thalassiosira weissflogii* incubation experiment. The number beneath each bar refers to the linkage site on each monosaccharide (i.e. carbon 1 and 6 as 1,6), and T refers to linkages through carbon 1 only. Only linkages which constitute  $> 5\%$  of each sugar are listed. .... 139

Figure 3.9 The change in the concentration of total neutral monosaccharides in HMW DOM and the change in APS as a percentage of the total neutral monosaccharides (as calculated in the text) over the course of the *Thalassiosira weissflogii* incubation experiment..... 147

## Chapter 4

Figure 4.1 Two scenarios for the delivery of surface produced DOM to the deep ocean. Scenario A shows the delivery of DOM to the deep ocean *via* deep water formation. Scenario B shows that in addition to advection, DOM may also be delivered to the deep ocean *via* bacterial degradation and disaggregation of sinking POM..... 165

Figure 4.2. A flow chart of the various analytical steps involved with the separation of hydrolyzed monosaccharides from HMW DOM. Boxes in bold denote HPLC steps. Silver column refers to the cation exchange steps and amino column refers to the reverse phase separation..... 169

Figure 4.3 (A) Reproducibility of six consecutive injections of a monosaccharide mixture on the Ag column. Standard deviations (% Stnd. Dev) for retention times (Ret. Times) and peak areas are reported as a percentage. (B) Calibrated detector response for the three different monosaccharide fractions ( $R^2$  for each linear fit to the data are reported on the figure). .... 173

Figure 4.4 (A) Reproducibility of six consecutive injections of a monosaccharide mixture on the amino column. Standard deviations (% Stnd. Dev) for retention times (Ret. Times) and peak areas are reported as a percentage. (B) Calibrated detector response for five monosaccharide fractions ( $R^2$  for each linear fit to the data are reported on the figure). .... 176



Figure 4.5 CRL sample after hydrolysis and neutralization, separated on the cation exchange column using Ag as the counterion. The figure shows the sample before (A) and after (B) desalting using an anion exchange resin. .... 182

Figure 4.6 HPLC of CRL on the Ag column, during the initial separation (A) and the second separation (B). .... 187

Figure 4.7 The separation of individual monosaccharides from unhydrolyzed HMW DOM using a combination of cation exchange and reverse phase HPLC. (A) Separation of glucose and rhamnose; (B) separation of mannose, xylose and galactose; (C) separation of fucose and arabinose. .... 190

Figure 4.8 Radiocarbon values for different fractions of carbon in the North East Pacific (Station M).  $\text{POC}_{\text{sus}}$  is the  $\Delta^{14}\text{C}$  value of suspended POC, and  $\text{POC}_{\text{sink}}$  is the  $\Delta^{14}\text{C}$  value of sinking POC. Depth profiles show DOC and DIC  $\Delta^{14}\text{C}$  values; filled circles are the  $\Delta^{14}\text{C}$  value of total HMW DOC (surface and 1600 m), and filled diamonds are the  $\Delta^{14}\text{C}$  value of the HMW Sugars (surface and 1600 m) DIC, POC and total DOC values were obtained from Druffel et al. 1996 and Bauer et al. 1998. .... 196

Figure 4.9 Variations in the concentration of total DOC ( $\mu\text{M}$ ) over the whole ocean (after Hansell and Carlson, 1998). .... 198

Figure 4.10 A comparison of the distribution of monosaccharides in HMW DOM (Average), Transparent Exopolymer Particles (Avg TEP) (after Mopper et al., 1995), and sediment trap material (POC) (after Cowie and Hedges, 1984). Monosaccharides are galactose (Ga), fucose (F), mannose (M), glucose (G), rhamnose and arabinose (R+A) and xylose (X). .... 200

Figure 4.11 The relative distribution of monosaccharides in HMW DOM injected onto the amino column compared to the relative distribution of monosaccharides in HMW DOM determined by GC (AA). .... 204

## Chapter 5

Figure 5.1 Cycling of APS in the Ocean. .... 215

Figure 5.2 The cycling of APS in the Surface Ocean. See text for an explanation of the terms. .... 216



## TABLE OF TABLES

### Chapter 2

Table 2.1 Ancillary data for each of the samples analyzed as part of this thesis. ....	39
Table 2.2 Relative abundance (in carbon) of the major biochemicals identified in HMW DOM by <sup>1</sup> HNMR. ....	43
Table 2.3 The relative distribution of neutral monosaccharides (as analyzed by alditol acetates) in HMW DOM. ....	58
Table 2.4 Results from the correlation coefficient analysis of the mole percent monosaccharide distributions in different HMW DOM samples. ....	75
Table 2.5 The mole percent distribution of amino acids in HMW DOM. ....	100

### Chapter 3

Table 3.1 Ancillary data for the HMW DOM isolated from the phytoplankton cultures. ....	106
Table 3.2 The relative distribution of monosaccharides in <i>T. weissflogii</i> , <i>E. huxleyi</i> , and <i>Phaeocystis</i> at the time of harvesting. ....	112
Table 3.3 Absolute concentrations of monosaccharides at the time of harvesting (TW2) and at each of the time points during the incubation experiment (TW3, TW4, TW5 and TW6) for <i>Thalassiosira weissflogii</i> . % C refers to the percent of total carbon in the sample accounted for by each of the monosaccharides. ....	131
Table 3.4 Concentrations of the individual amino acids in HMW DOM isolated during the degradation of the <i>T. weissflogii</i> exudate (TW3, TW4, TW5 and TW6). ....	132
Table 3.5 Monosaccharide composition of polysaccharides isolated from different species of algae. ....	142
Table 3.6 Degradation rate constant for the different organic carbon fractions in the <i>T. weissflogii</i> over the course of the incubation experiment. ....	148

### Chapter 4

Table 4.1 Sampling site and DOC data for the samples analyzed in this study. ....	167
Table 4.2 The recovery of carbon from the different purification steps performed in this analysis. Desalting was performed on an anion exchange column. Ag column and Amino column data, refer to recoveries during the HPLC procedure. ....	183
Table 4.3 The $\Delta^{14}\text{C}$ values of the different carbon fractions for each of the sites examined in this chapter. Refer to the text for descriptions of fm, fm* and $\Delta^{14}\text{C}$ . ....	192

### Chapter 5

Table 5.1 Numerical values for each of the terms shown in Figure 5.2. ....	208
----------------------------------------------------------------------------	-----



## 1. Introduction

### 1.1 The Role of DOM in the Carbon Cycle

Dissolved organic matter (DOM) constitutes the largest pool of reduced organic carbon in the ocean (Hedges, 1992) and has long been recognized to be an important part of the global carbon cycle. DOM is defined as the fraction of total organic matter in the ocean that passes through a 0.2  $\mu\text{m}$  filter. Seven hundred Gt of carbon are present in seawater as total organic carbon. Of this, 90% exists as DOM (Hedges 1992). This reservoir is nearly equal in size to the amount of organic carbon in the terrestrial biosphere, and the amount of carbon in the atmosphere as  $\text{CO}_2$ .

DOM has been shown to play an important role in a variety of oceanic processes. For example, DOM has been shown to be important in supporting microbial production. Between 15-25 Gt C/yr move *via* DOM into bacteria and the "microbial loop" (Azam et al., 1983; Fuhrman and Azam, 1982; Hagstrom et al., 1979). These large flux estimates are based on the high rates of heterotrophic bacterioplankton production throughout the surface ocean, and the high turnover rates observed for simple molecules such as amino acids and monosaccharides in seawater (Bada and Lee, 1977; Kirchman et al., 1991; Smith et al., 1992).

Apart from the importance of DOM as a substrate for bacteria, it has also been shown that DOM may be directly utilized by phytoplankton as a nutrient source. Recent work has shown that many phytoplankton have the capability to utilize DON for growth either by cell-surface deamination, amino acid transport systems or proteolysis (Martinez and Azam, 1993; Palenik and Morel, 1990). Studies have shown that the "brown tide" causing unicellular algae (*Aureococcus anophagefferens*) can use organic nitrogen

substrates in the field for growth, thereby giving this organism a possible ecological advantage (LaRoche et al., 1997).

DOM has also been shown to be important in determining the distribution of trace metals in the ocean. During the last several decades, convincing evidence has accrued demonstrating that a number of bioactive trace metals are strongly influenced by organic complexation. For example, >90% of the iron, copper and zinc in oceanic surface waters exists chelated with organic ligands (Bruland, 1989; Coale and Bruland, 1988; Moffet and Zika, 1987). It has been further suggested that the mean concentration of iron below 500 m in the ocean is primarily controlled by the complexation of iron with organic ligands (Johnson et al., 1997).

DOM has further been shown to play a role in the reduction of metals in the surface ocean. Organic complexes of Fe (III) can be reduced to Fe (II) by ligand to metal charge transfer reactions resulting from the absorption of both visible and ultraviolet light by DOM (Voelker et al., 1997). This absorption and fluorescence of chromophoric (or colored) DOM (CDOM) is particularly important because it can affect ocean color and thus interferes with the interpretation of remote sensing data (Blough et al., 1993).

## **1.2 Sources of DOM**

Despite the importance of marine DOM, little is known about its structure and its cycling. Depth profiles of DOC concentration in the ocean (Figure 1.1) have a characteristic shape. In surface water concentrations are between 60-80  $\mu\text{M}$ . Below the euphotic zone, concentrations decline to between 35-45  $\mu\text{M}$  by 600-1000 m, and remain relatively constant throughout the deep ocean (Peltzer and Hayward, 1996). The increased concentrations of DOM in surface waters indicates a surface source, and likely

results from a decoupling of production and removal processes over annual to decadal time scales (Carlson and Ducklow, 1995). Although the mechanisms by which DOM is added to surface waters is not well known, it has long been recognized that this carbon represents by-products generated by algal photosynthesis in the euphotic zone (Duursma, 1963; Mague et al., 1980; Menzel, 1974). Stable carbon isotope measurements of the standing stock of organic matter also support a largely marine source for DOM (-20 to -22 ‰) (Druffel et al., 1992; Williams and Gordon, 1970). However, there are little data

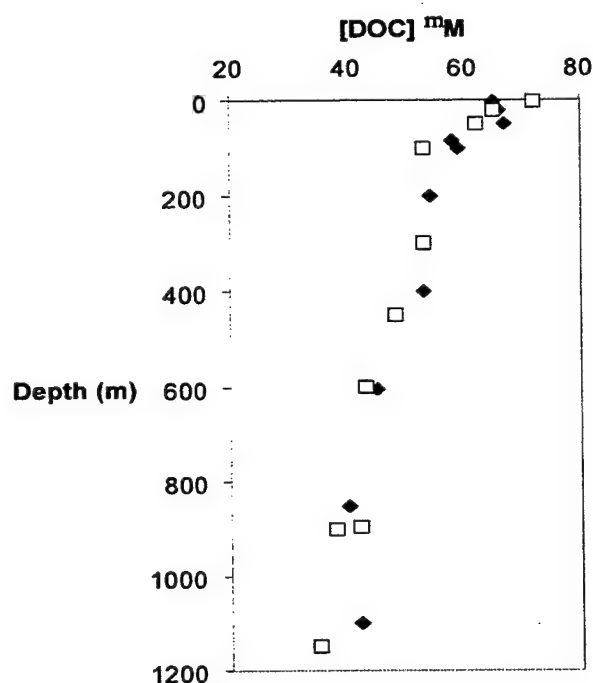


**Figure 1.1** Depth profiles of dissolved organic carbon (DOC) in the Sargasso Sea (filled diamonds) and the North Pacific Ocean (open squares) (data from Druffel et al. 1992).

directly linking the DOM present in seawater to a plankton source. For example, DOM concentrations, in general, are not well correlated with either phytoplankton biomass or primary productivity (Carlson et al., 1994; Chen et al., 1995; Morris and Foster, 1971),

indicating that other processes such as bacterial degradation of DOM must be important in maintaining steady state DOM concentrations.

Other possible sources of DOM are riverine DOM, which is expected to be intrinsically unreactive, and thus contribute disproportionately to the marine pool (Ertel et al., 1986), and input of DOM from sediment porewaters (Chen and Bada, 1989; McCorkle et al., 1985). The stable carbon isotope data and analysis of lignin oxidation products in seawater (Meyers-Schulte and Hedges, 1986) indicate that terrestrial DOM is not a large fraction of the total DOM dissolved in seawater. However, the stable carbon isotope data alone cannot be used to exclude riverborne DOM as a possible source, due to the presence of terrestrially derived DOM with heavy stable carbon isotopic values (e.g. C4 plants have  $\delta^{13}\text{C}$  values between  $-10$  and  $-18$  ‰) (Fry and Sherr, 1984).

### 1.3 Cycle of DOM in the Ocean

The cycle of DOM in the ocean has been studied using radiocarbon analyses. The  $\Delta^{14}\text{C}^1$  values of DOM isolated from the deep ocean range between  $-400$  ‰ (4000 radiocarbon years) in the deep Atlantic Ocean to  $-525$  ‰ (6000 radiocarbon years) in the Pacific Ocean (as shown in Figure 1.2, (Druffel et al., 1992)). The 2000 year age difference between the DOM in the deep Atlantic and Pacific Ocean is similar to the 1500 year ocean circulation time derived from measuring the  $\Delta^{14}\text{C}$  values of DIC. These

---


$$^1 \quad \Delta^{14}\text{C} = \delta^{14}\text{C} - 2\left(\delta^{13}\text{C} + 25\right)\left(1 + \frac{\delta^{14}\text{C}}{1000}\right); \delta^{14}\text{C} = \left[ \frac{\left(\frac{^{14}\text{C}}{^{12}\text{C}}\right)_{\text{sample}} - \left(\frac{^{12}\text{C}}{^{14}\text{C}}\right)_{\text{standard}}}{\left(\frac{^{14}\text{C}}{^{12}\text{C}}\right)_{\text{standard}}} \right] \times 1000$$

data reveal that (1) a large fraction of DOM escapes degradation on time scales of 6000 years, and (2) DOM must be transported between the two ocean basins by deep-water circulation. Also shown in Figure 1.2 is the  $\Delta^{14}\text{C}$  value of the total DOC in surface waters of the Atlantic and Pacific Ocean (-150 to -230 ‰). These values are more enriched in  $^{14}\text{C}$  than deep ocean values, but depleted compared to surface ocean DIC (approximately 130‰; the reported values are for the years 1987-1991). Given the 6000 year age of DOM in the deep Pacific, and the 1500 year ocean circulation time, it is clear that a large fraction of DOM is cycled over several ocean mixing cycles. The DOC concentration profile in Figure 1.1 shows that surface waters DOC concentrations are approximately double the deep-water values. Thus surface waters can be described as an admixture of refractory, deep ocean DOM (50%) and new, surface derived DOM (50%). Carrying out a simple mass balance calculation

$$(\Delta^{14}\text{C})_{\text{surfaceDOC}} = 0.5 \times (-525) + 0.5 \times (\Delta^{14}\text{C})_{\text{newDOM}} = -200$$

(the  $\Delta^{14}\text{C}$  value of surface waters is expressed as surface DOC, while the unknown  $\Delta^{14}\text{C}$  value for the new DOM produced in the surface ocean is expressed as new DOM), shows that the  $\Delta^{14}\text{C}$  value of the new DOM added at the surface is approximately 130 ‰, in good agreement with the  $\Delta^{14}\text{C}$  value of DIC in the surface ocean. This supports the conclusion that the new component of DOM, added in the surface ocean, is produced from DIC during photosynthesis.

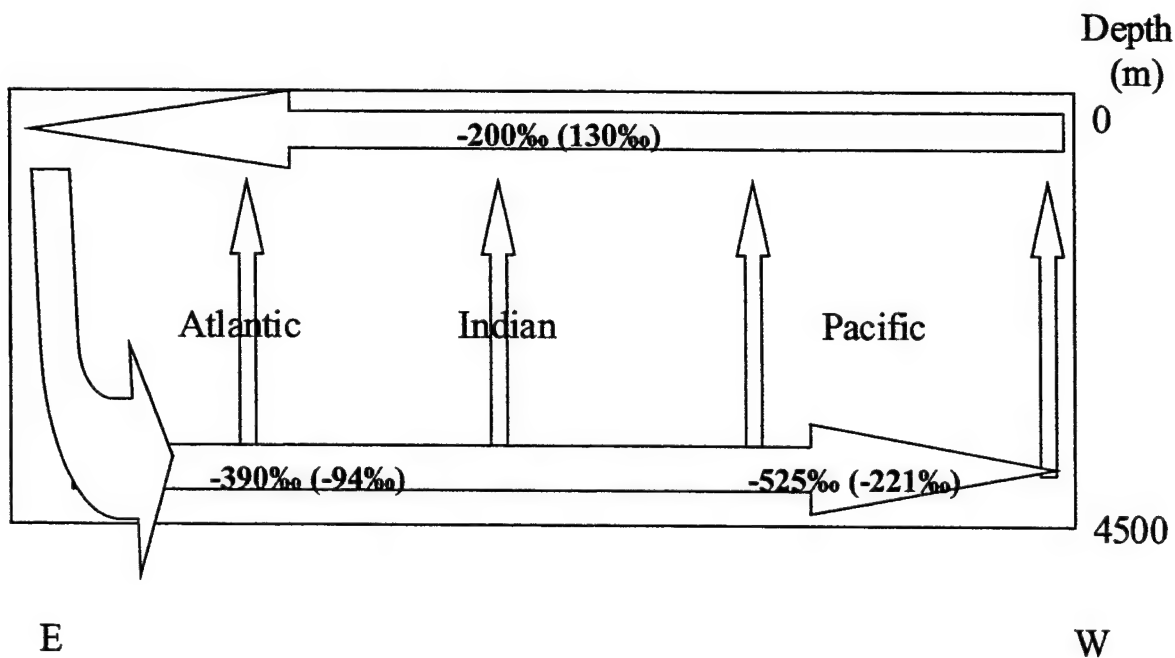


**Figure 1.2** The  $\Delta^{14}\text{C}$  values of DOC and DIC (in parentheses) in different parts of the World's Ocean. Arrows depict the direction of ocean circulation.

Using the age of total DOM in the deep ocean and the reservoir size (~600 Gt C), the flux of DOM out of the ocean can be calculated to be 0.1 Gt C/yr. This flux out can be supported entirely by the riverine flux into the ocean, and is only a small percentage of the total annual primary production (50 Gt C/yr). Given the rapid degradation rates of certain organic compounds and the high heterotrophic bacterioplankton production rates observed in the ocean (Fuhrman and Azam, 1982), it is clear that certain a fraction of DOM must cycle on shorter time scales.

(Carlson and Ducklow, 1995) showed that DOM can be sub-divided into at least three different reservoirs of differing reactivity: a "very reactive" fraction, consisting of soluble biochemicals, turning over on time scales of hours to days (Jorgensen et al., 1993; Vaccaro et al., 1968); a "refractory fraction" (6000 years old), which accounts for most of the measured DOM in the ocean, turning over on several thousand year time scales; and finally a third fraction, "reactive" DOM, which accounts for the 30-40  $\mu\text{M}$  difference



between surface and deep water DOC concentrations, likely turning over on annual to decadal timescales. Thus, while the radiocarbon results for the total DOM fraction in the seawater offers useful insights into the overall cycle of DOM, they clearly miss the more dynamic cycles that must exist for different components of the DOM pool.

In order to gain any further insight into the factors that control production and cycling of DOM we need a better understanding of the major chemical components of this pool.

### 1.5 Chemical Structure of DOM

Stuermer and Harvey, (1974) conducted a comprehensive investigation of the chemical structure of DOM isolated by adsorption on to XAD resins (humic substances). Shown in Figure 1.3 is a model structure for marine humic substances isolated from seawater (Gagosian and Stuermer, 1977). These humic substances accounted for

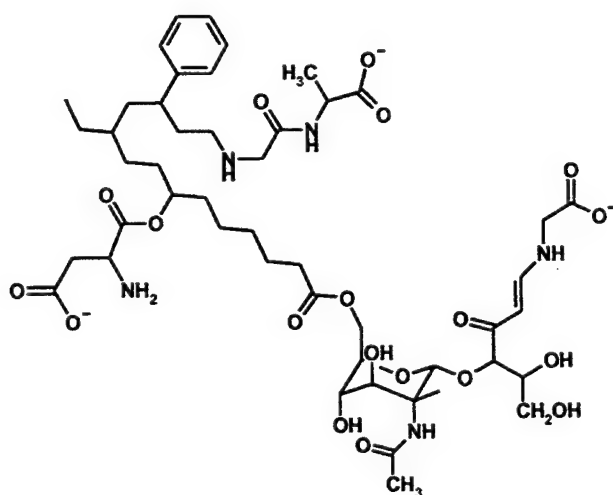


**Figure 1.3** Hypothetical structure for dissolved marine humic substances (Gagosian and Stuermer, 1977)

between 5-15% of the total DOM and were characterized by low aromaticity (compared to terrestrial humic substances), marine stable carbon isotopic values, carbon to nitrogen

ratios of 8, molecular weights < 700 daltons (73% of the total isolate), and an extremely complex mixture of amino acids, carbohydrates, lipids (of marine origin) and other biochemicals. This chemical data led these and other investigators to conclude the much of the DOM in seawater resulted from the random condensation, oxidation and polymerization of biochemicals present in seawater as proposed by (Kalle, 1966). Since XAD isolates account for between 5-15% of the total DOM, there is no *a priori* reason why the remaining fraction of DOM accumulating in the ocean should be formed by the *geopolymerization* of simple biochemicals.

## **1.5 Organization of this Thesis**

The isolation of DOM by adsorption onto XAD resins chemically fractionates DOM, and isolates only between 5-15% of the total (Hedges, 1992). The first goal of this thesis was to isolate and chemically characterize a more representative and larger fraction of DOM from the marine environment, and to test the theory of geopolymerization by structurally characterizing DOM from different sites within the ocean. This study used tangential flow ultrafiltration, which separates molecules based on their size (Benner et al., 1992; Carlson and Mayer, 1985), to isolate the > 1000 MW (nominal molecular weight) fraction of DOM (high molecular weight (HMW) DOM) for chemical characterization by a variety of different analytical methods. The results of this investigation are presented in Chapter 2, and show that up to 60% of the HWM DOM in surface waters, and 10-20 % of the HMW DOM in deep waters, consists of structurally related acylated polysaccharides (APS). These APS are characterized by a nearly fixed ratio of carbohydrate:acetate:lipid carbon and a very characteristic distribution of seven monosaccharides.

The IUPAC numbering of monosaccharide carbon atoms, and the two possible orientations of the anomeric carbon proton (C-1) are shown in Figure 1.3. This anomeric carbon is particularly important because it is a key linkage site for most carbohydrates, including APS isolated in this study. Figure 1.4 shows the structures for the 10 different monosaccharides discussed in Chapter 2.

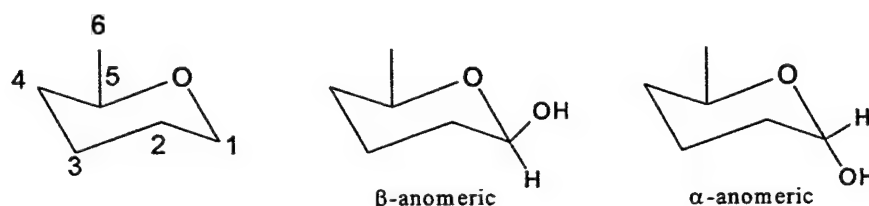


**Figure 1.4** Monosaccharide structure: carbon and protons are labeled 1-6 as shown (a),  $\beta$  anomer (b) and  $\alpha$  anomer (c).

The discovery that the major biochemicals in HMW DOM were present in a near constant ratio at all the diverse sites examined in this study is surprising and suggests a direct biological source (biosynthesis). However, the constant ratio of biochemicals in HMW DOM does not exclude the geopolymerization model. If DOM consists of refractory geopolymers with residence times longer than the mixing time of the ocean, then these geopolymers would exist well mixed throughout the oceanic reservoir. To test the conclusion of Chapter 2, that a large fraction of "reactive" DOM is from biosynthesis, we chemically characterized the HWM DOM exudates of three common phytoplankton. It was found that organic matter with chemical characteristics similar to APS were present in the exudates of two of the three species of phytoplankton, indicating that the source of this APS is direct biosynthesis.

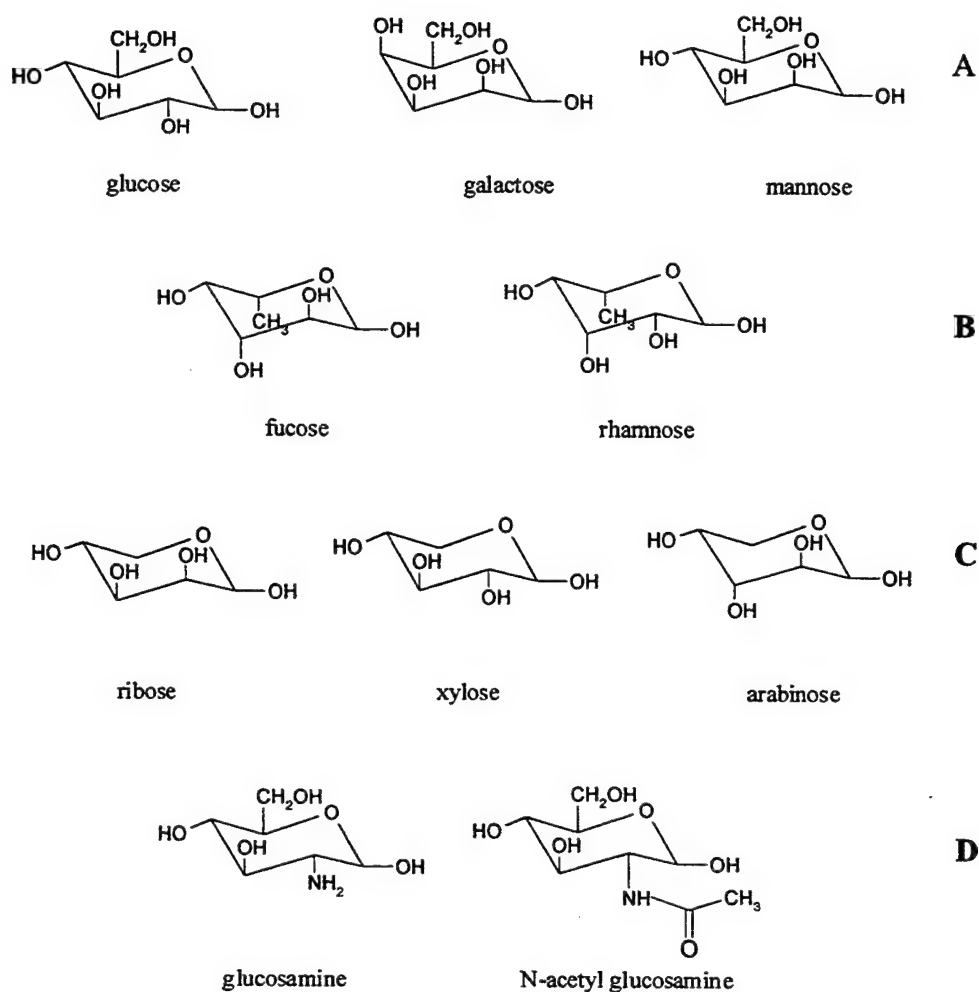


**Figure 1.5 Eight neutral monosaccharides identified in HMW DOM: hexoses (A); deoxy hexoses (B); pentoses (C). Glucosamine in its acetylated and non-acetylated form (D) is also shown.**

Finally, we attempted to use the chemical data and radiocarbon measurements to determine the mechanisms that control the cycling of APS in the ocean. The results from this investigation, presented in Chapter 4 shows that the individual monosaccharides that constitute APS are of contemporary origin both in the surface and deep ocean, with  $\Delta^{14}\text{C}$

values similar to surface DIC. The presence of DOM with contemporary with  $\Delta^{14}\text{C}$  values in the deep sea indicates recent, autochthonous production. The radiocarbon data further confirm that the constant biochemical ratio observed for seawater APS do not result from a well mixed reservoir, but from a ubiquitous marine source as shown in Chapter 3.

These data require a shift from the currently accepted paradigm that geopolymerization is the mechanism which forms the accumulating DOM in the ocean. While it is likely and possible that some fraction of DOM is formed by these mechanisms, our data suggests that at least 20% of the DOM accumulating in seawater is produced by direct biosynthesis. Further, contrary to the picture of DOM cycling generated by using  $\Delta^{14}\text{C}$  values of total DOM, the data presented in this thesis indicates that there are more dynamic cycles for certain fractions of DOM within the larger cycle of passive transport by ocean circulation.

## **1.6 Goals of this Thesis**

The goal of this thesis was to chemically characterize dissolved organic matter (DOM) isolated by ultrafiltration (20-30% of the total DOM), and use the chemical information to better understand the cycle of DOM in the ocean. The thesis is divided into three parts: (1) the chemical characterization of high molecular weight ( $> 1 \text{ k Da}$ ) (HMW) DOM isolated from different oceanic regimes; (2) the use of the chemical data to identify possible sources of HMW DOM to the marine environment; and (3) the use of radiocarbon measurements to understand the cycle of HWM DOM in the ocean.

## 1.7 References

- Azam F., Fenchel T., Field J. G., Gray J. S., Meyer-Reil L. A., and Thingstad F. (1983) The ecological role of water-column microbes in the sea. *Marine Ecology Progress Series* 10, 257-263.
- Bacastow R. and Maier-Reimer E. (1991) Dissolved organic carbon in modeling oceanic new production. *Global Biogeochemical Cycles* 5(1), 71-85.
- Bada J. L. and Lee C. (1977) Decomposition and alteration of organic compounds dissolved in seawater. *Marine Chemistry* 5, 523-534.
- Benner R., Pakulski J. D., McCarthy M., Hedges J. I., and Hatcher P. G. (1992) Bulk chemical characteristics of dissolved organic matter in the ocean. *Science* 255, 1561-1564.
- Blough N. V., Zafiriou O. C., and Bonilla J. (1993) Optical absorption spectra of waters from the Orinoco River outflow: terrestrial input of colored dissolved organic matter to the Caribbean. *Journal of Geophysical Research* 98(C2), 2271-2278.
- Bruland K. W. (1989) Oceanic zinc speciation: Complexation of zinc by natural organic ligands in the North Pacific. *Limnology and Oceanography* 34, 267--283.

- Carlson C. A. and Ducklow H. W. (1995) Dissolved organic carbon in the upper ocean of the central equatorial Pacific Ocean, 1992: Daily and finescale vertical variations. *Deep-Sea Research* **42**(2-3), 639-650.
- Carlson C. A., Ducklow H. W., and Michaels A. F. (1994) Annual flux of dissolved organic carbon from the euphotic zone in the northern Sargasso Sea. *Nature* **371**, 405-408.
- Carlson D. J. and Mayer L. M. (1985) Molecular weight distribution of dissolved organic materials in seawater as determined by ultrafiltration: A re-examination. *Marine Chemistry* **16**, 155-171.
- Chen R. F. and Bada J. L. (1989) Seawater and porewater fluorescence in the Santa Barbara Basin. *Geophysical Research Letters* **16**, 687-690.
- Chen R. F., Fry B., Hopkinson C. S., Repeta D. J., and Peltzer E. T. (1995) Dissolved organic carbon on Georges Bank. *Continental Shelf Research* **16**, 409-420.
- Coale K. H. and Bruland K. W. (1988) Copper complexation in the North East Pacific. *Limnology and Oceanography* **33**, 1084-1101.

- Druffel E. R. M., Williams P. M., Bauer J. E., and Ertel J. R. (1992) Cycling of dissolved and particulate organic matter in the open ocean. *Journal of Geophysical Research* **97**(10), 15639-15659.
- Duursma D. K. (1963) The production of dissolved organic matter in the sea, as related to the primary gross production of organic matter. *Netherlands Journal of Sea Research* **2**, 85-94.
- Ertel J. R., Hedges J. I., Devol A. H., and Richey J. E. (1986) Dissolved humic substances of the Amazon River system. *Limnology and Oceanography* **31**, 739-754.
- Frew N. M., Goldman J., Dennet M. R., and Johnson A. S. (1990) Impact of phytoplankton generated surfactants on Air-Sea gas exchange. *Journal of Geophysical Research* **95**(c3), 3337-3352.
- Fry B. and Sherr E. B. (1984)  $\delta^{13}\text{C}$  measurements as indicators of carbon flow in marine ecosystems. *Contributions in Marine Science* **27**, 13-47.
- Fuhrman J. A. and Azam F. (1982) Thymidine incorporation as a measure of heterotrophic bacterial production in marine surface waters: Evaluation and field results. *Marine Biology* **66**(2), 109-120.



- Gagosian R. B. and Stuermer D. H. (1977) The cycling of biogenic compounds and their diagenetically transformed products in seawater. *Marine Chemistry* **5**, 605-632.
- Hagstrom A., Larsson A., Horstedt P., and Normark S. (1979) Frequency of dividing cells, a new approach to the determination of bacterial growth rates in aquatic environments. *Applied Environmental Microbiology* **37**, 805-812.
- Hedges J. I. (1992) Global Biogeochemical cycles: progress and problems. *Marine Chemistry* **39**, 67-93.
- Johnson K. H., Gordon R. M., and Coale K. H. (1997) What controls dissolved iron concentrations in the World Ocean? *Marine Chemistry* **57**, 137-161.
- Jorgensen N. O. G., Kroer K., Coffin R. B., Yang X. -H., and Lee C. (1993) Dissolved free amino acids and DNA as sources of carbon and nitrogen to marine bacteria. *Marine Ecology Progress Series* **98**, 135-148.
- Kalle K. (1966) The problem of Gelbstoff in the sea. *Oceanography and Marine Biology, Annual Review* **4**, 91-104.
- Kirchman D. L., Suzuki Y., Garside C., and Ducklow H. W. (1991) High turnover rates of dissolved organic carbon during a spring phytoplankton bloom. *Nature* **352**, 612-614.

- LaRoche J., Nuzzi R., Waters R., Wyman K., Falkowski P. G., and Wallace D. W. R. (1997) Brown tide blooms in Long Island's coastal waters linked to interannual variability in groundwater flow. *Global Change Biology* **3**(3), 397-410.
- Mague T. H., Friberg E., Hughes D. J., and Morris I. (1980) Extracellular release of carbon by marine phytoplankton a physiological approach. *Limnology and Oceanography* **25**(2), 262-279.
- Martinez J. and Azam F. (1993) Amino-peptidase activity in marine cyanobacteria. *Applied Environmental Microbiology* **59**(11), 3701-3707.
- McCorkle D. C., Emerson S. R., and Quay P. D. (1985) Stable carbon isotopes in marine porewaters. *Earth and Planetary Science Letters* **74**, 13-26.
- Menzel D. W. (1974) Primary productivity, dissolved and particulate organic matter, and the sites of oxidation of organic matter. In: E. D. Goldberg (Ed.), *The Sea* (John Wiley & Sons Ltd.), 659-678.
- Meyers-Schulte K. and Hedges J. I. (1986) Molecular evidence for a terrestrial component of organic matter dissolved in ocean water. *Nature* **321**, 61-63.
- Moffet J. W. and Zika R. G. (1987) Solvent extraction of copper acetylacetonate in studies of copper (II) speciation in seawater. *Marine Chemistry* **21**, 301-313.

Morris A. W. and Foster P. (1971) The seasonal variation of dissolved organic carbon in the inshore waters of the Menai Strait in relation to primary production.

*Limnology and Oceanography* **16**, 987-989.

Palenik B. and Morel F. M. M. (1990) Amino acid utilization by marine phytoplankton:

A novel mechanism. *Limnology and Oceanography* **35**(2), 260-269.

Peltzer E. T. and Hayward N. A. (1996) Spatial and temporal variability of total organic carbon along 140 W in the Equatorial Pacific Ocean in 1992. *Deep Sea Research Special EqPac* **43**(4-6), 1155-1180.

Rue E. L. and Bruland K. W. (1995) Complexation of iron (III) by natural ligands in the Central North Pacific as determined by a new competitive ligand

equilibration/adsorptive cathodic stripping voltammetric method. *Marine*

*Chemistry* **50**(1-2), 117-138.

Smith D. C., Simon M., Alldredge A. L., and Azam F. (1992) Intense hydrolytic enzyme activities on marine aggregates and implications for rapid particle dissolution.

*Nature* **359**, 139-142.

Stuermer D. H. and Harvey G. R. (1974) Humic substances from seawater. *Nature* **250**,

480-481.

Vaccaro R. F., Hicks S. E., Jannasch H. W., and Carey F. G. (1968) The occurrence and role of glucose in seawater. *Limnology and Oceanography* **13**, 356-360.

Voelker B. M., Morel F. M. M., and Sulzberger B. (1997) Iron redox cycling in surface waters: effects of humic substances and light. *Environmental Science and Technology* **31**(4), 1004-1011.

Williams P. and Gordon L. (1970) Carbon-13: Carbon-12 ratios in dissolved and particulate organic matter in the sea. *Deep-Sea Research* **17**(19-27).

## **2. Structural Characterization of Marine Dissolved High Molecular Weight Organic Matter**

### **2.1 Introduction**

In order to fully understand the relationship between the production, accumulation and removal of dissolved organic matter (DOM) in the ocean, it is important to first investigate its chemical composition. Until the mid 1990's direct chemical analyses of DOM in seawater typically accounted for less than 15% of total mixture (Hedges, 1992)), and it was believed that the characterization of the remainder of DOM had been frustrated by its heteropolycondensate nature (Degens, 1970; Gagosian and Lee, 1981). The study of DOM has been further impeded by the fact that many techniques that can provide comprehensive structural information, such as nuclear magnetic resonance spectroscopy (NMR), mass spectrometry (MS) and infrared spectroscopy (IR), require the technically difficult isolation of DOM from the much more abundant salts in seawater. As discussed in the Chapter 1, past studies on DOM have focused on the compounds isolated by the adsorption of acidified DOM onto non-ionic XAD resins (Gagosian and Stuermer, 1977). This separation requires large manipulations of the pH, which may alter the DOM and chemically fractionates the DOM during isolation. The recent use of tangential flow ultrafiltration has allowed investigators to isolate DOM from seawater based on molecular size, and requires no chemical manipulation of the sample. Using filters with a nominal cutoff of 1 nm (> 1000 daltons) several investigators have shown that up to 30% of the total DOM can be isolated from seawater (Carlson and Mayer 1985; Benner et al. 1992; Santschi et al., 1995) using this method. Bulk chemical characteristics of this high

molecular weight (HMW) DOM show that contrary to what was expected (from the XAD resin isolates) a large fraction of HMW DOM consists of recognizable biochemicals. Using  $^{13}\text{C}$ NMR for example, Benner et al. (1992) showed carbohydrate resonances were the major fraction of HMW organic carbon in surface waters (54%) and significant fraction in deep waters (25%). In fact, several investigators in the past, using a variety of different methods, also showed that up to 20% of the total carbon dissolved in seawater can be identified as polysaccharides (Burney et al., 1979; Ittekkot et al., 1981; Mopper, 1977; Sakugawa and Handa, 1983; Sakugawa and Handa, 1985b). In accordance with these findings, a large body of work has emerged over the last several years showing that 17-50% of the carbon in HMW DOM, and thus at least 7-15% of the total DOC, is carbohydrate (Aluwihare et al., 1997; Borch and Kirchman, 1997; McCarthy et al., 1996; Skoog and Benner, 1997).

The large concentration of polysaccharides in HMW DOM would suggest that it is nitrogen poor, however C/N ratios in both the surface and deep waters are approximately 15 (Benner et al., 1992; McCarthy et al., 1996), suggesting that HMW DOM must contain nitrogen. Using  $^{15}\text{N}$ NMR, McCarthy et al., (1998) showed that the major nitrogen resonance in HMW DOM was amide, arising from proteins or acetylated amino sugars. In accordance with the carbohydrate data, identifiable biochemicals, for example bacterial membrane proteins (Tanoue et al., 1995) have also been isolated from the HMW dissolved organic nitrogen pool. However, amino acid analysis accounts for only 4-5% of the total carbon in HMW DOM and approximately 11-29% of the total nitrogen in HMW DOM (McCarthy et al. 1996). Acetylated amino sugars have also been identified in HMW DOM by GC (Aluwihare et al., 1997), HPLC (Skoog and Benner,

1997) and mass spectrometry (Klap, 1997). Quantification by the two former methods show that acetylated amino sugars do not account for more than 10% of the total carbon in HMW DOM.

The purpose of this chapter was to identify the major carbon and nitrogen - containing components of DOM isolated by ultrafiltration and to investigate if the HMW DOM isolated from different parts of the ocean was chemically distinct. The chapter begins with a synopsis of the sampling sites, and sampling methods, and includes data from  $^1\text{H}$ ,  $^{13}\text{C}$  and  $^{15}\text{N}$  NMR, monosaccharide composition and some carbohydrate linkage, lipid, and amino acid analyses.

## **2.2 Materials and Methods**

### **2.2.1 Sampling Site**

In order to investigate the hypothesis that DOM from different locations is compositionally similar, samples spanning diverse oceanographic environments were collected and analyzed (Figure 2.1). A suite of samples from the Mid Atlantic Bight were collected during the Ocean Margins Program sponsored by the Department of Energy. In addition, two samples from the Northeast Pacific Ocean (Station M), and one sample each from the Eastern North Atlantic, Hawaii and Woods Hole (Coastal Research Laboratory) were also analyzed. Sample locations, depths and sampling time are listed in Table 2.1 (see results section 2.3.1).

### **2.2.2 Sample Collection and Isolation**

All surface samples were collected using a Teflon lined hose, and pumped onboard ship with a pneumatic, teflon-lined diaphragm pump (Lutz Pumps, Inc., Norcross, GA). Deep samples were collected via Niskin bottles. Seawater samples were

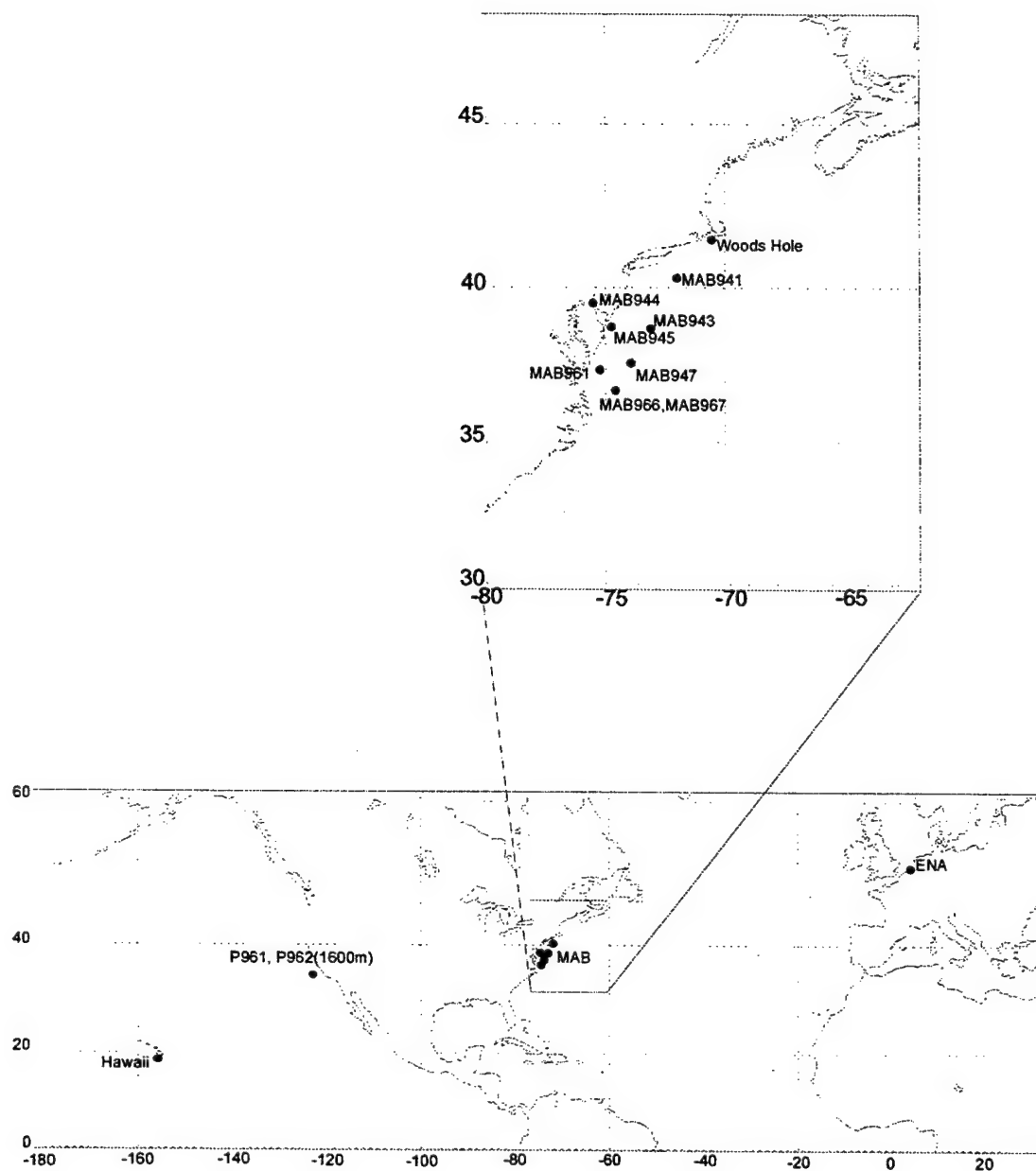


**Figure 2.1 Map showing the locations of the different samples analyzed for this thesis**

pre-filtered through both pre-combusted (450°C, 12 hours) 293mm, Whatman GF/F (0.7  $\mu\text{m}$ ) or Gelman A/E (1.0  $\mu\text{m}$ ) filters and acid (0.1 N HCl) rinsed, 0.2  $\mu\text{m}$ , Gelman Criticap 100 capsules. Filters were changed when the flow rates decreased. Pre filtered



samples were stored (< 5 h) in Teflon coated barrels (Fluoropure, Chaska, MN) until they were ultrafiltered. All tubing and fittings were Teflon except for the 273 mm filter holder (polycarbonate) and the Criticap capsule filters (polycarbonate).

#### 2.2.2.1 Ultrafiltration

Ultrafiltration (the generic term for cross flow filtration and tangential flow filtration (Carlson and Mayer, 1985), is the only practical technique for processing the large volume samples (10-1000 l) required for the isolation of DOM for more sophisticated analytical techniques such as NMR, MS and infrared spectroscopy (IR). In ultrafiltration, a pre-filtered sample solution flows parallel to the ultrafiltration membrane, and hydrostatic pressure drives solutes with an effective molecular size less than the membrane pore diameter, through the membrane (permeate) (Buesseler et al., 1996). The remaining solution (retentate), containing some of the smaller solutes and all of the bigger solutes, is transported along the membrane surface and recycled through the retentate reservoir. Thus the molecules which are rejected by the membrane (i.e. bigger than the membrane pore diameter) are increasingly concentrated in the retentate over time (Buesseler et al. 1996).

A schematic for the system used in this study is shown below (Figure 2.2). An Amicon DC-10L ultrafiltration unit was used in this study, and was routinely run with two spiral-wound polysulphone membrane cartridges, stacked in series. These membranes have a 1 nm pore diameter and are designed to have a nominal molecular weight cutoff of 1000 daltons (1 k Da) (Millipore, Bedford, MA; Amicon S10N1). Thus these membranes retain compounds whose molecular weights are greater than 1kD. With

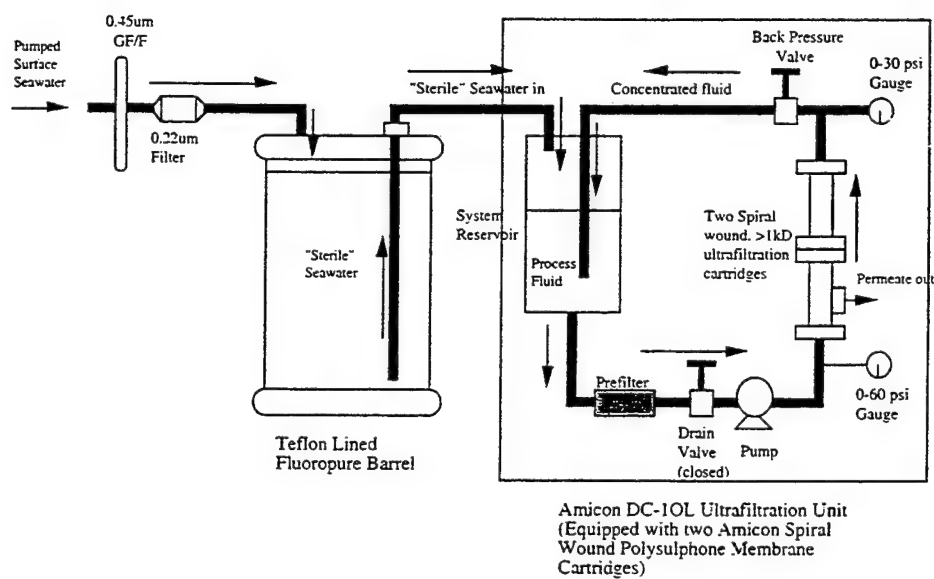


**Figure 2.2 Schematic representation of the procedure for the isolation of HMW DOM**

two cartridges in series, the Amicon system can be run with a 20 psi (pounds per square inch) pressure differential between the inlet and the outlet. At no time during ultrafiltration was the inlet pressure allowed to exceed 50 psi, and thus the outlet pressure never exceeded 30 psi. Samples were delivered from the teflon-lined barrels to the ultrafiltration system by applying slight air pressure to the barrels. In this manner 10s to 100s of liters of seawater were processed continuously. A 200 l surface sample of seawater typically took 8-12 h to concentrate to approximately 2 l. Unless samples were desalted by diafiltration (described in section 2.2.2.2) on site (Hawaii and CRL), concentrated samples were frozen ( $-4^{\circ}\text{C}$ ) in pre-combusted glass bottles, or acid rinsed (concentrated HCl) teflon bottles. Directly after processing each sample, the ultrafiltration unit was then rinsed with 4 l of Milli Q water, which was collected and frozen as above.

Membranes were calibrated using two compounds with molecular weights close to the membrane pore diameter, maltoheptaose (Sigma, St. Louis, MO), molecular weight 1.15 k Da, and Gramicidin S (Sigma, St. Louis, MO), molecular weight 1.2 k Da. Samples were dissolved in Milli Q water (DOC concentrations 10-19  $\mu\text{M}$ ), at a concentration of 1 mg C/l. The concentration factor in all cases was 4. Recoveries were determined by measuring the DOC concentration in sample prior to ultrafiltration and in the retentate following ultrafiltration. Purity of the samples following ultrafiltration was also determined using  $^1\text{H}$ NMR spectroscopy. Retention characteristics were  $80\pm 10\%$  and 50 % for the carbohydrate and protein, respectively. Other investigators have found higher values, typically 80% for vitamin B-12 (1.2 k Da) and  $> 93\%$  for molecules larger than 6 k Da (Guo and Santschi, 1996; Gustafsson et al., 1996).

#### 2.2.2.1.1 Cleaning The Membranes

In all cases, water other than seawater, was collected from a Millipore Milli Q system, (four cartridge system with 1 pre-filter cartridge, a carbon removal cartridge (Super C), and two ion exchange cartridges (Ion X)). Water was collected after the resistivity increased beyond 18 ohms and was filtered through a 0.2  $\mu\text{m}$  filter prior to collection. The water isolated directly from the system had a DOC blank of 15  $\mu\text{M}$ . New cartridges, and cartridges that were stored for over three weeks were thoroughly cleaned before use. Cartridges were cleaned by sequentially passing 4 l liters of Micro detergent (1%), 0.01 N sodium hydroxide (NaOH) and hydrochloric acid (HCl) solutions in Milli Q water through the system (Guo et al., 1994). Between each cleaning solution, the cartridges were rinsed with 20 l of Milli Q water. The pH of the permeate was measured after the last Milli Q rinse to insure that it was between 6-7 units (that of unprocessed Milli Q water). Between samples, on board ship, cartridges were only cleaned with base and acid solutions (MAB941 through MAB947, MAB961), except when a deep sample followed a surface sample (before MAB966, MAB967, and between P961 and P962) when all three cleaning solutions were used. Before ultrafiltering each sample, 3-4 l of seawater were used to condition the cartridges.

#### 2.2.2.2 Diafiltration

Diafiltration or desalting was performed in the laboratory (except in the case of Hawaii and CRL) on thawed samples. During diafiltration, the sample was added to the ultrafiltration reservoir along with 2 l of Milli Q water and ultrafiltered to between 1.5-2 l. Following this, another 2 l of Milli Q water was added and re-concentrated to 1.5 l. This procedure was repeated until the permeate from the last 2 l rinse gave no visible

precipitate when added to a saturated solution of silver nitrate (0.5g/50 ml). In most cases 10 dilutions (for a total of 20 l) were used in diafiltering each sample. Following diafiltration, samples were concentrated to approximately 2 l and stored at  $-20^{\circ}\text{C}$  in glass or teflon bottles for a few weeks to several months.

Prior to analysis, all samples were lyophilized and stored at room temperature or  $-4^{\circ}\text{C}$ .

#### 2.2.2.3 Desalting

Prior to the linkage analysis, samples (CRL, Hawaii and ENL) were further desalted using a cation exchange resin. Lyophilized samples were applied, dissolved in 1 ml of Milli Q water (5 mg sample/2 ml of resin bed), to the cation exchange resin (AG 50W-X8, BioRad Laboratories, Hercules, CA) in the hydrogen form, and eluted with water (3 column bed volumes). The resin was rinsed with  $3 \times 3$  ml of Milli Q water prior to packing. Columns were packed in 6" combusted glass pipettes (6 or 8 mm I. D.), using Milli Q water.

Mass balances after desalting showed that material was lost to the column, but in all cases removal of salt could account for this loss. Three samples from the deep ocean (UF967, UF948, and UF9412 (750 m)), in addition to the three samples mentioned above, were tested to determine changes in the C/N ratios incurred during desalting. Samples containing between 1-10% carbon (C/N ratios between 1 to 4) showed an order of magnitude change in their C/N ratios following desalting, while samples with  $> 25\%$  C showed only a 20% increase in their C/N ratio. Neither charged sugar (galactouronic acid and glucosamine) standards nor Bovine Serum Albumin (BSA) showed losses to the

column during desalting. Recovery of monosaccharides and changes in the distribution of monosaccharides following desalting are discussed more fully in Chapter 4.

### **2.2.3 Dissolved Organic Carbon (DOC) Analysis**

Total DOC concentrations were measured by filtering 20-40 ml of seawater through pre-combusted GF/F filters (47 mm, Whatman) and collecting the filtrate in pre-combusted glass vials fitted with teflon-lined caps. Any surface that came into contact with seawater was teflon, stainless steel or glass. High molecular weight (HMW) DOC concentrations were obtained by directly sampling the retentate and diluting with a known volume of Milli Q water. All samples were acidified with 50% phosphoric acid  $\text{H}_3\text{PO}_4$  (0.5 M) immediately after collection and stored at room temperature or 4°C. Samples were analyzed for DOC by high temperature catalytic oxidation (Peltzer and Brewer, 1993) after purging with nitrogen to remove inorganic carbon. Precision for triplicate analyses were better than  $\pm 3.5\%$  and the upper limit for the blank was 25  $\mu\text{M}$  based on the DOC concentration of acidified distilled water.

### **2.2.4 Elemental Analysis**

DOC samples were analyzed for carbon, hydrogen and nitrogen content using an EA 1108 elemental analyzer with Eager 200 data acquisition software (Fisons Instruments, Inc., Beverly, MA). Between 300-1000  $\mu\text{g}$  of lyophilized DOM was weighed into 8  $\times$  6 mm tin cups using a Sartorius Micro balance, and folded with forceps into very small packages prior to analysis. Samples were run with blank cups and known standards in order to correct for the C and N associated with the tin cups.

## 2.2.5 Nuclear Magnetic Resonance Spectroscopy

### 2.2.5.1 General Principles

Nuclear magnetic resonance spectroscopy (NMR) is a non-destructive technique for the determination of chemical structure and conformation. Today, with the development of magnets with high field strengths ( $> 750$  MHz) and multi-dimensional techniques, NMR is used to routinely analyze the primary, secondary and tertiary structures of complex chemicals.

NMR is based on the principle that the magnetic moment of nuclei with spin numbers of  $\frac{1}{2}$  (for example  $^1\text{H}$ ,  $^{13}\text{C}$  and  $^{15}\text{N}$ ) will align with or against an externally applied magnetic field. At equilibrium, according to the Boltzmann distribution, there are more nuclei aligned with the applied magnetic field, than against. The nuclei aligned with the magnetic field are in the lower energy state (spin  $+\frac{1}{2}$ ) and those aligned against the magnetic field are in the higher energy state (spin  $-\frac{1}{2}$ ). In a NMR experiment, the nuclei of interest are excited to a higher energy state by the application of a radio frequency (rf) pulse at right angles to the applied magnetic field. This deviation from the Boltzmann distribution, resulting from the rf pulse, changes the direction of the net magnetization vector of the nuclei from its orientation with the applied magnetic field (the positive z axis by convention) to an orientation in the x-y plane. Once the rf pulse turns off, the individual nuclei relax back to their ground state at a rate that is dependent on the immediate chemical environment of each nucleus. This relaxation, or loss of energy to the environment, is enabled by two processes known as longitudinal relaxation (whereby a nucleus dissipates its energy to surrounding molecules) and transverse relaxation (whereby energy is dissipated among nuclei). As the nuclei relax back to their ground state (alignment with the z-axis) the magnitude of the magnetization vector in the

x-y plane begins to decrease. This decrease is detected by the receiver (which measures the size of the vector in the x-y plane) and is referred to as the free induction decay (FID). The FID, which is a function of time, is Fourier transformed to yield peaks as a function of frequency. Thus the x-axis of the NMR spectrum shows peaks as a function of frequency.

The difference in the absorption position of a particular proton from the absorption position of a reference proton is called its chemical shift. One of the major and more easily understood factors that influence chemical shift is electronegativity. For example, since carbon is more electropositive than hydrogen, the sequence of proton absorptions in the series  $\text{CH}_4$ ,  $\text{RCH}_3$ ,  $\text{R}_2\text{CH}_2$  and  $\text{R}_3\text{CH}$  is from lower frequency to higher frequency (and higher field to lower field). Furthermore, the chemical shift of protons in  $\text{RCOCH}_3$  is downfield (lower field) from  $\text{R}_x\text{CH}_x$ , while the non-alcohol proton of  $\text{RCHOH}$ , absorbs even further downfield (higher chemical shift). These latter chemical shifts are caused by the influence of the oxygen atom, which draws the electron density away from the proton nucleus, thus decreasing its shielding by electrons.

Units of  $\delta$  (in p.p.m) are usually employed to report chemical shifts because they are dimensionless and are independent of the applied magnetic field. Higher  $\delta$  values correspond to higher frequencies and lower field.

#### 2.2.5.2 Experimental Conditions for Proton NMR ( $^1\text{H}$ NMR)

All spectra were acquired using a Bruker AC300, 300 MHz spectrometer (Bruker Instruments, Inc., Manning Park, Billerica, MA) in conjunction with an Aspect 3000 data system (Spectrospin AG, Industriestrasse 26, CH-8117 Faellanden, Switzerland). The quantity of sample used for each acquisition depended on the solubility of the material



and the spectrometer availability. Typically, 10 mg of DOM was used with acquisition times ranging between 1-2 days. Spectra can be acquired on much smaller quantities of material ( $< 100 \mu\text{g}$ ), but much longer acquisition times are necessary for these experiments. All samples were dissolved in 750  $\mu\text{l}$  to 1 ml of  $>99.9$  atom % purity  $\text{D}_2\text{O}$  (Aldrich Chemical Company, Milwaukee, WI) and acquired at  $298^\circ\text{K}$ . In most cases samples were first dissolved in 1-2 ml of 99.9 atom %  $\text{D}_2\text{O}$  and freeze-dried. This was repeated 1-2 times in order to insure that the exchangeable protons in the sample were saturated with deuterium. In all cases, chemical shifts are reported in the standard " $\delta$ " notation (units of p.p.m), relative to HDO ( $\delta = 4.8$  p.p.m). Acquisition parameters for a typical  $^1\text{H}$ NMR spectrum are given in the Appendix. The resonance from HDO (deuterated water) was suppressed in all cases (irradiation power was between  $1.5 \times 10^{-3}$  and  $1.5 \times 10^{-4}$  Watts). All samples were run in 5 mm emperor glass NMR tubes (Wilma Glass Co., Buena, N.J.), and transferred using combusted glass NMR pipettes (Wilma Glass Co.). NMR tubes were reused and cleaned between each sample by soaking in a 2:1 solution of concentrated  $\text{HNO}_3$  and  $\text{HCl}$ , followed by rinsing with copious quantities of tap water, distilled water and Milli Q water, and oven drying at  $60^\circ\text{C}$ .

The area under each peak in the NMR spectrum (in solution state) is proportional to the number of nuclei in the sample which absorb at that frequency. Thus, it is possible to determine the relative ratios of the different proton functional groups that are present in the sample by comparing the areas under each peak. In order to obtain the relative areas spectra were photocopied and each peak was weighed out in triplicate.

### 2.2.5.3 $^{13}\text{C}$ and $^{15}\text{N}$ NMR

Both carbon and nitrogen NMR are based on the same general principles discussed in 2.2.5.1. However, greater amounts of sample and/or much longer acquisition times are necessary to obtain a  $^{13}\text{C}$  NMR spectrum, since the natural abundance of the  $^{13}\text{C}$  atom is 1.1% of all carbon atoms, and the sensitivity of the  $^{13}\text{C}$  nucleus for NMR is 1.6% that of the  $^1\text{H}$  nucleus. Due to the large amount of sample needed,  $^{13}\text{C}$  NMR and  $^{15}\text{N}$  NMR were performed on samples isolated in Woods Hole only (CRL).

For  $^{13}\text{C}$  NMR, up to 100-200 mg of samples were prepared as above and finally dissolved in  $\text{D}_2\text{O}$  (chemical shifts are reported relative to carboxylic acid (176 p.p.m)). Due to the large quantity of sample needed, all spectra were obtained in 10 mm tubes (Wilmad Glass Company, Buena, NJ). The  $^{13}\text{C}$  NMR spectrum shown in this chapter was acquired using the Bruker AC300, 300 MHz spectrometer described above, in 27 000 scans, using a pulse width of 4 ms, and a recycle delay of 2 ms, with the decoupler on (0.15 Watts) for 100  $\mu\text{s}$ .

In the case of  $^{15}\text{N}$  NMR, the sample was analyzed in solid state. The natural abundance of  $^{15}\text{N}$  is 0.37% of all nitrogen atoms, and its relative NMR sensitivity for equal numbers of nuclei is only 1/1000 times that of protons, making natural abundance  $^{15}\text{N}$  NMR often impractical because of the long acquisition times necessary to obtain useful spectra (Gust et al., 1975). However, the greater frequency separation of nitrogen resonances as compared to both hydrogen and carbon (Gust et al., 1975) makes Nitrogen NMR a very useful tool for determining the forms of nitrogen present in a sample.

Solid state spectra were acquired by Dr. Anthony Bielecki of Bruker (Billerica, MA), using 240 – 400 mg of sample (3% nitrogen). Solid state NMR is typically performed on approximately 300 mg of material. Spectra were acquired with a Bruker Avance 400 MHz NMR instrument in 250, 000 scans, using a spin rate of 5000 MHz. In this chapter chemical shifts for  $^{15}\text{N}$ NMR are reported relative to liquid ammonia.

In this study,  $^{15}\text{N}$ NMR spectra were acquired for two samples of HMW DOM. In one case, 420 mg of HMW DOM (13 mg of nitrogen) isolated from Woods Hole seawater (November, 1998) as described in section 2.2.2.1, using a combination of both polysulphone and regenerated cellulose membrane cartridge filters (both from Millipore), were submitted for  $^{15}\text{N}$ NMR analysis. In the second case 1.3 g sample, containing 39 mg of nitrogen, (ultrafiltered as above) was hydrolyzed in 1 M HCl at 105°C for 17 h and lyophilized prior to acquiring the  $^{15}\text{N}$ NMR. In the latter case, 15 mg of pyridine was added as an external standard (206 p.p.m) prior to data acquisition.

## **2.2.6 Carbohydrate Analysis**

### **2.2.6.1 Monosaccharide Analysis**

The monosaccharide composition of HMW DOM was determined according to York et al. (1985). Hydrolysis of the HMW DOM was carried out by heating a mixture of 300 - 700  $\mu\text{g}$  of dry sample in 0.5 ml of 2 M trifluoroacetic acid (TFA), containing 20  $\mu\text{g}$  of myo-inositol as an internal standard, at 121°C for 2 h in a tightly capped glass vial. Samples were cooled to room temperature and the acid was removed by drying under a stream of nitrogen. Monosaccharides were reduced to alditol acetates using 250  $\mu\text{l}$  of a solution of sodium borohydride ( $\text{NaBH}_4$ ) dissolved (10 mg/ml) in 1 M  $\text{NH}_4\text{OH}$ , and incubated at room temperature for a minimum of 2-3 h. The reaction was quenched with

glacial acetic acid (250  $\mu$ l) to decompose the excess borohydride. Glacial acetic acid and trace amounts of water were removed by adding methanol (3 $\times$ 250  $\mu$ l) and then drying under a stream of nitrogen. The dry alditols were per-acetylated with 100  $\mu$ l of acetic anhydride and 20  $\mu$ l of 1-methyl imidazole and mixed thoroughly. After 15 minutes at room temperature, the excess acetic anhydride was quenched with 0.5 ml of Milli Q water. After a further 10 minutes at room temperature, 0.5 ml of dichloromethane was added. The solution was vortex mixed, and the alditol acetates were extracted into the lower, dichloromethane layer. This layer was withdrawn and dried over Na<sub>2</sub>SO<sub>4</sub> (anhydrous), transferred and the dichloromethane was removed under a stream of nitrogen. The alditol acetates (Figure 2.3) were then re-dissolved in 100  $\mu$ l of methanol and analyzed using an HP 5890 gas chromatograph equipped with a 30 m, DB-5 fused silica column (0.25 mm ID, and 0.20  $\mu$ m film), using a temperature program of 150(1)/2/240(15), (initial temperature (time)/ramp/final temperature (time)).

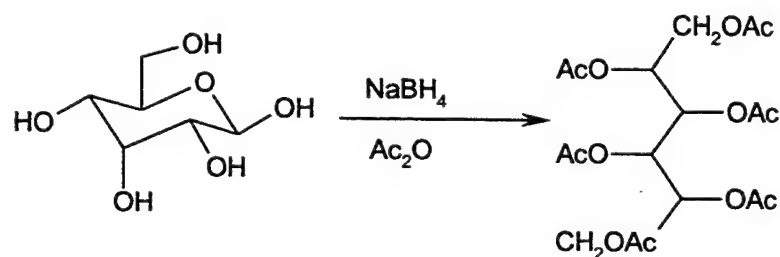


**Figure 2.3** Synthesis of alditol acetates from monosaccharides

#### 2.2.6.2 Linkage Analysis

Glycosyl linkage analysis was performed on the HMW DOM by preparing partially methylated alditol acetates according to the method of Hakomori (1964), with a few modifications (Figure 2.4). Freeze dried samples were first desalted as described in

section 2.1.3. Up to 1 mg of the desalted, dry sample was dissolved in 0.5 ml of dry dimethylsulphoxide (DMSO), under nitrogen with stirring. Methylation of the sample was initiated by adding 0.5 ml of dry 2M potassium dimethyl sulphanyl (dmsyl) anion prepared earlier by adding 4.8 g of potassium hydride (the Hakomori procedure uses NaH) to 10 ml of dry DMSO.

Following the addition of the dmsyl anion, the reaction tube was flushed with nitrogen, capped, and stirred. After 8 h the sample tube was cooled in an ice bath until frozen, and 1.0 ml of iodomethane was slowly added to complete the methylation. The tube was then vortex-mixed gently, capped, and stirred overnight at room temperature. Following this, 0.5 ml of Milli Q water was added, and the tube vortex-mixed. Finally, the reaction mixture was evaporated under a stream of nitrogen at room temperature until all the methyl iodide was removed (i.e. until the solution was clear and homogeneous). The methylated HMW DOM was purified by solid phase extraction using a C-18 reverse phase cartridge (Waters Sep-Pak). The cartridge was preconditioned with 8 ml of acetonitrile, followed by 8 ml of Milli Q water. The methylated sample was applied slowly to the top of the cartridge, washed with 8 ml of Milli Q water, and eluted with 2-3 ml of acetonitrile. (For Hawaii and CRL, <sup>1</sup>HNMR spectra of methylated polysaccharides were obtained prior to hydrolysis).

The dry, permethylated polysaccharide was hydrolyzed at 121°C for 2 hr in 0.5 ml of 2M trifluoroacetic acid containing 20 µg of myo-inositol. The reduction and acetylation of the generated monosaccharides were carried out as described above for alditol acetates, but substituting sodium borodeuteride for sodium borohydride in the reduction step. The partially methylated alditol acetates, finally dissolved in 100 µl of

methanol, were analyzed by GC-MS, using a VG-Autospec Mass Spectrometer equipped with a HP 5890 Gas Chromatograph. Samples were run on a Supelco, SP2330 30 m

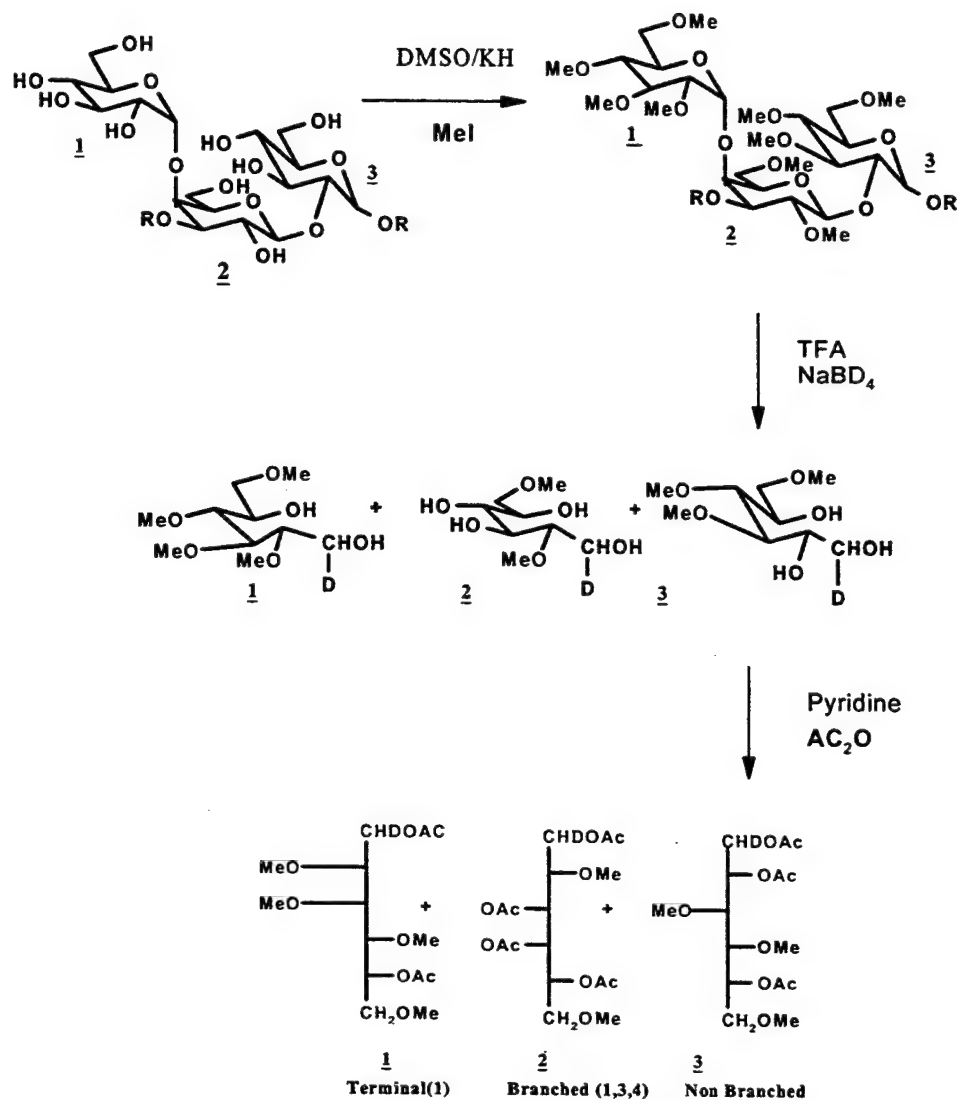


**Figure 2.4** The reaction scheme for the preparation of partially methylated alditol acetates for linkage analysis of polysaccharides.

fused silica column (0.25 mm ID, and 0.20  $\mu$ m film), using a temperature program of 80(2)/30/170/4/240(10) (temperature (hold time)/ramp rate/temperature/ramp rate/temperature (hold time)) with Helium as the carrier gas. Methylated monosaccharides were identified by comparing chromatographic and mass spectral properties with known standards.

#### 2.2.7 Lipid Analysis

High molecular weight DOM (8-10 mg C in 10–15 ml) samples were analyzed for the presence of bound fatty acids by acid hydrolysis (HCl (4 N, 4-22 h at 100°C)) and saponification (KOH (20%, 24 h at 100°C)) (Sidorczyk et al., 1983). HMW DOM samples (8-10 mg C in 10–15 ml) were also analyzed for the presence of ether bound lipids with boron tribromide (BBr<sub>3</sub>, Aldrich) (90°C for 4h) according to Benton and Dillon (1942). All reactions were performed in sealed tubes under nitrogen. All glassware was combusted and extracted with methanol and dichloromethane. Acids, bases, and samples dissolved in water were pre extracted with ethyl ether or dichloromethane to remove any free lipids. The organic extracts were analyzed by <sup>1</sup>HNMR to insure that samples and reagents were free of lipids. Following hydrolysis, the pH of the aqueous layer was adjusted to 3-4 units (using NaOH), and extracted with chloroform or diethyl ether (for the ester bound lipids) and hexane (for the ether bound lipids). The extracts were dried (by rotary evaporation, at room temperature) and re-dissolved in deuterated methylene chloride for <sup>1</sup>HNMR. Prior to gas chromatography, dry extracts were derivatized using *N,O*-bis [trimethylsilyl] trifluoroacetamide (BSTFA, Pierce, Rockford, IL) in pyridine (heat at 60°C for 15 min), for fatty acid analysis and derivatized with acetic anhydride and pyridine (room temperature, 15 min) for alcohol

analysis. Samples were then dried and re-dissolved in dichloromethane and separated on a DB-5 (J&W Scientific, Folsom, CA) column using a temperature program of 55(5)/4/320(10).

After drying the extracts, samples were re-dissolved in water and analyzed for low molecular weight fatty acids (lipids) using ion chromatography (samples were analyzed by Dr. J. Seewald, WHOI, using a Dionex Ion Chromatograph with suppressed conductivity detection).

#### **2.2.8 Amino Acid Analysis.**

Amino acids were analyzed by high pressure liquid chromatography (HPLC) using o-phthaldialdehyde derivatives, by Dr. S. Pantoja (according to Pantoja et al., 1997).

Four hydrolysis methods were compared in this study. Two mg of CRL HMW DOM (containing 60 µg of nitrogen), were hydrolyzed using: (a) 2M TFA, for 2 h at 121°C, (b) 1N HCl for 11 h at 105°C, (c) 7N HCl for 1.5 h at 150°C and (d) 4N HCl for 17 h at 100°C. Following hydrolysis, samples were neutralized with sodium hydroxide, prior to O-phthaldialdehyde derivatization. Amino acids were separated by HPLC using a Beckman Ultrasphere C<sub>18</sub> column (5 µm, 250×4.6 µm), and detected by fluorescence using a Hitachi 1000 Fluorometer (with excitation and emission wavelengths set at 330 nm and 450 nm respectively). Individual amino acids were separated and eluted in 35 minutes using a gradient of sodium acetate (25 mM, pH 5.7. with 2% tetrahydrofuran) and methanol (18-100%), with a flow rate of 1 ml/min.



## 2.3 Results

### 2.3.1 Ancillary Data

The ancillary data for each of the samples discussed in this chapter are shown in Table 2.1. As shown in this table, the samples analyzed in this study spanned a range of DOC concentrations (40–210  $\mu\text{M}$ ). Carbon to nitrogen ratios in the HMW DOM samples ranged from 11 to 21. This range is larger than that previously observed by other investigators (15–22 (Benner et al., 1992; McCarthy et al., 1996)), but the samples in Table 2.1, span more diverse environments. The average C/N value for this data set (not including UF945) was 15.

Two numbers for the recovery of HMW DOC from total DOC are given for each sample. The first number, (% HMW1), is the recovery of HMW DOC (from total DOC) after ultrafiltration, calculated using the concentration of HMW DOM in the retentate). The second number is the recovery of HMW DOC after ultrafiltration, diafiltration and lyophilization (%HMW2). Typically, ultrafiltration isolates between 20–30% of the total DOC (Benner et al., 1992; Carlson and Mayer, 1985). The average amount of HMW DOC isolated in this study was approximately 26% in accordance with earlier studies (% HMW1). However, marked losses in HMW DOC occurred following diafiltration, with >50% loss of carbon for most samples. Except in the case of MAB961, the samples which were most efficiently diafiltered (i.e. samples that contained >20% carbon) showed the highest losses of carbon. Other investigators have also noted carbon losses during diafiltration, for example, Guo and Santschi (1996) observed that 35–39% of the HMW carbon was lost during diafiltration. These investigators suggest that the

Sample	Depth	Latitude	Longitude	Date	DOC( $\mu$ M)	C/N	%C	HMW DOM (mg)	%HMW1	%HMW2
MAB941	Surface	40.33	72.03	Apr-94	89	14	11.4	51.4	22	10.7
MAB943	Surface	38.7	73.15	Apr-94	72	16.5	6.2	41.0	37	17.1
MAB944	Surface	39.3	75.5	Apr-94	209	20.4	7.3		21	
MAB945	Surface	38.93	75.06	Apr-94	132	2	12.3		37	
MAB947	Surface	37.18	74.27	Apr-94	121	21	8.5	39.5	26	16.5
MAB948	750 m	37.18	74.27	Apr-94	47	13.8	3.29	29.1	13	7.6
MAB961	Surface	36.78	75.87	Jul-96	160	12	37	222.0	18	23.1
MAB966	300 m	36.7	74.58	Jul-96	40		28	20.0		4.2
MAB967	750 m	36.7	74.58	Jul-96	40	16.1	28.7	26.9		5.6
P961	Surface	34.83	123.15	Oct-96	72	12.4	26.3	38.4	33	9.1
P962	1600 m	34.83	123.15	Oct-96	40	12.8	17.3	28.9	22	5.6
ENA	Surface	51.6	40.11	Apr/Jun-96	200	12		N/D	27	
Hawaii	600 m	19.67	156	Jan-95	80	11	10.3	N/D		

Table 2.1 Ancillary data for each of the samples analyzed as part of this thesis.

The prefixes for each of the samples are as follows: MAB is the Mid-Atlantic Bight; P is the North East Pacific Ocean; ENA is the Eastern North Atlantic (a sample from the Sint Annaland salt marsh in the Oosterschelde estuary (Dr. V. Klap), and Hawaii was filtered at the Natural Energy Laboratory in Hawaii. %HMW1 was calculated from the concentration of the retentate following ultrafiltration. %HMW2 was calculated using the HMW DOM (mg) yield after ultrafiltration, diafiltration with 20 l of Milli Q water, and lyophilization. %C and C/N are reported for HMW DOM (after ultrafiltration and diafiltration)

loss of material during diafiltration may be caused by the incomplete ultrafiltration of LMW DOM.

Riverine and coastal samples were highly colored (clear, bright yellow), while deep samples showed more color than open ocean surface samples (suggesting photo bleaching of surface HMW DOM). Lyophilized samples were powdery and colors ranged between white and yellow.

### **2.3.2 Nuclear Magnetic Resonance Data**

#### **2.3.2.1 Proton NMR**

The major resonances present in HMW DOM spectra were from carbohydrates (4 – 5.5 p.p.m. (anomeric), 3 – 4.0 p.p.m (CHOH), and 1.3 p.p.m (CH<sub>3</sub>)). Resonances for acetate (2.0 p.p.m (CH<sub>3</sub>COO/N)) and low-molecular weight, non-acetate lipids were also present (0.9 p.p.m (CH<sub>3</sub>) and 1.3 p.p.m (CH<sub>2</sub>)) (Figure 2.5). The peak centered at 4.8 p.p.m in all the <sup>1</sup>HNMR spectra arises from partially deuterated water (HDO). Proton NMR spectroscopy of HMW DOM showed similar spectra for all surface ocean samples (Figure 2.6 and Figure 2.7A).

Given the monosaccharide data that are discussed in section 2.3.3, the lipid data discussed in section 2.3.4, and the area under each of the major peaks identified above, the relative proportion of major biochemicals in surface water HMW DOM can be calculated. The monosaccharide data are used determine the contribution of deoxy sugars (rhamnose and fucose) to the area of the lipid peak at 1.3 p.p.m. The monosaccharide data presented in section 2.3.3 show that deoxy sugars are 30% of the total neutral monosaccharides in each of the samples. Thus 30% of the peak area between 3 – 4 p.p.m comes from the deoxy sugars. Since 3 out of the 8 non-alcohol

protons in deoxy sugars give rise to lipid resonances, the contribution of deoxy sugars to the total lipid peak (at 1.3 p.p.m) can be further calculated.

Since the carbon to hydrogen ratios of these biochemicals are known (C/H ratios are 1 carbohydrates, 0.67 for acetate and 0.5 for lipids), the measured areas in the  $^1\text{H}$ NMR spectra may be expressed in terms of carbon. Table 2.2 shows results from the integration for 20 surface seawater samples (including all the samples listed in Table 2.1).

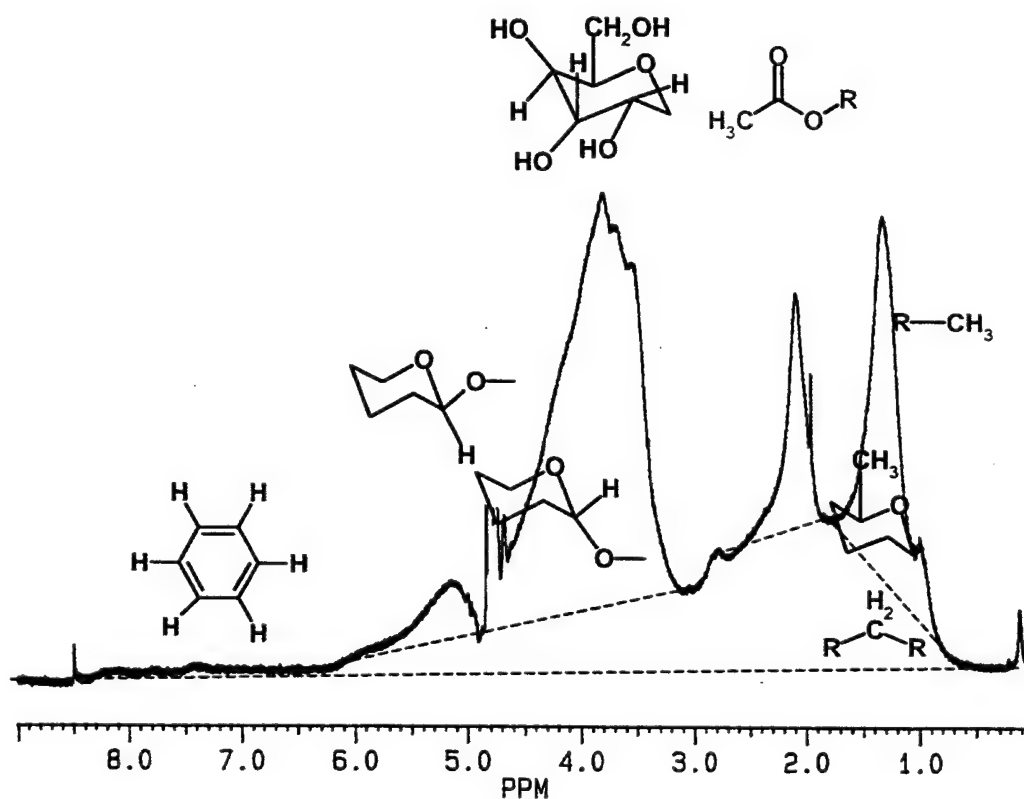


**Figure 2.5** The major  $^1\text{H}$ NMR resonances identified in HMW DOM. The baseline for each of the major peaks and the whole spectrum are shown on the figure as dashed lines.

As can be seen from Figure 2.6, the resonances from the major biochemicals identified above were superimposed on a featureless background of overlapping resonances. The amount of HMW carbon contained within the background was calculated using the C/H ratios listed above, and measuring the baseline area under each of the three major peaks. According to the data in Table 2.2, identifiable biochemicals, carbohydrates, acetate and lipid, accounted for 70% of the total carbon in the sample. Thus the data shown in Table 2.2 can be recast to determine the contribution of each of the three major biochemicals to the total identifiable carbon. This ratio is  $80 \pm 4 : 10 \pm 2 : 9 \pm 4$  for carbohydrate:acetate:lipid carbon and stays remarkably constant in the surface water HMW DOM samples analyzed thus far (see Figure 2.6 and 2.7 A).

	Carbohydrate C	Acetate C	Lipid C	Baseline C
Surface Water(n=20)	56 $\pm$ 4	7 $\pm$ 2	6 $\pm$ 4	30 $\pm$ 3
Deep Water(n=8)	25 $\pm$ 4	2 $\pm$ 0.5	7 $\pm$ 3	64 $\pm$ 7
Deep Water*(n=2)	32	2	4	62

\* Refers to ratios after the sample was desalted using a cation exchange resin.

**Table 2.2** Relative abundance (in carbon) of the major biochemicals identified in HMW DOM by  $^1\text{H}$ NMR.

Shown in Figure 2.7 B is a typical  $^1\text{H}$ NMR spectrum of HMW DOM isolated from the deep ocean (P962). Comparing the spectra shown in Figure 2.7 A and 2.7 B it is apparent that all the major resonances identified in surface seawater (spectrum A) are still present, including acetate. However, the relative proportions of these biochemicals are quite different from surface water, as shown by the data in Table 2.2. The major differences between the two spectra are a substantial decrease in the acetate and

carbohydrate peaks relative to the lipid peak and a relative increase in the area under the base line.

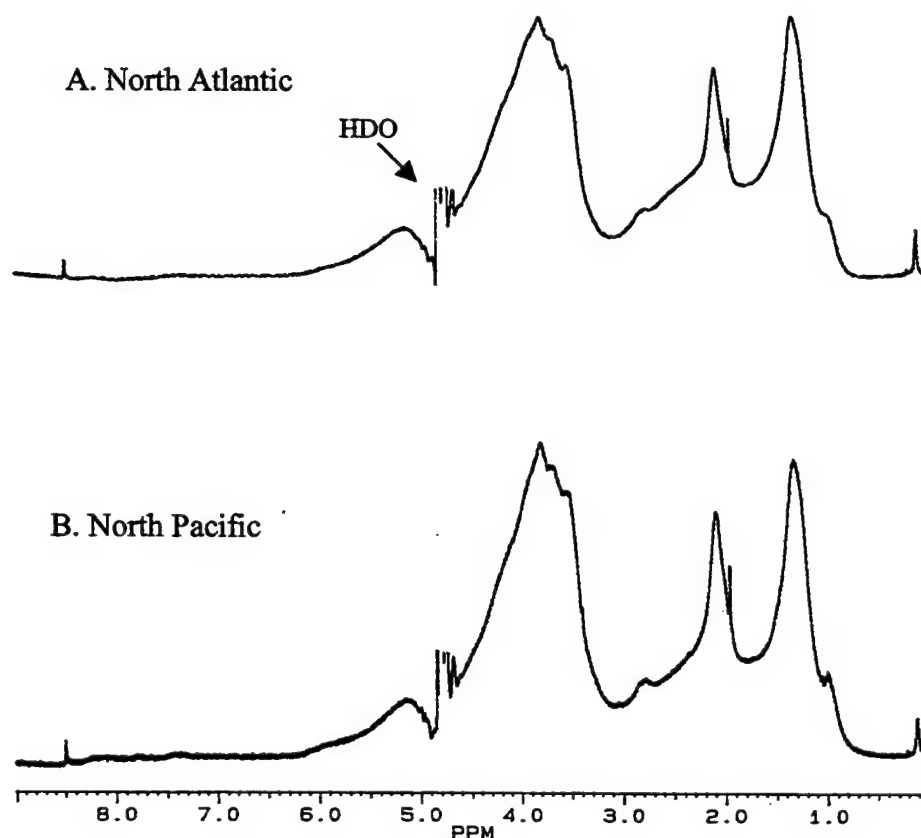


**Figure 2.6** Two  $^1\text{H}$ NMR spectra for surface HMW DOM isolated from the North Atlantic (MAB943) (A) and North Pacific (B) (P961). Note the similarities in the resonances present and the relative proportion of each resonance.

The carbohydrate: lipid ratio decreased from 9 in surface waters to 4 in deep water while the ratio of carbohydrate:acetate increased from 8 to 12.5. As shown in Table 2.2, the relative contribution of uncharacterized carbon, calculated using the background area in  $^1\text{H}$ NMR spectra from the deep ocean, doubled compared to surface values (64% (deep) vs. 30% (surface)). This data indicates that the component containing carbohydrate and acetate decreases with depth, or that the background component increases with depth.

This depth related decrease in the relative fraction of carbohydrates is consistent with the  $^{13}\text{C}$ NMR data of Benner et al. (1992).

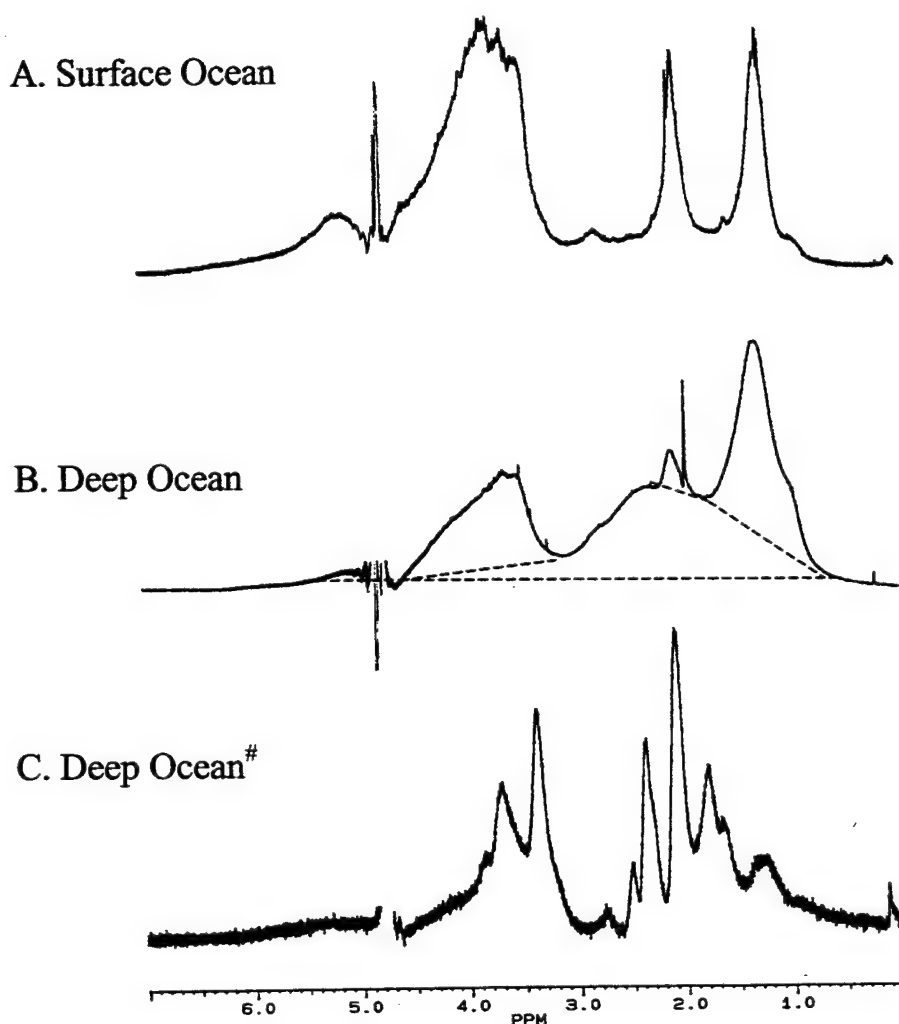


**Figure 2.7** The figure shows  $^1\text{H}$ NMR spectra for a typical surface ocean sample (A) (CRL), a typical deep ocean sample (B) (P962) and a spectrum seen for two of the eight deep samples analyzed (C) (MAB944). Dashed lines in Spectrum B show the baseline for each of the identified peaks.

Much of the relative increase in background resonances (seen in Figure 2.7C) resides between 1.0 and 2.5 p.p.m, indicating a relative increase in methyl and methylene protons. Thus, HMW DOM isolated from the deep ocean appears to contain a larger

relative amount of reduced compounds. For both surface and deep HMW DOM samples the baseline contains a "smear" of resonances (i.e. a variety of resonances that are not well resolved). As discussed in section 2.2.5.1, as the excited proton nuclei relax back to the ground state they dissipate energy at a rate that is dependent on the immediate chemical environment of each nucleus. The "smear" of resonances in the baseline indicate that the sample contains several protons with a slightly different chemical environment. Molecules that are coiled or molecules whose functional groups are closely associated may give rise to a variety of poorly resolved resonances. A mixture of closely related molecules or large molecules that rotate very slowly in solution may also give rise to poorly resolved resonances.

Neither surface nor deep ocean spectra show significant contribution from aromatic protons (< 1% of the carbon in the samples).

The third spectrum shown in Figure 2.7 C is one that has been observed for two of the eight deep samples examined by <sup>1</sup>HNMR spectroscopy (a sample from a depth of 750 m in the MAB (35.5°N, 74.7°W), and a sample from 1000 m in the Sargasso Sea (36.5°N, 65.5°W)). Although carbohydrate, acetate and lipid resonances are present in this spectrum, additional resonances (compared to Figure 2.7 A and B) are apparent in the region 1.9 – 2.8 p.p.m. When Figure 2.7 C is compared to the spectrum shown in Figure 2.9, which shows a mixture of two standards, maltoheptose and Gramicidin S (protein), some of the same resonances are apparent. For example, the resonances in the region 1 – 3.0 p.p.m in the standard mixture arise entirely from Gramicidin S. Spectra similar to Figure 2.7C have also been identified in culture work (see Chapter 3).



Figure 2.8 shows the spectrum of a deep ocean sample (MAB948) before desalting (A), after desalting (B) and following hydrolysis with 4M HCl (as in section 2.2.7). The spectrum of the desalted sample resembles the surface seawater samples

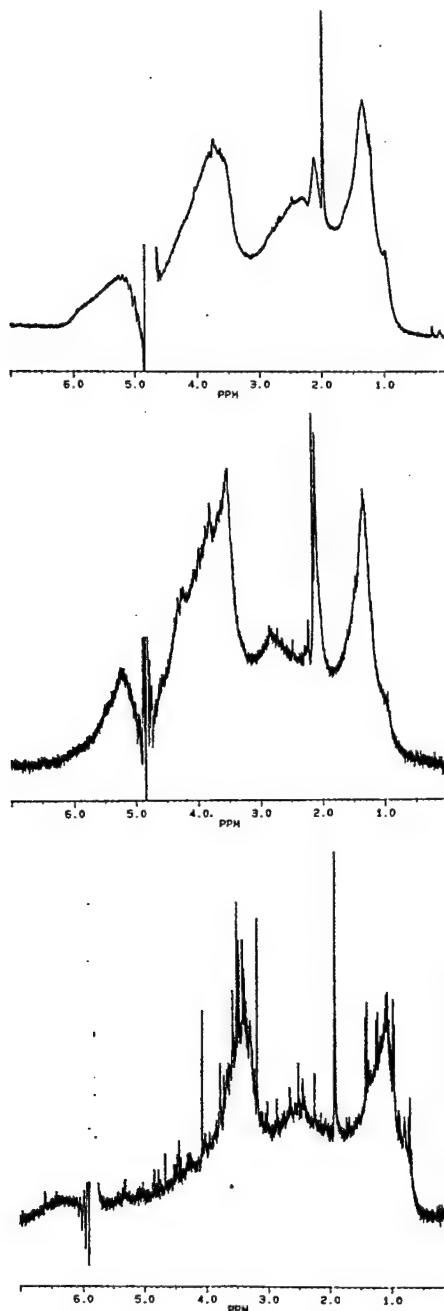
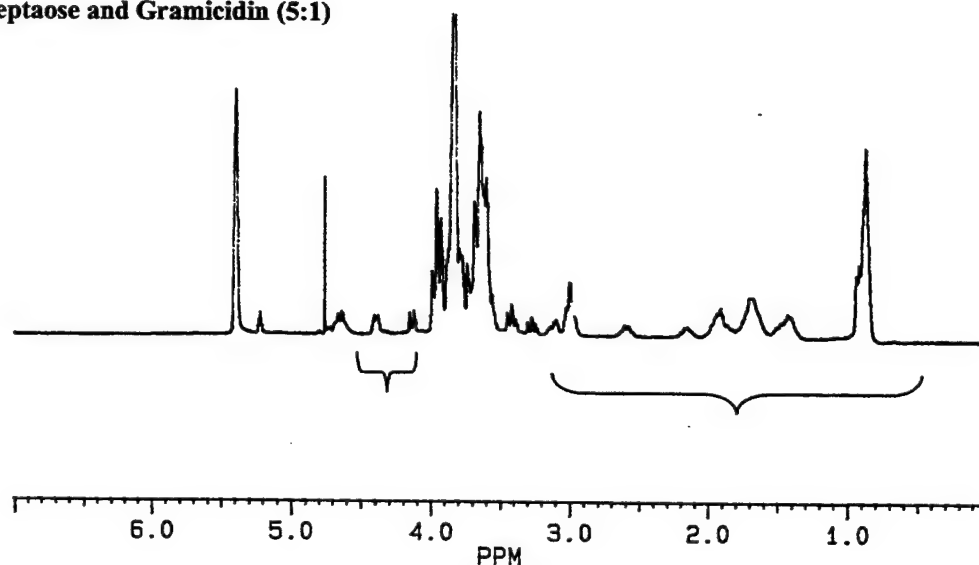


Figure 2.8  $^1\text{H}$ NMR spectra of MAB948, a HMW DOM sample from a depth of 750 m before desalting (A), after desalting with a cation exchange resin (B) and after hydrolysis (C)

more closely than Figure 2.8A, and clearly shows that both the surface and deep samples contain the same resonances, but that deep samples have a much more pronounced baseline. In spectrum 2.8 B, the acetate peak is more easily identified and the carbohydrate peak is relatively more pronounced, however, no overall loss (< 4%) of carbon is incurred between 2.8A and 2.8B. The spectrum shown in Figure 2.8 C illustrates that hydrolysis of both the acetate and carbohydrate fractions yield similar results to those observed for HMW DOM isolated from the surface ocean.

**Maltoheptaose and Gramicidin (5:1)**



**Figure 2.9 Proton NMR spectrum of a 5:1 mixture of maltoheptaose and Gramicidin S, in D<sub>2</sub>O. Resonances enclosed in brackets arise from proteins.**

### 2.3.2.2 Carbon NMR

The individual carbon resonances in HMW DOM can also be observed directly using  $^{13}\text{C}$  NMR. A  $^{13}\text{C}$  NMR spectrum of surface seawater HMW DOM (CRL) is shown in Figure 2.12. The major resonances arise from carbohydrates (20 – 50 p.p.m ( $\text{CH}_3$ ), 60 – 85 p.p.m ( $\text{CHOH}$ ), 85 – 115 p.p.m (anomeric)), acetate (20-50 p.p.m ( $\text{CH}_3$ ), 160-180 p.p.m ( $\text{COO}$ )) and lipids (20 – 50 p.p.m ( $\text{CH}_3$ ,  $\text{CH}_2$ )). As expected, the anomeric carbons from carbohydrates fall in the region centered at 100 p.p.m, and the secondary carbohydrate peak at 65 p.p.m likely arises from  $\text{C}^6$  of non-deoxy hexoses. Aromatic and unsaturated carbons give rise to resonances between 120-140 p.p.m. In our  $^{13}\text{C}$  NMR spectra there are no clear resonances in this region.

The relative proportions of the major biochemicals calculated from Figure 2.10 are 64:11:25 (carbohydrate:carboxylic:lipid). If the area under the lipid and carbohydrate peaks are adjusted according to the contribution from deoxy sugars (deoxy sugars are 30% of the carbon in the sample, and the  $\text{C}^6$  resonance (in the lipid region) is 1/6 of this), the relative ratios change to 67:11:22 (carbohydrate:carboxylic:lipid). The ratio of carbohydrate to acetate carbon determined from both  $^1\text{H}$  NMR and the lipid analysis is  $8 \pm 2$ . Using this ratio, the amount of acetate carbon resonances in the sample can be calculated (8). Half of this acetate carbon is buried in the lipid resonances, and thus the carbon distribution in HMW DOM, determined by  $^{13}\text{C}$  NMR spectroscopy, can be further expressed as 65:8:18 (carbohydrate:acetate:lipid). The ratio of identifiable carbon:baseline carbon in this spectrum is 60:40. Benner et al., (1992) found similar carbohydrate:carboxylic:lipid carbon ratios using  $^{13}\text{C}$  NMR spectroscopy for HMW DOM isolated from the surface Pacific Ocean (54:13:26).

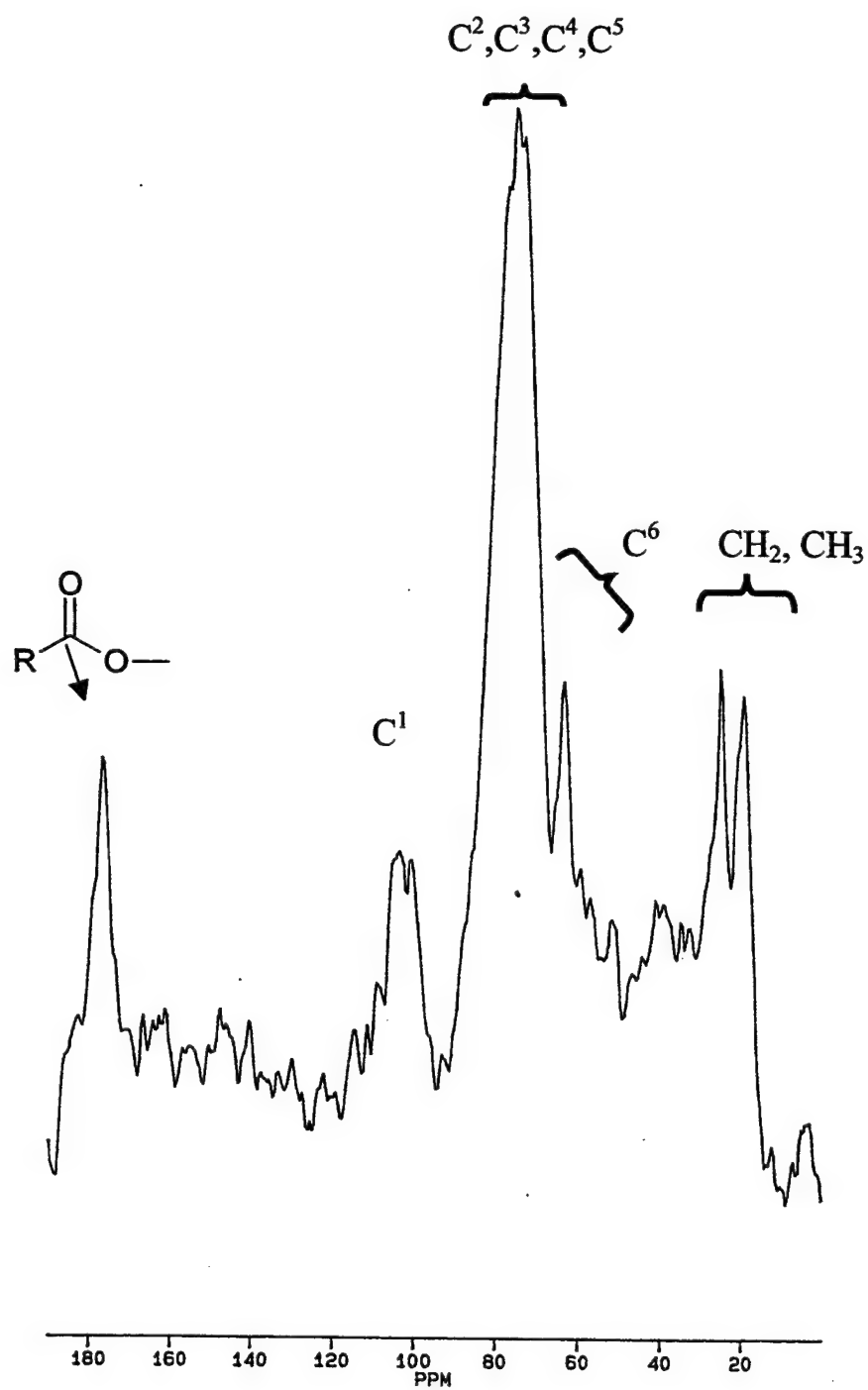


Figure 2.10  $^{13}\text{C}$ NMR spectrum of HMW DOM in  $\text{D}_2\text{O}$

Both the  $^1\text{H}$ NMR and the  $^{13}\text{C}$ NMR data (presented in this thesis and present in the literature) are in good agreement and show that the major biochemicals identified by NMR are present in a relatively fixed ratio throughout the ocean. It is the initial data obtained by NMR that led the way for the other analyses presented in this chapter, and highlights the utility of NMR spectroscopy in characterizing even very complex mixtures of biochemicals.

#### 2.3.2.3 Nitrogen NMR

In order to determine the major types of nitrogen present, HMW DOM was also analyzed by  $^{15}\text{N}$  NMR spectroscopy. Shown in Figure 2.11 A is the solid state  $^{15}\text{N}$ NMR spectrum of CRL HMW DOM. The spectrum was dominated by one peak at 122 p.p.m (92% of the total area) belonging to amide nitrogen ( $\text{CNCO}$ ). Two other peaks were also present in this spectrum: a spinning sideband at -23 p.p.m from the peak at 122 p.p.m, and a peak at 40 p.p.m from free amines ( $\text{CNH}_2$ , or  $\text{C}_2\text{NH}$ , 8% of the total area).

The amide resonance likely arises from the peptide bond of proteins or from N-acetylated sugars (such as N-acetylated glucosamine or galactosamine). The amine arises from free amines in proteins (terminal amino acids, and amino acids such as arginine and lysine which have two or more nitrogen atoms) and/or amino sugars (glucosamine, and galactosamine). In order to differentiate between the amide resonances from N-acetylated sugars and other amide resonances (such as peptide bonds), the DOM sample was hydrolyzed with 1M HCl for 17 hours at 105°C. Proton NMR confirmed the hydrolysis of the acetate group (Figure 2.12 A and B), indicating that any N-acetylated sugars were converted to amino sugars.

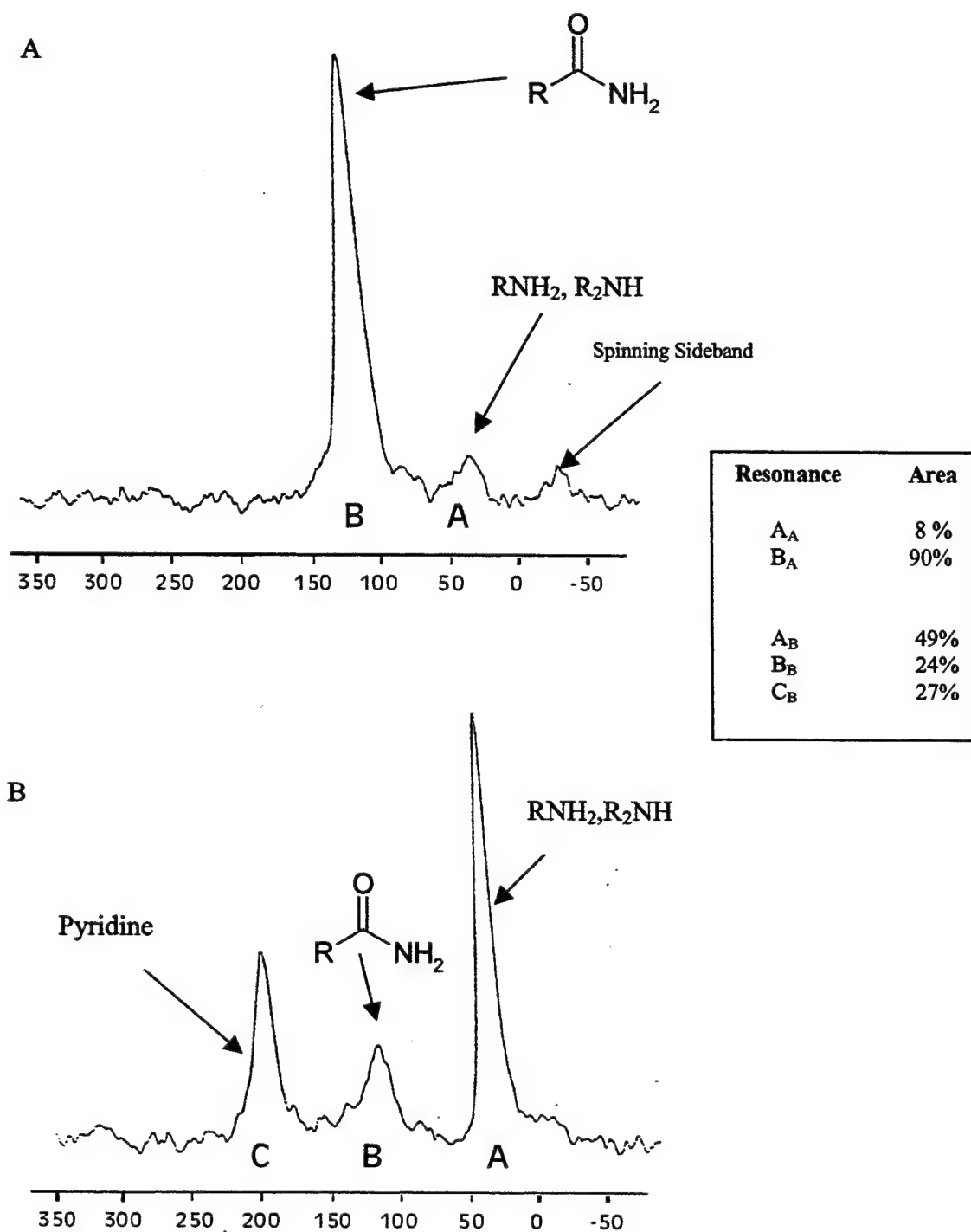
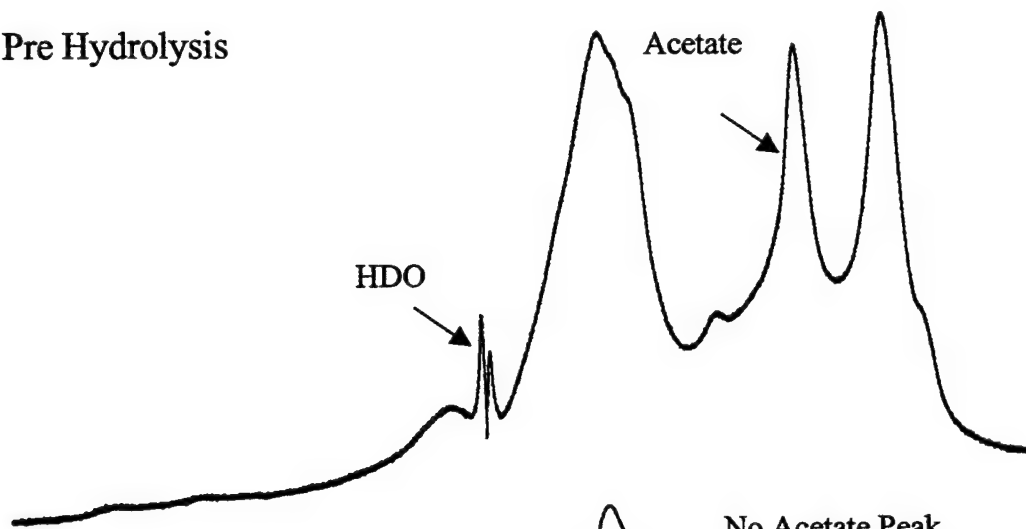


**Figure 2.11** Solid state  $^{15}\text{N}$  NMR spectra of HMW DOM, before (A) and after (B) 1 M HCl hydrolysis for 11 h at  $105^\circ\text{C}$ . Resonances are reported relative to  $\text{NH}_3$ . Pyridine was added as an external standard to quantify the total nitrogen detected by  $^{15}\text{N}$  NMR.

A. Pre Hydrolysis



B. Post Hydrolysis and Freeze Drying

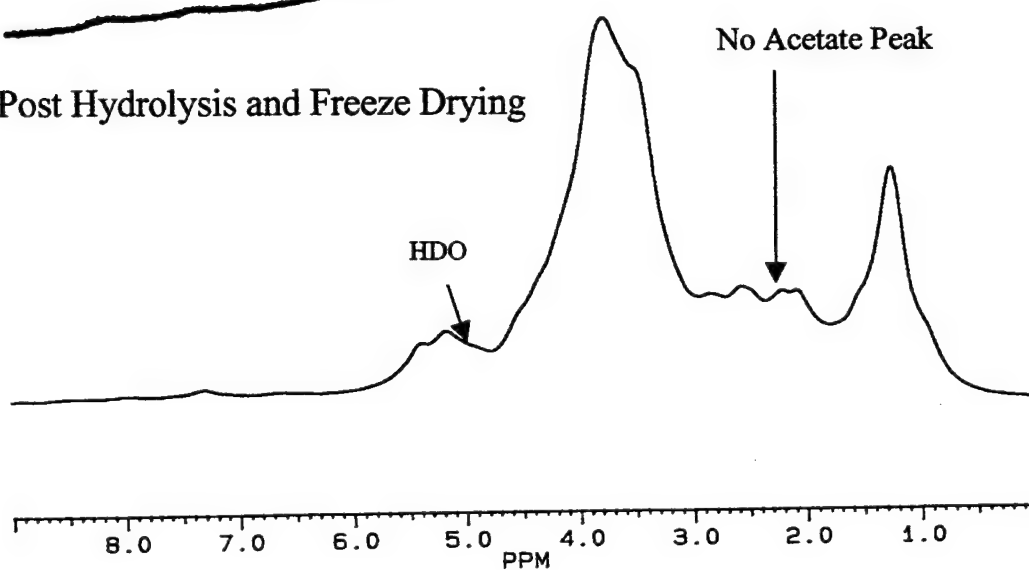


Figure 2.12  $^1\text{H}$  NMR spectra of HMW DOM, before (A) 1 N HCl hydrolysis for 11 h at 105°C and after hydrolysis and freeze drying to remove acetic acid (B).

The hydrolyzed sample should contain no amide resonances if all the amide signals in the  $^{15}\text{N}$  NMR spectrum arise from N-acetylated sugars. A  $^{15}\text{N}$  NMR spectrum of the sample after hydrolysis is shown in Figure 2.12 B. The resonance at 204 p.p.m arises from 0.95 mmoles of pyridine added as an internal standard to calculate the recovery of nitrogen (103%). In contrast to the unhydrolyzed sample, the major resonance in the hydrolyzed sample is at 40 p.p.m, previously identified as the amine region. This peak accounts for 67% of the total nitrogen in the sample (not including pyridine). Some amide resonances remain after hydrolysis (120 p.p.m) and they represent the remaining 33% of the total nitrogen resonances in the sample (not including pyridine). The  $^1\text{H}$ NMR (Figure 2.12) confirms that all the acetate is hydrolyzed, insuring that the remaining amide signal does not arise from N-acetylated sugars. Thus the remaining amide nitrogen likely arises from unhydrolyzed proteins in the sample. However, we cannot rule out the possibility that the remaining amide in sample may arise from a yet unidentified type of amide nitrogen.

In order to determine the origin of the amine nitrogen, the hydrolyzed sample was analyzed for the presence of amino acids (by Dr. Silvio Pantoja, WHOI) and N-acetylated sugars. Amino acid analysis was able to account for 15-18% of the nitrogen in the hydrolyzed sample. This yield of amino acids is in accordance with literature values (11-28% (McCarthy et al., 1996)). OPA derivatization (Section 2.2.8) of the sample also showed the presence of glucosamine which accounted for 5% of the total nitrogen. Further hydrolysis of the CRL sample (Section 2.2.8) by various methods (including 4M HCl, for 19 hours at 100°C) did not increase the yield of either amino acids or amino



sugars. Thus the remaining 73 – 80% of the amine signal in the NMR spectrum was not directly accounted for as amino acids or amino sugars.

### 2.3.3 Lipid Results

Hydrolysis of HMW DOM caused a change in the  $^1\text{H}$ NMR of each sample (Figure 2.8C, Figure 2.13 B), especially in the region of 2.0 p.p.m. Following the hydrolysis, fatty acids were extracted from the aqueous phase (section 2.2.7) and derivatized for GC analysis. No fatty acids were detected by GC. Ether cleavage with  $\text{BBr}_3$  yielded no lipids either; however this analysis was only performed on one sample and may give different results for other samples. Proton NMR of the organic layer after extraction (Figure 2.13 D) showed one resonance at 2.0 p.p.m (not including peaks from the solvent (diethyl ether)). The extracted aqueous layer (Figure 2.13 C) showed the removal of the peak at 2.0 p.p.m. The lack of other peaks at 0.9 and 1.3 p.p.m ( $\text{CH}_3$  and  $\text{CH}_2$  from lipids) in the  $^1\text{H}$ NMR spectrum of the organic extract, coupled with the chemical shift of the single peak, indicated the presence of acetic acid, which must be present within HMW DOM as acetate. The absence of  $\text{CH}_3$  and  $\text{CH}_2$  resonances in the organic layer confirms the absence of fatty acids detected by GC, since the temperature program was designed to detect fatty acids of chain lengths greater than sixteen carbons. The presence of acetic acid in the organic layer was further confirmed by ion chromatography. The amount of acetic acid determined by ion chromatography ( $9 \pm 2.7$   $\mu\text{moles}$ ) was not statistically distinguishable from the amount of acetic acid expected from the  $^1\text{H}$ NMR spectrum (10.8  $\mu\text{moles}$ ).

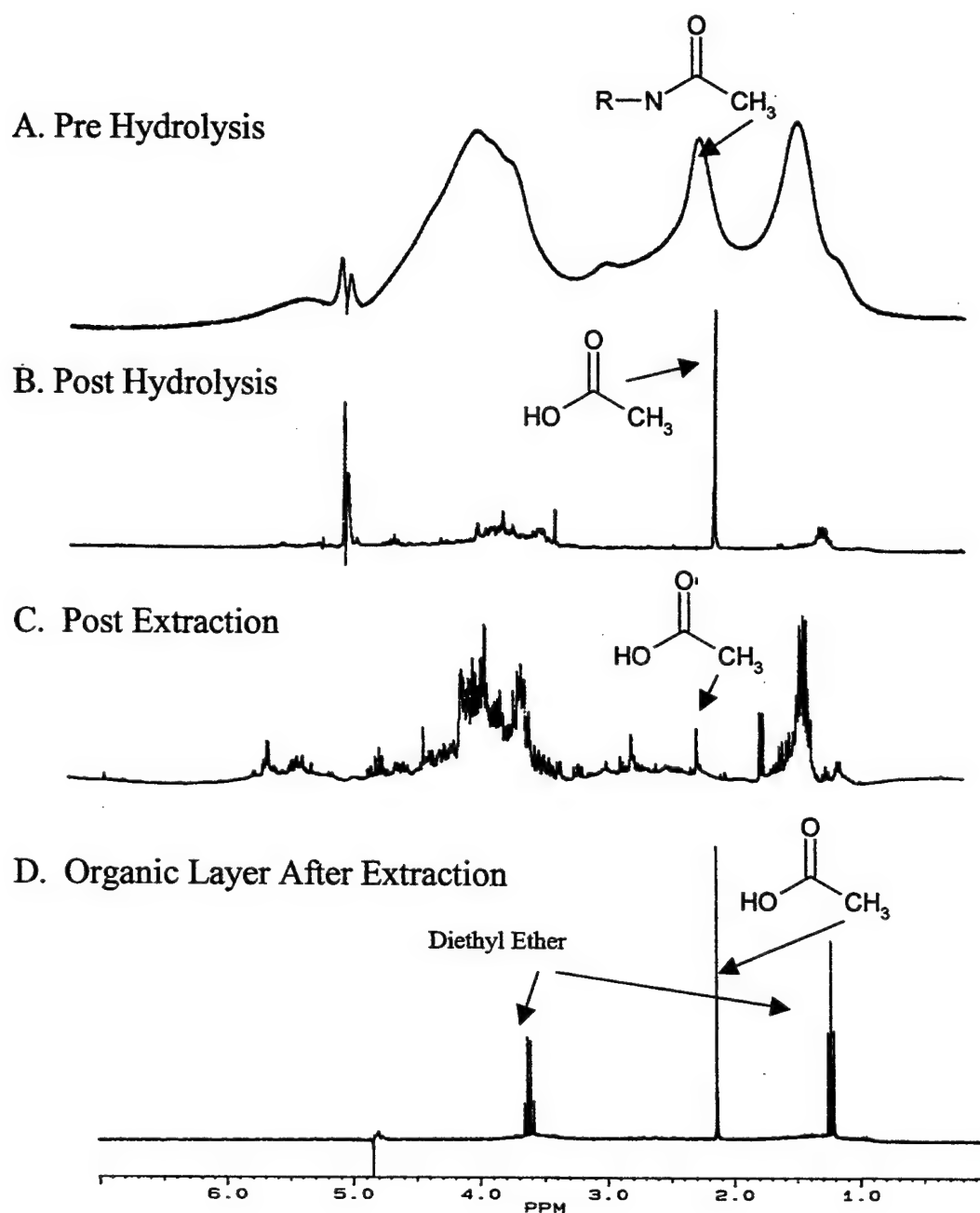


Figure 2.13  $^1\text{H}$  NMR of HMW DOM prior to 4 N HCl hydrolysis (A), following hydrolysis (B), the aqueous layer (pH = 3) after extraction with ethyl ether (C) and the ethyl ether layer (D).

#### 2.3.4 Monosaccharide Analyses

The HMW DOM samples were hydrolyzed and analyzed for monosaccharides as discussed in Section 2.2.6.1 (Figure 2.14) and the relative mole percent of monosaccharides in each of the samples is shown in Table 2.3. All samples showed the presence of the same neutral monosaccharides. Galactose was observed to be the most abundant monosaccharide, with glucose, mannose, xylose, rhamnose and fucose being only slightly less abundant, and arabinose usually being the least abundant neutral monosaccharide. Analysis of some of the samples (MAB941, MAB943, MAB944, MAB945, and MAB947) for uronic acids and amino sugars showed that these sugars comprised <12 % of the total monosaccharides. In the case of surface samples (MAB961, MAB965, CRL, P961, ENL and Hawaii), the neutral monosaccharides comprised between 15-20 % of the total carbon in the sample. Deep ocean samples (MAB964, MAB967 and P962) contained smaller amounts of neutral monosaccharides (between 4-9% of the total HMW DOM carbon). This depth associated decrease in the total monosaccharides coincides with the  $^1\text{H}$ NMR data which shows decreasing carbohydrate resonances with depth. The monosaccharides yields observed in this study are comparable with existing data (6-15% in surface waters vs. 1.6-3.5% in deep water (Borch and Kirchman, 1997; McCarthy et al., 1996; Skoog and Benner, 1997)).

The data in Table 2.3 are plotted in Figure 2.15 to better illustrate the mole percent monosaccharide distribution. Despite the differences in the total amount of monosaccharide between surface and deep waters, the relative distribution of

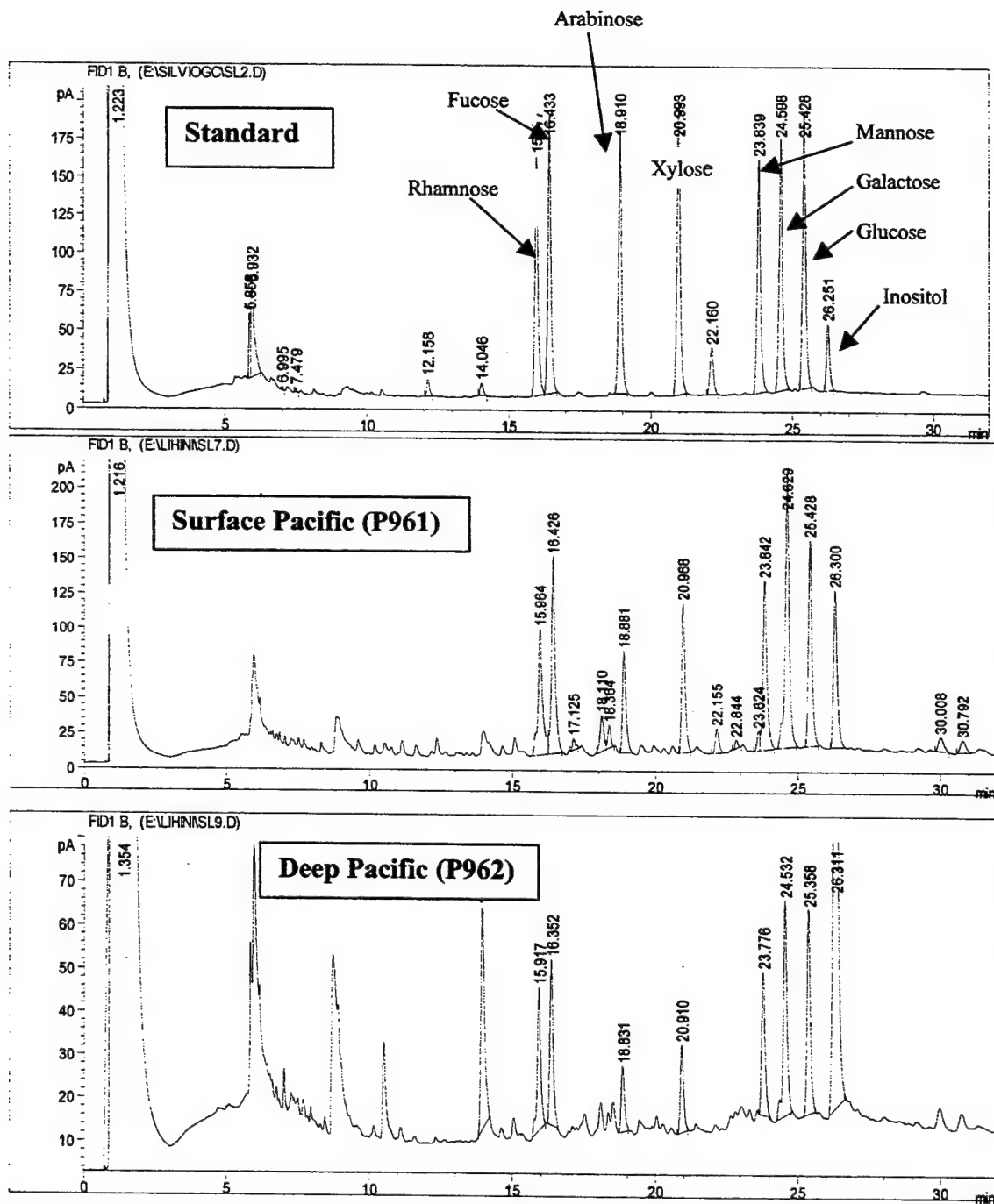


Figure 2.14 Raw gas chromatograms of alditol acetates.

Sugars	MAB941	MAB943	MAB944	MAB945	MAB946	MAB947	MAB961	MAB961
Rhamnose	0.16	0.16	0.18	0.17	0.18	0.17	0.20	0.19
Fucose	0.15	0.17	0.16	0.14	0.13	0.16	0.17	0.17
Arabinose	0.05	0.05	0.08	0.09		0.08	0.07	0.08
Xylose	0.13	0.15	0.15	0.11	0.16	0.15	0.11	0.11
Mannose	0.14	0.12	0.12	0.18	0.14	0.13	0.13	0.13
Galactose	0.19	0.21	0.15	0.22	0.15	0.18	0.21	0.22
Glucose	0.19	0.14	0.16	0.09	0.25	0.13	0.10	0.10

Sugars	MAB964	MAB965	MAB967	CRL96	ENA	Hawaii	P961	P962
Rhamnose	0.17	0.14	0.18	0.12	0.14	0.10	0.13	0.17
Fucose	0.20	0.16	0.16	0.16	0.17	0.15	0.17	0.18
Arabinose	0.09	0.09	0.09	0.05	0.08	0.09	0.09	0.07
Xylose	0.13	0.11	0.10	0.15	0.15	0.13	0.11	0.08
Mannose	0.12	0.15	0.17	0.15	0.15	0.17	0.14	0.15
Galactose	0.18	0.23	0.16	0.22	0.18	0.21	0.23	0.20
Glucose	0.12	0.12	0.14	0.15	0.13	0.16	0.13	0.15

Table 2. 3 The relative distribution of neutral monosaccharides (as analyzed by alditol acetates) in HMW DOM.

All samples (except MAB964 and MAB965) are listed in table 2.1. MAB965 is the surface counterpart of MAB966 and MAB967. MAB964 was taken from a depth of 750 M at 35.5°N and 74.7°W. MAB941, MAB943, MAB944, MAB945 and MAB947 were also analyzed for uronic acid and amino sugars. In all cases, these sugars were 10% of the total sugars in each sample, except in the case of mab945 where they accounted for 12% of the sample. Glucose distributions varied  $\pm 25\%$  of their mean distribution, arabinose distributions varied  $\pm 20\%$ , and all other sugars varied between  $\pm 13-15\%$ . Replicate monosaccharide analyses varied  $\pm 5\%$ .

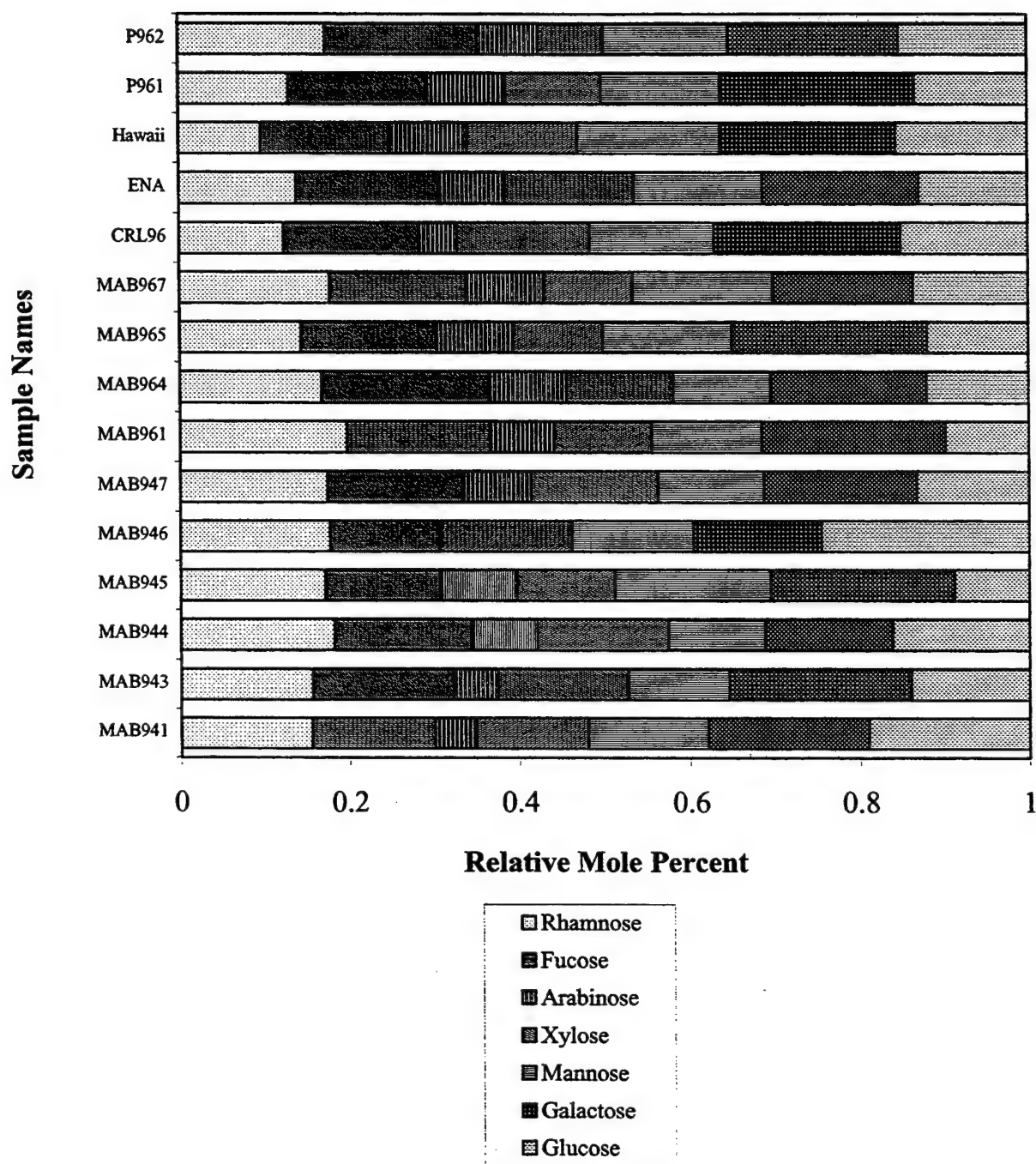


**Figure 2.15** The mole percent distribution of the seven neutral monosaccharides identified in HMW DOM.

monosaccharides is remarkably similar for all samples and compares well to distributions observed by other investigators (McCarthy et al., 1996; Sakugawa and Handa, 1985b).

In order to determine how closely the monosaccharide distributions in each sample were related a correlation coefficient analysis was performed on the samples shown in Figure 2.16. The results of the analysis are given in Table 2.4, and as an example, the results for the extent of correlation of all the samples with MAB941 are shown plotted in Figure 2.16. Most samples correlate well with MAB941, showing the close relationship between the monosaccharide distributions in HMW DOM isolated from diverse locations. The sugar distribution of P962 and MAB967 are closely correlated ( $>0.9$ ). These are both deep ocean samples, but their sugar distributions are poorly correlated with MAB964, which is also a deep ocean station. However, MAB964 had high monosaccharide yields (9% of HMW DOM) and its  $^1\text{HNMR}$  was unique (Figure 2.7C). In fact MAB964 is not well correlated with any of the samples (except MAB944). The sugar distribution in the Hawaii sample is closely correlated (0.85) with P961, which is also a Pacific Ocean surface sample. The correlation coefficient data for the MAB samples shown in Table 2.4 correspond well to the direction of water flow established for this region (Figure 2.17) (Beardsley et al. 1976). The correlation coefficient data for this region demonstrates that although the monosaccharide distributions among samples are closely correlated, there are subtle differences that differentiate samples in this region driven by the advection of DOM by different water masses. This is consistent with the DOM concentrations which increase southward along the shelf of the MAB indicating that at each location the DOM consists of DOM advected along the shelf, DOM produced at that location and/or DOM brought in by rivers (e.g. MAB 95, MAB961 and MAB967).

If the correlation coefficient analysis is repeated without glucose the degree of correlation increases between most samples. The greater variability in glucose compared to other monosaccharides is not surprising given the importance of glucose in energy storage polysaccharides. Thus while the other neutral monosaccharides likely occur together in a single polysaccharide, a larger fraction of glucose is present in other polysaccharides as well.

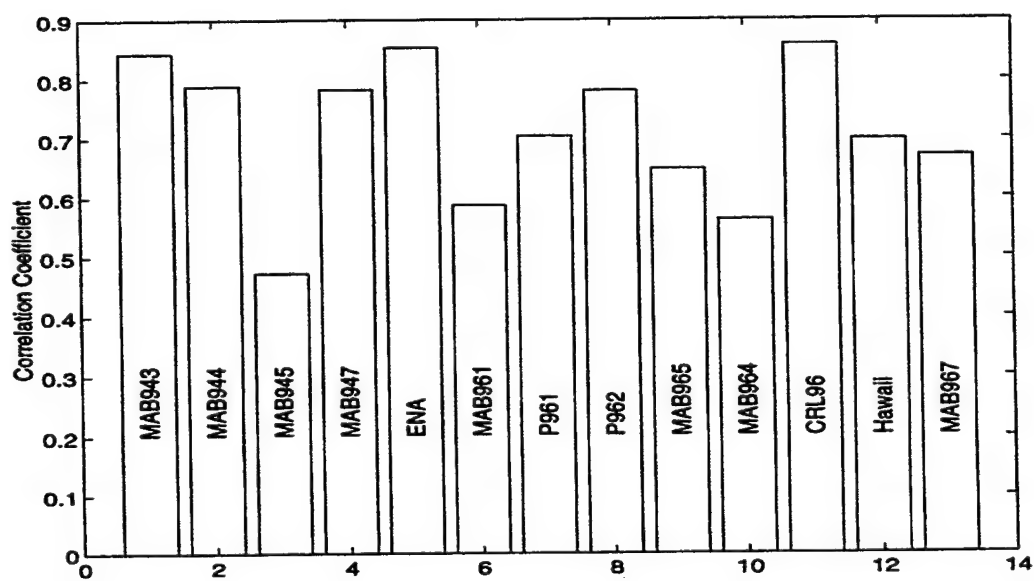
	MAB941	MAB943	MA944	MAB945	MAB947	MAB961	MAB964
MAB941	1	0.84	0.79	0.47	0.78	0.59	0.56
MAB943	0.84	1	0.77	0.64	0.95	0.83	0.44
MAB944	0.79	0.77	1	0.26	0.87	0.62	0.8
MAB945	0.47	0.64	0.26	1	0.66	0.84	-0.09
MAB947	0.78	0.95	0.87	0.66	1	0.9	0.52
ENA	0.85	0.96	0.62	0.65	0.84	0.72	0.31
MAB961	0.59	0.83	0.62	0.84	0.9	1	0.33
P961	0.7	0.85	0.41	0.75	0.72	0.79	0.23
P962	0.78	0.76	0.63	0.69	0.76	0.83	0.57
MAB965	0.65	0.82	0.37	0.87	0.73	0.86	0.14
MAB964	0.56	0.44	0.8	-0.09	0.62	0.33	1
CRL	0.85	0.94	0.62	0.62	0.82	0.66	0.32
HAWAII	0.7	0.68	0.22	0.57	0.46	0.42	0.08
MAB967	0.67	0.63	0.6	0.76	0.73	0.81	0.51

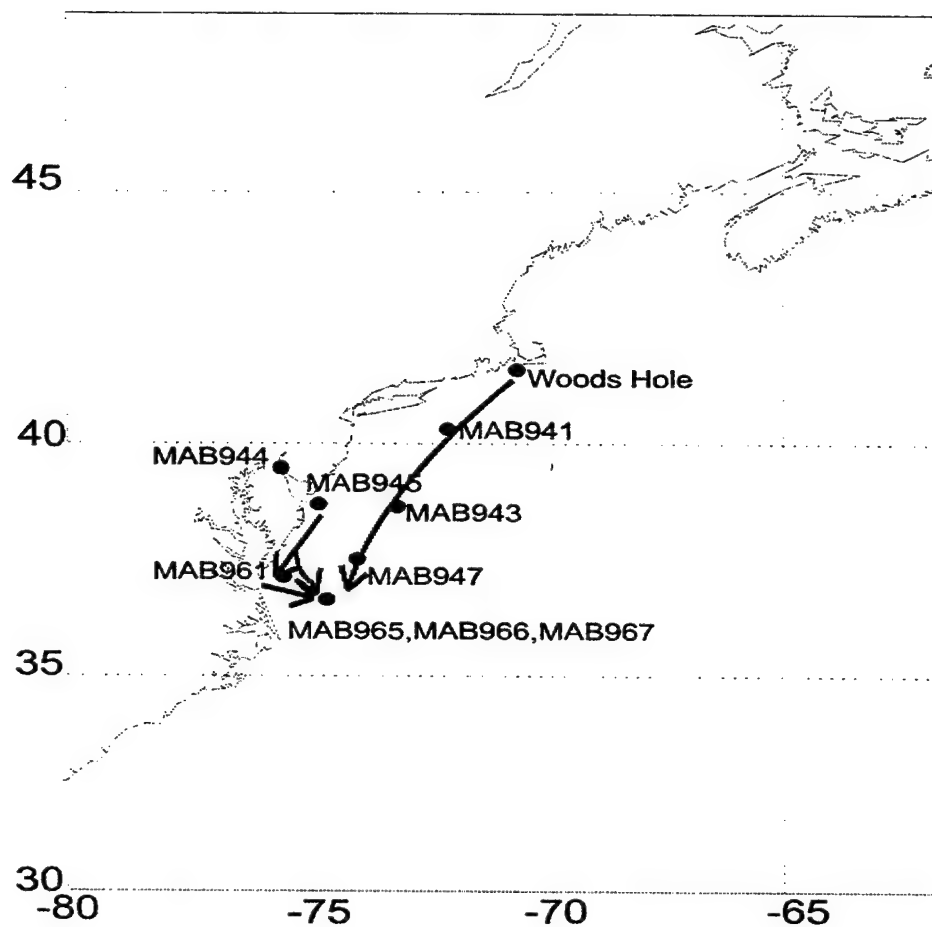
	MAB965	MAB967	CRL	ENA	HAWAII	P961	P962
MAB941	0.65	0.67	0.86	0.85	0.7	0.7	0.78
MAB943	0.81	0.63	0.94	0.96	0.68	0.85	0.76
MAB944	0.37	0.6	0.62	0.62	0.22	0.41	0.63
MAB945	0.87	0.76	0.62	0.65	0.57	0.75	0.69
MAB947	0.73	0.73	0.82	0.84	0.46	0.72	0.76
ENA	0.85	0.57	0.99	1	0.85	0.9	0.72
MAB961	0.86	0.81	0.66	0.72	0.42	0.79	0.83
P961	0.98	0.65	0.85	0.9	0.85	1	0.84
P962	0.84	0.92	0.68	0.72	0.6	0.84	1
MAB965	1	0.72	0.8	0.85	0.78	0.98	0.85
MAB964	0.14	0.51	0.32	0.31	0.08	0.23	0.57
CRL	0.8	0.56	1	0.99	0.87	0.85	0.68
HAWAII	0.78	0.44	0.87	0.85	1	0.85	0.6
MAB967	0.72	1	0.56	0.57	0.44	0.65	0.92

Table 2.4 Results from the correlation coefficient analysis of the mole percent monosaccharide distributions in different HMW DOM samples.





**Figure 2.16 Correlation coefficient data for the mole percent monosaccharide distribution of each HMW DOM sample. All correlations are reported relative to MAB941**



**Figure 2.17** A schematic representation of the flow of water in the MAB constructed using the correlation coefficient data for the mole percent monosaccharide distributions.

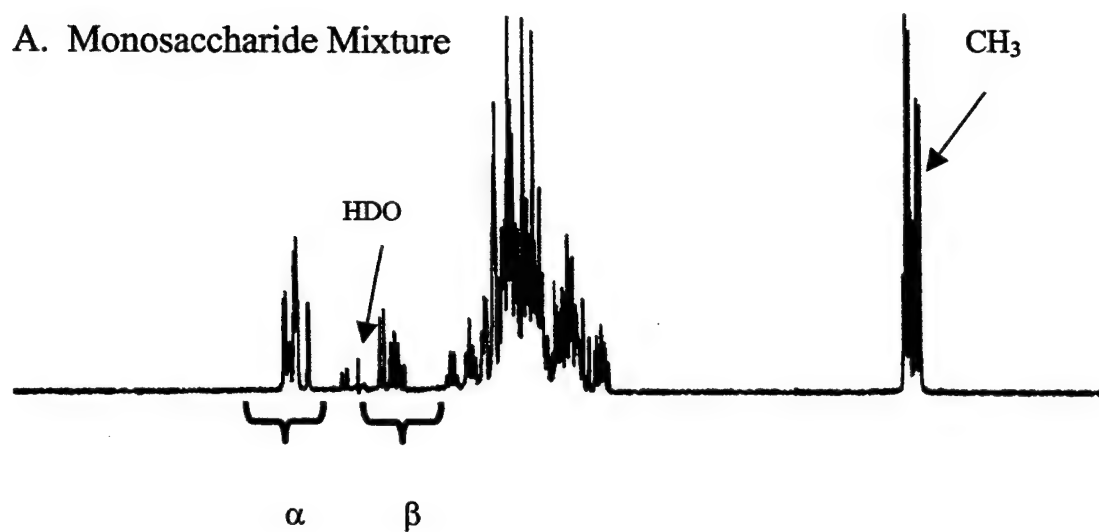
A standard mixture of seven monosaccharides was made using the monosaccharide distributions determined by the alditol acetate analyses, and its  $^1\text{H}$ NMR is shown in Figure 2.18 A. Also shown in Figure 2.18 is a  $^1\text{H}$  NMR spectrum of a hydrolyzed HMW DOM sample (B). The similarities between these two spectra are remarkable and confirm that much of the DOM in surface water is carbohydrate.

However, there is a discrepancy between the monosaccharide yields determined from the alditol acetate data and the  $^1\text{H}$ NMR. The combined hydrolysis yields of neutral and charged monosaccharides do not exceed 30%. However, NMR data estimate that carbohydrates account for between 50-60% of the total carbon in HWM DOM. Thus, either biochemicals other than carbohydrates give rise to the resonances in the region 3-4.5 p.p.m in the  $^1\text{H}$ NMR spectrum or HMW DOM contains carbohydrates (neutral and charged) that are not hydrolyzed or identified by conventional analytical methods.

#### 2.3.5 Methylation Analysis

Several attempts were made to methylate the polysaccharides in HMW DOM according to the method in section 2.2.6.2 (UF941, UF947, CRL, Hawaii). Following methylation, polysaccharides were extracted into dichloromethane and analyzed by  $^1\text{H}$ NMR. Proton NMR spectra of each of the methylated samples were very similar. Shown in Figure 2.19 are spectra for an aqueous sample prior to methylation (A) and the organic extract of methylated CRL (B). The R-O-CH<sub>3</sub> groups of the methylated carbohydrates give resonances at 3.0 p.p.m. There are some large peaks in the methylated sample near this region (2.8 p.p.m) that may be the peaks of interest. However, the high ratio of anomeric (4.5 to 6.0 p.p.m) to non-anomeric (3 to 4.5 p.p.m) carbohydrate protons, and the large peaks between 1 and 2 p.p.m suggest that the sample contains other compounds besides polysaccharides. If polysaccharides

A. Monosaccharide Mixture



B. Hydrolyzed Surface Water DOM

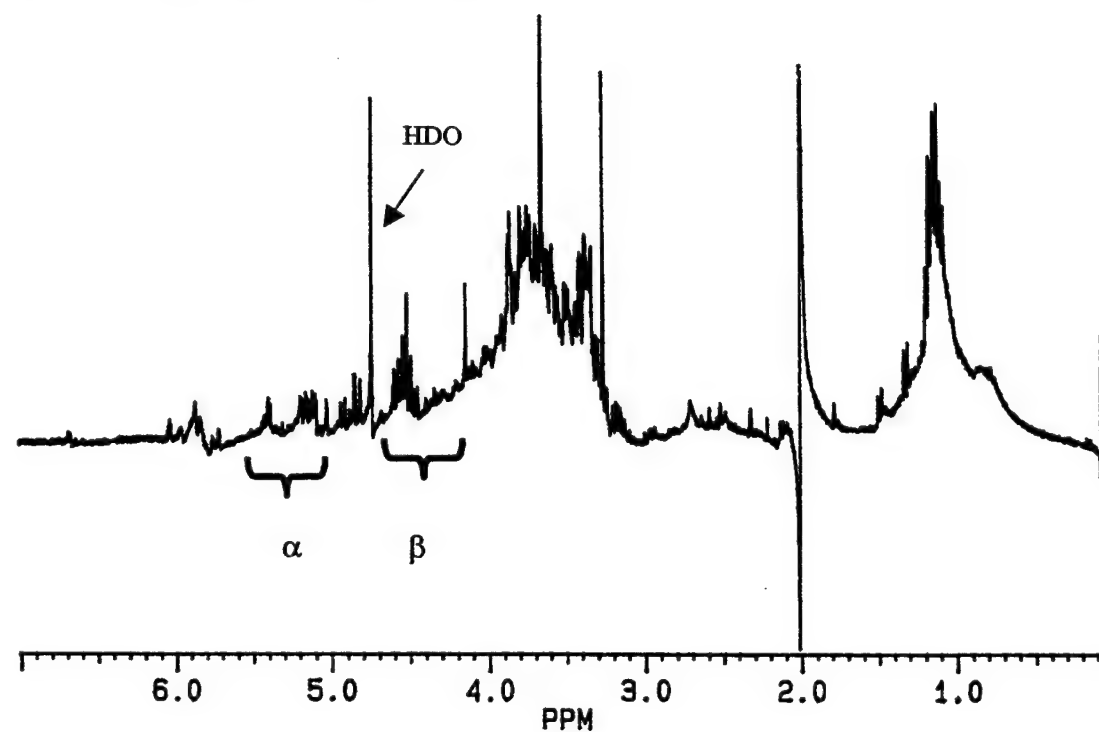
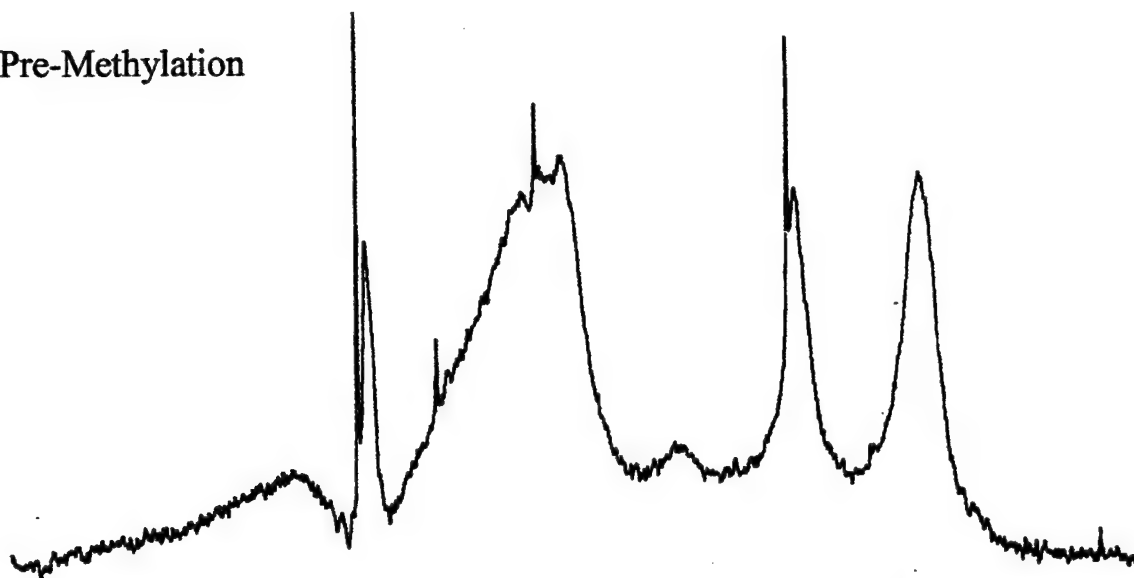


Figure 2.18 The  $^1\text{H}$  NMR spectrum of a standard mixture of monosaccharides (A) and a hydrolyzed HMW DOM sample (B).

A. Pre-Methylation



B. Organic Layer After Methylation

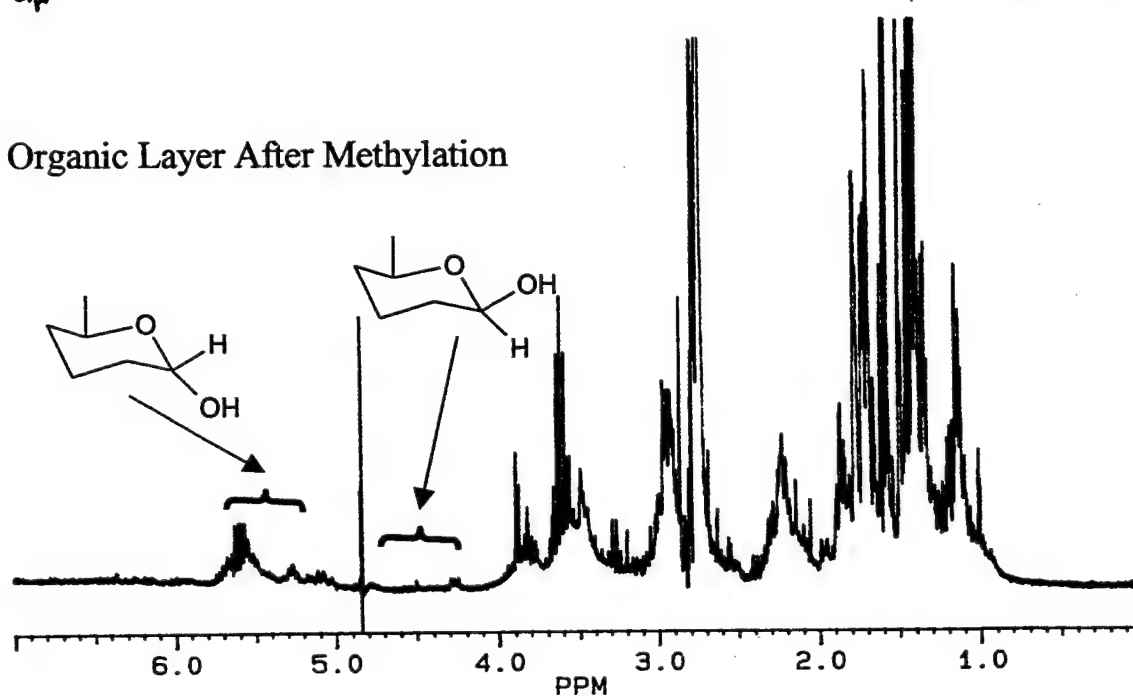


Figure 2.19  $^1\text{H}$ NMR spectra of HMW DOM prior to methylation (A) and following methylation and extraction into an organic solvent (B).

are present in these extracts, even in small concentrations, the NMR data imply that the majority of anomeric hydrogen atoms are in the  $\alpha$  orientation (5.0-6.0 p.p.m).

This methylation reaction should be performed using  $\text{CD}_3\text{I}$  to determine which of the peaks in Figure 2.19 B arise from the reaction of polysaccharides and other compounds with the  $\text{CD}_3$  group. It may also be important to methylate the sample several times to insure that polysaccharides are completely methylated and to desalt the sample as thoroughly as possible prior to methylation. If performed correctly this is likely to be the best method for isolating the carbohydrate fraction from the total HMW DOM.

#### 2.3.6 Linkage Analysis

A typical total ion trace of partially methylated alditol acetates (PMAA) from HMW DOM is shown in Figure 2.20. PMAA's were identified by their mass spectra and retention time. Shown in Figure 2.22 A, B and C are the mass spectra of four different linkage types identified in each sample. Accompanying each spectrum is the typical fragmentation pattern expected from a particular compound. Some common fragments of PMAA's are  $m/z$  118 and 101/102 peaks that can be generated as shown in Figure 2.21. Other characteristic peaks are  $m/z$  129 for 1,2-linked sugars, and  $m/z$  131 for deoxy hexoses (Figure 2.21B and C).

Also given in the appendix of this chapter is a list of the retention times of known standards that are necessary to make the correct peak identifications.

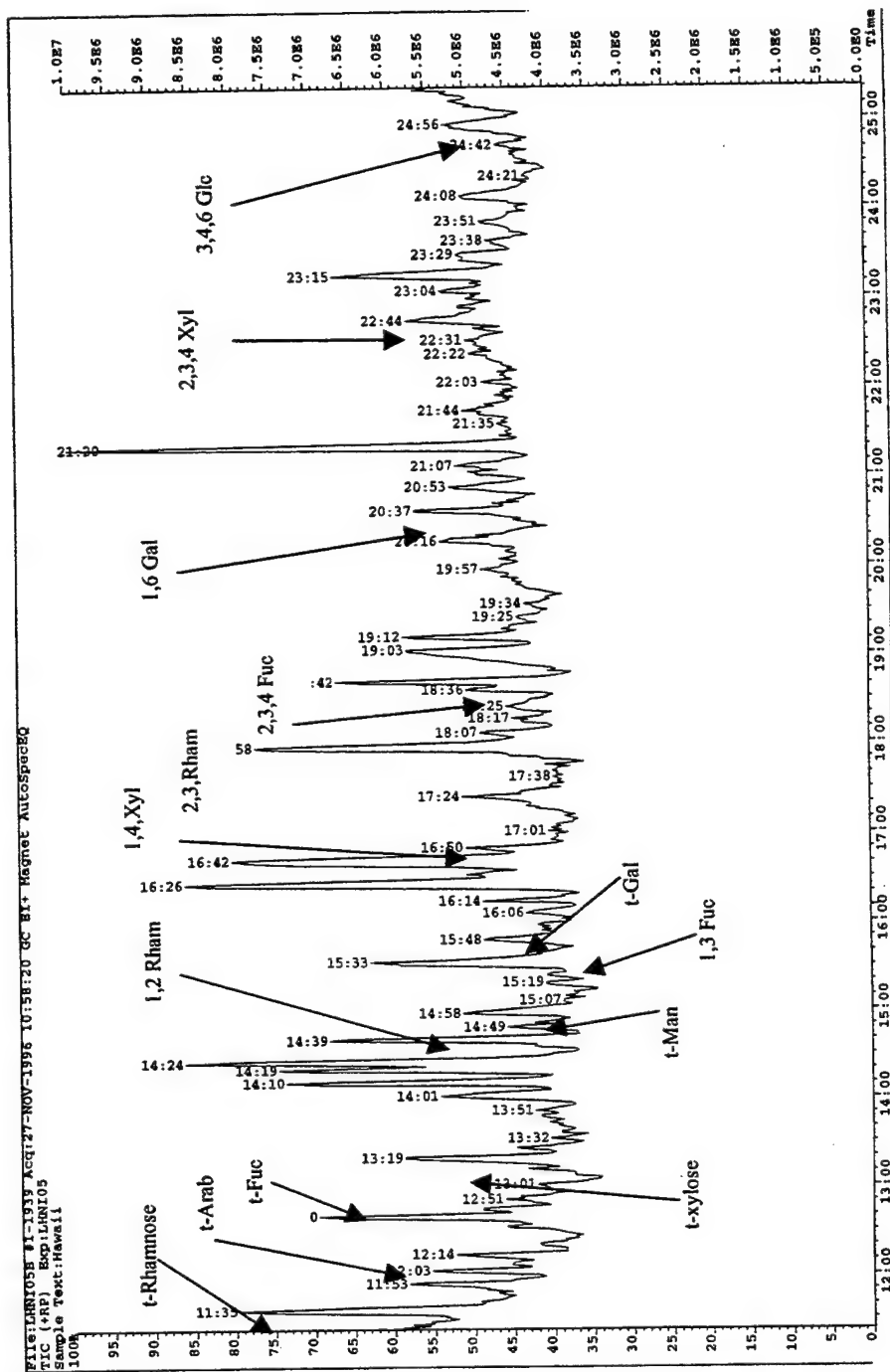
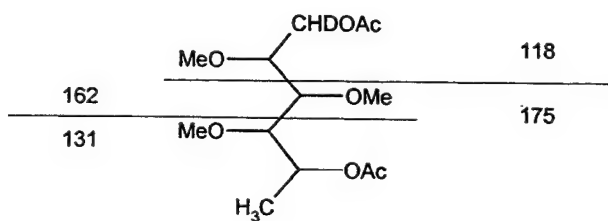
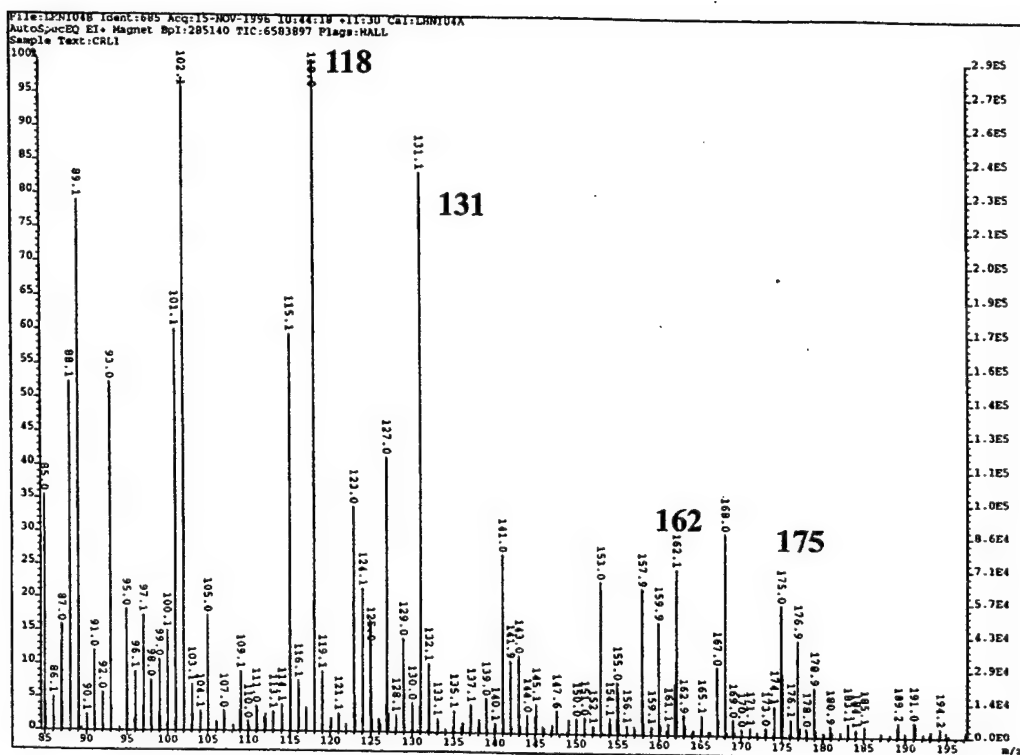


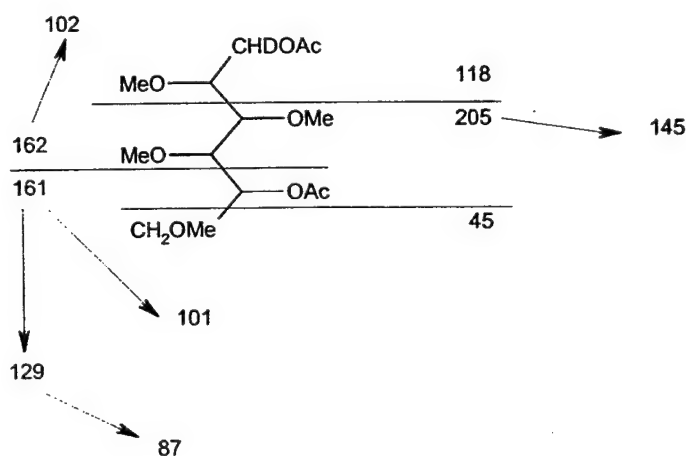
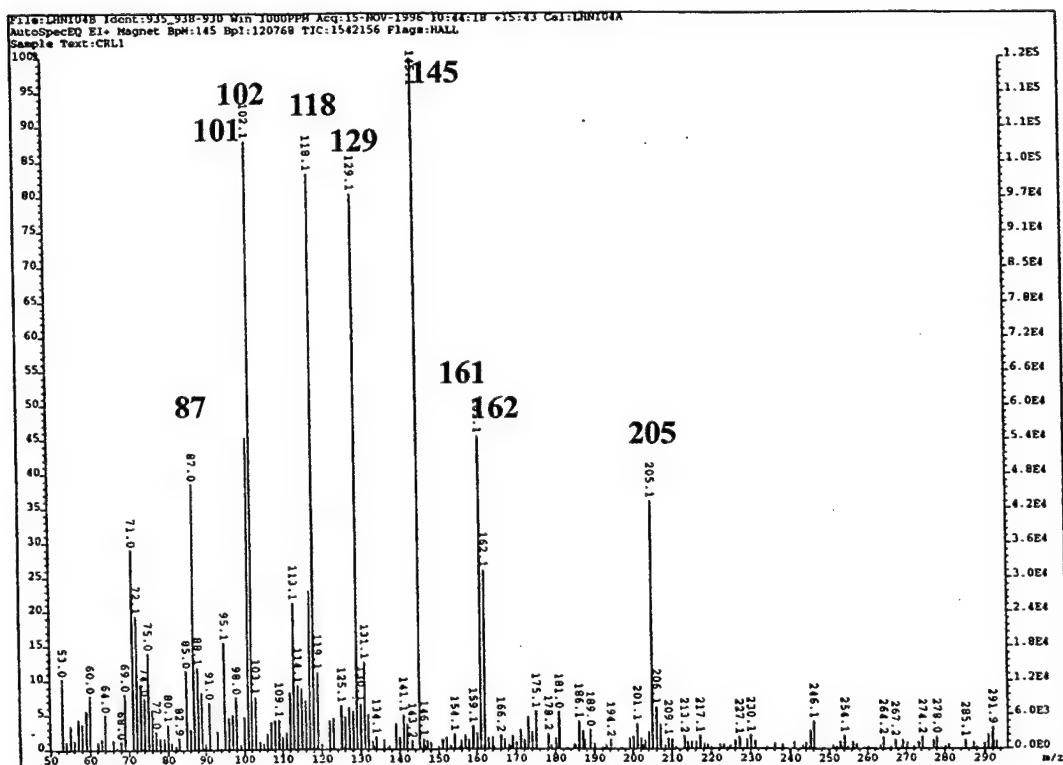
Figure 2.20: The total ion current of partially methylated alditol acetates from a HMW DOM sample. Each peak was identified using mass spectral data and retention time data.

# A. Terminal Rhamnose





## B. Terminal Mannose



## C. 1,4 Galactose

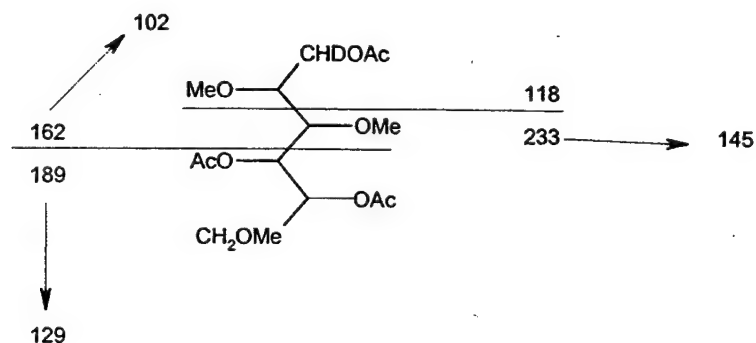
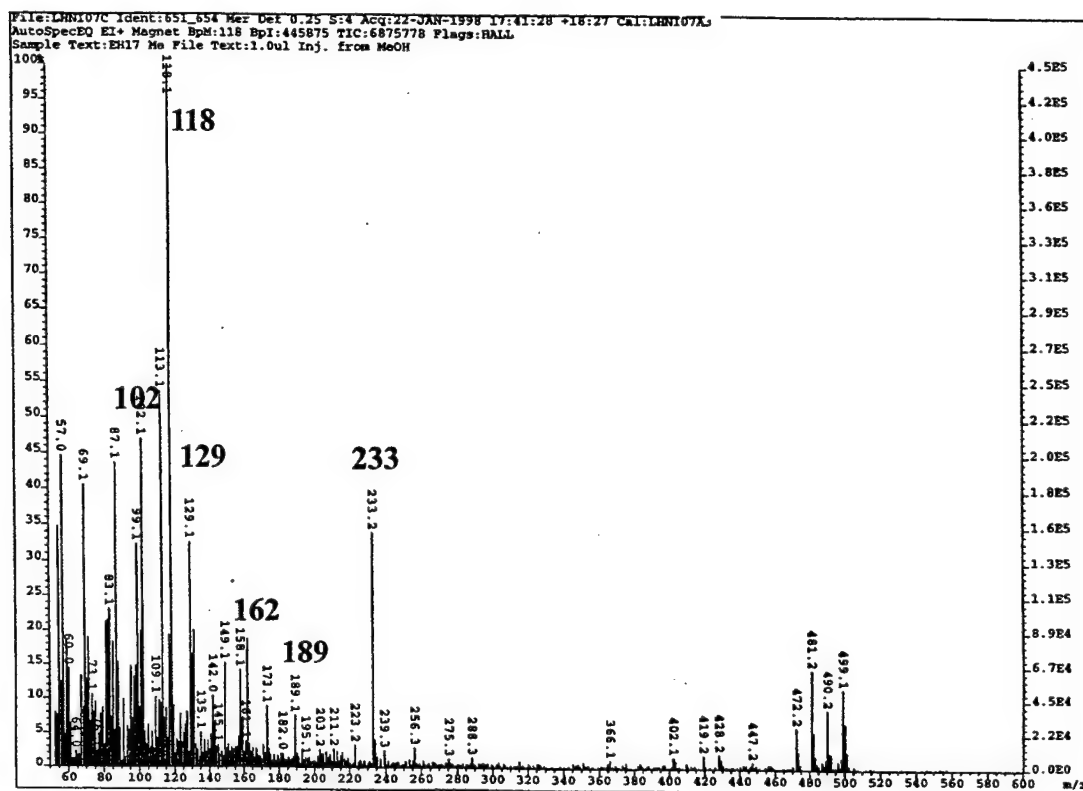


Figure 2.21 Mass spectra of terminally linked rhamnose (A), terminally linked mannose (B), 1,4-linked galactose (C).

The linkage patterns for three different HMW DOM samples isolated from the surface ocean are shown in Figure 2.22. The abundance of each type of linkage is expressed as a percent of the total linkages present for each sugar. Linkage type "T" refers to monosaccharides linked only at carbon 1, while linkage type 1,3 refers to monosaccharides linked at both carbon 1 and carbon 3, etc.

Of the pentoses, only arabinose is present as both the pyranose (*p*) (six membered ring) and the furanose (*f*) (five membered ring) form. Arabinose (*f*) was only present at a terminal site. In most cases, the most abundant type of linkage was the terminally linked monosaccharide. The large percentage of terminal linkages may be an artifact of the analysis. If the polysaccharide is only partially methylated, then the sites that are most accessible (i.e. monosaccharides present at the terminus of the polymer) will be methylated preferentially.

As shown in the Figure 2.22, each monosaccharide is linked at several different sites. Glucose has the fewest different linkages; for example, the HMW DOM sample ENA contains only terminally linked glucose. Furthermore, glucose only appears at the terminus of a polymer or linked at 3 or more positions. All other monosaccharides show a variety of different linkages.

It is clear from Figure 2.22 that linkage patterns are complex and distinct in the three samples analyzed in this study. The use of linkage analysis is imperative in understanding and comparing the structure of polysaccharides isolated from these

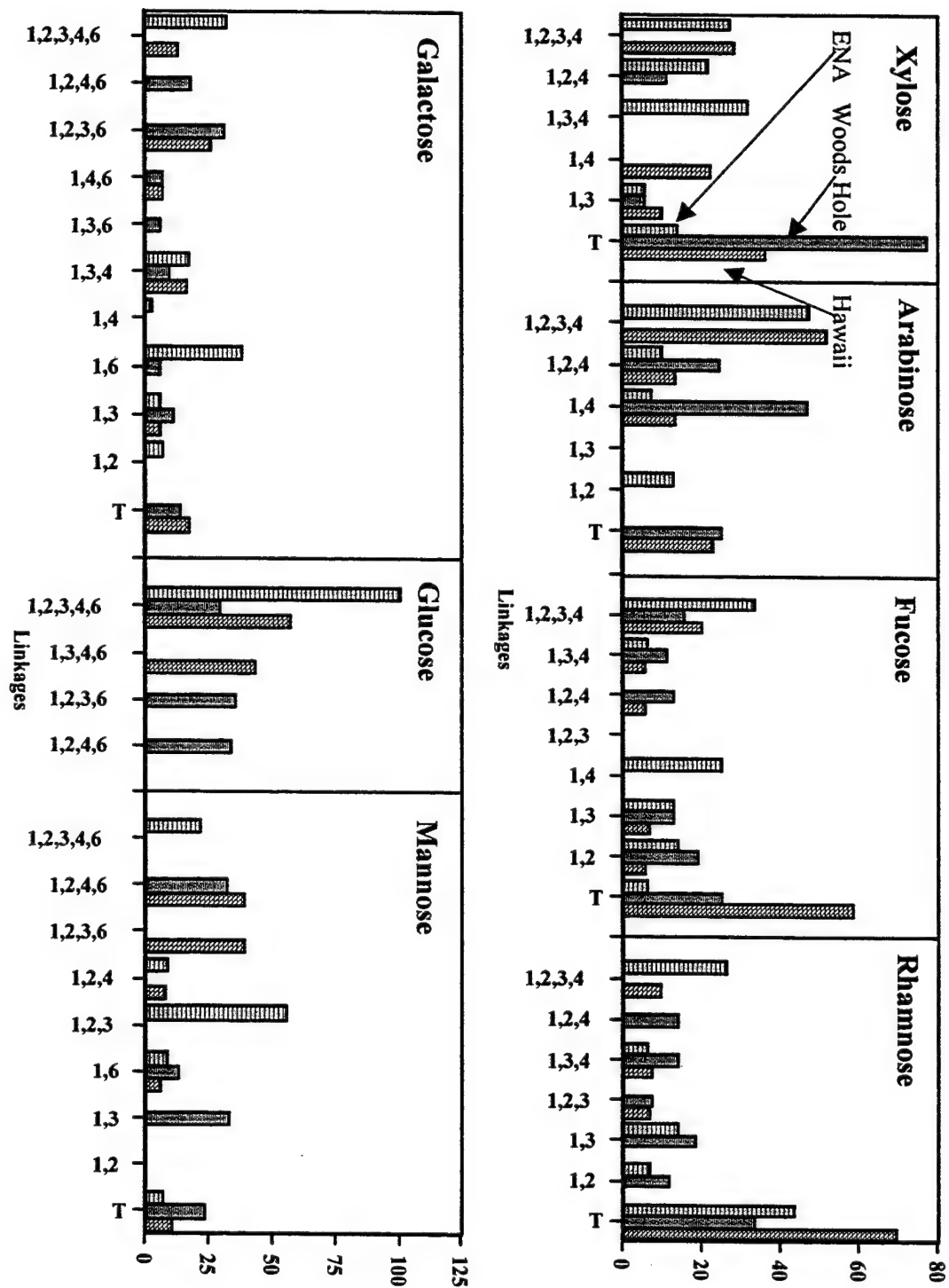


Figure 2.22 The relative distribution of different types of linkages per sugar for three different HMW DOM samples.

different sites. Thus, it is important to determine if the differences exhibited in the linkage patterns are real or an artifact of the experimental method. This is the first time an analysis of this type has been performed on such a complex natural substrate and as such, the method needs refinement to be more certain of the its results.

### **2.3.7 Amino Acid Analysis**

The relative distribution of amino acids in CRL determined in this study are shown in Table 2.4 (for CRL) along with the average distribution of amino acids in seawater HMW DOM (McCarthy et al.1996). Different acid strengths, temperatures and time of hydrolysis had no systematic effect on the yield of amino acids but affected the relative distribution of amino acids in the sample (as illustrated by the standard deviation data). In all cases, total amino acid yields did not exceed 20% of the total nitrogen and 4-5% of the total HMW carbon. CRL1, CRL2, CRL3 and CRL4 were all initially hydrolyzed with 1 M HCl at 105 °C for 11 hours. Following this hydrolysis, CRL2 was hydrolyzed with 2M TFA at 121°C for 2 h (the standard hydrolysis method used in this thesis), CRL3 was hydrolyzed with 7 N HCl at 150 °C for 1.5 h (the hydrolysis method used by McCarthy et al. (1997)), and CRL4 was hydrolyzed with 4 N HCl at 100 °C for 17 h (the standard method used to liberate muramic acid from peptidoglycans (Discussion section)). The variation in amino acid distributions resulting from different hydrolysis methods is unexpected. These differences may reflect degradation of amino acids during certain hydrolysis procedures. Amino acid standards were not tested for each method.

Amino acid AA	Mole% Literature	Mole% CRL1	Mole% CRL2	Mole% CRL3	Mole% CRL4	Average	% Standard Deviation
Aspartic Acid	11.3	23.8	16.1	12.1	21.9	18.5	29.0
Glutamic Acid	16.3	8.6	6.9	7.9	7.9	7.8	8.7
Serine and Histidine	10.4	8.8	12.2	12.8	10.4	11.1	16.5
Glycine	16.0	13.1	18.0	15.2	12.1	14.6	18.1
Threonine and Arginine	11.8	8.2	7.8	10.2	9.1	8.8	12.2
Alanine	14.8	14.1	16.6	15.5	14.6	15.2	7.0
Tyrosine	2.0	2.5	1.4	1.2	1.8	1.7	33.2
Methionine	0.8	1.3	0.0	0.6	1.6	0.9	80.1
Valine	3.9	2.8	3.1	4.4	4.4	3.7	22.8
Ph-Alanine	2.2	2.4	2.1	3.1	2.6	2.6	16.2
Isoleucine	3.2	10.0	10.9	14.8	9.2	11.2	22.0
Leucine	4.0	3.4	3.4	0.4	2.7	2.5	58.0
Lysine	1.4	1.1	1.5	0.2	1.7	1.1	59.8

**Table 2.5 The mole percent distribution of amino acids in HMW DOM.**

Literature, refers to the data published by McCarthy et al. (1996). Despite large variations in the distribution of amino acids for the CRL series, total yields ranged from 15-19 % (of the total nitrogen in the sample).

Using the fact that arginine and lysine contain 3 and 1 moles of nitrogen, respectively, that do not participate in peptide bonds, the relative percent of free amines in a protein containing the relative distribution of amino acids shown in Table 2.4, can be estimated to be approximately 12% of the total nitrogen. This calculation assumes that all the amino acids are present in one protein, thus an additional mole of free amine nitrogen (from a terminal amino acid) is also included in this percentage. These amino acids account for approximately 20% of the total nitrogen in the sample and thus the free amine

contribution to the  $^{15}\text{N}$ NMR spectrum shown in Figure 2.10A is approximately 2.4 % of the total nitrogen in the sample, leaving approximately 5-6% of the free amine unaccounted for. These remaining free amines may come from either amino sugars (~5% N by hydrolysis in section 2.3.2.3) or other proteins.

## 2.4 Discussion

The goal of this chapter was to determine the chemical characteristics HMW DOM isolated from the ocean by ultrafiltration. Furthermore, by isolating and characterizing HMW DOM for different parts of the ocean, this study attempted to determine the overall variation in the chemical structure of HMW DOM.

In accordance with other published studies (Benner et al., 1992; McCarthy et al., 1996; Sakugawa and Handa, 1985b; Vernonclark et al., 1995), using  $^1\text{H}$ NMR spectroscopy this study found that a major fraction of HMW DOM in surface waters (60-70% of the total carbon), and a significant fraction of HMW DOM isolated from deep waters (30-40% of the total carbon) consisted of identifiable (Table 2.2). The results in Table 2.1 indicated that on average, 27 % of the total DOC was isolated by ultrafiltration. Thus, in the surface and deep ocean, the major biochemicals identified above respectively account for 16-19 and 8-11 % of the total DOC.

The major identifiable biochemical in both surface and deep waters was carbohydrate, consisting of a fixed ratio of neutral monosaccharides ( $16\pm 3$  % rhamnose,  $16\pm 2$  % fucose,  $8\pm 3$  % arabinose,  $13\pm 2$  % xylose,  $14\pm 2$  % mannose,  $20\pm 3$  % galactose, and  $14\pm 4$  % glucose). Due to the constant mole percent distribution of monosaccharides in both surface and deep water HMW DOM isolated from these diverse locations, the

monosaccharides are postulated to be present together in a single class of polysaccharides. In addition, the relatively constant carbohydrate: acetate ratio in all these samples implies that acetate is also present in these polysaccharides, linked to O-acetylated or N-acetylated sugars. These polysaccharides, containing acetate and the relative distribution of monosaccharides that were identified above, are referred to as acylated polysaccharides or APS, for the purpose of this study.

Hydrolysis of HMW DOM and subsequent monomer analysis showed quantitative differences in the yield of major biochemicals compared with NMR data. Neutral monosaccharides as analyzed by alditol acetates accounted for 15-20% of the total carbon in surface waters (compared with the 50-60% yield expected by NMR spectroscopy). Amino sugars and uronic acids accounted for approximately 5-10% of the total carbon (amino sugar yields by both GC and HPLC are comparable at 5%), thus increasing the carbohydrate carbon yield to approximately 25%. Lipid analysis showed only acetate as the major lipid in HMW DOM, accounting for approximately 8% of the total carbon. In addition amino acid analysis showed that 4% of the carbon in HMW DOM could be accounted for as hydrolyzable amino acids. When these latter carbon yields are added to the carbohydrate carbon yield of 25%, it is clear that hydrolysis products can account for only 37% of the carbon in HMW DOM.

The same calculation can be done for the nitrogen in HMW DOM. The O-phthalaldehyde derivatization performed by Dr. Silvio Pantoja (as in section 2.28) showed that 20 and 5% of the nitrogen in hydrolyzable HMW DOM were amino acids and amino sugars, respectively.



The ultrafiltration data given in Table 2.1, together with published data (Benner et al., 1992; Guo et al., 1997; McCarthy et al., 1996), suggest that there is no systematic depth related difference in the fraction of DOM isolated by ultrafiltration. Thus, since DOM concentrations in the surface ocean are double those in the deep ocean (and DOM is recycled over several ocean mixing cycles), surface waters can be assumed to be a mixture of 50 % deep water HMW DOM (refractory) and 50 % surface water HMW DOM (newly added). Assuming that the compounds labile to acid hydrolysis (APS for example) are derived solely from the newly added surface water component, then 70-75% of this new carbon can be accounted for by the hydrolysis products. This calculation is illustrated schematically in Figure 2.23.

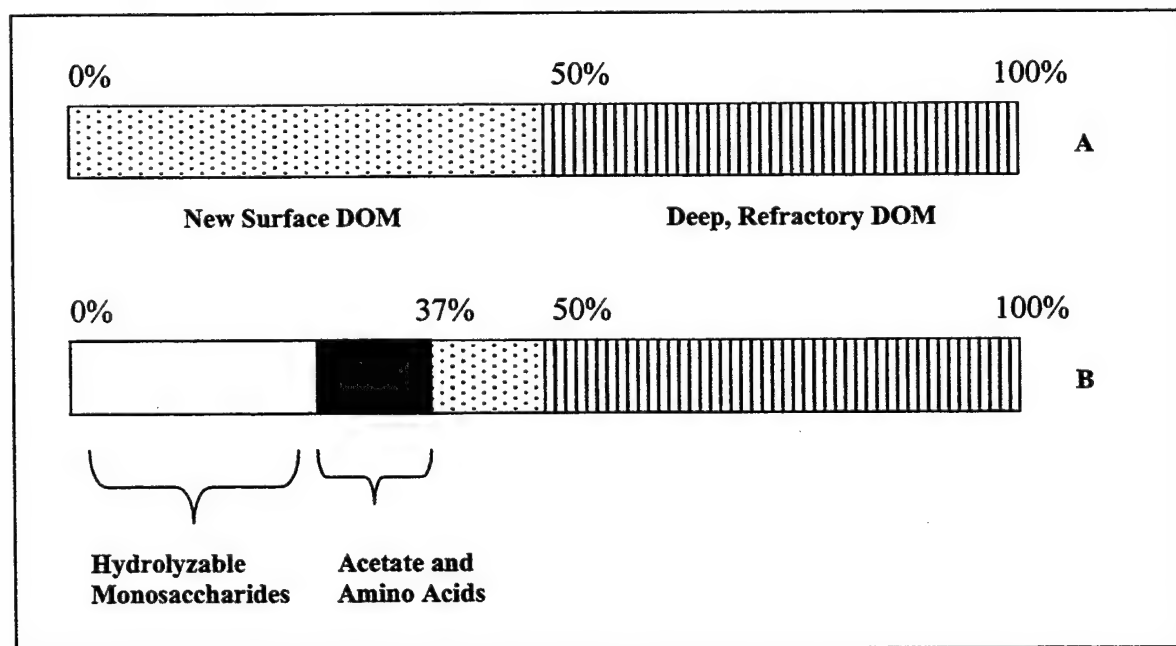


**Figure 2.23** The total amount of carbon in surface water HMW DOM derived from refractory deep ocean HMW DOM, and HMW DOM newly added at the surface (A) and the relative amount of carbon accounted for by the hydrolysis products (B), assumed to be derived from new HMW DOM only.

As discussed earlier, the hydrolysis products identified in Figure 2.23 accounted for only 25% of the total nitrogen in HMW DOM. In Section 2.3.1 it was shown that there was no depth related change in the C/N ratio of HMW DOM. In both surface and deep waters, the average C/N ratio was shown to be 15, indicating that both the newly added component of HMW DOM in the surface ocean, and the upwelled refractory HMW DOM component must have a C/N ratio close to 15. In order to balance the carbon and nitrogen budget for surface waters, the remaining 25% of the new HMW DOM (Figure 2.23B) in surface waters (and thus 13% of the total) must have a C/N ratio  $\leq 6$ . Common biochemicals with C/N ratios similar to this value are N-acetylated (8) sugars and proteins ( $< 5$ ). In order to close the carbon budget for the new HMW DOM component added to surface waters, more compositional information is needed for the nitrogen containing compounds in HMW DOM.

The  $^{15}\text{N}$ NMR data presented in section 2.3.2.3, showed that 92% of the nitrogen in surface HMW DOM is present as amide nitrogen derived from N-acetylated sugars or proteins. Mild hydrolysis of this HMW DOM converts approximately 70% of the amide nitrogen to amine nitrogen. The remaining amide (33% of the total nitrogen) must be derived from non-hydrolyzable proteins and not N-acetylated sugars, because the NMR data suggest complete hydrolysis of the acetate peak. Several studies have shown the presence of refractory, and hydrolysis resistant proteins both in the water column and in sediments (Keil and Kirchman, 1991; Knicker et al., 1996; Tanoue et al., 1995), indicating that unhydrolyzable proteins may be the nitrogen component upwelled from deep waters. As mentioned before, the hydrolysis products showed the presence of amino acids, accounting for 20% of total nitrogen in the sample. Thus 53% of the total

nitrogen in the samples can be accounted for by hydrolyzable and non-hydrolyzable proteins. Thus the remaining 46 % of the nitrogen in hydrolyzed HMW DOM is amine nitrogen. The remaining amine compounds are derived from the hydrolysis of compounds containing amide bonds (not proteins, unless the amino acids generated upon hydrolysis are not identifiable by HPLC).

If 46 % of the nitrogen in HMW DOM (present as amines after hydrolysis) is derived from amino sugars, then given their C/N ratio of 6, amino sugars could account for approximately 20% of the carbon in HMW DOM (average C/N ratio of 15). As shown in Figure 2.23, the amount of carbon needed to close the carbon budget for the new component of HMW DOM added in surface waters, is 13 %. Thus, amino sugars could easily account for the missing new HMW DOM component in surface waters. Furthermore, combining the amino sugar carbon with the amount of carbon derived from hydrolyzable monosaccharides increases the total carbohydrate yield to 45 %. This value is similar to the amount of carbohydrates estimated by both  $^1\text{H}$  and  $^{13}\text{C}$ NMR. The amount of acetylated amino sugars in HMW DOM can also be calculated if all the acetate (8%) in HMW DOM is assumed to be present within these sugars. This calculation indicates that 30% of the total HMW DOM carbon should be derived from amino sugars, and is higher than the  $^{15}\text{N}$  NMR estimate. However, the NMR data ( $^1\text{H}$ ,  $^{13}\text{C}$  and  $^{15}\text{N}$ ), the constant ratio of carbohydrate to acetate, and the nitrogen and carbon budget in HMW DOM, are all consistent with the presence of N-acetylated sugars, (Figure 2.24). Other authors have also proposed that amino sugars are abundant in HMW DOM (Boon et al., 1999; McCarthy et al., 1998)). McCarthy et al. (1998) proposed that the major fraction of nitrogen in HMW DOM is derived from peptidoglycans, a resistant bacterial

membrane component. These compounds contain two acetylated amino sugars, N-acetyl glucosamine and muramic acid, in equal abundance. However, repeated attempts to hydrolyze the amino sugars in our study, using the different hydrolysis methods discussed in section 2.3.5 were unsuccessful even though standard glucosamine polymers (Chitin) were completely hydrolyzed by three of the four methods. Thus no direct identification of amino sugars was possible to confirm the data shown in Figure 2.24. However, hydrolysis of whole bacterial cells with 4 M HCl at 100°C for 19 h, yielded both muramic acid and N-acetyl glucosamine, indicating that peptidoglycans are hydrolyzable. No muramic acid was detected upon hydrolysis of HMW DOM indicating that if peptidoglycans are a significant fraction of HMW DOM, they are resistant to hydrolysis and must therefore be modified compared to intact bacterial cell walls. Furthermore, the relatively constant relationship between neutral monosaccharide yields and acetate concentrations indicate that the N-acetylated sugars are closely coupled with the neutral monosaccharides. This relationship would not be expected if amino sugars and neutral monosaccharides were present within distinct biochemicals, as would be the case if amino sugars were derived from peptidoglycans. Thus the data from this chapter suggests that peptidoglycans are not a significant source of the N-acetylated sugars in HMW DOM.

The preceding discussion determined that acylated polysaccharides (APS) isolated from the surface ocean consist of seven neutral monosaccharides, and N-acetylated amino sugars. A hypothetical structure for APS based on this data is shown in Figure 2.25. Since acid hydrolysis gave high neutral monosaccharide recoveries but poor amino sugar recoveries, this figure shows the amino sugars bonded to each other within APS.

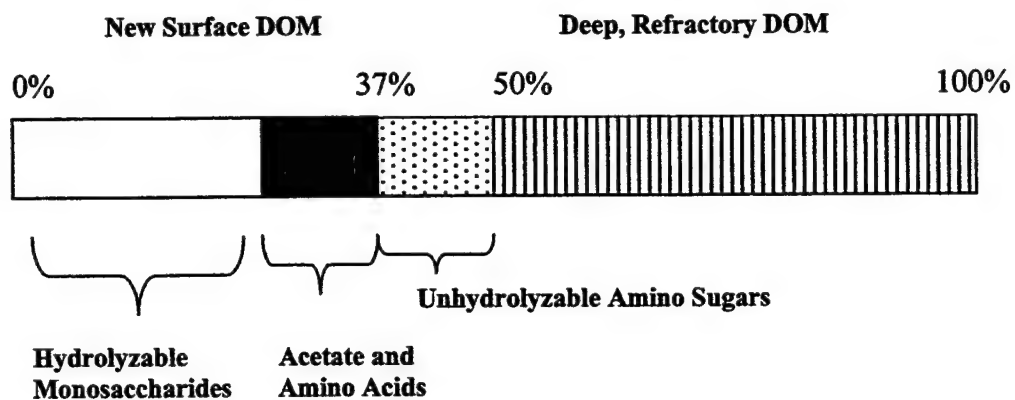


**Figure 2.24** The total carbon in surface water HMW DOM accounted for by the biochemicals identified in this study. Also refer to Figure 2.23

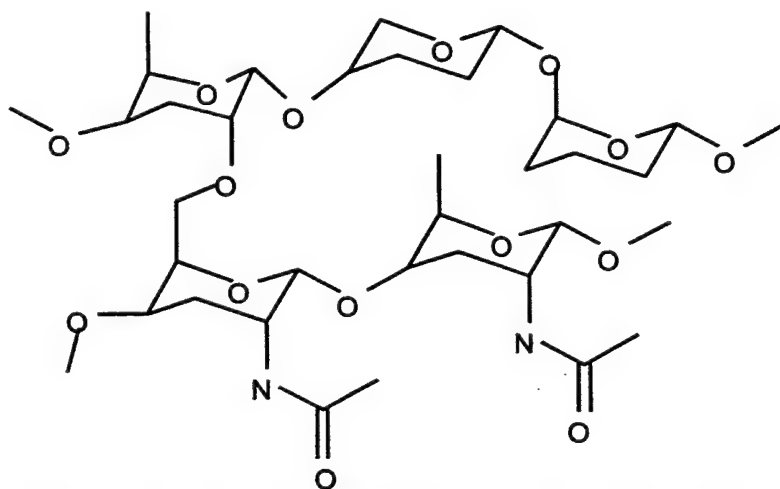


**Figure 2.25** Hypothetical structure for APS, containing neutral monosaccharides and N-acetylated sugars.

Both the amount of monosaccharide carbon in HMW DOM and the acetate and carbohydrate resonances in the NMR spectra decrease with depth indicating that APS

decreases with depth. This is consistent with the idea that the source of APS resides in surface waters and APS is thus the new component of HMW DOM added to upwelled deep water in the surface ocean. If the new nitrogen in surface waters is accounted for by amino sugars, then most of the nitrogen in the deep ocean must be protein (from the  $^{15}\text{N}$ NMR data), consistent with the presence of non-hydrolyzable (likely refractory) proteins. The elevated concentration of proteins in deep waters relative to surface waters is also consistent with the  $^1\text{H}$ NMR spectra of HMW DOM isolated from deep waters, which showed a relative increase in the area of the baseline between 1 and 3.0 p.p.m (Figure 2.7 B). Resonances in this region are abundant in proteins (Figure 2.9). However, since the C/N ratio of HMW DOM in the deep ocean is 15, there must be a significant fraction of compounds other than proteins (C/N = 5) in deep ocean HMW DOM that remain to be identified. A  $^{15}\text{N}$ NMR experiment similar to that conducted in section 2.3.2.3 should be performed on HMW DOM isolated from the deep ocean to confirm that proteins are the major nitrogen component.

## 2.5 Conclusions

The data presented in this chapter show that HMW DOM isolated from different parts of the ocean is chemically related. The chemical analyses performed in this chapter show that HMW DOM consists of identifiable biochemicals, namely carbohydrates, proteins and lipids. The carbohydrate component referred to as APS has been shown to consist of seven neutral monosaccharides, rhamnose, fucose, arabinose, xylose, mannose, galactose and glucose. In addition to the neutral monosaccharides, the presence of acetate and the results from  $^{15}\text{N}$ NMR infer that N-acetylated sugars are also a major

component (~50% of the total carbohydrates) of APS. However, no direct detection of these amino sugars was possible indicating that they are resistant to hydrolysis. The data also indicate that APS is 50% of the total carbon in HMW DOM isolated from surface waters and 15-20% of the carbon isolated from deep waters (calculated using the relative amount of acetate present in the deep ocean). Twenty percent of the nitrogen in surface waters is recoverable as proteins. Nitrogen NMR further indicates that the major nitrogen containing component in the deep ocean are hydrolysis resistant proteins, while in surface waters amino sugars are an equally dominant fraction of the nitrogen.

## 2.6 References

- Aluwihare L. I., Repeta D. J., and Chen R. F. (1997) A major biopolymeric component to dissolved organic carbon in surface seawater. *Nature* **387**, 166-169.
- Benner R., Pakulski J. D., McCarthy M., Hedges J. I., and Hatcher P. G. (1992) Bulk chemical characteristics of dissolved organic matter in the ocean. *Science* **255**, 1561-1564.
- Beardsley R. C., Boicourt W. C., and Hausen, D. (1976) Physical Oceanography of the Middle Atlantic Bight. *Limnology and Oceanography, Special Symposium* **2**, 20-34.
- Benton F. L. and Dillon T. E. (1942) *Journal of the American Chemical Society* **64**, 1128.
- Boon J. J., Klap V. A., and Eglinton T. I. (1999) Molecular characterization of microgram amounts of oceanic colloidal organic matter by Direct Temperature resolved ammonia Chemical Ionization Mass Spectrometry. *Organic Geochemistry* submitted.



- Borch N. H. and Kirchman D. L. (1997) Concentration and composition of dissolved combined neutral sugars (polysaccharides) in seawater determined by HPLC-PAD. *Marine Chemistry* **57**, 85-95.
- Buesseler K. O., Bauer J. E., Chen R. F., Eglantine T. I., Gustafsson O., Landing W., Mopper K., Moran S. B., Santschi P. H., VernonClark R., and Wells M. L. (1996) An intercomparison of cross-flow filtration techniques used for sampling marine colloids: Overview and organic carbon results. *Marine Chemistry* **55**, 1-31.
- Burney C. M., Johnson K. M., Lavoie D. M., and Sieburth J. M. (1979) Dissolved carbohydrate and microbial ATP in the North Atlantic: concentrations and interactions. *Deep Sea Research* **26**, 1267-1290.
- Carlson D. J. and Mayer L. M. (1985) Molecular weight distribution of dissolved organic materials in seawater as determined by ultrafiltration: A re-examination. *Marine Chemistry* **16**, 155-171.
- Degens E. T. (1970) Molecular nature of organic nitrogen compounds in seawater and recent marine sediments. In: D. W. Hood (ed.), *Organic Matter in Natural Waters*. Univ. of Alaska. , pp. 77-106.

- Gagosian R. B. and Lee C. (1981) Processes controlling the distribution of biogenic organic compounds in seawater. In: E. K. Duursma and R. Dawson (ed.). Elsevier, Amsterdam. *Marine Organic Chemistry*, pp. 91-123.
- Gagosian R. B. and Stuermer D. H. (1977) The cycling of biogenic compounds and their diagenetically transformed products in seawater. *Marine Chemistry* **5**, 605-632.
- Guo L., Coleman C. H. J., and Santschi P. H. (1994) The distribution of colloidal and dissolved organic carbon in the Gulf of Mexico. *Marine Chemistry* **45**, 105-119.
- Guo L. and Santschi P. H. (1996) A critical evaluation of the cross-flow ultrafiltration technique for sampling colloidal organic carbon in seawater. *Marine Chemistry* **55**, 113-1127.
- Guo L., Santschi P. H., Cifuentes L. A., Trumbore S., and Southon J. (1997) Cycling of high molecular weight dissolved organic matter in the Middle Atlantic Bight as revealed by carbon isotopic ( $^{13}\text{C}$  and  $^{14}\text{C}$ ) signatures. *Limnology and Oceanography*.
- Gust D., Moon R. B., and Roberts J. D. (1975) Applications of natural abundance nitrogen-15 nuclear magnetic resonance to large biochemically important molecules. *Proceedings of the National Academy of Science* **72**(12), 4696-4700.

Gustafsson O., Buesseler K. O., and Gschwend P. M. (1996) On the integrity of the cross-flow filtration for collecting marine organic colloids. *Marine Chemistry* **55**.

Hakomori S.-I. (1964) A rapid permethylation of glycolipid, and polysaccharide catalyzed by methylsulfinyl carbanion in dimethyl sulfoxide. *Journal of Biochemistry* **55**(2), 205-208.

Hedges J. I. (1992) Global Biogeochemical cycles: progress and problems. *Marine Chemistry* **39**, 67-93.

Ittekkot V., Brockman U., Michaelis W., and Degens E. T. (1981) Dissolved free and combined carbohydrates during a phytoplankton bloom in the Northern North Sea. *Marine Ecology Progress Series* **4**, 299-305.

Keil R. G. and Kirchman D. L. (1991) Dissolved combined amino acids in marine waters as determined by a vapor-phase hydrolysis method. *Marine Chemistry* **33**, 243-259.

Klap V. A. (1997) Biogeochemical aspects of salt marsh exchange processes in the SW Netherlands. *Ph. D. Thesis, Netherlands Institute of Ecology*.

Knicker H. A., Scaroni A. W., and Hatcher P. G. (1996)  $^{13}\text{C}$  and  $^{15}\text{N}$  NMR spectroscopic investigation on the formation of fossil algal residues. *Organic Geochemistry* **24**, 661-669.

- McCarthy M., Hedges J. I., and Benner R. (1996) Major biochemical composition of dissolved high molecular weight organic matter in seawater. *Marine Chemistry* **55**, 282-297.
- McCarthy M. D., Pratum T., Hedges J. I., and Benner R. (1998) Chemical composition of dissolved organic nitrogen in the ocean. *Nature* **390**, 152-153.
- Mopper K. (1977) Sugars and uronic acids in sediment and water from the Black Sea and North Sea with emphasis on analytical techniques. *Marine Chemistry* **5**, 585-603.
- Pantoja S., Lee C., and Lee C. (1999) Molecular weight distribution of proteinaceous material in Long Island Sound sediments. *Limnology and Oceanography* (in press).
- Peltzer E. T. and Brewer P. G. (1993) Some practical aspects of measuring DOC - sampling artifacts and analytical problems with marine samples. *Marine Chemistry* **41**, 243-252.
- Sakugawa H. and Handa N. (1983) Chemical studies of dissolved carbohydrates in seawater. Part 1. The concentration and separation of dissolved carbohydrates. *Journal of Oceanography of the Society of Japan* **39**, 279-288.

- Sakugawa H. and Handa N. (1985) Isolation and chemical characterization of dissolved and particulate polysaccharides in Mikawa Bay. *Geochimica et Cosmochimica Acta* **49**, 1185-1193.
- Santschi P. H., Guo L., Baskaran M., Trumbore S., Southon J., Bianchi T. S., Honeyman B., and Cifuentes L. (1995) Isotopic evidence for the contemporary origin of high molecular weight organic matter in oceanic environments. *Geochimica et Cosmochimica Acta* **59**(3), 625-631.
- Sidorczyk Z., Zahringer U., and Rietschel E. T. (1983) Chemical structure of the lipid A component of the lipopolysaccharide from a *Proteus mirabilis* Re-mutant. *European Journal of Biochemistry* **137**, 15-22.
- Skoog A. and Benner R. (1997) Aldoses in various size fractions of marine organic matter: implications for carbon cycling. *Limnology and Oceanography* **42**, 1803-1813.
- Tanoue E., S. N., Kamo M., and Tsugita A. (1995) Bacterial Membranes: A possible source of a major dissolved protein in seawater. *Geochimica et Cosmochimica Acta* **59**(12), 2643-2648.
- Vernonclark R., Goldberg E. D., and Bertine K. E. (1995) Organic and inorganic characterization of marine colloids. *Chemistry and Ecology* **11**, 69-83.

York W. S., Darvill A. G., McNeil M., Stevenson T. T., and Albersheim P. (1985)

Isolation and characterization of plant cell walls and cell wall components.

*Methods in Enzymology* **118**(3-40).

## 2.7 Appendix

### 2.7.1 Nuclear Magnetic Resonance Spectroscopy Conditions

#### <sup>1</sup>H NMR

AU PROG:

PRESAT.AUR

SF 300.134  
SY 210.0  
O1 5533.103  
SI 32768  
TD 16384  
SW 4201.681  
HZ/PT .256

PW 6.0  
RD 0.0  
AQ 1.950  
RG 80  
NS 12108  
TE 297

FW 5300  
O2 5533.103  
DP 28L

LB 0.0  
GB 0.0  
CX 19.0  
CY 10.0  
F1 9.000P  
F2 0.001P  
HZ/CM 142.168  
PPM/CM .474  
SR 4092.46

#### <sup>13</sup>C NMR

SF 75.469  
SY 75.0  
O1 6271.031  
SI 1024  
TD 1024  
SW 18518.519  
HZ/PT 36.169

PW 4.0  
RD 2.0  
AQ 0.028  
RG 320  
NS 271325  
TE 297

FW 23200  
O2 4350.000  
DP 16H  
P9 100

LB 100  
GB 0.0  
CX 19.0  
CY 10.0  
F1 225.205P  
F2 -19.000P  
HZ/CM 972.755  
PPM/CM 12.890  
SR -1465.63

## 2.7.2 Linkage Data for Seawater

	1	2	3	4	5
	Sugars	Linkages	Vincent Klap	CRL	Hawaii
1	Rhamnose	T	42.8	32.9	69
2		1,2	6.47	11.4	
3		1,3	13.4	18.2	
4		1,2,3		6.7	6.3
5		1,3,4	6	13.6	6.8
6		1,2,4		13.4	
7		1,2,3,4	26.1		9.2
8					
9	Fucose	T	6.11	25	57.9
10		1,2	13.6	18.4	5.3
11		1,3	12.7	12.6	6.3
12		1,4	24.6		
13		1,2,3			
14		1,2,4		12.6	5.3
15		1,3,4	6.11	10.9	5.3
16		1,2,3,4	33.3	15.5	20
17					
18	Arabinose	T		24.7	22.4
19		1,2	12.3		
20		1,3			
21		1,4	6.9	46.2	13.2
22		1,2,4	9.9	23.9	13.2
23		1,2,3,4	47		51.3
24					
25	Xylose	T	13.8	76.7	35.8
26		1,3	5.3	5.4	9.7
27		1,4	0		22
28		1,3,4	31.2	0	
29		1,2,4	21.5	11.1	
30		1,2,3,4	26.8	0	28
31					



	1	2	3	4	5
	Sugars	Linkages	Vincent Klap	CRL	Hawaii
3 2	Mannose	T	6.64	23.4	10
3 3		1,2			
3 4		1,3		32.3	
3 5		1,6	8.07	12.2	6
3 6		1,2,3	54.9		
3 7		1,2,4	8.5		7
3 8		1,2,3,6			38.6
3 9		1,2,4,6		32	38.6
4 0		1,2,3,4,6	21.1		
4 1					
4 2	Glucose	1,2,4,6		33.4	
4 3		1,2,3,6		35	0
4 4		1,3,4,6			42.9
4 5		1,2,3,4,6	100	28.7	57
4 6					
4 7	Galactose	T		13.4	16.6
4 8		1,2	6.11		
4 9		1,3	5.27	10.7	5.8
5 0		1,6	37.7	5.7	0
5 1		1,3,4	16.7	9.5	16
5 2		1,3,6		5.7	0
5 3		1,4,6		6.2	6.4
5 4		1,2,3,6		30.9	25.4
5 5		1,2,4,6		17.9	
5 6		1,2,3,4,6	31.9		12.2

### 2.7.3 Retention Times for Partially Methylated Alditol Acetates

As of: 22 Mar 96	RRT (relative to myo-Inositolhexaacetate)	
	SP2330	DB1
terminal-Ribo	0.383	
terminal-Rhap	0.392	
terminal-Araf	0.410	
terminal-Fucp	0.441	
terminal-Arap	0.446	
terminal-Xylo	0.455	
2-linked-Ribf	0.468	
2-linked-Rhap	0.497	
2-linked-Araf	0.498	
3-linked-Ribf	0.503	
3-linked-Rhap	0.504	
terminal-Mano	0.505	
4-linked-Rhap	0.507	
3-linked-Ribo	0.511	
2-linked-Ribo	0.517	
4-linked-Ribo	0.517	
terminal-Glcp	0.523	
3-linked-Araf	0.524	
3-linked-Fucp	0.525	
terminal-Galp	0.533	
4-linked-Fucp	0.540	
2-linked-Fucp	0.547	
3-linked-Xylo	0.556	
5-linked-Araf	0.558	
4-linked-Arap	0.558	
3-linked-Arap	0.561	
2-linked-Arap	0.564	
2,3-linked-Ribf	0.565	
3,4-linked-Rhap	0.570	
2-linked-Xylo	0.584	
4-linked-Xylo	0.584	
3,4-linked-Fucp	0.585	
2,3-linked-Araf	0.586	
2,3-linked-Rhap	0.591	
3-linked-Glcp	0.607	
2,4-linked-Rhap	0.609	
3-linked-Mano	0.613	
2-linked-Mano	0.613	
2,3,4-linked-Rhap	0.616	
2-linked-Glcp	0.617	
2,3-linked-Fucp	0.620	
2,4-linked-Ribo	0.621	
2,4-linked-Fucp	0.623	
2,3-linked-Ribo	0.628	
3,4-linked-Ribo	0.628	

As of: 22 Mar 96

RRT (relative  
to myo-Inositolhexaacetate)

<u>Compound</u>	<u>SP2330</u>	<u>DB1</u>
3-linked-Galp	0.628	
4-linked-Manp	0.630	
2,3,4-linked-Fucp	0.630	
2-linked-Galp	0.648	
6-linked-Manp	0.649	
3,5-linked-Araf	0.651	
3,4-linked-Arap	0.651	
6-linked-Glcp	0.652	
4-linked-Galp	0.654	
2,3-linked-Arap	0.662	
4-linked-Glcp	0.666	
2,5-linked-Araf	0.667	
2,4-linked-Arap	0.667	
2,3,4-linked-Ribp	0.690	
2,3-linked-Manp	0.691	
3,4-linked-Xylp	0.691	
2,3-linked-Xylp	0.691	
2,4-linked-Xylp	0.691	
3,4-linked-Manp	0.695	
6-linked-Galp	0.700	
3,4-linked-Galp	0.710	
2,3,5-linked-Araf	0.715	
2,3,4-linked-Arap	0.715	
2,3-linked-Galp	0.716	
3,4-linked-Glcp	0.722	
2,3-linked-Glcp	0.731	
2,4-linked-Manp	0.736	
2,4-linked-Glcp	0.742	
2,3,4-linked-Manp	0.742	
2,4-linked-Galp	0.743	
4,6-linked-Manp	0.749	
2,3,4-linked-Galp	0.764	
3,6-linked-Glcp	0.764	
3,6-linked-Manp	0.770	
2,6-linked-Manp	0.778	
4,6-linked-Glcp	0.782	
2,6-linked-Glcp	0.783	
2,3,4-linked-Xylp	0.786	
4,6-linked-Galp	0.790	
2,3,4-linked-Glcp	0.792	
3,6-linked-Galp	0.797	
2,6-linked-Galp	0.815	
3,4,6-linked-Manp	0.815	
3,4,6-linked-Galp	0.841	
3,4,6-linked-Glcp	0.849	

As of: 22 Mar 96

RRT (relative  
to myo-Inositolhexaacetate)

<u>Compound</u>	<u>SP2330</u>	<u>DB1</u>
2,3,6-linked-Manp	0.871	
2,4,6-linked-Manp	0.873	
2,4,6-linked-Glcp	0.878	
2,3,4,6-linked-Manp	0.881	
2,3,6-linked-Galp	0.905	
2,4,6-linked-Galp	0.905	
2,3,4,6-linked-Galp	0.915	
2,3,6-linked-Glcp	0.916	
2,3,4,6-linked-Glcp	0.953	
terminal-GlcpNAc		0.965
terminal-GalpNAc		1.022
terminal-ManpNAc		1.024
4-linked-GlcpNAc		1.071
4-linked-GalpNAc		1.091
4-linked-ManpNAc		1.103
3-linked-ManpNAc		1.122
3-linked-GlcpNAc		1.132
3-linked-GalpNAc		1.146
6-linked-GlcpNAc		1.150
3,4-linked-ManpNAc		1.152
3,4-linked-GalpNAc		1.176
3,4-linked-GlcpNAc		1.177
6-linked-ManpNAc		1.197
6-linked-GalpNAc		1.198
4,6-linked-GlcpNAc		1.239
4,6-linked-ManpNAc		1.261
4,6-linked-GalpNAc		1.273
3,6-linked-ManpNAc		1.286
3,4,6-linked-ManpNAc		1.306
3,6-linked-GlcpNAc		1.307
3,6-linked-GalpNAc		1.323
3,4,6-linked-GlcpNAc		1.338
3,4,6-linked-GalpNAc		1.343

<u>Temperature Program</u>	<u>SP2330</u>	<u>DB1</u>
Initial Temp	80.0	140.0
Init Time (min)	2.0	0.5
Rate (deg/min)	30.0	2.0
Final Temp (deg C)	170.0	220.0
Final Time (min)	0.0	0.0
Rate A (deg/min)	4.0	20.0
Final Temp A (deg C)	240.0	300.0
Final Time A (min)	20.0	5.0

### **3. A comparison of the chemical characteristics of oceanic HMW DOM and extracellular DOM produced by marine algae.**

#### **3.1 Introduction**

Dissolved organic matter (DOM) in the ocean is a by-product of marine primary production (Carlson and Ducklow, 1995; Mague et al., 1980; Williams and Gordon, 1970). Several processes may act to transfer organic matter from plankton to seawater, for example: direct exudation by phytoplankton (Baines and Pace, 1991; Fogg, 1966; Fogg, 1971; Hellebust, 1965; Mague et al., 1980) and heterotrophs (Nagata and Kirchman, 1992; Stoderegger and Herndl, 1998; Tanoue et al., 1995; Tranvik, 1994), indirect production through "sloppy feeding" (Lampert, 1978), dissolution of fecal pellets, marine snow (Alldredge et al., 1993) or other marine aggregates, and cell lysis (Fuhrman, 1992). While all of these processes have been shown to occur, there is little data that directly links the DOM released by these mechanisms to DOM which accumulates in seawater. Thus, we do not yet understand how the process of DOM introduction may affect its ultimate fate. For example, DOM that is directly released by plankton may be more labile than reworked DOM introduced by grazing.

Using  $^{13}\text{C}$ -labeled bicarbonate in a mesocosm experiment, Norrman et al. (1995) induced a mixed algal bloom, dominated by diatoms, and stimulated the release of DOM. Bacteria preferentially utilized labeled DOM, suggesting that newly synthesized DOM is labile, but a fraction of the labeled DOM persisted after one year of incubation. By using stable isotopes, Norrman et al. (1995) were able to quantify recently synthesized DOM, and trace its production, accumulation and utilization. However, the dynamics of labeled DOM alone do not show if the long-lived fraction of DOM was directly produced by

phytoplankton, or resulted from a reworking of the extracellular DOM by bacteria. It was also not determined if the experimentally produced DOM was chemically related to DOM that accumulates in seawater.

As shown in Chapter 2, a fraction of oceanic DOM retained by a 1kD (nominal molecular weight) ultrafiltration membrane (hereafter HMW DOM), is rich in acylated polysaccharides (APS) which have a characteristic acetate/carbohydrate/lipid ratio (Aluwihare et al., 1997). The carbohydrate fraction of APS contains at least seven major neutral monosaccharides which occur in a relatively fixed ratio and which are linked together at specific positions. High molecular weight DOM with a similar distribution of neutral monosaccharides has been isolated from geographically diverse locations (Aluwihare et al., 1997; Borch and Kirchman, 1997; McCarthy et al., 1996; Sakugawa and Handa, 1985a; Skoog and Benner, 1997), which together with our structural data led us to conclude that a large fraction of persistent DOM in seawater is produced by direct algal biosynthesis.

This chapter investigates the HMW fraction of extracellular DOM produced in laboratory cultures of three algal species, *Thalassiosira weissflogii*, a diatom, *Emiliania huxleyi* sp., and *Phaeocystis* sp., both prymnesiophytes. These algae were chosen to represent classes of phytoplankton important in oceanic primary production, and because previous laboratory studies have shown that the extracellular DOM produced by these phytoplankton is rich in carbohydrates. *T. weissflogii* and other diatoms are abundant in both coastal and ocean open areas; *E. huxleyi* is a cosmopolitan algae and a major contributor to primary production in the open ocean, and *Phaeocystis* sp. are mucus producing algae important in high latitude environments. The extracellular DOM

isolated from each culture was studied in extensive chemical detail in order to determine which algae could be a potential source for APS isolated from the surface ocean. Our data show that all three species do indeed exude DOM in culture and that 20-30% of the extracellular DOM from both *T. weissflogii* and *E. huxleyi* is spectrometrically and chemically similar to APS isolated from surface seawater. Furthermore, degradation of the *T. weissflogii* exudate shows that APS is metabolically more resistant to degradation than other polysaccharides.

## 3.2 Materials and Methods

### 3.2.1 Phytoplankton Cultures

All algae grown for this study were obtained from the Center for Culturing Marine Phytoplankton (CCMP), at Bigelow Laboratory, in Boothbay Harbor, Maine. Species included, *Thalassiosira weissflogii*, (CCMP 1336), *Phaeocystis* sp. (CCMP 628), and *Emiliania huxleyi* (CCMP 373). *T. weissflogii* and *E. huxleyi* were obtained as axenic seed cultures. The seawater used for the *T. weissflogii* was collected from a depth of 1000 m, south of Nantucket Island, Massachusetts (39° 49' N, 70° 20' W), and the seawater used for *E. huxleyi*, and *Phaeocystis* was collected in Great Harbor, Vineyard Sound, Woods Hole, Massachusetts. All seawater was prefiltered (0.2 µm) and ultrafiltered twice to remove high molecular weight (> 1kD) dissolved organic carbon (HMW DOC). Prior to adding *T. weissflogii*, seawater was enriched with nutrients, vitamins and trace metals added as f/2 concentrations according to Guillard & Ryther (1962), with an additional enrichment of sodium selenite (NaSeO<sub>3</sub>) to a final concentration of 10<sup>-8</sup> M. In the case of *E. huxleyi*, the media was enriched with F/2 - Si medium (Guillard and Ryther, 1962), and *Phaeocystis* sp. was grown in K medium

(Keller et al., 1987). Care was taken to keep bacterial populations low throughout the experiment by sterilizing all culture and sampling apparatus. A flow diagram of the experimental set up is shown in Figure 3.1. *T. weissflogii* and *E. huxleyi* were grown at 23°C, in 18 l glass carboys which were continuously aerated, and illuminated at 900  $\mu\text{E}/\text{m}^2\text{s}$ , 24:0 L:D (light:dark) and 14:10 L:D respectively. The cultures were sampled daily for particulate organic carbon (POC), dissolved organic carbon (DOC), chlorophyll *a* (chl-*a*), nutrients and cell numbers. *Phaeocystis* was grown in an 18 l glass carboy, at 26°C, in an incubator on a 14/10 L:D cycle, by Dr. Steven Morton at the CCMP. The *T. weissflogii* culture was harvested during late log phase growth determined by previous culture experiments and chl-*a* absorbance. *E. huxleyi* and *Phaeocystis* were also harvested during late log phase growth, based on chl-*a* absorbance and cell counts, respectively. All algae were removed by filtering (Whatman GF/F) and the exudates isolated as shown in Figure 3.1.

Subsamples (9 ml) for counting bacterial and phytoplankton cells (*E. huxleyi*) were collected daily, preserved with 1 ml of 10% glutaraldehyde and stored at 4 °C. Samples were filtered onto blackened Nuclepore 0.2  $\mu\text{m}$  polycarbonate filters and stained using a final concentration of 0.005 % v/v acridine orange (Hobbie et al., 1977). Five vertical and horizontal fields were counted for each slide using a standard Zeiss microscope with epifluorescence microscopy. The microscope was fitted with a bandpass 450-490 exciter, a FT510 chromatic beam splitter and a LP520 barrier filter. Bacterial



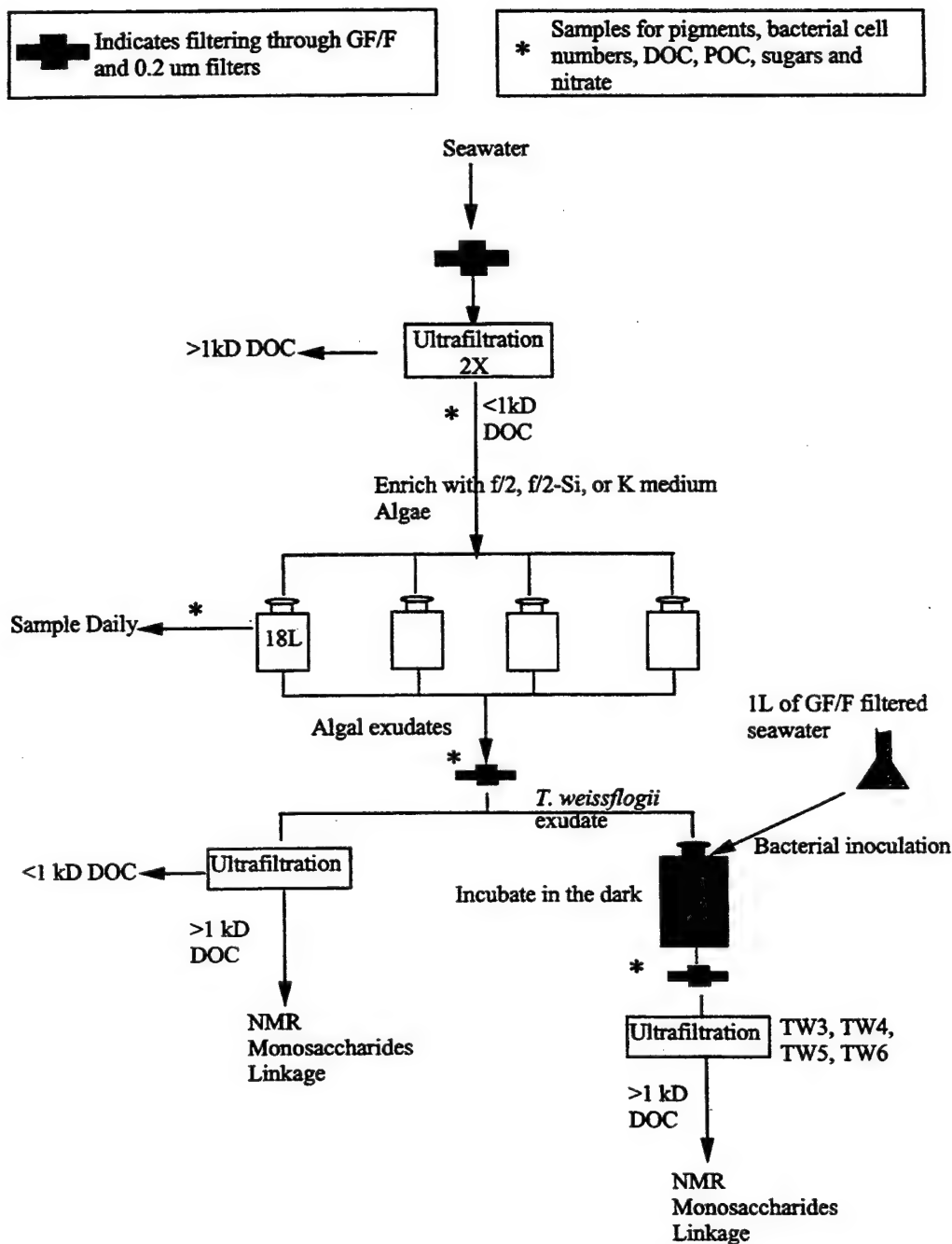


Figure 3.1 Experimental set up for the culture experiments. Seawater was pre-filtered through 0.2 µm and 1 nm membranes. Both the *Emiliania huxleyi* and *Phaeocystis* experiments were terminated after the algae were removed without further degradation of the exudate. TW3, TW4, TW5 and TW6 refer to samples taken during the degradation of the *Thalassiosira Weissflogii* exudate (dates are given in Figure 3.3).

cell numbers were converted to carbon using a conversion factor of 20 fg C/cell (Lee and Fuhrman, 1987).

The cultures were monitored daily for chl-a concentrations by filtering 15 - 45 ml of the culture medium onto Whatman GF/F filters, extracting with 100 % acetone, and measuring the absorbance at 664 nm. Conversion from absorbance to concentration was achieved assuming a molar extinction coefficient ( $\epsilon$ ) of  $8 \times 10^5 \text{ M}^{-1} \text{ cm}^{-1}$  and a molecular weight of 900 for chlorophyll a. POC analyses were performed according to the acidification method of Hedges (1991). Culture samples (20 ml) were filtered onto precombusted Whatman GF/F filters and frozen ( $-20^\circ\text{C}$ ) until analysis (1- 6 months). Prior to analysis, filters were oven dried overnight at  $60^\circ\text{C}$ , exposed to HCl vapors in a desiccator under vacuum (in the case of *E. huxleyi* acidified with 100  $\mu\text{l}$  of 2N HCl), and oven dried again, overnight at  $60^\circ\text{C}$ . After acidification, the filters were subsampled for triplicate analysis of carbon, nitrogen and hydrogen using a Fisons automated elemental analyzer.

The filtrates from the POC samples were collected in combusted vials fitted with teflon-lined caps, acidified with 50%  $\text{H}_3\text{PO}_4$  (5 $\mu\text{l}$   $\text{H}_3\text{PO}_4/\text{ml}$ ), and stored at room temperature or at  $4^\circ\text{C}$ . The samples were analyzed for DOC by high temperature catalytic oxidation (Peltzer and Brewer, 1993). Precision for triplicate analyses was better than  $\pm 3.5\%$ , and the upper limit for our system blank was 25  $\mu\text{M}$ , based on the DOC concentration of our acidified carbon-free distilled water.

The *T. weissflogii* exudates isolated from the five carboys at the end of the experiment (day 8 in Figure 3.2) were combined (80 l), filtered and subjected to microbial degradation. The degradation was initiated by inoculating the exudate with 1 l

of pre-filtered (Whatman GF/F) Woods Hole seawater. Following inoculation, the exudate was incubated in the dark for 8 months to monitor compositional changes in the DOC due to microbial degradation. Samples were taken periodically for ultrafiltration, and DOC concentration measurements.

### 3.2.2 Ultrafiltration

Cultures were filtered through a pre-combusted Whatman GF/F filter and a pre-rinsed 0.2  $\mu\text{m}$  polysulphone cartridge filter, and ultrafiltered to isolate the HMW DOM using an Amicon DC-10L system equipped with two spiral wound polysulphone filter membranes (1 nm, nominally  $>1$  k Da). Filters were cleaned between samples as described in Chapter 2, section 2.2.2. Eight to 10 l were ultrafiltered for each of the *T. weissflogii* samples, and 14 l were ultrafiltered for the *E. huxleyi* and *Phaeocystis* samples. Samples were concentrated to approximately 1-2 l and diafiltered ( $10\times$ ), as in section 2.2.2.2, using 2 l of de-ionized (Milli Q) water. Permeate from the final Milli Q rinse no longer gave a visible precipitate when added to a solution of silver nitrate (0.5 g/50 ml). Mass balances of DOM for the ultrafiltration were  $95 \pm 15\%$ , prior to diafiltration. High molecular weight DOM concentrates were stored frozen in glass or teflon bottles and lyophilized prior to analysis.

### 3.2.3 Analyses

Proton Nuclear Magnetic Resonance ( $^1\text{H}$ NMR) spectroscopy and monosaccharide, linkage and amino acid analyses were performed as described in Chapter 2.

### 3.2.4 Dissolved Oxygen Measurements

Samples for dissolved oxygen were collected in replicate. Sixty ml glass bottles (BOD bottles) were filled to the point of overflowing, capped with no headspace and

stored in the dark until analysis. Oxygen concentration measurements were made by Ms. Amy Nolin at the Marine Biological Laboratory (Woods Hole, MA), using an automated Winkler titration system designed by (Knapp et al., 1990).

### 3.3 Results

#### 3.3.1 Phytoplankton Cultures

##### 3.3.1.1 POC, DOC, and HMW DOC

Over the eight days of the experiment, chl-a and POC values in the *T. weissflogii* culture rose steadily to 1.8 mg/L and 82 mg/L respectively, while total DOC values fluctuated. DOC comprised 9% of the total organic carbon (TOC) in the system on day 8; HMW DOC comprised 27 % of DOC, and thus 2-3% of the TOC. *E. huxleyi* grew slowly over the first 10 days of the experiment followed by exponential growth from days 10-22 (Figure 3.2), when the culture was harvested. At the time of harvesting (day 22) the maximum POC value was 1.8 mM while DOC comprised 9-10% of the TOC. Also at this time, HMW DOC was 25% of the total DOC or 2-3% of the TOC. For the

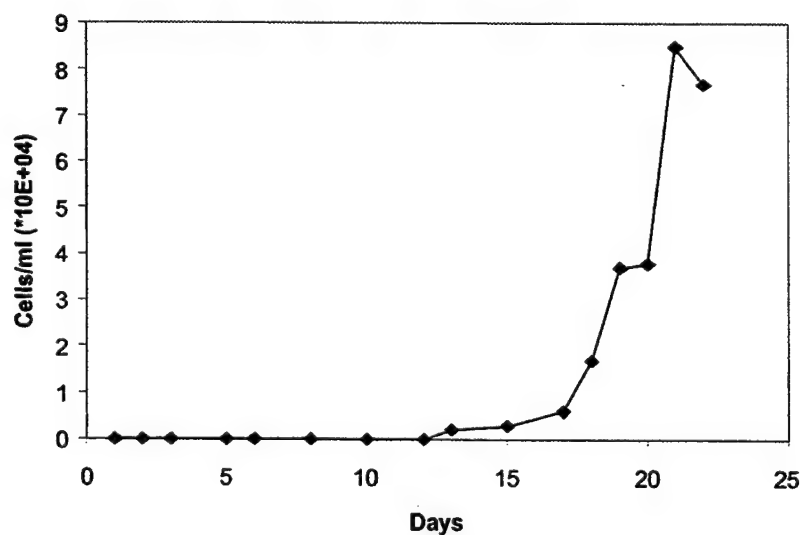


Figure 3.2 Growth curve for the *E. huxleyi* culture expressed in cell numbers/ml.

Sample	Time (day)	[DOC] ( $\mu\text{M C}$ )	[HMWDOC] ( $\mu\text{M C}$ )	%HMW	HMW Sugar ( $\mu\text{M C}$ )	C/N (HMW)
TW2	9	632	171	27	48	14.0
TW3	17	484	179	37	39	10
TW4	31	320	63	20	10	7.2
TW5	61	269	58	21	3	5.6
TW6	218	161	12	7	1	8.85
<i>E. huxleyi</i>	22	194	49	25	17	9.6
<i>Phaeocystis</i>	10	520	111	21	54	12.0

**Table 3.1** Ancillary data for the HMW DOM isolated from the phytoplankton cultures.

Day 0, in all cases (*T. weissflogii* (TW2, TW3, TW4, TW5 and TW6), *E. huxleyi* and *Phaeocystis*), marks the beginning of the phytoplankton cultures.

*Phaeocystis* culture, HMW DOC comprised 21% of the total DOC at the time of harvesting. HMW DOC and total DOC concentrations in these cultures at the time of harvesting are given in Table 3.1.

Figure 3.3 outlines the dynamics of the *T. weissflogii* culture in more detail. Chl-a (mg/l) and POC (mM) increased steadily from inoculation to harvesting, reaching a POC/Chl-a ratio of 45 (Figure 3.3A). In contrast, the changes in the carbon to nitrogen (C/N) ratio of the POC, shown in Figure 3.3B, are more dynamic over this time period. Values rose from 4 to 6 during the first two days of the culture, remained approximately constant for the next 3 days, and rose again sharply on day 5 to a value of 10, with little change thereafter. The final C/N ratio of the POC was 10.6 (day 8) corresponding to a PON concentration of 640  $\mu\text{M}$ . This value agrees well with the 600  $\mu\text{M}$  loss of nitrate from the medium (1217  $\mu\text{M}$  starting concentration (f/2 concentrations) and 615  $\mu\text{M}$  on day 8).

DOC concentrations in the culture also fluctuate, as shown in Figure 3.3B. There was no measurable change in DOC concentration until day 5, when the value rose sharply by 560  $\mu\text{M}$  to a maximum concentration of 842  $\mu\text{M}$ . This maximum was followed by a rapid decrease of 260  $\mu\text{M}$  to 582  $\mu\text{M}$  between days 5 and 6, and a slower, total increase of 53  $\mu\text{M}$ , over the course of the next three days to day 8, at which time the culture was harvested (TW2 on Figure 3.3B).

The density of the bacterial population in the diatom culture, prior to harvesting, was monitored in order to determine the extent of the bacterial contribution to DOM. The amount of bacterial carbon was only a small percentage of the total DOC ( $< 1\%$ ) throughout the culture and a small percentage of the total HMW DOC ( $< 2\%$ ) present at the end of the culture. Coincident with the rapid decrease in DOC concentration from day 5 to 6, bacterial cell numbers also increase. Although the increase in cell numbers between day 5 and 6 corresponds to a three-fold increase in the amount of bacterial carbon, this change accounts for only 3% of the loss in total DOC. If bacterial degradation alone was responsible for this DOC loss, nearly all the DOC (97%) must have been respired as  $\text{CO}_2$  and not incorporated into the bacterial biomass. Bacterial growth yields are usually in the range of 10 - 20 % (Kirchman et al., 1991; Smith et al., 1995). As the growth yields of 3% calculated above for our culture are unusually low, it is unlikely that bacteria are solely responsible for the loss of DOC. Other mechanisms, such as flocculation of DOC, must have played a role in the removal of DOC from our system. Bacteria were also present in the *E. huxleyi* and *Phaeocystis* cultures throughout the growth period, but accounted for less than 2% of the total DOC.

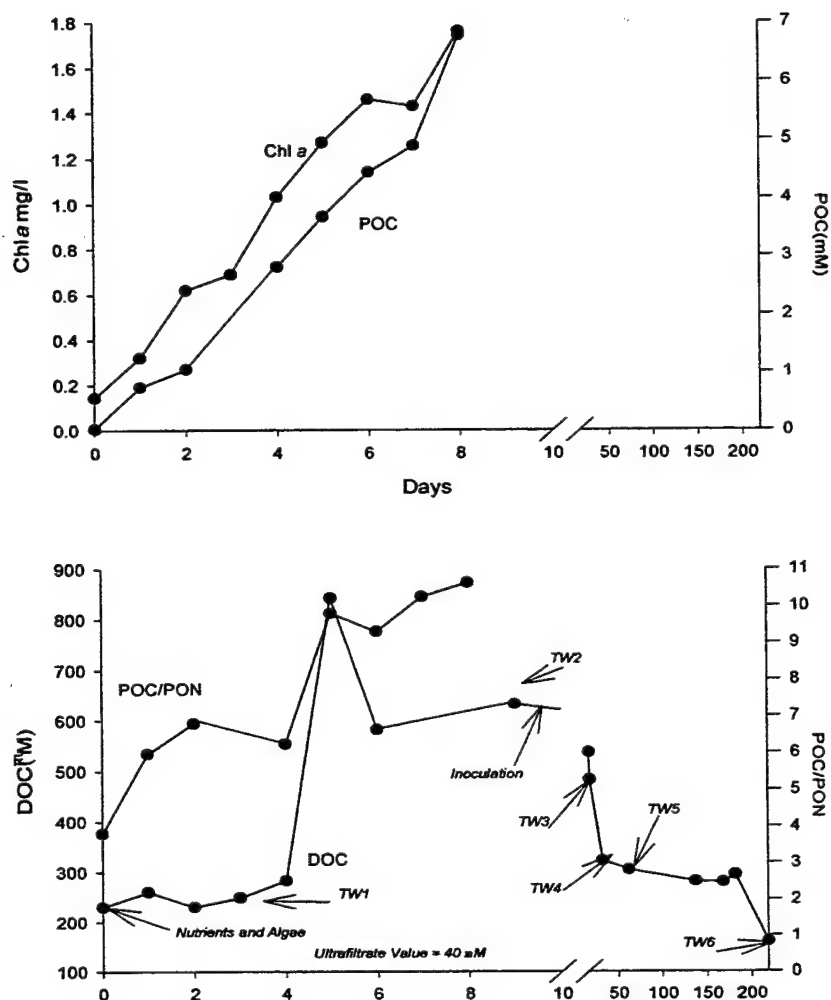


Figure 3.3 Ancillary data from the *Thalassiosira weissflogii* culture. (A) Changes in chl-*a* (filled squares) and POC (filled triangles). (B) Changes in the DOC (filled squares) concentration and C/N ratios of the POC (open triangles). Algae were removed on day 8. TW1, refers to the ultrafiltration sample taken during early log phase, TW2 was taken during late log phase, and TW3, 4, 5 and 6 were taken during the course of the degradation experiment after the algae had been removed. After day 9, changes in DOC concentration result from the action of microorganisms present in the incubation, or from physical removal mechanisms.

### 3.3.1.2 $^1\text{H}$ NMR Data

Proton nuclear magnetic resonance ( $^1\text{H}$ NMR) spectroscopy can be used to determine the major biochemicals present in each of the phytoplankton exudates. The  $^1\text{H}$ NMR spectra for HMW DOM isolated from the cultures at the time of harvesting are shown in Figure 3.4, along with a spectrum typical for seawater (Coastal Research Laboratory, Woods Hole, Massachusetts; Figure 3.4A). In all spectra, carbohydrate resonances dominate, with resonances between 3.2 and 4.7 p.p.m ( $\text{CHOH}$ ), 5 and 5.8 p.p.m (anomeric protons), and 1.3 p.p.m ( $\text{CH}_3$ , from rhamnose and fucose). Resonances at 2.0 p.p.m ( $\text{CH}_3\text{COO}$ ) arise from acetate and resonances at 0.9 p.p.m ( $\text{CH}_3$ ), and other resonances at 1.3 p.p.m ( $\text{CH}_2$ ) may arise from lipids. There is a close resemblance between the spectra of seawater and the exudates from *T. weissflogii* and *E. huxleyi* (Figure 3.4B and C). Although both exudates show the presence of carbohydrates, acetate and lipids, the proportions of these constituents are different from seawater. The ratio of carbohydrates:acetate:lipid carbon, calculated as in Chapter 2 (section 2.3.2.1), using  $^1\text{H}$ NMR peak areas, is 89:7:4 for the *T. weissflogii* exudate, and 89:6:3 for the *E. huxleyi* exudate. For comparison, this ratio in seawater HMW DOM is  $80 \pm 4:10 \pm 2:9 \pm 4$ . The  $^1\text{H}$ NMR spectrum of the *Phaeocystis* exudate is different (Figure 3.4 D) from the other exudates. In this spectrum, as with the others, the carbohydrate resonances dominate between 3.2 and 4.7 p.p.m. However, the acetate resonance at 2.0 p.p.m is smaller and the lipid resonance at 1.3 p.p.m is larger compared to the other exudates. The ratio of carbohydrate:acetate:lipid carbon in this sample is 90:2:5, showing the relative excess of carbohydrates compared to seawater. For all spectra (including seawater), the



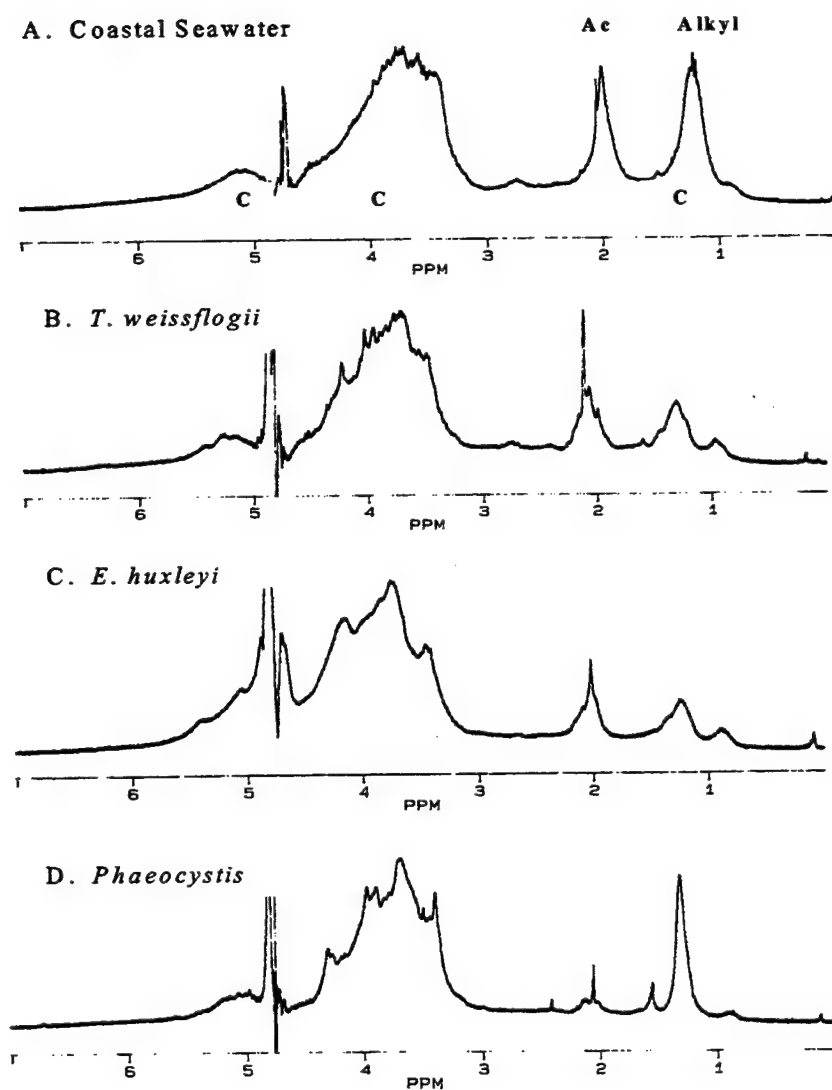


Figure 3.4  $^1\text{H}$ NMR spectra for HMW DOM isolated from seawater (Woods Hole) (A), and the exudates of *Thalassiosira weissflogii* (B), *Emiliania huxleyi* (C), and *Phaeocystis* (D). Carbohydrate resonances are between 3.2- 4.7 p.p.m (CHOH), 5-5.8 p.p.m (anomerics) and 1.3 p.p.m ( $\text{CH}_3$  from deoxy sugars). Spectra also show proton resonances for acetate (2.0 p.p.m) and lipids (1.3 and 0.9 p.p.m). The ratios of carbohydrate:acetate:lipid reported in the text are based on the areas under the peaks denoted C (for carbohydrates), Ac (for acetate) and Alkyl (lipids). To convert from hydrogen to carbon we use a C/H ratio of 1 for carbohydrates, 0.67 for acetate and 0.5 for lipids.

carbohydrate, acetate and lipid resonances discussed above account for approximately 70% of the total carbon in each HMW DOM sample.

#### 3.3.1.3 Monosaccharide Data

The relative distribution of neutral monosaccharides in the HMW fraction of each of the three exudates and seawater, analyzed as alditol acetates, are listed in Table 3.2 and shown in Figure 3.5. The seawater sample shown in Figure 3.5 is the average monosaccharide distribution in ten APS samples. Average seawater shows equal proportions of rhamnose, fucose, xylose, mannose and glucose ( $14 \pm 1\%$ ) with galactose being slightly enriched (21%) and arabinose being slightly depleted (6%) (Figure 3.5). While the exudates shown in Figure 3.5 also contain the same seven neutral monosaccharides, the relative proportions of these monosaccharides differ substantially for each sample. The relative distribution of monosaccharides in the *T. weissflogii* exudate shows  $4.3 \pm 1\%$  each, of rhamnose, fucose, arabinose and glucose; 15% xylose, 37% mannose and 30% galactose. In the case of *E. huxleyi*, the proportions are 5% fucose,  $9 \pm 1\%$  each of rhamnose, mannose and glucose, 12% xylose, 30% arabinose, and 24% galactose. The major monosaccharides in the *Phaeocystis* exudate are mannose (30%), rhamnose (21%), arabinose (17%) and galactose (16%). Xylose, glucose and fucose are also present, but in smaller quantities (6, 4 and 2% respectively). This exudate also contains an additional neutral monosaccharide, ribose, in a small quantity.

Samples	Rhamnose	Fucose	Arabinose	Xylose	Mannose	Glucose	Galactose	Ribose
Seawater	0.15	0.15	0.07	0.14	0.15	0.15	0.19	0
<i>T. weissflogii</i>	0.04	0.03	0.05	0.15	0.34	0.05	0.3	0
<i>E. huxleyi</i>	0.09	0.05	0.27	0.11	0.10	0.11	0.3	0
<i>Phaeocystis</i>	0.21	0.02	0.17	0.06	0.30	0.40	0.16	0.04

**Table 3.2** The relative distribution of monosaccharides in *T. weissflogii*, *E. huxleyi*, and *Phaeocystis* at the time of harvesting.

Monosaccharides accounted for 15% (Seawater), 28% (*T. weissflogii*), 35±10% (*E. huxleyi*), and 49±9% (*Phaeocystis*) of the total carbon in the HMW exudates. Seawater is the average distribution in 10 samples from the Northwest Atlantic, an estuary in Oosterschelde (Aluwihare et al. 1997), the Sargasso Sea and the Gulf of Mexico (McCarthy et al., 1996), and Mikawa Bay (Sakugawa and Handa, 1985b).

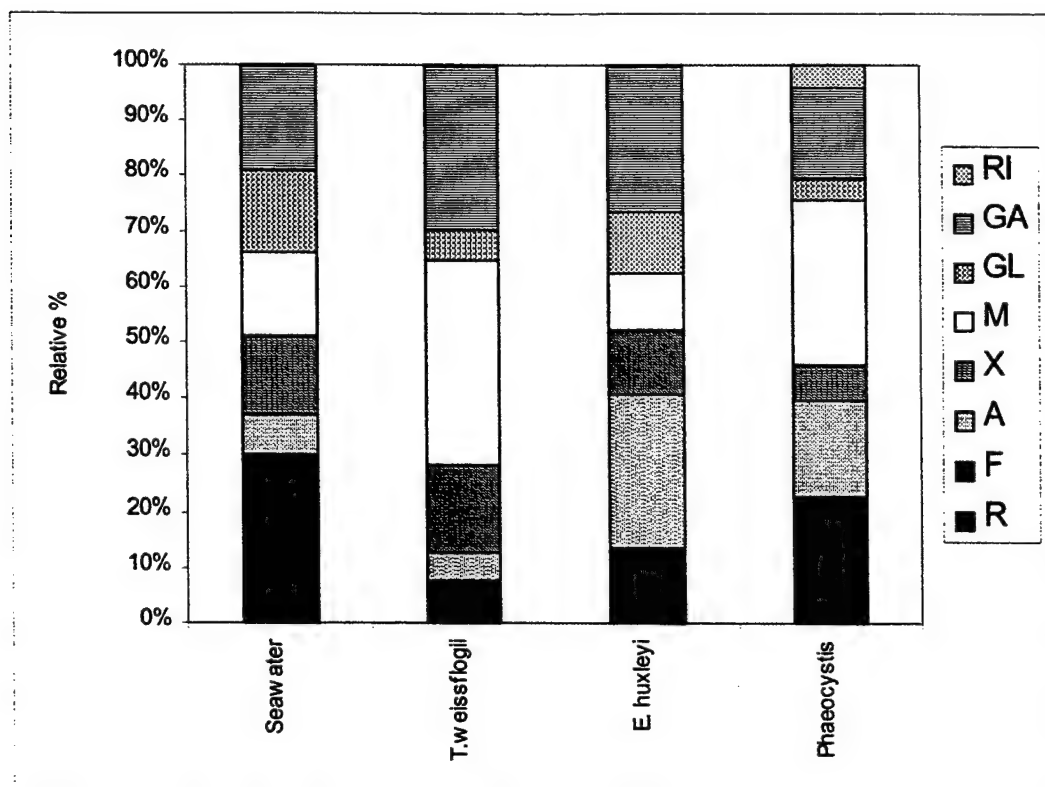


**Figure 3.5** The relative distribution of monosaccharides in HMW DOM isolated from seawater, and the exudates of *Thalassiosira weissflogii*, *Emiliania huxleyi*, and *Phaeocystis*. R is rhamnose, F is fucose, A is arabinose, X is xylose, M is mannose, GL is glucose, GA is galactose, and RI is ribose. The seawater sample represents the average distribution of monosaccharides in ten seawater samples (the standard deviation is less than  $\pm 3\%$  for each monosaccharide).

### 3.3.2 Bacterial Degradation of the *T. weissflogii* Exudate.

#### 3.3.2.1 Changes in DOC

In order to observe chemical changes in the exuded DOM due to bacterial degradation, *T. weissflogii* were harvested by filtering on day 8 and the filtrate inoculated with Whatman GF/F filtered seawater. The changes in total DOC after inoculation are also shown in Figure 3.3B (days 9-218) and listed in Table 3.1.

Three hundred  $\mu\text{M}$  C were lost from the DOC pool during the first three weeks (days 9-31) of the incubation experiment. Approximately 50% of this DOC removal

occurred over the first week of the incubation (day 9 through 17, TW2 to TW3 from Figure 3.2 and Table 3.1), during which time the concentration of HMW DOC showed no change. Over this time period there must have been a balance between the production and removal of DOC within the HMW fraction (note the changes in the  $^1\text{H}$ NMR spectra (Figure 3.6)), total hydrolyzable monosaccharide concentrations and C/N ratios in HMW DOM (Table 3.1) between these two time points). Thus, the net change in DOC concentration reflects the reactivity of the <1kD (low molecular weight) fraction of DOC during the first week of the degradation, and suggests some synthesis of HMW DOM from LMW DOM by microbes. During the next two weeks (days 17-31; TW3 to TW4 from Figure 3.3 and Table 3.1) the concentration of HMW DOC decreased by 100  $\mu\text{M}$  accounting for 70% of the loss in total DOC. After the first three weeks, the removal of DOC slows down considerably. From day 31 to 61 (TW4 to TW5, Figure 3.3 and Table 3.1), the 50  $\mu\text{M}$  decrease in total DOC concentration is accompanied by little change in the concentration of HMW DOC (but HMW monosaccharide concentration decrease over this time period (Table 3.1)). Removal rates continue to decrease over the last five months of the experiment (TW5 to TW6) resulting in a 100  $\mu\text{M}$  decrease in the total DOC concentration. The concentration of HMW DOC also decreases over this time period, and can account for approximately 30% of the loss from the total DOC pool.

At day 218 of the experiment, when DOC concentrations had reached 161  $\mu\text{M}$ , the filtrate was re-inoculated to determine if any microbially labile DOC remained in the culture. Following the inoculation, oxygen concentration measurements yielded a total consumption of 7  $\mu\text{M}$  oxygen over a three month period, indicating that the remaining

organic matter was refractory to bacterial degradation (nutrient concentrations remained high throughout this period).

### 3.3.2.2 $^1\text{H}$ NMR Data

Proton nuclear magnetic resonance ( $^1\text{H}$ NMR) spectroscopy was used to monitor the changes in HMW DOM as the total *T. weissflogii* exudate was degraded. Shown in Figure 3.6 are spectra for the HMW exudate one week (Figure 3.6A, day 17, TW3) and three weeks (Figure 3.6B, day 31, TW4) after the inoculation. The  $^1\text{H}$ NMR spectra of TW5 and TW6 (not shown) are very similar to the  $^1\text{H}$ NMR spectra of TW3 and TW4. However, between TW4 and TW5, there is a decrease in carbohydrate resonances relative to other resonances (between 1 and 3 p.p.m) (the ratio of carbohydrate carbon/other carbon decreases from 3 to 2). When these spectra are compared to the  $^1\text{H}$ NMR spectrum of the *T. weissflogii* exudate at the time of harvesting (day 9 of the experiment) shown in Figure 3.4B, new resonances in the region between 1.9 and 3.1 p.p.m are apparent. These resonances may be attributed to proteins excreted into the medium by microorganisms, or to small microbes ( $< 0.2\ \mu\text{m}$ ) concentrated in the sample during ultrafiltration. Protein resonances were removed by passage through a cation exchange column (BioRad AG 50W-X8), which increases the C/N ratios of the samples from 10 and 7 (prior to passage through the column) to 14 (after passage through the cation exchange column), consistent with removal of protein (nitrogen containing fraction). The  $^1\text{H}$ NMR spectra of these cleaned samples (Figure 3.6 insets) closely resemble the spectrum of HMW DOM isolated when the algae were harvested (Figure 3.4 B) and the seawater spectrum shown in Figure 3.4 A.

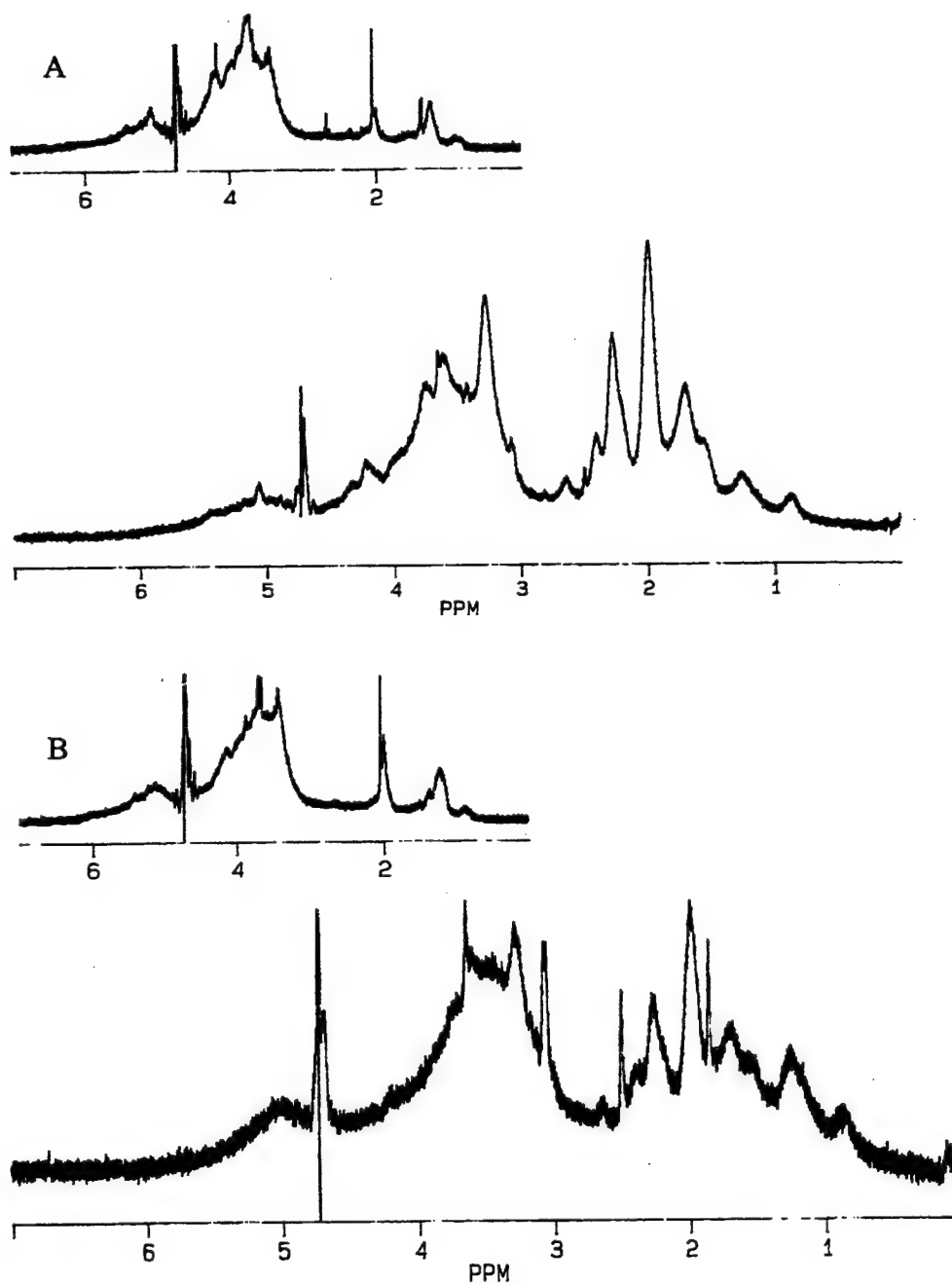


**Figure 3.6**  $^1\text{H}$ NMR spectra of two HMW DOM samples isolated during the degradation of the *Thalassiosira weissflogii* exudate, TW3 (A) and TW4 (B). Resonances between 1.9-3.1 p.p.m are thought to arise from proteins which can be removed by passage through a cation exchange column (insets).

### 3.3.2.3 Monosaccharide Data

The removal of polysaccharides during the incubation of the *T. weissflogii* exudate was followed using the changes in monosaccharide concentrations. These data are shown in Table 3.3. The overall changes occur in three stages. During the first stage which spans the first three weeks of the incubation (TW2 (day 9) to TW4 (day 31)), polysaccharide concentrations (Table 3.1) decrease by 80% accounting for 40% of the decrease in the HMW DOC concentration. Mannose and galactose are preferentially removed, compared to other monosaccharides, with an overall 90% decrease in mannose concentration, and a 75% decrease in galactose concentration. At the end of the third week, galactose, mannose and xylose are still the most abundant sugars but their dominance is diminished, making the relative distribution of sugars more even. Between TW4 (day 31) and TW5 (day 61), there is a decrease in the concentrations of all monosaccharides (except arabinose). Rhamnose, xylose, mannose and galactose all experience an 80-90% decrease in concentration, indicating removal of these sugars during the second month of the degradation. Over the last five months of the degradation (TW5 to TW6) there is an increase in fucose concentrations, and a decrease in arabinose concentration.



Monosaccharide Data											
Sugars	TW2 %C	TW2 Concentration $\mu\text{M C}$	TW3 %C	TW3 Concentration $\mu\text{M C}$	TW4 %C	TW4 Concentration $\mu\text{M C}$	TW5 %C	TW5 Concentration $\mu\text{M C}$	TW6 %C	TW6 Concentration $\mu\text{M C}$	
NAG	0.8	1.4	0.6	1.1	0.8	0.5	0.1	0.06	0.5	0.06	
G	1.7	2.9	1	1.8	1.4	0.9	1.2	0.70	2	0.24	
R	1.2	2.1	1.1	2.0	1.4	0.9	0.3	0.17	0.5	0.06	
F+A	2.3	3.9	1.1	2.0	1.7	1.1	2.2	1.28	1.5	0.18	
X	3.9	6.7	3	5.4	2.6	1.6	0.3	0.17	0.3	0.05	
M	11.3	19.3	9.8	17.5	3.3	2.1	0.5	0.29	0.5	0.06	
GA	9.2	15.7	6.7	12.0	5.6	3.5	0.4	0.23	0.4	0.05	
TOTAL	30.4	51.984	23.3	41.7	16.8	10.6	5	2.9	5.7	0.7	

Table 3.3 Absolute concentrations of monosaccharides at the time of harvesting (TW2) and at each of the time points during the incubation experiment (TW3, TW4, TW5 and TW6) for *Thalassiosira weissflogii*. % C refers to the percent of total carbon in the sample accounted for by each of the monosaccharides.

### 3.3.2.4 Amino Acid Data

The  $^1\text{H}$ NMR data discussed in section 3.3.2.2 indicated the presence of protein resonances in HMW DOM isolated from the incubation experiment. The data for the amount of nitrogen and carbon associated with hydrolyzable proteins are shown in Table

3.4. Consistent with the  $^1\text{H}$ NMR data, all samples isolated from the incubation

<b>Amino Acid Data</b>								
<i>Amino Acids</i>	<i>TW3</i>		<i>TW4</i>		<i>TW5</i>		<i>TW6</i>	
	%C	%N	%C	%N	%C	%N	%C	%N
Aspartic	0.64	2.01	1.04	2.34	0.04	0.07	0.32	0.90
Glutamic	1.01	2.53	0.65	1.16	0.09	0.13	0.83	1.87
Serine+Histidine	6.46	17.93	4.40	8.80	0.16	0.27	1.80	4.50
Glycine	0.43	2.70	0.40	1.80	0.06	0.23	0.42	2.37
Threonine+Arganine	2.65	8.28	1.40	3.15	0.07	0.13	0.34	0.96
Alanine	0.64	2.68	0.56	1.69	0.12	0.30	0.34	1.29
Tyrosine	0.23	0.32	0.24	0.24	0.95	0.79	0.49	0.61
Methionine	0.18	0.44	0.18	0.33	0.05	0.07	0.03	0.08
Valine	0.50	1.26	0.39	0.69	0.07	0.10	0.17	0.37
Ph-Alanine	0.62	0.87	0.54	0.54	0.10	0.08	0.25	0.31
Isoleucine	0.41	0.85	0.30	0.45	0.06	0.08	0.15	0.28
Leucine	0.67	1.40	0.64	0.96	0.09	0.11	0.24	0.45
Lysine	0.12	0.51	0.12	0.36	0.01	0.04	0.13	0.50
<b>Total %</b>	<b>15</b>	<b>42</b>	<b>11</b>	<b>22</b>	<b>2</b>	<b>2</b>	<b>5</b>	<b>14</b>
<b>Concentration (<math>\mu\text{M}</math>)</b>	<b>27.0</b>	<b>7.5</b>	<b>7</b>	<b>2</b>	<b>1.2</b>	<b>0.2</b>	<b>0.6</b>	<b>0.2</b>

**Table 3.4 Concentrations of the individual amino acids in HMW DOM isolated during the degradation of the *T. weissflogii* exudate (TW3, TW4, TW5 and TW6).**

experiment contain proteins. Amino acid yields for TW3 and TW4 account for a large fraction of the nitrogen in these samples (44 and 24%, respectively). Although the fraction of carbon and nitrogen derived from amino acids increases from TW5 to TW6, there is an overall decrease in the concentration of carbon and nitrogen associated with these amino acids over the course of the incubation. As expected, the C/N ratio of the

total amino acid fraction is constant (between 3 and 4) during the incubation, except in the case of TW5, when this ratio increases to 6. This data is consistent with the relative distribution of amino acids which shows a marked relative increase in tyrosine at TW5 (30% of the total amino acid nitrogen, and 50% of the amino acid carbon), which has C/N ratio of 9. The relative distribution of amino acids in HMW DOM isolated from the incubation is shown in Figure 3.7. There is considerable variation in the relative distribution of amino acids in these samples suggesting that the protein fraction is dynamic.

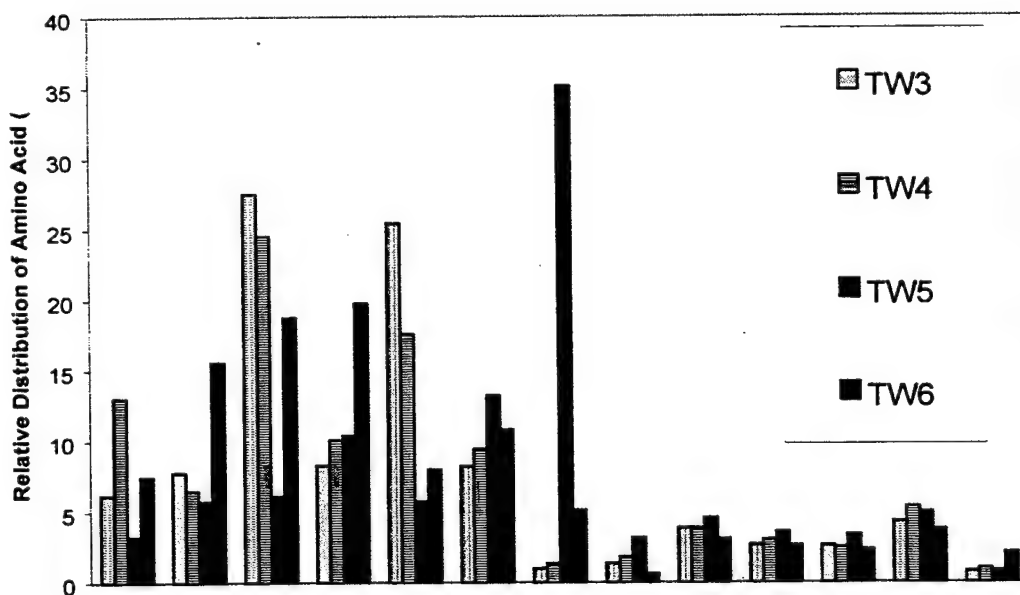


**Figure 3.7** The relative distribution of amino acids in HMW DOM isolated during the degradation of the *Thalassiosira weissflogii* exudate, expressed as the percentage of each amino acid accounted for by the culture sample. Amino acid are: aspartic acid, glutamic acid, serine and histidine, glycine, threonine and arginine, alanine, tyrosine, methionine, valine, phenylalanine, isoleucine, leucine and lysine.

### 3.4 Discussion

#### 3.4.1 Phytoplankton Cultures

The major goals of this study were to determine if polysaccharides produced by algae chemically resemble acylated polysaccharides (APS) isolated from seawater and to monitor changes in the chemical characteristics of the exuded polysaccharides during microbial degradation. As shown by  $^1\text{H}$ NMR, seawater APS consist mainly of carbohydrates ( $80\pm 4\%$  of the total carbon), acetate ( $10\pm 2\%$  C) and lipid ( $9\pm 4\%$  C). Monosaccharide analyses have shown that APS are composed of seven major neutral monosaccharides, rhamnose, fucose, xylose, arabinose, mannose, glucose and galactose present in a relatively fixed ratio (Aluwihare et al. 1997).

The nuclear magnetic resonance ( $^1\text{H}$ NMR) spectra shown in Figure 3.4 indicate that the HMW DOM produced by *T. weissflogii* and *E. huxleyi* have spectral characteristics similar to seawater APS. However, the relative areas under each of resonances in these spectra indicate an excess of carbohydrate in extracellular HMW DOM isolates (89:7:4 (carbohydrate:acetate:lipid carbon) for *T. weissflogii* and *E. huxleyi*) compared to seawater ( $80\pm 4:20\pm 2:10\pm 4$ ). In the case of *Phaeocystis*, the  $^1\text{H}$ NMR spectrum shows very little acetate (90:2:5, for carbohydrate:acetate:lipid carbon).

When the distribution of monosaccharides in each of the exudates (Figure 3.5) is compared to seawater, the presence of polysaccharides other than APS is apparent. Unlike seawater, where the major polysaccharide is APS, the algal exudates are comprised of a mixture of polysaccharides, including APS. The abundance of polysaccharides in the exudates relative to seawater HMW DOM was indicated by the yield of monosaccharides upon hydrolysis (Table 3.1 and Table 3.3). As shown in

Chapter 2, neutral monosaccharides contribute between 7-20% of the carbon in HMW DOM (Aluwihare et al., 1997; Borch and Kirchman, 1997; McCarthy et al., 1996; Skoog and Benner, 1997) isolated from surface seawater. At the time of harvesting, neutral monosaccharides were 28% of the total HMW DOC in the *T. weissflogii* exudate,  $35 \pm 10\%$  of the *E. huxleyi* exudate, and  $49 \pm 9\%$  of the *Phaeocystis* exudate. In all cases including seawater, the amount of carbohydrate carbon determined by  $^1\text{H}$ NMR spectroscopy (section 3.3.2) is approximately double the alditol acetate monosaccharide yield.

In order to investigate the similarity between seawater APS and the algal exudates, we calculated the correlation between the relative distribution of monosaccharides in each culture sample and seawater. The correlation coefficient between samples is calculated by dividing the covariance in the monosaccharide distribution of two samples (e.g. seawater vs. *T. weissflogii*) by the product of their standard deviations ( $\sigma$ ). In all cases, the absolute values of the correlation coefficients are reported. The *T. weissflogii* sample (at the time of harvesting) exhibits only a weak correlation with seawater (0.34), confirming that the monosaccharide distribution in these two samples is quite different. Two correlation coefficients were calculated for *E. huxleyi*. The first (0.32) was generated using the monosaccharide distribution shown in Figure 3.5, while the second (0.85) was generated after arabinose (the dominant sugar in the distribution) was removed from the analysis. Without arabinose (which contributed 30% of the monosaccharides in HMW DOM), the monosaccharide distribution in the exudate closely resembled the distribution seen for seawater. This analysis is consistent with the conclusion that the HMW exudate from *E. huxleyi* mainly comprised mainly of

APS and an arabinose dominated polymer. For *Phaeocystis*, the sugar distribution cannot be easily manipulated to increase the correlation coefficient (0.28) because several of the monosaccharides dominate the exudate (see Figure 3.5).

While the  $^1\text{H}$ NMR data support the idea that the *T. weissflogii* and *E. huxleyi* exudates contain APS, the monosaccharide and correlation coefficient analyses imply that if APS is present, it is only a fraction of the total polysaccharides in each exudate. In the case of *Phaeocystis*, the relative distribution of monosaccharides together with the  $^1\text{H}$ NMR data suggests that APS (if present), is only a very small component of the total HMW exudate.

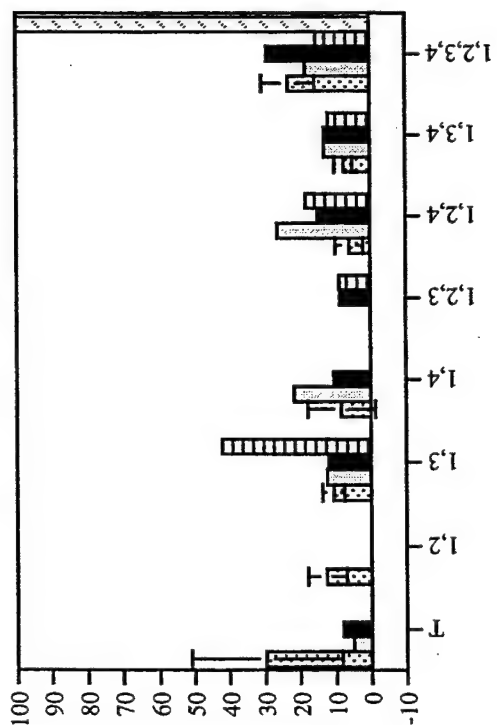
Non APS monosaccharides in the exudates were estimated by subtracting the APS associated monosaccharides from the total. Monosaccharides associated with APS in the *T. weissflogii* and *E. huxleyi* exudates were calculated using the relative distribution of monosaccharides observed in seawater, and assuming that all the rhamnose present in the exudates was derived from APS. The data were normalized to rhamnose because it was the least abundant monosaccharide in these exudates. The relative distribution of non APS monosaccharides in the *T. weissflogii* exudate was dominated by mannose and galactose (~40% each of the total excess). In the case of *E. huxleyi*, the dominant non APS monosaccharides were arabinose (50%), and galactose (35%). The abundance of neutral hexoses in the non APS fraction may be explained by the presence of storage polysaccharides in the exudates. Furthermore, in contrast to the heterogeneous monosaccharide distribution in APS, non APS polysaccharides contain mostly 2 or 3 monosaccharides. In the case of *Phaeocystis*, fucose was the least abundant monosaccharide and was thus used for the calculation of APS. However, due to the low

concentration of fucose in this sample, the removal of APS associated monosaccharides did not significantly change the overall distribution of monosaccharides in this sample.

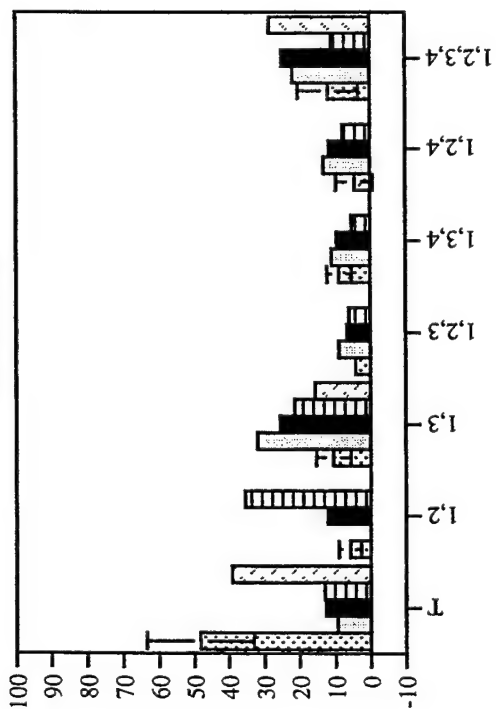
Results from the linkage analysis for rhamnose, fucose, xylose, glucose and galactose in the total HMW DOM isolated from seawater and the cultures at the time of harvesting are shown in Figure 3.8 as TW2, *E. huxleyi*, and *Phaeocystis*. Most of the linkages present in seawater are found in the culture samples, and in all cases, their relative abundance in the culture samples fall within the range observed for seawater. From this data it is apparent that the exudates from *T. weissflogii* and *E. huxleyi* could contain compounds related to APS. The *Phaeocystis* sample shows some significant differences compared to the other two samples and compared to seawater. With the exception of rhamnose (the second most abundant sugar), this sample has fewer linkages per sugar, for example, 50% of arabinose present is linked at all positions; 40% of rhamnose is terminal and 69% of xylose is linked at carbon 1,2, and 3. Fucose was only identified linked at all positions; however, this is the least abundant sugar in the sample, and other linkages may be present in very small quantities. The simplicity of the *Phaeocystis* linkage data suggests that this exudate probably contains a much simpler mixture of polysaccharides compared with the other two exudates.

The presence of polysaccharides in the exudates of diatoms grown in culture, has been noted in numerous studies (Allan et al., 1972; Biersmith and Benner, 1998; Haug and Myklestad, 1976; Hecky et al., 1973; Myklestad, 1974; Myklestad et al., 1972; Percival et al., 1980; Smestad et al., 1975) Table 3.5). The exudates examined in Table 3.5, contain many different monosaccharides with different linkage types, consistent with

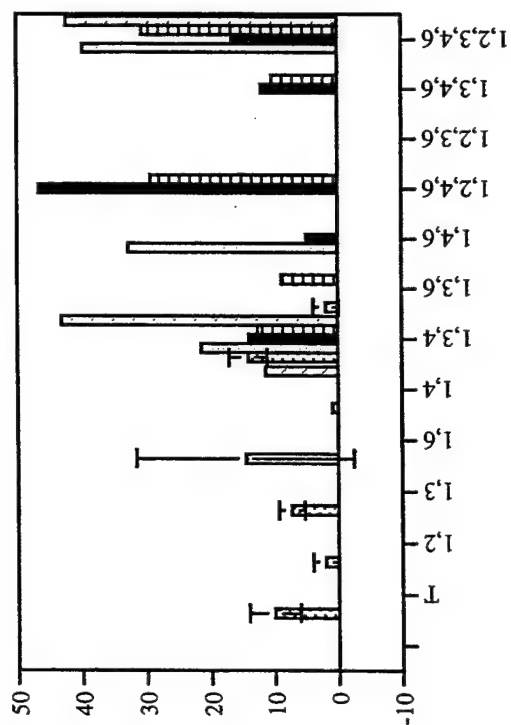
# Fucose



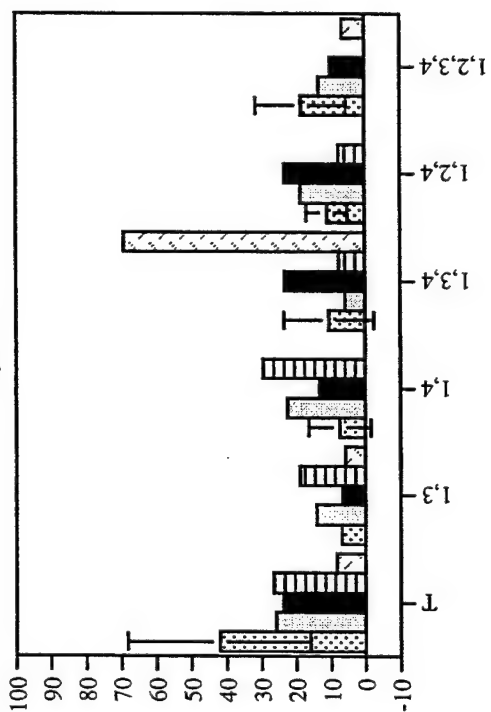
# Rhamnose



# Glucose



# Xylose



- Seawater
- TW2
- TW4
- E. Huxleyi*
- Phaeocystis*



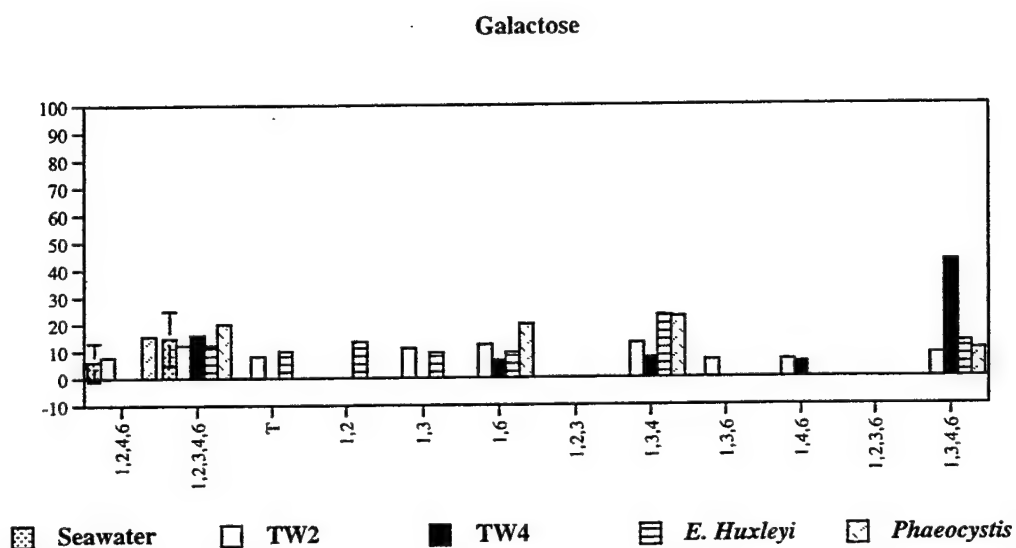


**Figure 3.8** Carbohydrate linkage data for the exudates. TW2, *E. huxleyi* and *Phaeocystis* samples were taken when the cultures were harvested. TW4 was isolated during the *Thalassiosira weissflogii* incubation experiment. The number beneath each bar refers to the linkage site on each monosaccharide (i.e. carbon 1 and 6 as 1,6), and T refers to linkages through carbon 1 only. Only linkages which constitute > 5% of each sugar are listed.

the data for *T. weissflogii* presented in this chapter. All the species examined produced extracellular DOM with varying amounts of rhamnose and galactose. When fucose was present it was a major fraction of the total monosaccharides, while xylose, arabinose, mannose, and glucose were found in varying amounts in most of the exudates. These data demonstrate the heterosaccharide nature of the exuded polymers in accordance with what is observed in this study. In contrast, the extraction of whole diatom cells with water mainly yields homopolymers such as glucans (see Table 3.5). However, cell walls and the alkali soluble fraction of whole cells (listed in Table 3.5 under water insoluble at pH = 7) have also been shown to contain many of the different monosaccharides discussed above, indicating that structural polysaccharides are heterogeneous. Direct comparison of the relative distribution of these monosaccharides indicates that for the diatoms considered in these studies, clear compositional differences exist between intracellular and extracellular carbohydrates. Some chemical data are also available on extracellular DOM produced by *Phaeocystis* (Table 3.5). The organic mucus which surrounds the cell has been shown to be polysaccharide (Painter, 1983), but the monosaccharide composition of this gel-like material seems to vary among species. The studies listed in Table 3.5 (Biersmith and Benner, 1998; Guillard and Hellebust, 1971; Janse et al., 1996) reported the presence of rhamnose, arabinose, xylose, mannose, galactose and glucose in the *Phaeocystis* exudate. In some cases, fucose, uronic acids and small amounts of O-methylated sugars were also detected. The *Phaeocystis* species grown in this study (CCMP 628) was an isolate from coastal Surinam and contained the

Taxon	Extracellular	Extract Monosaccharides		Reference	
		Water Insoluble (at pH=7)	Water Soluble (pH=7)		
<i>Diatoms</i>					
<i>Asionella socialis</i>	R(70), F(tr), M(7), X(tr), GA(tr), GL(tr), ?(8), ?(15)	R(tr), F(tr), M(22), X(tr), GA(5), GL(tr), ?(29), ?(10)	GL	3.2 Allan et al., 1972	
<i>Chaetoceros affinis</i>	R(35), F(39), GA(26)	R(25), F(7), RI(15), M(11), X(8), GA(22), GL(3)		Myklestad et al., 1972 Smestad et al., 1972 Haug and Myklestad, 1976	
<i>Chaetoceros curvisetus</i>	R(3), F(35), GA(10)	R(13), F(14), R(18), M(12), X(8), GA(30), GL(5)		Smestad et al., 1972 Haug and Myklestad, 1976	
<i>Chaetoceros debilis</i>	R(17), F(30), M(10), X(9), GA(29), GL(5)	R(22), F(8), RI(31), M(2), X(19), GA(23), GL(4)		Haug and Myklestad, 1976	
<i>Chaetoceros decipiens</i>	R(34), F(32), M(7), X(5), GA(17), GL(5)	R(27), F(5), RI(10), M(24), X(2), GA(10), ?(22)		Haug and Myklestad, 1976	
<i>Chaetoceros socialis</i>		R(10), F(10), RI(20), M(15), X(12), GA(19), GL(7), ?(7)	GL	Haug and Myklestad, 1976	
<i>Chaetoceros species</i>				Haug and Myklestad, 1976	
<i>Corethron hystrix</i>		R(3), F(31), RI(17), M(12), X(12), GA(13), GL(12)		Haug and Myklestad, 1976	
<i>Coscinodiscus nobilis</i>	R(15), F(34), M(19), X(6), GA(tr), GL(16)			Percival et al., 1980	
<i>Cyclotella cryptica</i>		R(7), F(12), M(37), X(18), GA(12), GL(13)		Hecky et al., 1973	
<i>Cyclotella nana</i>	R(33), F(tr), RI(8), M(10), X(7), GA(14), GL(11), ?(4), ?(13)			Allan et al. 1972	
<i>Cyclotella stelligera</i>		F(0.6), A(2), M(14), X(18), GA(22), GL(43)		Hecky et al., 1973	
<i>Nitzschia angularis</i>	R(20), F(16), A(8), M(7), X(7), GA(17), GL(tr), ?(4), ?(21)	R(tr), F(64), M(11), X(tr), GA(4), GL(14), ?(7)		Allan et al. 1972	
<i>Nitzschia brevisstris</i>		R(2), F(43), RI(5), A(2), M(20), X(4), GA(10), GL(15)		Hecky et al. 1973	

Taxon	Extracellular	Extract Monosaccharides Water Insoluble (at pH=7)	Water Soluble (pH=7)	Reference
<b>Diatoms</b>				
<i>Skeletonema costatum</i>		R(12),F(10),R(1),A(2), M(55),X(11),GA(3),GL(6)		Handa, 1969
<i>Thalassiosira gravida</i>		F(25),R(27),M(12),X(12), GA(17),GL(7)		Haug and Mykleslad, 1976
<i>Skeletonema costatum</i>	R(5), A(2),X(4),F(12), M(14), GA(4), GL(60)			Biersmith and Benner 1998
<b>PHAEOCYSTIS</b>				
sp.				
<i>Phaeocystis</i> *	R(5),A(40),M(15),X(17), GA(15),Me(8),[GL (variable)]			Janse et al. 1996b
<i>Phaeocystis globosa</i>			GL	Janse et al. 1996a
<i>Phaeocystis poucheti</i> (Woods Hole)	R(19.5),R(3),A(5),M(27), X(3),GA(5.5),GL(30)			Guillard and Hellebust, 1971
<i>Phaeocystis poucheti</i> (Surinam)	R(16),R(8),M(64),X(1.5), GA(2),GL(4.5)			Guillard and Hellebust, 1971
<i>Phaeocystis</i> sp	R(6),R(2),M(16),X(13), GA(4),GL(17),A(13),F(4)			Biersmith and Benner, 1998

\*average estimates of the data plotted in the paper – relative distribution without glucose

**Table 3.5 Monosaccharide composition of polysaccharides isolated from different species of algae.**

Linkage analysis was performed on (A) *Chaetoceros affinis* extracellular polysaccharide: terminal rhamnose; 1,2-, 1,3-, and 3,4-rhamnose; terminal fucose; 1,3-, 1,3,4-, 1,2,3-fucose; terminal galactose and 1,3-, 1,4- galactose; (B) *Chaetoceros curvisetus* extracellular polysaccharide: terminal rhamnose; 1,2-rhamnose; terminal fucose; 1,2-, 1,3-, 1,2,3-, 1,3,4-fucose; terminal galactose; 1,3-, 1,2,3-galactose, (C) *Coscinodiscus nobilis* extracellular polysaccharide: terminal rhamnose; 1,2-, 1,2,3-, 1,2,4- and 1,3,4-rhamnose; terminal fucose; 1,3-, 1,2,4-, 1,3,4-fucose; terminal xylose; 1,4-xylose; terminal mannose; 1,3-, 1,4-, 1,6-, 1,2,4-, 1,2,6-, 1,3,6 –mannose; terminal glucose; 1,3-, 1,4-, 1,2,4-, 1,3,6 glucose were detected.

complex mixture of neutral monosaccharides (including ribose) observed by other investigators. In our samples the dominant sugars are arabinose, rhamnose, and mannose, with fucose present only in a very small amount. Fucose has not been reported in the literature to be abundant in *Phaeocystis* extracellular polysaccharides. While the monosaccharide distributions discussed above were qualitatively similar to APS isolated from seawater, these distributions alone do not allow a definitive comparison between the polymers isolated from seawater and those exuded by phytoplankton in culture.

#### 3.4.2 Degradation of the *T. weissflogii* exudate

Norrman et al. (1995) demonstrated that DOM with a range of turnover times, was produced by algae in culture. Here, we expanded on their study by following the compositional changes within the polysaccharide fraction, including APS, as the total *T. weissflogii* exudate was subjected to microbial degradation. These data can be used to determine if the chemical composition of the refractory material persisting in culture differs from the chemical composition of the compounds present at the time of exudation. In addition, we directly compare the DOM present at the end of the degradation to the DOM isolated from seawater.

To quantitatively compare HMW DOM left in the degradation experiment with APS isolated from seawater (Figure 3.4 A), we used the carbohydrate to acetate carbon ratio in each of these samples. This ratio varies little in seawater APS ( $8 \pm 2$ ), and is well established by our previous studies (Aluwihare et al. 1997). Although both inset spectra in Figure 3.6 contain the same resonances, there is a difference in the relative abundance of acetate. The carbohydrate/acetate carbon ratio at the time of harvesting (Figure 3.3 B) was 15, and at TW3, after one week of degradation, (Figure 3.6 A, inset), was comparable at 18. Two weeks later, at TW4, (Figure 3.6 B, inset) the ratio drops to 10,

not significantly different from the ratio of 8 ( $\pm 2$ ) observed for seawater. One month later, at TW 5, this ratio was still 10. However, at TW6 (5 months later), the ratio of carbohydrate/acetate carbon increased to 13, consistent with the changes in the monosaccharide data discussed below. The overall decrease in this ratio is brought about by a more rapid loss of total carbohydrate compared to the acetate containing (perhaps APS) fraction. This indicates that the different polysaccharides within the exudate have different removal rates, consistent with the findings of Norrman et al. (1995), and as the exudate is degraded, the remaining polysaccharide component resembles APS more closely. Collectively, the NMR data indicate that a component closely resembling seawater APS is produced by *T. weissflogii* in culture (Figure 3.3 B) and is present throughout the incubation (Figure 3.5 A and B). Furthermore, carbohydrate/acetate carbon ratios indicate that this APS component is concentrated relative to other HMW components as the degradation proceeds.

The neutral monosaccharide data, for the different time points during the incubation, also supports the accumulation of APS as HMW DOM is degraded. During the degradation there is a shift in the monosaccharide distribution from one that is dominated by the hexoses (mannose and galactose) to one that is more evenly distributed amongst the seven neutral sugars. Consistent with the NMR data, the monosaccharide data indicate that a polysaccharide resembling APS exists within the algal exudate, but that its presence is partially obscured by hexose-dominated polysaccharides.

Correlation coefficient analysis was used to determine the similarity between the relative distribution of monosaccharides in each of the samples isolated from the incubation and seawater. TW2 and TW3 are closely correlated with each other (0.9) but

only exhibit a small correlation with seawater (0.32 and 0.33, respectively). TW4 and TW5 exhibit a stronger correlation with seawater, 0.7 and 0.8, respectively, showing that as the exudate is degraded, the monosaccharide distribution in the HMW exudate approaches the distribution observed for seawater. At the end of the incubation (TW6), the correlation coefficient is lower than at the beginning of the experiment (0.15), due to a relative increase in glucose and fucose. These sugars may be preferentially concentrated with time and/or added (in the case of fucose) during the incubation. The low correlation at TW6 is consistent with the increase in the carbohydrate to acetate ratio calculated from the NMR spectrum, indicating a change in the relative abundance of APS between TW5 and TW6. As shown by the correlation coefficient analysis, there is a considerable change in the relative distribution of monosaccharides over the course of the incubation. Given these changes in the monosaccharide distribution, we were interested to see if the linkage data showed similar variations. The linkage data from two time points, TW2 and TW4, are compared in Figure 3.8. The linkage pattern of each monosaccharide falls within the range observed for seawater. For certain sugars (for example the deoxy hexoses and pentoses) the linkage pattern in TW4 more closely approached the average seawater distribution, consistent with the correlation coefficient analysis. However, the variations in the linkage patterns between these two time points are not reflective of the much more pronounced difference in their relative monosaccharide distribution. Before any specific conclusions can be drawn from these results, however, more data and analyses are necessary.

An accumulation of the APS-like component relative to other polysaccharides in the incubation experiment is suggested by the changes in the carbohydrate:acetate carbon

ratio calculated from the  $^1\text{H}$ NMR spectra and the relative distribution of monosaccharides. Given these data, we attempted to compare the change in the concentration of total polysaccharides (as analyzed by alditol acetates), to the change in the relative concentration of the component resembling APS, over the course of the degradation (Figure 3.9). The APS fraction was calculated by assuming that all the rhamnose in HMW DOM is present within APS at each of the time points sampled during the incubation. Total APS concentrations are calculated using the seawater monosaccharide distribution shown in Figure 3.5. The monosaccharide data were normalized to rhamnose because it was the least abundant monosaccharide at the beginning of the incubation and thus estimates the maximum possible loss of APS over the course of the incubation. Both APS and total polysaccharide concentrations decreased over the course of the incubation, however, the initial rate of degradation was slower for the calculated APS fraction than for the total polysaccharides. Thus, the percentage of APS in the total polysaccharide fraction increases from 31 to 68%, over the course of the incubation. This data suggests that although APS is labile, there are other polysaccharides within the exudate that are degraded faster than APS.



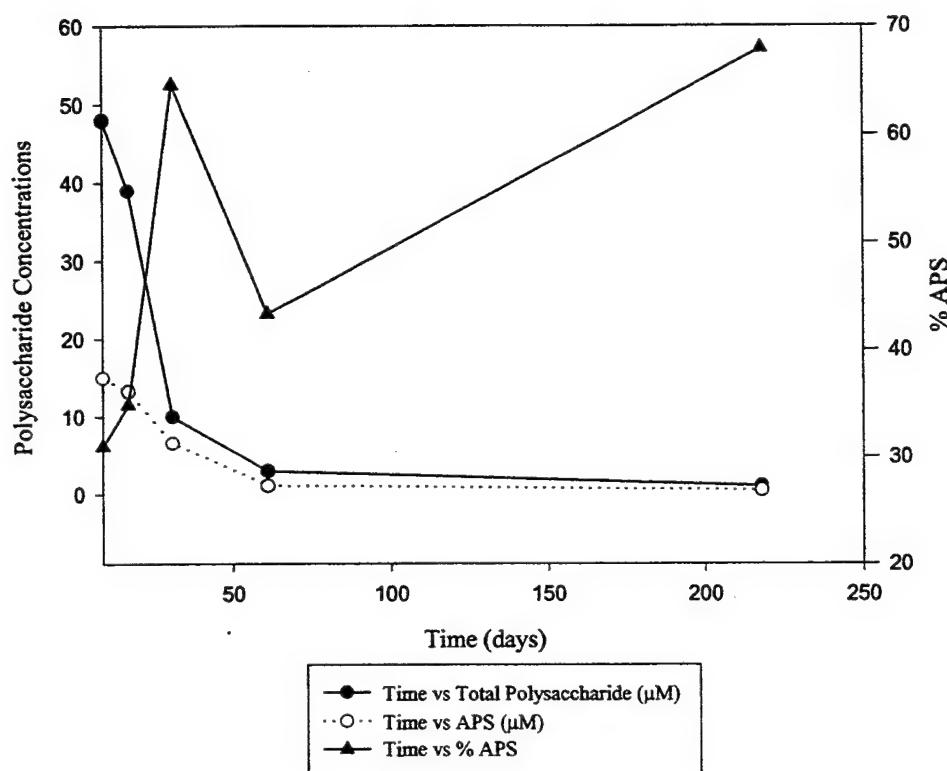


**Figure 3.9** The change in the concentration of total neutral monosaccharides in HMW DOM and the change in APS as a percentage of the total neutral monosaccharides (as calculated in the text) over the course of the *Thalassiosira weissflogii* incubation experiment

The data in Figure 3.9 can be used to calculate the degradation rate of the total polysaccharide fraction in HMW DOM (Table 3.6). The decrease in the total polysaccharide concentration can be modeled as a pseudo first order removal process. The rate constant for the degradation of the total polysaccharide fraction over the course of the entire incubation (TW2 to TW6) is 0.055/day ( $\pm 0.012$ ). The initial rate constant (between TW2 and TW4) is even faster: 0.07/day ( $r^2 = 0.90$ ). In comparison, the rate constant for the degradation of the calculated APS fraction is 0.042 /day ( $\pm 0.009$ ) over

Substrate	$k_{R[\text{initial}]}$	Correlation( $r^2$ )	$k_{R[\text{total}]}$	Standard Error
[DOC]	-0.015	0.85	-0.015	0.007
HMWDOC	-0.023	0.73	-0.028	0.01
TP	-0.055	0.96	-0.055	0.012
TP <sub>TW2-TW4</sub>	-0.07	0.90		
APS	-0.055	0.98	-0.042	0.009
APS <sub>TW2-TW4</sub>	-0.044	0.91		
M	-0.08	0.96	-0.06	0.02
GA	-0.09	0.99	-0.06	0.01
X	-0.07	0.99	-0.06	0.01
R	-0.05	0.98	-0.04	0.01
F+A	-0.02	0.50	-0.04	0.02
GL	-0.03	0.82	-0.05	0.006

$k_{R[\text{TOTAL}]}$  is the rate constant for the loss of each substrate over the course of the entire incubation (in /day)

$k_{R[\text{initial}]}$  is calculated for TW2 to TW5, unless otherwise noted

**Table 3.6 Degradation rate constants for the different organic carbon fractions in the *T. weissflogii* over the course of the incubation experiment.**

the entire incubation period and 0.044  $\mu\text{M C/day}$  ( $r^2 = 0.91$ ) between TW2 and TW4, confirming that APS is degraded more slowly than the total monosaccharide fraction.

The initial degradation rates of TP and APS will not be the same if other polysaccharides besides APS in the TP fraction are degraded faster than APS. However, the similarity in

the degradation constant for both the TP and the APS over the course of the *whole* experiment is expected if APS is the dominant polysaccharide in the TP fraction remaining towards the *end* of the experiment ( $k_{R[\text{total TP}]}$  not significantly different from  $k_{R[\text{total APS}]}$ ). Consistent with the degradation of the polysaccharide fraction, the decrease in the concentration of individual monosaccharides can also be modeled well as a pseudo first order removal process. The overall degradation rate constant for mannose, xylose and galactose is 0.06 /day, while the degradation rate between TW2 and TW4 is even faster (between 0.07 and 0.09 /day ( $r^2 > 0.96$ )). The overall degradation rate of rhamnose can also be modeled as above, and is 0.04/day. The slower degradation rate of rhamnose compared with the hexoses further confirms the fact that these monosaccharides are initially present in different polysaccharides (e.g. hexoses are present in APS and other polysaccharides, and rhamnose is present in APS).

Many factors can control the rates of degradation of individual polysaccharides by bacteria (Arnosti 1994). First these molecules must be hydrolyzed extracellularly, and second the bacteria must be able to produce enzymes that recognize the individual bonds within the polymer. It has been speculated that structural polysaccharides are synthesized to be particularly resistant to bacterial degradation (Thingstad and Billen, 1994). As shown in Table 3.5 for example, several investigators have noted the heterogeneity in the distribution of monosaccharides in diatom cell walls. This heterogeneity may impart a resistance to bacterial degradation. Both the culture exudates and seawater APS exhibit complex monosaccharide distributions. The ubiquity of APS and their presence at depth in the ocean (Chapter 2 and Chapter 4) lead us to hypothesize that APS would be

refractory due to its complex monosaccharide distribution, consistent with the data presented in Figure 3.9, showing the accumulation of APS in the incubation experiment.

In a recent study, Carlson et al. (1998) investigated the quality of DOM available to bacteria in the Ross Sea polynya and the Sargasso Sea. The bloom in the Ross Sea was dominated by an Antarctic *Phaeocystis* species, while the Sargasso Sea bloom was dominated by picoplankton (with some haptophytes and diatoms also present). A comparison between the two sites showed that the DOM produced in the Ross Sea was readily available to bacteria, while approximately 50% of the new DOM produced in the Sargasso Sea escaped microbial degradation, suggesting an inherent difference in the DOM produced at these locations. This study supports our findings on the interspecies (*Phaeocystis* vs. *T. weissflogii* and *E. huxleyi*) differences we observe in the chemical composition of HMW DOM exudates, and the differences in the relative lability of dissolved organic compounds produced during algal photosynthesis.

### 3.5 Conclusions

The chemical characteristics of extracellular HMW DOM from three species of marine phytoplankton were compared to HMW DOM in seawater. *Thalassiosira weissflogii*, *Emiliania huxleyi*, and *Phaeocystis* sp., were grown in nutrient enriched seawater that had been previously ultrafiltered to remove HMW DOM. The extracellular HMW DOM produced in these cultures was isolated by ultrafiltration and characterized using <sup>1</sup>HNMR, and molecular level analyses. All species exude DOM rich in polysaccharides, and the exudates of *T. weissflogii* and *E. huxleyi* closely resemble APS, previously identified as a major constituent of naturally occurring marine HMW DOM. APS may comprise up to 2-3% of the total organic carbon and 30% of the HMW DOC at

the time of production. Degradation of the *T. weissflogii* exudate alters the chemical composition of the HMW DOM, which we attribute to differences in the reactivity of specific polysaccharides. The component within the exudate that most resembles seawater HMW DOM has a slower degradation rate relative to the total polysaccharide fraction. This study indicates that APS isolated from the surface ocean can have a direct algal source and that APS may accumulate in seawater as a result of its metabolic resistance.

### 3.6 References

- Allan G., Lewin J., and Johnson P. G. (1972) Marine Polymers IV Diatom polysaccharides. *Botanica Marina* **15**, 102-108.
- Aldredge A. L., U. P., and Logan B. E. (1993) The abundance and significance of a class of large, transparent organic particles in the ocean. *Deep Sea Research I* **40**(6), 1131-1140.
- Aluwihare L. I., Repeta D. J., and Chen R. F. (1997) A major biopolymeric component to dissolved organic carbon in surface seawater. *Nature* **387**, 166-169.
- Arnosti C. and Repeta, D. J. (1994) Rapid Bacterial degradation of polysaccharides in anoxic marine sediment. *Geochimica et Cosmochimica Acta* **58**(12), 1639-2652.
- Baines S. B. and Pace M. L. (1991) The production of dissolved organic matter by phytoplankton and its importance to bacteria: Patterns across marine and freshwater systems. *Limnology and Oceanography* **36**(6), 1078-1090.
- Biersmith A. and Benner R. (1998) Carbohydrates in phytoplankton and freshly produced dissolved organic matter. *Marine Chemistry* **63**, 131-144.
- Borch N. H. and Kirchman D. L. (1997) Concentration and composition of dissolved combined neutral sugars (polysaccharides) in seawater determined by HPLC-PAD. *Marine Chemistry* **57**, 85-95.

- Carlson C. A., Ducklow H. W., Hansell D. A., and Smith Jr. W. O. (1998) Organic carbon partitioning during the spring phytoplankton blooms in the Ross Sea polynya and the Sargasso Sea. *Limnology and Oceanography* **43**(3), 375-386.
- Carlson C. A. and Ducklow H. W. (1995) Dissolved organic carbon in the upper ocean of the central equatorial Pacific Ocean, 1992: Daily and finescale vertical variations. *Deep-Sea Research* **42**(2-3), 639-650.
- Fogg G. E. (1966) The Extracellular Products of Algae. *Annual Review of Oceanography and Marine Biology* **4**, 195-212.
- Fogg G. E. (1971) Extracellular products of algae in fresh water. *Archive of Hydrobiology* **5**, 1-25.
- Fuhrman J. (1992) Bacterioplankton roles in the cycling of organic matter: The microbial food web. In: Primary productivity and biogeochemical cycles in the sea. **Plenum Press, New York**, 361-383.
- Guillard R. R. L. and Hellebust J. A. (1971) Growth and the production of extracellular substances by two strains of *Phaeocystis pouchetii*. *Journal of Phycology* **7**, 330-338.

- Guillard R. R. L. and Ryther J. H. (1962) Studies on marine planktonic diatoms I, *Cyclotella nana* Hustedt and *Detonula confervacea* (Cleve). *Grand Canadian Journal of Microbiology* **8**, 229-239.
- Haug A. and Mykelstad S. (1976) Polysaccharides of marine diatoms with special reference to *Chaetoceros* species. *Marine Biology* **34**, 217-222.
- Hecky R. E., Mopper K., Kilham P., and T. D. E. (1973) The amino acid and sugar distribution compositions of diatom cell walls. *Marine Biology* **19**, 323-331.
- Hedges J. I. (1991) Marine Particles: Analysis and Characterization: Lignin, cutin, amino acid and carbohydrate analyses of marine particulate organic matter. *Geophysical monograph* **63**, 129-137 ( Under Chpt. 4).
- Hellebust J. A. (1965) Excretion of some organic compounds by marine phytoplankton. *Limnology and Oceanography* **10**, 192-206.
- Hobbie J. E., Daley R. J., and Jasper S. (1977) Use of nucleopore filters for counting bacteria by fluorescence microscopy. *Applied Environmental Microbiology* **33**(5), 1225-1228.



- Janse I., van Rissel M., Gottschal J. C., Lancelot C., and Gieskes W. W. C. (1996) Carbohydrates in the North Sea during spring blooms of *Phaeocystis*: a specific fingerprint. *Aquatic Microbial Ecology* **10**, 97-103.
- Keller M. D., Selvin R. C., Claus W., and Guillard R. R. L. (1987) Media for the culture of oceanic ultraphytoplankton. *Journal of Phycology* **23**, 663-638.
- Kirchman D. L., Suzuki Y., Garside C., and Ducklow H. W. (1991) High turnover rates of dissolved organic carbon during a spring phytoplankton bloom. *Nature* **352**, 612-614.
- Knapp G. P., Stalcup M. C., and Stanley R. J. (1990) Automated oxygen titration and salinity determination. Woods Hole Oceanographic Institution Technical Report. WHOI-90-35. .
- Lampert W. (1978) Release of dissolved organic carbon by grazing phytoplankton. *Limnology and Oceanography* **23**, 831-834.
- Lee S. and Fuhrman J. A. (1987) Relationships between biovolume and biomass of naturally-derived marine bacterioplankton. *Applied Environmental Microbiology* **52**, 1298-1303.

- Mague T. H., Friberg E., Hughes D. J., and Morris I. (1980) Extracellular release of carbon by marine phytoplankton a physiological approach. *Limnology and Oceanography* **25**(2), 262-279.
- McCarthy M., Hedges J. I., and Benner R. (1996) Major biochemical composition of dissolved high molecular weight organic matter in seawater. *Marine Chemistry* **55**, 282-297.
- Myklestad S. (1974) Production of carbohydrates by marine planktonic diatoms. I. Comparison of nine different species in culture. *Journal of Experimental Marine Biology and Ecology*(15), 261-274.
- Myklestad S., Haug A., and Larsen B. (1972) Production of carbohydrates by the marine diatom *Chaetoceros affinis* var. *Willei* (Gran) Hustedt. II. Preliminary investigation of the extracellular polysaccharide. *Journal of Experimental Marine Biology and Ecology* **9**, 137-144.
- Nagata T. and Kirchman D. L. (1992) Release of macromolecular organic complexes by heterotrophic marine flagellates. *Marine Ecology Progress Series* **83**, 233-240.
- Norrman B., Zwiefel U. L., Hopkinson C. S., and B. F. (1995) Production and utilization of dissolved organic carbon during an experimental diatom bloom. *Limnology and Oceanography* **40**(5), 898-907.

Painter T. J. (1983) Algal Polysaccharides. *The Polysaccharides* 2, 195-285.

Peltzer E. T. and Brewer P. G. (1993) Some practical aspects of measuring DOC - sampling artifacts and analytical problems with marine samples. *Marine Chemistry* 41, 243-252.

Percival E., Rahman M. A., and Wiegel H. (1980) Chemistry of the polysaccharides of the diatom *Coscinodiscus Nobilis*. *Phytochemistry* 19, 809-811.

Sakugawa H. and Handa N. (1985a) Chemical studies on dissolved carbohydrates in the water samples collected from the North Pacific and Bering Sea. *Oceanologica Acta* 8(2), 185-196.

Sakugawa H. and Handa N. (1985b) Isolation and chemical characterization of dissolved and particulate polysaccharides in Mikawa Bay. *Geochimica et Cosmochimica Acta* 49, 1185-1193.

Skoog A. and Benner R. (1997) Aldoses in various size fractions of marine organic matter: implications for carbon cycling. *Limnology and Oceanography* 42, 1803-1813.

- Smestad B., Haug A., and Mykelstad S. (1975) Structural studies of the extracellular polysaccharide produced by the diatom *Chaetoceros curvisetus* Cleve. *Acta Chemica Scandinavia B.* **29**, 337-340.
- Smith D. C., Steward G. F., Long R. A., and Azam F. (1995) Bacterial-mediation of carbon fluxes during a diatom bloom in a mesocosm. *Deep-Sea Res. II* **42**(1), 75-97.
- Stoderegger K. and Herndl G. J. (1998) Production and release of bacterial capsular material and its subsequent utilization by marine bacterioplankton. *Limnology and Oceanography* **43**, 877-884.
- Tanoue E., S. N., Kamo M., and Tsugita A. (1995) Bacterial Membranes : A possible source of a major dissolved protein in seawater. *Geochimica et Cosmochimica Acta* **59**(12), 2643-2648.
- Thingstad F. and Billen G. (1994) Microbial degradation of Phaeocystis material in the water column. *Journal of Marine Systems* **5**, 55-65.
- Tranvik L. (1994) Colloidal and dissolved organic matter excreted by a mixotrophic flagellate during bacterioivory and autotrophy. *Applied Environmental Microbiology* **60**(6), 1884-1888.

Williams P. and Gordon L. (1970) Carbon-13:Carbon-12 ratios in dissolved and particulate organic matter in the sea. *Deep-Sea Research* 17(19-27).

### 3.7 Appendix

#### 3.7.1 Linkage date for the Cultures

	1	2	3	4	5	6
	Sugars	Linkages	TW2	TW4	E. huxleyi	Phaeocystis
1	R	T	9.4	12.8	13	39.1
2		1,2		12.2	35.5	
3		1,3	32	25.6	21.4	15.6
4		1,2,3	8.9	6.7	6.2	
5		1,3,4	10.8	9.4	5.4	
6		1,2,4	13	11.7	7.7	
7		1,2,3,4	21.7	24.8	10.8	28.3
8						
9	F	T	5.2	7.9		
10		1,2	0	0		
11		1,3	12.4	12	41.9	
12		1,4	21.5	10.3		
13		1,2,3		8.4	8.7	
14		1,2,4	26.1	14.7	18	
15		1,3,4	12.8	12.8	11.8	
16		1,2,3,4	18	29	15	100
17						

18	A	T		38	27.3	10.8
19		1,2			13.9	24.4
20		1,3			16.8	
21		1,4		10.3		
22		1,2,4	100	51.7	42	
23		1,2,3,4				52.8
24						
25	X	T	25.7	23.6	26.5	8.3
26		1,3	14.1	6.6	18.9	5.8
27		1,4	22.4	13.2	29.4	
28		1,3,4	5.8	23.2	7.5	69.1
29		1,2,4	18.6	23.2	7.5	
30		1,2,3,4	13.3	10		6.5
31						
32	M	T		5.8	16.8	
33		1,2			8.2	
34		1,3	26.7	11.6	8.2	12
35		1,6		5.7	8.4	18.5
36		1,2,3	5.7		6.4	33.9
37		1,2,4				5.8
38		1,3,6	18.7	11.6	6.8	
39		1,4,6		14.5	14.7	
40		1,2,3,4				10.5
41		1,3,4,6	8.2	5.6		
42		1,2,3,6	12.2	17.4	14	
43		1,2,4,6				
44		1,2,3,4,6	20.8	24.9	15.8	
45						

46	Q	1,4				11.3
47		1,3,4	21.4	14	12.6	43.1
48		1,3,6			8.8	
49		1,4,6	32.7	5		
50		1,2,4,6		46.6	29.2	
51		1,2,3,6				
52		1,3,4,6		11.9	10.2	
53		1,2,3,4,6	39.7	16.5	30.5	42.3
54						
55	GA	T	8.1		10	
56		1,2			13.4	
57		1,3	11		9.3	
58		1,6	12.3	6.5	9.3	19.9
59		1,2,3				
60		1,3,4	12.8	7.3	23.1	22.5
61		1,3,6	6.5			
62		1,4,6	6.5	5.6		
63		1,2,3,6				
64		1,2,4,6	7.7			15.4
65		1,3,4,6	8.7	42.9	13	10.3
66		1,2,3,4,6	12.2	15.9	12.2	20.1



## 4. Radiocarbon values of individual monosaccharides isolated from oceanic HMW DOM

### 4.1 Introduction

Carbon has three naturally occurring isotopes,  $^{12}\text{C}$ ,  $^{13}\text{C}$  and  $^{14}\text{C}$ .  $^{12}\text{C}$  is the most abundant (99%) isotope, followed by  $^{13}\text{C}$  (1%), while only 1 in  $10^{12}$  atoms in modern carbon is present as  $^{14}\text{C}$ . While  $^{12}\text{C}$  and  $^{13}\text{C}$  are stable,  $^{14}\text{C}$  is radioactive ( $\lambda = 1.2 \times 10^{-4}/\text{y}$ ). Naturally occurring  $^{14}\text{C}$  is produced in the upper atmosphere from spallation reactions of  $^{14}\text{N}$  and rapidly combines with oxygen to form carbon dioxide ( $\text{CO}_2$ ). This carbon dioxide mixes throughout the atmosphere, dissolves in the oceans and, *via* photosynthetic fixation of  $\text{CO}_2$  to organic carbon, enters the biosphere. Aboveground nuclear weapons testing in the 1950's and 1960's introduced large amounts of radiocarbon into the atmosphere. Atmospheric levels of  $\Delta^{14}\text{C}$  (see section 1.3), expressed relative to the pre 1950's value (i.e.  $\Delta^{14}\text{C} = 0 \text{ ‰}$ ), increased to approximately 1000 ‰ (Broecker and Peng, 1982).

Diffusion of  $\text{CO}_2$  from the atmosphere introduced bomb radiocarbon into the ocean such that the  $\Delta^{14}\text{C}$  value of surface dissolved inorganic carbon (DIC) reached a maximum of approximately 200 ‰ between 1973-1975. There has been a steady decrease in both the atmospheric and oceanic reservoirs of  $^{14}\text{C}$  since their peak in the 1960's and 1970's, respectively. Today, surface ocean  $\Delta^{14}\text{C}$  values of DIC are approximately 70 ‰. Since the decay constant for radiocarbon is approximately 10 ‰ every 80 years, these atmospheric and surface ocean decreases, result from mixing processes and not from radioactive decay. In particular, the decrease observed in the

surface ocean results from the more rapid vertical mixing of radiocarbon compared with the slower diffusion rate of radiocarbon into the surface ocean from the atmosphere (isotopic equilibration time scales are about 10-15 years).

The presence of bomb radiocarbon in the surface ocean has proven to be a useful tracer for different ocean processes such as deep water formation and ocean circulation. Of particular interest is its use as a tracer of recent, autochthonous organic matter. Any organic matter produced by both autotrophic and heterotrophic organisms in the surface ocean since the 1960's will contain post-bomb radiocarbon concentrations ( $\Delta^{14}\text{C} > -50\text{‰}$ ). The data presented in Chapters 2 and 3 suggest that polysaccharides (APS) isolated from HMW DOM are produced in the surface ocean during photosynthesis, indicating that APS must have a modern (post-bomb)  $\Delta^{14}\text{C}$  value. The presence of APS in the deep ocean, as revealed by the distribution of monosaccharides and the presence of acetate in DOM, implies that surface-produced APS must be transported to the deep ocean.

Dissolved organic matter synthesized in surface waters can be delivered down to the deep ocean by two possible mechanisms. Shown in Figure 4.1 are the two possible scenarios for the delivery of APS, and therefore DOM, to the deep ocean. Both scenarios show the production of DOM in the surface ocean, but differ in the mechanisms of DOM transport to the deep ocean. Figure 4.1A emphasizes APS transport to the deep ocean by the formation of deep water at high latitudes, while Figure 4.1B emphasizes that particle dissolution in the deep ocean may also be an important source of DOM. This chapter is based on the hypothesis that concentrations of  $^{14}\text{C}$  in APS can be used to differentiate between the two scenarios presented above. Since the formation of deep water is the dominant mode of DIC

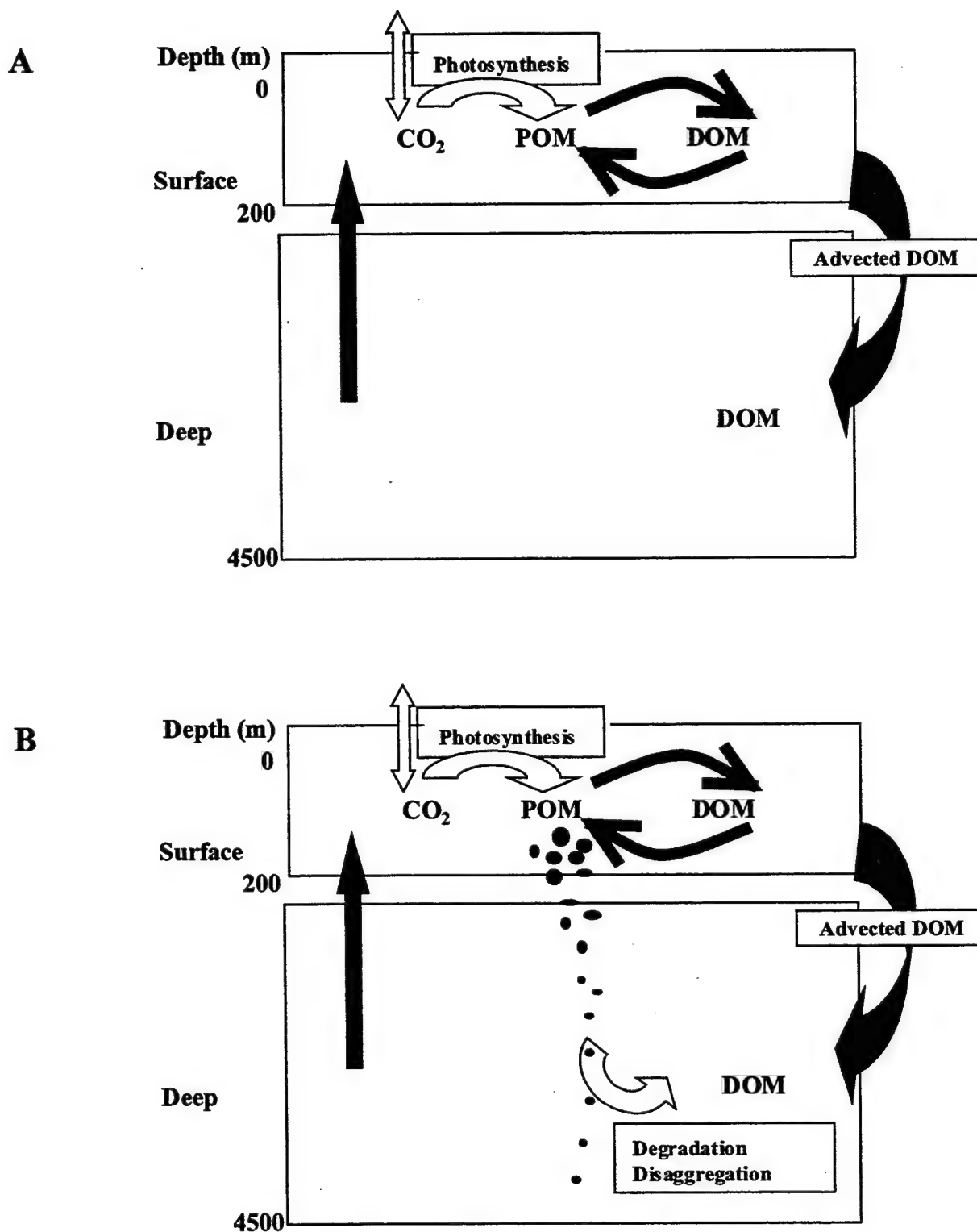


**Figure 4.1** Two scenarios for the delivery of surface produced DOM to the deep ocean. Scenario A shows the delivery of DOM to the deep ocean *via* deep water formation. Scenario B shows that in addition to advection, DOM may also be delivered to the deep ocean *via* bacterial degradation and disaggregation of sinking POM.

transport to the deep ocean, there should be no difference between the radiocarbon value of APS (corrected for isotopic fractionation during photosynthesis) and DIC, in the case of Fig. 4.1A. The vertical transport of POM, on the other hand, occurs on much faster time-scales compared to deep water formation. Thus, if POM delivers APS to the deep ocean (as in Fig. 4.1B), the radiocarbon values of APS should be more modern than DIC.

APS cannot be isolated from HMW DOM. However, it is possible to isolate the individual monosaccharides that constitute APS and measure their  $\Delta^{14}\text{C}$  values. This chapter focuses on the development of a method to isolate monosaccharides from HMW DOM for radiocarbon measurements in order to gain insight into the cycling of APS in the ocean.

## **4.2 Materials and Methods**

### **4.2.1 Sampling**

Surface samples were collected from a depth of 5 m in the North West Atlantic (CRL), Mid Atlantic Bight (MAB961) and Pacific Ocean (P961). Seawater was pumped through a teflon hose using a diaphragm pump and pre-filtered to remove large particles (Whatman GF/F) and bacteria (0.2  $\mu\text{m}$  Gelman Criticap cartridge filter). Deep water samples were collected using Niskin bottles from the Mid Atlantic Bight (MAB966 and MAB967), Sargasso Sea (SS972) and Pacific Ocean (P962) and pre-filtered as above. All seawater samples (with the exception of the sample from the Sargasso Sea) were ultrafiltered on board ship as described in section 2.2.2.1. Ultrafiltration membranes and filters were cleaned as in section 2.2.2.1. Following ultrafiltration, the HMW DOM was frozen ( $-20$  and  $-40^\circ\text{C}$ ). Blanks for each sample were obtained as a 4 l Milli Q water

rinse of the ultrafiltration system immediately prior to sample processing. The Sargasso Sea sample was stored in the dark, in teflon lined barrels, and ultrafiltered 2-3 weeks after collection. After returning to the laboratory, frozen samples were thawed and diafiltered to reduce salts as in section 2.2.2.2, lyophilized and stored at -20 °C until further analysis.

Seven samples were prepared for this study (Table 4.1). The samples included two surface water samples from the North Atlantic Ocean: MAB961 from the Middle Atlantic Bight, and CRL, collected at Woods Hole; a depth profile from the Middle Atlantic Bight: MAB966 and MAB967 (300 and 750 m); a depth profile from the North East Pacific Ocean: P961 and P962 (surface and 1600 m) and a deep water sample from the Sargasso Sea: SS972 (1000 m depth in the Sargasso Sea).

Sample	Depth	Latitude	Longitude	Date	[DOC] $\mu$ M	Liters	HMWDOC mg C	%HMW	HMWDOC2 mg C
CRL	Surface	41.5	70.5	Aug-94	102	1300			135
MAB961	Surface	36.78	75.87	Jul-96	160	800	276	18	163.0
MAB966	300 m	36.7	74.58	Jul-96	40	400			20.0
MAB967	750 m	36.7	74.58	Jul-96	40	400			26.9
SS972	1000 m	36.5	65.46	Feb-97	43	400	39	19	14.0
P961	Surface	34.83	123.15	Oct-96	72	350	100	33	38.4
P962	1600 m	34.83	123.15	Oct-96	40	431	45	22	28.9

**Table 4.1.1 Sampling site and DOC data for the samples analyzed in this study.**

HMW DOC refers to the DOC measured in the retentate following ultrafiltration. HMWDOC2 refers to the amount of carbon recovered following both ultrafiltration and diafiltration.

#### 4.2.2 Chemical Analyses

All the glassware used in this study was combusted (450°C) for 12 h. All tubing and fittings used for high-performance liquid chromatography (HPLC) were teflon, stainless steel or Upchurch PEEK (polyetheretherketone) (Upchurch Scientific, Oak Harbor, WA). Samples were lyophilized on a system containing two water traps: one that was a refrigerated isopropanol trap (at -30°C) and one containing isopropanol and dry ice (at -70°C).

A flow chart of the analyses is shown in Figure 4.2. Subsamples (100- 500 µg C) were archived for radiocarbon analysis of total HMW DOM. The remaining samples and blanks were hydrolyzed by adding 0.5 ml of Trifluoroacetic Acid (TFA) per 4 mg of C, and heating in a sand bath for 2 h at 121°C.

Following hydrolysis, samples were lyophilized, re-dissolved in Milli Q water and neutralized to between pH 7 and 8 with NH<sub>4</sub>OH. Samples were then desalted using an anion exchange resin (BioRex® 5) in the chloride form. The ion exchange resin was rinsed with 3×3 ml of Milli Q water and the columns were packed in 6", combusted pasteur pipettes (6 or 8 mm I. D.). Samples were applied on to the column dissolved in Milli Q water (10 mg of sample/ 2 ml of resin bed) and were eluted with 3 column bed volumes. After desalting, some samples (UF961, SS972, P961 and P962) were filtered (GF/F) to remove particles. Prior to HPLC separation, samples were lyophilized, re-dissolved in 1 – 3 ml of Milli Q water and centrifuged for 1-2 minutes in conical vials.

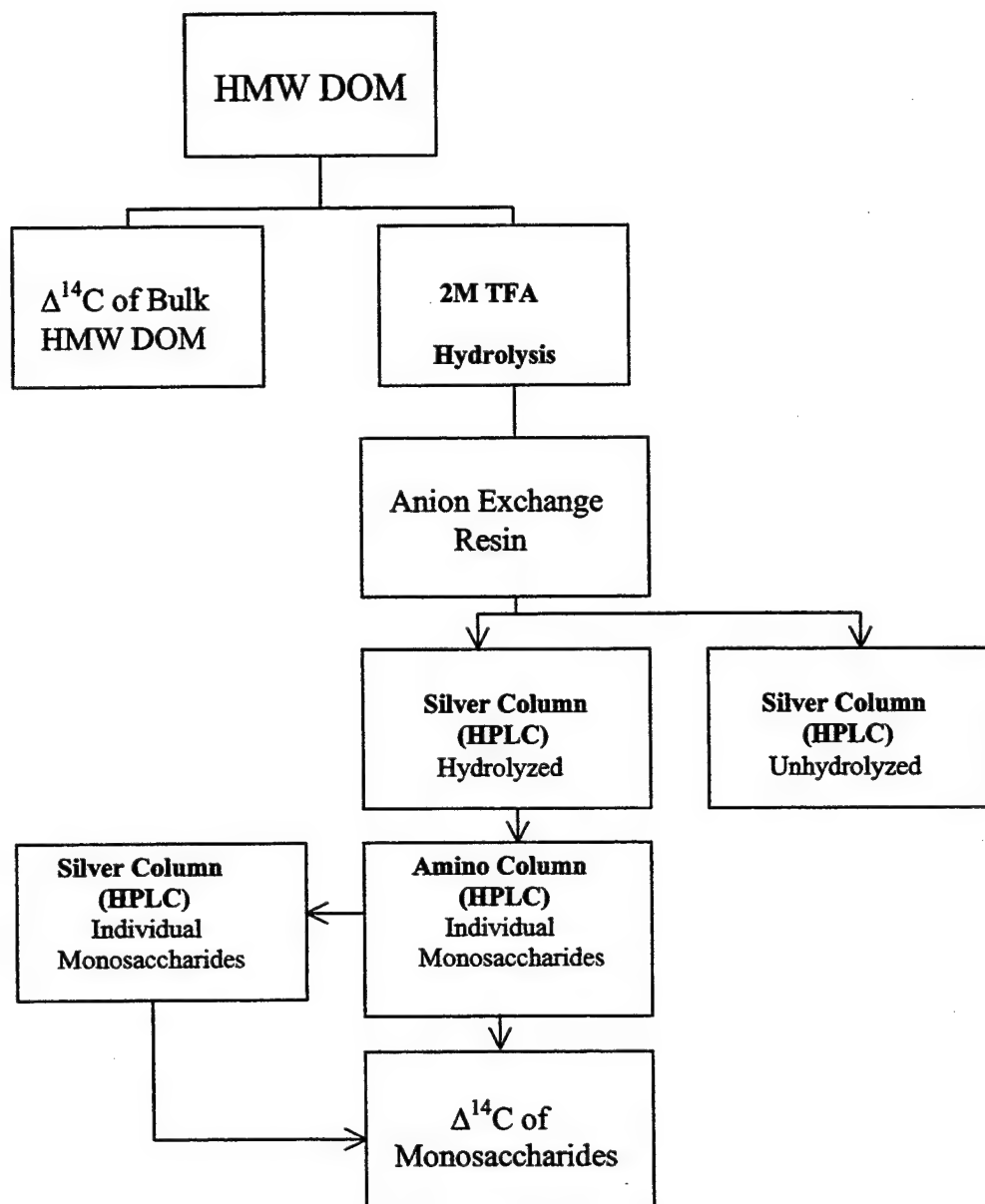


**Figure 4.2.** A flow chart of the various analytical steps involved with the separation of hydrolyzed monosaccharides from HMW DOM. Boxes in bold denote HPLC steps. Silver column refers to the cation exchange steps and amino column refers to the reverse phase separation.

#### 4.2.3 High-Performance Liquid Chromatography (HPLC)

Instrumentation included a Waters Model 510 (Waters Corporation, Milford, MA) HPLC pump equipped with a Shodex (Showa Denko K.K., Tokyo, Japan) RI-71 refractive index detector, and a Timberline (Alltech Associates, Inc., Deerfield, IL), TL-430 column heater, programmed using a Timberline TL-50 temperature controller. A Rheodyne 7125 Syringe Loading Sample Injector (Rheodyne, Inc., Cotati, CA) was mounted directly onto the column heater, and was fitted with a 1000  $\mu$ l stainless steel sample loop. Data acquisition was performed using HP Chemstation LC software (Hewlett-Packard Company). The detector and injector were interfaced with the computer through a Hewlett-Packard 35900E Analog to Digital Interface.

##### 4.2.3.1 Ion Exchange

Following hydrolysis, the total monosaccharide fraction in each sample was purified from unhydrolyzed material (Figure 4.2) using cation exchange chromatography with silver as the counterion, on a sulphonated styrene-divinylbenzene gel. Two different manufacturers were used, Supelco (Supelcogel™ Ag, cat # 5-9315, Supelco, Inc, Bellefonte, PA) and Alltech (Benson carbohydrate, BC-100, Ag<sup>+</sup>; cat # 33802, Alltech Associates, Inc, Deerfield, IL). The performance and the retention time of monosaccharide standards on these two columns were identical. Column dimensions were 30 cm x 7.8 mm I. D., and the bead size was 10  $\mu$ m. Columns were eluted with Milli Q water at a flow rate of 0.5 ml/min, with the column heated to 80°C. Contrary to the instructions which accompany these columns, the column should be heated to 80 °C before connecting the flow in order to minimize large increases in back pressure. When



the column is disconnected for storage, the flow path should be disconnected while the column is still at 80 °C.

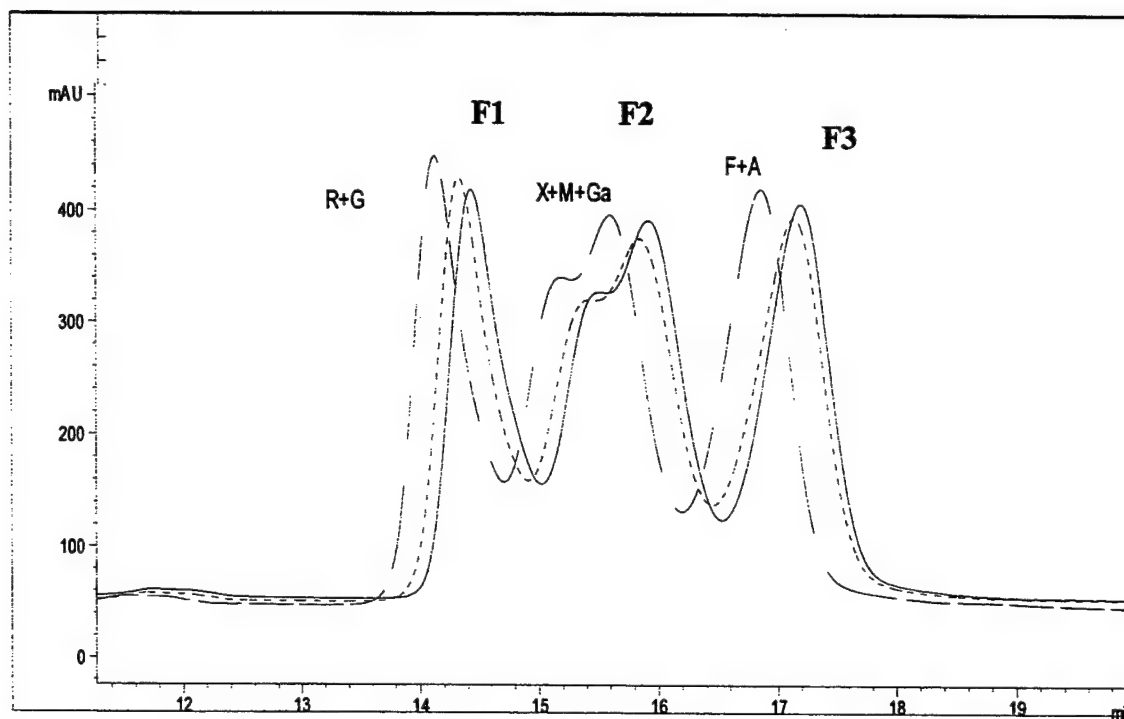
The total weight of the sample injected on to the column did not exceed 1 mg/injection. In some cases (UF961, UF967, CRL, P961), samples were re-injected onto the Ag column to further purify the monosaccharide fraction from unhydrolyzed material.

During injection and sample collection, samples were stored on ice to reduce bacterial degradation of saccharides. Monosaccharide fractions were lyophilized immediately after collection and prior to the second HPLC purification step. Monosaccharides detected by HPLC were quantified by calibrating the detector using a standard mixture of seven monosaccharides. The calibration was based on 6 injections of increasing amounts of the standard mixture (between 5 –250 µg of each monosaccharide) and was performed once per each sample and blank set. Twenty µl of the standard monosaccharide mixture (20 µg of each sugar) was injected at least twice a day to insure that there was no fluctuation in response factor over time.

Data from the six consecutive injections of a sugar standard on the Ag column (Alltech Associates, Bodman Carbohydrate Column) showed good reproducibility in retention time and peak area (Figure 4.3 A). Rhamnose and glucose eluted first with an average retention time (flow rate 0.5 ml/min) of  $14.24 \pm 0.11$  minutes (F1), followed by one peak for xylose, mannose and galactose, at  $15.675 \pm 0.16$  minutes (F2). Fucose and arabinose elute together at  $16.907 \pm 0.2$  minutes (F3). For six consecutive injections of equal monosaccharide concentration, the percent standard deviations for the areas under each of the three peaks was between 3.4 to 5 %. All six monosaccharides examined

(rhamnose, fucose, arabinose, xylose, mannose, glucose and galactose) show similar response factors on this column (0.0059 – 0.0081 µg/unit area) (Figure 4.3B).

**A**



Sugar	Ret. Time	% Stnd. Dev.	Area	% Stnd . Dev.
R+G	14.241	0.8	12316.9	3.4
X+Ga+M	15.675	1	20270.4	3.5
F+A	16.907	1.2	14816.6	5

**B**

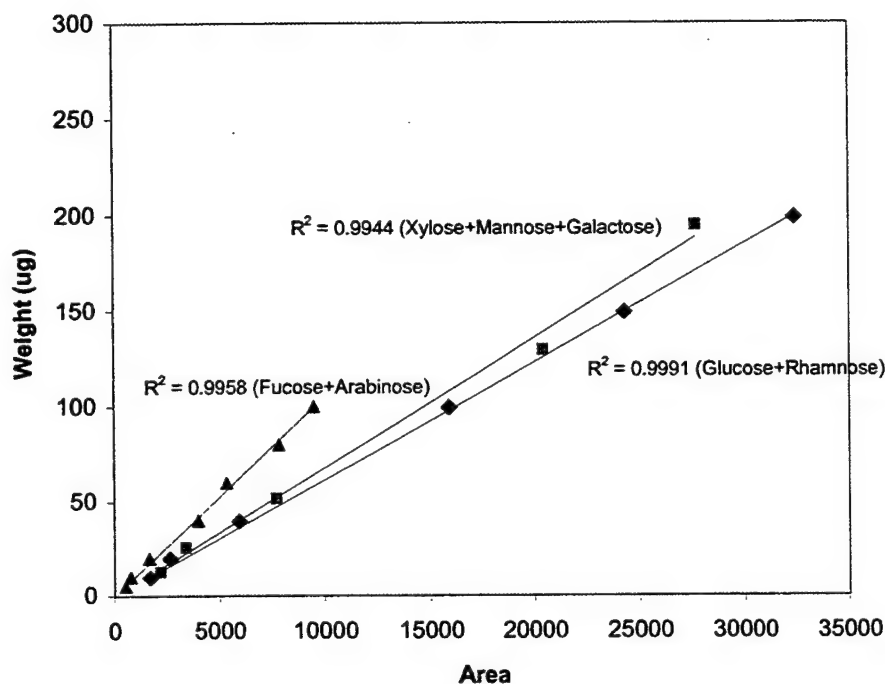


Figure 4.3 (A) Reproducibility of six consecutive injections of a monosaccharide mixture on the Ag column. Standard deviations (% Stnd. Dev) for retention times (Ret. Times) and peak areas are reported as a percentage. (B) Calibrated detector response for the three different monosaccharide fractions ( $R^2$  for each linear fit to the data are reported on the figure).

#### 4.2.3.2 Normal Phase Chromatography

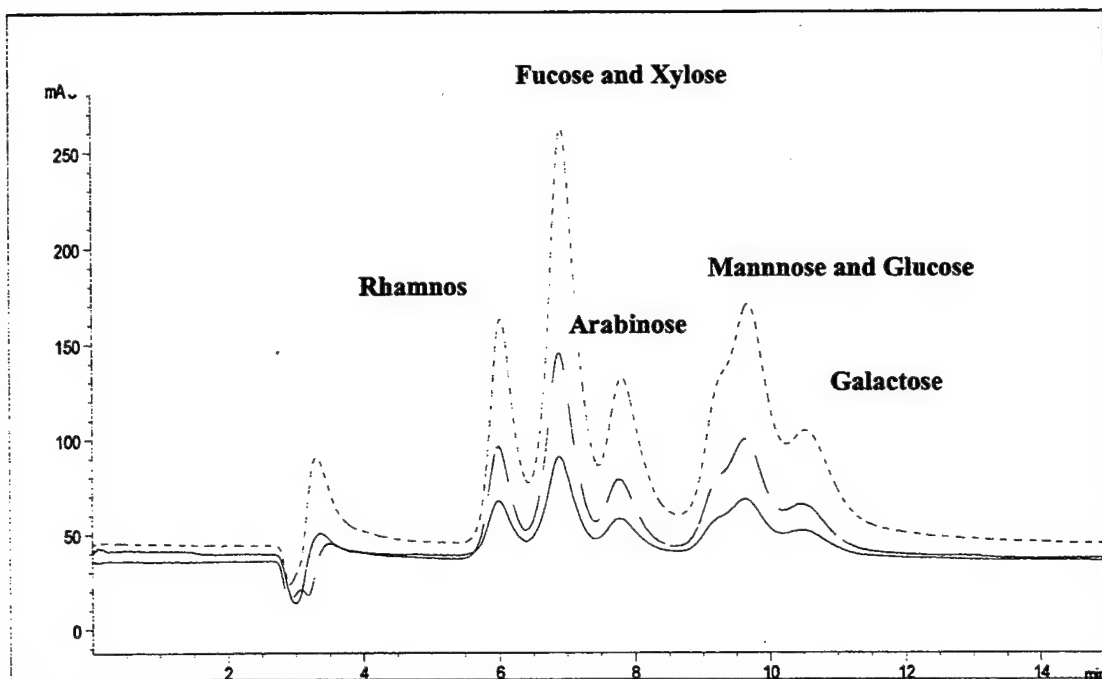
Separation of individual monosaccharides was achieved using a silica column, with an aminopropyl silyl bonded phase (5 µm Supelcosil LC-NH<sub>2</sub>, cat # 508338, from Supelco; an Adsorbosphere NH<sub>2</sub>, 3 µm column, cat # 287283, or Carbohydrate, 10 µm column, cat # 35642 both from Alltech). The two Alltech columns differed in bead size, and stability. The Alltech Carbohydrate column is more highly cross-linked than the Alltech Adsorbosphere column, increasing its stability to hydrolysis. Column dimensions

in all cases were 25 cm x 4.6 mm I. D. All three columns gave similar retention times for monosaccharide standards. Columns were operated at room temperature using a degassed mobile phase of 75/25 acetonitrile/water (v/v), at a flow rate of 1 ml/min. Attempts were made to increase the relative amount of water in the mobile phase (to insure complete dissolution of monosaccharides), but rapid loss in peak resolution was observed. Thus, we found that 75% acetonitrile gave us the best combination of resolution, recovery and sugar solubility. The mobile phase must be delivered in a capped solvent delivery system to prevent evaporation of the acetonitrile, which will cause a rapid drift of the RI detector.

The samples were dissolved in the mobile phase prior to injection. After sample collection, the acetonitrile was removed by evaporating under nitrogen using a TurboVap LV Evaporator (Zymark) at 50 °C. The remaining water was lyophilized, and a fraction (5-10 %) of each sample was re-injected onto the amino column to insure that the separation of was complete.

Retention times and reproducibility in peak areas were calibrated by sequentially injecting larger sample amounts. Up to 200 µg of each monosaccharide was injected with 100% recovery off the column. As shown in Figure 4.4A, retention times for seven consecutive injections of increasing sample size (5-100 µg of each sugar/inj) did not shift more than ±0.5% for each sugar. The standard deviation for the calculated areas under each of the individual monosaccharide peaks ranged from 5-12%. The calibrated response factors differed for individual monosaccharides, with arabinose, mannose and galactose showing lower responses than rhamnose, fucose, xylose and glucose.

**A**



Sugar	Ret. Time	% Stnd Dev.	Area	% Std.Dev.
R	6.022	0.5	914.3	9.6
F+X	6.924	0.4	1859.5	5.7
A	7.81	0.31	968.8	10.4
M+G	9.667	0.32	1916.5	5.5
Ga	10.504	0.36	908.3	12.2

**B**

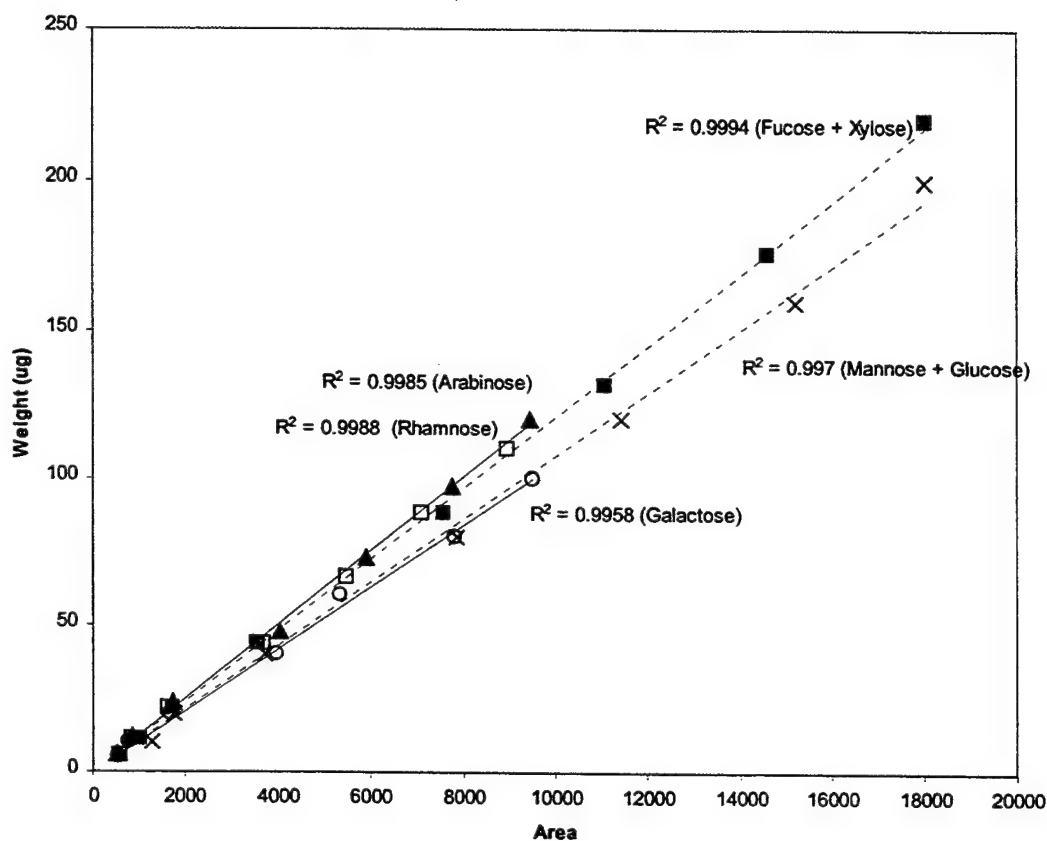


**Figure 4.4 (A)** Reproducibility of six consecutive injections of a monosaccharide mixture on the amino column. Standard deviations (% Std. Dev) for retention times (Ret. Times) and peak areas are reported as a percentage. **(B)** Calibrated detector response for five monosaccharide fractions ( $R^2$  for each linear fit to the data are reported on the figure).

In the case of UF961, CRL, and P961, purified monosaccharide fractions were re-injected onto the ion exchange column to remove bleed from the amino column.

#### 4.2.4 Sample Preparation for Accelerator Mass Spectrometry (AMS)

After the final HPLC purification step (Figure 4.2), samples were lyophilized and re-dissolved in 1-2 ml of Milli Q water. Using pre-combusted 13" NMR pipettes (Cat # 803A, Wilmad Glass Co, Buena, NJ), samples were transferred to the bottom of 8" Vycor quartz tubes (9 mm O.D  $\times$  7 mm I. D., Anderson Glass Co, Inc, Fitzwilliams, NH). These quartz tubes, containing 300-500 mg of CuO (copper oxide wires, fine wires 4 mm  $\times$  0.5 mm (sieved), Elemental Microanalysis, Manchester, MA, (stored in a dessicator)), had been combusted at 850°C for 5 h prior to the addition of each sample. Care was taken to avoid dripping the samples along the side of the quartz tubes in order to minimize losses during the flame sealing step. The copper oxide was pre-weighed using an aluminum boat and placed at the bottom of each combustion tube using a long-stemmed funnel. All weighing equipment was sprayed with an Aero Duster® (Miller Stephson Chemical Company, Danbury, CN) to remove any dust. The samples, in quartz tubes, were lyophilized overnight, covered with pre combusted aluminum foil (450°C) and flame sealed the following day.

Prior to flame sealing, quartz tubes containing the sample and CuO were attached to a vacuum manifold and evacuated. Connections were first cleaned using the Aero Duster®. The samples were gradually placed under vacuum using a needle valve and evacuated for at least 1 h. Prior to sealing, the samples were closed off to the vacuum pump and the bottom 2" of each tube was placed in a liquid nitrogen bath to avoid any sample loss through volatilization. Samples were then sealed using a butane/oxygen torch. All tubes were annealed in the mixed gas flame, followed by a butane flame, for one minute after the sealing was complete. The pyrolytic decomposition of CuO, yielding oxygen for the oxidation of sugar carbon to CO<sub>2</sub>, occurs at temperatures above 500 °C

(Boutton, 1991). Thus, sealed samples were combusted at 850°C for five hours. In the case of larger samples (>300 µg), or samples likely to contain salts, ceramic blocks were used to separate individual tubes in the muffle furnace to avoid damaging surrounding tubes in case of an explosion. The copper that is reduced during the oxidation of organic matter will also help strip halogens such as chloride. The total HMW DOM sample tubes contained 100 mg of Ag (silver shot, Alfa Aesar, Ward Hill, MA), in addition to CuO, to react with other sea salt contaminants.

The CO<sub>2</sub> generated during the combustion was quantified 2-3 days later. Sample tubes were scored, placed in crackers, and connected to a vacuum manifold. Samples were cracked individually and CO<sub>2</sub> was quantified by measuring the partial pressure of the gas in a pre-calibrated volume at a known temperature. Prior to quantification, the gas was passed over a dry ice/isopropanol slush bath to trap any water produced during the combustion. The CO<sub>2</sub> was then trapped in a liquid nitrogen bath and any remaining gas (i.e., gases with freezing points lower than -200°C) was removed by evacuating the manifold. Quantified CO<sub>2</sub> samples were then transferred to 6 mm pyrex tubes (Anderson Glass Co, Fitzwilliams, NH) by trapping the CO<sub>2</sub> in the bottom of the tubes with liquid nitrogen, and flame sealed. If splits of gas were taken for δ<sup>13</sup>C analysis, the samples were allowed to equilibrate for 3 minutes to prevent any isotopic fractionation.

Samples with > 70 µg of carbon, (the seven blanks for CRL combined as one sample, all the individual monosaccharide samples from CRL, and rhamnose, fucose and xylose from MAB961) were submitted as quantified CO<sub>2</sub> to Lawrence Livermore National Laboratory (Livermore, CA) and prepared into graphite and dated by Dr. Michael Kashgarian. Smaller samples (combined blanks from MAB961, combined



blanks from P961, individual monosaccharides from P961, and both the blank and the combined monosaccharides (rhamnose, fucose and xylose) from P962), were prepared into graphite according to the microscale AMS sample preparation protocol (Pearson et al. 1998). In all cases CO<sub>2</sub> was reduced to graphite on a 325 mesh spherical cobalt catalyst, that was cleaned at 400°C for 0.5 h under 0.7 atm H<sub>2</sub>. A carbon:cobalt ratio of 60 µg/ 1 mg was used, but no less than 1 mg of Co was used (thus smaller samples have a lower carbon to cobalt ratio). The graphite was pressed into targets by NOSAMS, and analyzed along with standards and process blanks. Two primary standards NBS Oxalic Acid I (NIST-SRM-4990) and Oxalic Acid II (NIST-SRM-4990C) are used during all <sup>14</sup>C measurements. The process blank material is a Johnson-Mathey 99.9999% pure graphite powder.

All the radiocarbon data reported in this chapter were determined by AMS, and are reported as fm: fraction modern, or fm\*: fraction modern blank-corrected (MAB961 and P962). Fraction modern is a measurement of the deviation of the <sup>14</sup>C/<sup>12</sup>C ratio of a sample from “modern” values. Modern is defined as 95% of the radiocarbon concentration (in 1950) of NBS Oxalic Acid I normalized to δ<sup>13</sup>C<sub>VPDB</sub> = -19 ‰ (Olsson, 1970). AMS results are calculated using the internationally accepted modern value of 1.176±0.010×10<sup>-12</sup> (Karlen et al. 1968) and a final <sup>13</sup>C correction is made to normalize the sample fm to a δ<sup>13</sup>C<sub>VPDB</sub> value of -25‰.

Thus fm is calculated according to:

$$fm = \frac{A_{SN}}{A_{abs}} = \frac{A_s \left( 1 - \frac{2(25 + \delta^{13}C)}{1000} \right)}{0.95 A_{ox} \left( 1 - \frac{2(19 + \delta^{13}C)}{1000} \right)} \quad (1)$$

where  $A_s$  is the sample activity,  $A_{ox}$  is the activity of oxalic acid,  $\lambda$  is the decay constant for  $^{14}\text{C}$  ( $1/8267 \text{ yr}^{-1}$ ), (Stuiver and Polach, 1977). The quantity  $fm^*$  is calculated as:

$$fm^* = \left[ fm_{sample} - \left( fm_{blank} \left\{ \frac{M_{blank}}{M_{sample}} \right\} \right) \right] \times \frac{M_{sample}}{(M_{sample} - M_{blank})} \quad (2)$$

$M_{sample}$  is the carbon mass of the total sample, and  $M_{blank}$  is the carbon mass of the corresponding blank. Masses are determined after combustion to  $\text{CO}_2$ . In order to convert  $fm$  to  $\Delta^{14}\text{C}$  and radiocarbon age, the Libby half life of 5568 years is used ( $\lambda = 1/8033 \text{ yr}^{-1}$ ). Also the present time,  $y$ , is taken to be 1997. Thus:

$$\Delta^{14}\text{C} = (fm^* \times e^{\lambda(1950-y)} - 1) \times 1000 \quad (3)$$

$$^{14}\text{C Age} = 8033 \ln(fm) \quad (4)$$

A  $\delta^{13}\text{C}$  value of  $-22\text{‰}$  was used for all the monosaccharides, HMW DOC samples and blanks. Blank samples were too small to remove a split for  $\delta^{13}\text{C}$  analysis, thus a value of  $-22\text{‰}$  was assumed. This assumption may be incorrect, but the age correction is approximately +16 years for every +1‰ difference from the standards'  $-25\text{‰}$  value, which in this case is only a small fraction of the radiocarbon age of the blanks.

Radiocarbon values for the blanks were  $-770 \text{‰}$  prior to the final purification (Ag column) (Table 4.3). Following the final purification steps, blanks for CRL were  $-431.4 \pm 10.3 \text{‰}$ . Blanks for the ultrafiltration cartridges were  $-999.5 \text{‰}$  (Santschi et al., 1995).

### 4.3 Results

A list of recoveries following each of the purification steps is reported in Table 4.2. All samples (with the exception of MAB966 and MAB967) were desalted using an anion exchange resin. Between 20-40% of the total sample applied on to the column was lost during desalting (Desalting I). Consistent with this removal of material following desalting, the chromatograms showed a marked difference in the size of the peak eluting in the dead-volume of the column, as shown in Figure 4.5 (CRL (20 mg ) sample).

Although good separation of the monosaccharides from the unhydrolyzed material is achieved in both steps, desalting via anion exchange, reduces the area under the peak eluting at 6 minutes in (B) by 90 %. Monosaccharide recoveries, following desalting, were between  $70 \pm 10\%$ . Other investigators have also observed similar losses of monosaccharides during desalting using a mixed ion exchange (40-50 %, (Borch and Kirchman, 1997)). No systematic relationship between the amount of sample lost and the total amount of carbon applied onto the anion exchange resin was observed.

Following desalting (some samples were desalted twice) and filtration, the fraction of monosaccharide carbon recovered from total HMW DOM ranged from  $< 1\%$  to  $5\%$ . Of the total carbon recovered following the initial desalting step (Desalting I), between  $4-5\%$  and  $1.5-2.5\%$  of the carbon in the surface and deep water samples were recovered as monosaccharides. Recoveries of monosaccharide carbon following the final separation on the amino column were approximately  $50\%$  lower than silver column recoveries.

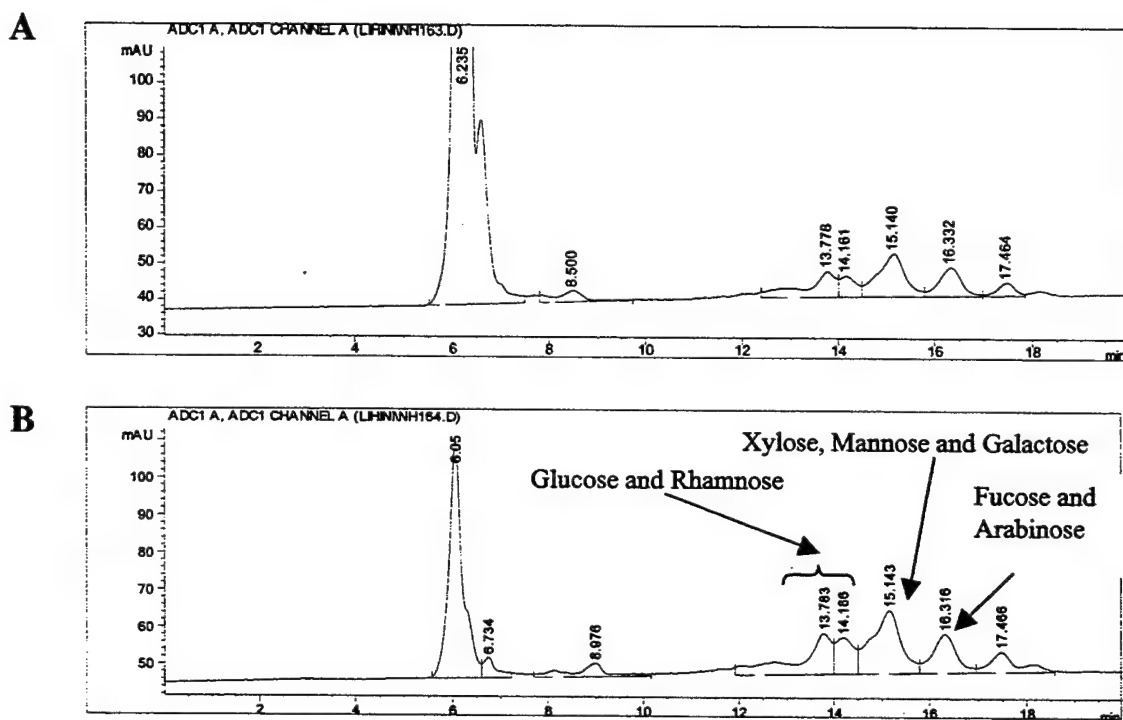


**Figure 4.5** CRL sample after hydrolysis and neutralization, separated on the cation exchange column using Ag as the counterion. The figure shows the sample before (A) and after (B) desalting using an anion exchange resin.

Sample	HMW DOM Mg	HMW DOM mg C	Desalting I mg C (Total)	Desalting I mg C (Sugars)	Desalting II GF/F Filtering mg C (Sugars)	Ag Column mg C (Sugars)	Amino Column mg C (Sugars)	Combustion mg C (Sugars)
CRL	217	58.6	36.3	2.1		1.4	1.1	0.48
MAB961	210.6	82	67.2	8.1	2.7	4.0 <sup>\$</sup>	2.7	0.51
MAB966*	61.6	17.9	14.3			0.7		
MAB967	84.4	24.5				0.7		0.25
P961	145.8	37.9	30.3		1.8	1.8	0.8	0.40
P962	167	36.9	29.1		0.4 <sup>#</sup>	0.4	0.1	0.21 <sup>&amp;</sup>
SS971	234	15.9	10.8	0.3		0.3	0.1	0.2 <sup>&amp;</sup>

\* MAB966 was collected using a cation exchange column in the Pb form not the Ag form

# P962 was also treated with AgNO<sub>3</sub> to precipitate chloride.

\$ Recoveries are the sum of a fraction collected after Desalting I and another collected after Desalting II.

& These samples had high blanks from indicating contamination.

Table 4.1.2 The recovery of carbon during each of the different purification steps performed for this analysis. Desalting was performed on an anion exchange column. Ag column and Amino column data, refer to recoveries during the HPLC procedure

The deep Pacific Ocean sample (P962) had the lowest carbon recovery. In addition to being desalted twice and filtered, it was also mixed with 10 ml of a saturated solution of  $\text{AgNO}_3$  (dissolved in Milli Q water) to try and precipitate the chloride ions prior to HPLC. The precipitate was removed by centrifuging the sample and pipetting out the water (repeated 3-4 times). The  $\text{AgCl}$  precipitation was performed because the deep sample processed prior to P962 (SS971) stripped Ag ions from the cation exchange column as  $\text{AgCl}$ .

In all cases, the low recovery of monosaccharides is likely due to the presence of high concentrations of cations in these samples, which interfered with the separation and generated a mixed ligand cation exchange column. Also, the use of the anion exchange column in the  $\text{Cl}^-$  form for desalting the samples introduced large concentrations of chloride ions to the cation exchange column, causing the removal of Ag ions as  $\text{AgCl}$ .

The relative distribution of monosaccharides and the amount of carbon in HMW DOM accounted for by these monosaccharides was also determined by gas chromatography (GC). The method and the results of the analysis for UF961, P961 and P962, and UF967 are reported in Chapter 2. Briefly, samples were hydrolyzed with 2M TFA as in Section 4.2.2, but were not desalted or filtered. Monosaccharides were derivatized and analyzed as alditol acetates by GC. In all cases, monosaccharides were shown to account for 15% of the carbon in surface water and between 4-6 % of the carbon in deep water HMW DOM. Comparing this data to the yields in Table 4.2, it is clear that the HPLC method underestimates the relative amount of monosaccharides in HMW DOM compared to the GC analysis. For comparison, monosaccharide recoveries in other studies range between 6-20% in surface waters and 1.6-3.5% in deep waters

(Borch and Kirchman, 1997; McCarthy et al., 1996; Skoog and Benner, 1997). In all cases, quantitation of monosaccharides by GC (this study and McCarthy et al. (1996) gave higher yields than HPLC (Borch and Kirchman, 1997; Skoog and Benner, 1997)).

For deep samples, carbon was added between the separation of monosaccharides on the amino column and the final combustion step (Table 4.2). This resulted from the contamination of the samples and blanks with bleed from the amino column (propyl amine was observed in the waste fraction by  $^1\text{H}$ NMR spectroscopy). The combustion yields for contaminated individual blanks (galactose blanks from MAB961 and P961) and combined blanks (P962 and SS971) were between 34-53  $\mu\text{g}$  and 90-104  $\mu\text{g}$  carbon. The surface ocean samples (MAB961, CRL, and P961) were subsequently re-injected onto the Ag column to remove the bleed from the amino column. For these samples, further losses of carbon were incurred between the amino column and the final combustion of the sugars to  $\text{CO}_2$ . Following the final clean-up step, blanks for CRL were  $5.7 \pm 1.18$   $\mu\text{g}$  of C,  $6.72 \pm 0.13$   $\mu\text{g}$  for MAB961 and  $4.91 \pm 0.82$   $\mu\text{g}$  for P961. Blanks for the lyophilizing system were 2.2  $\mu\text{g}$  of carbon, and combustion blanks were  $<1.0$   $\mu\text{g}$  of carbon.

High-performance liquid chromatography of all blanks showed a peak eluting between 17-18 minutes on the silver column which was 5% of the area of the total monosaccharide fraction. This peak was also present in the blanks of each of the different hydrolysis procedures that were tested, indicating that it did not result from either a contaminant in the TFA or the ultrafiltration and diafiltration procedures. In the case of samples (UF961, P961 and P962) that were filtered using a Whatman GF/F filter, an additional peak was detected, eluting 13-13.5 minutes. Individual monosaccharide

blanks on the amino column showed a peak eluting at approximately 6.3 minutes (between the rhamnose and the fucose + xylose peak).

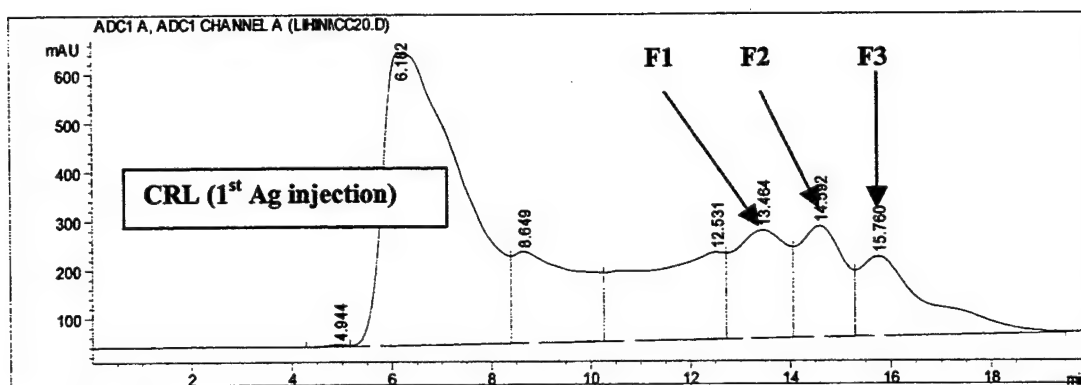
Shown in Figure 4.6 A is a chromatogram of the CRL sample during the initial separation of monosaccharides from unhydrolyzed material (Ag). All samples were characterized by a large initial peak and a large baseline. This baseline was present in the monosaccharide region of the chromatogram as well, and was thus collected with the monosaccharide fraction. Figure 4.6B shows the re-injection of each of the collected monosaccharide fractions (F1, F2 and F3) onto the silver column for further purification. Subsequent re-injection of the monosaccharide fractions (F1, F2 and F3) shows the presence of some of the baseline material following the initial collection. The second injection of CRL onto the cation exchange column greatly increases the separation of the monosaccharide fractions from the total unhydrolyzed material.

Following the Ag column separation (as shown in Figure 4.2), each dried monosaccharide fraction was injected re-dissolved in 75/25 acetonitrile/water (v/v) and injected onto the amino column. Figures 4.7 A through C show the separation of each of the fractions (F1, F2 and F3) collected from the Ag column by reverse phase chromatography (amino column). As shown in the Figure 4.7, F1, F2 and F3 separate well into their individual monosaccharide components on the amino column allowing clean separation individual monosaccharides.

Subsequent combustion of some blanks and samples (as above) showed contamination from the amino column. Thus the remaining individual monosaccharide fractions were re-injected and separated by cation exchange chromatography (Ag column) (Figure 4.2). This separation is also shown in Figures 4.7 A though C.



**A**



**B**

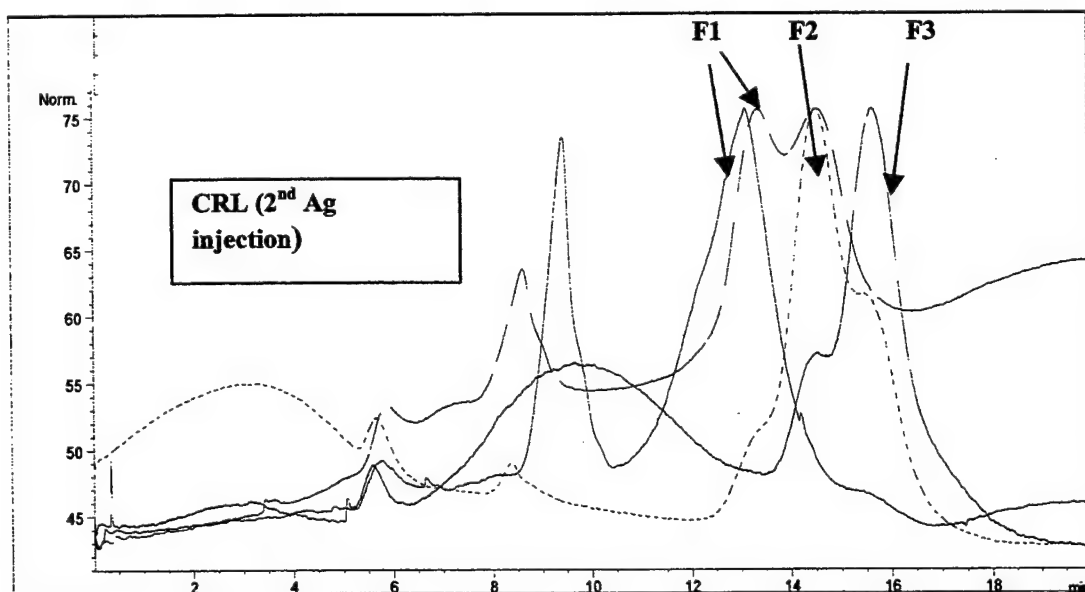
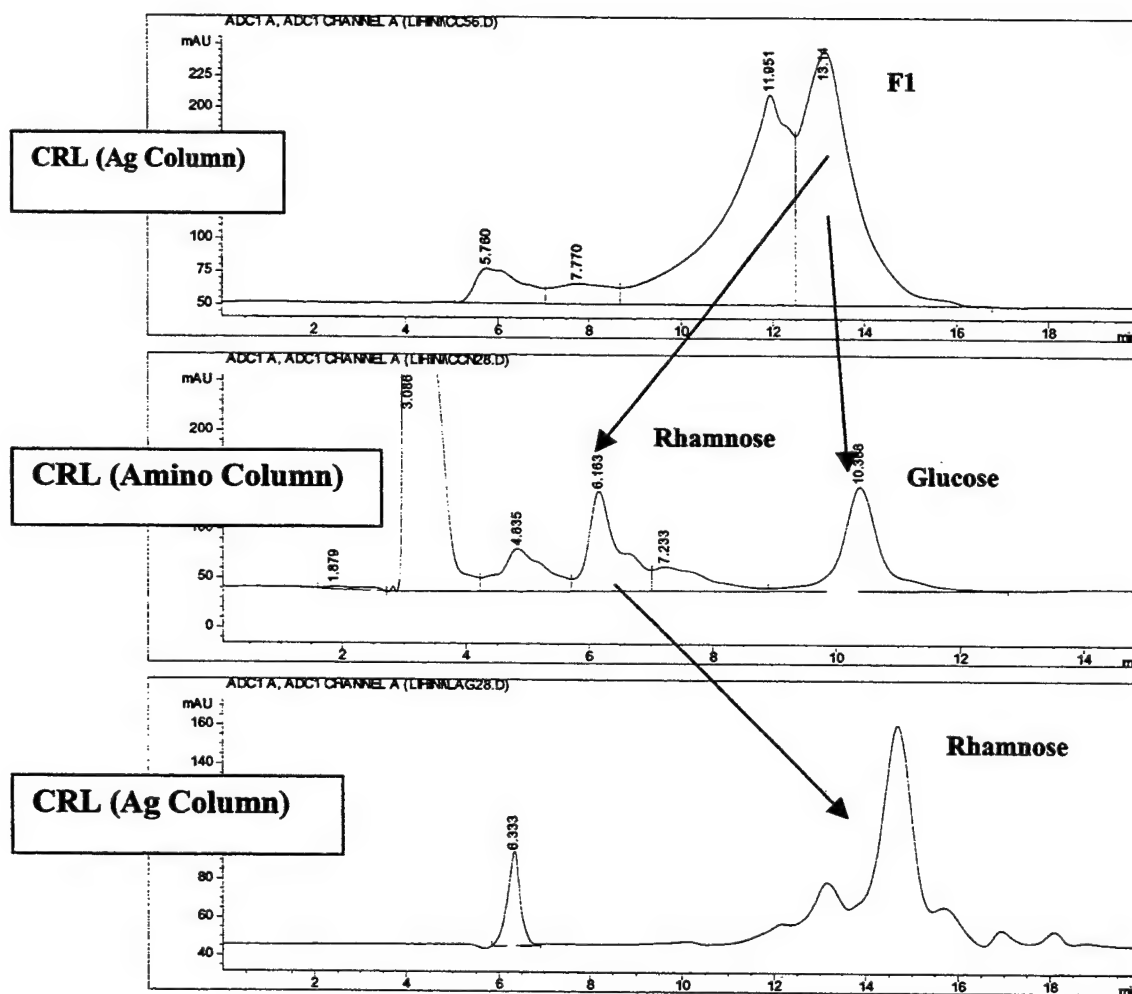
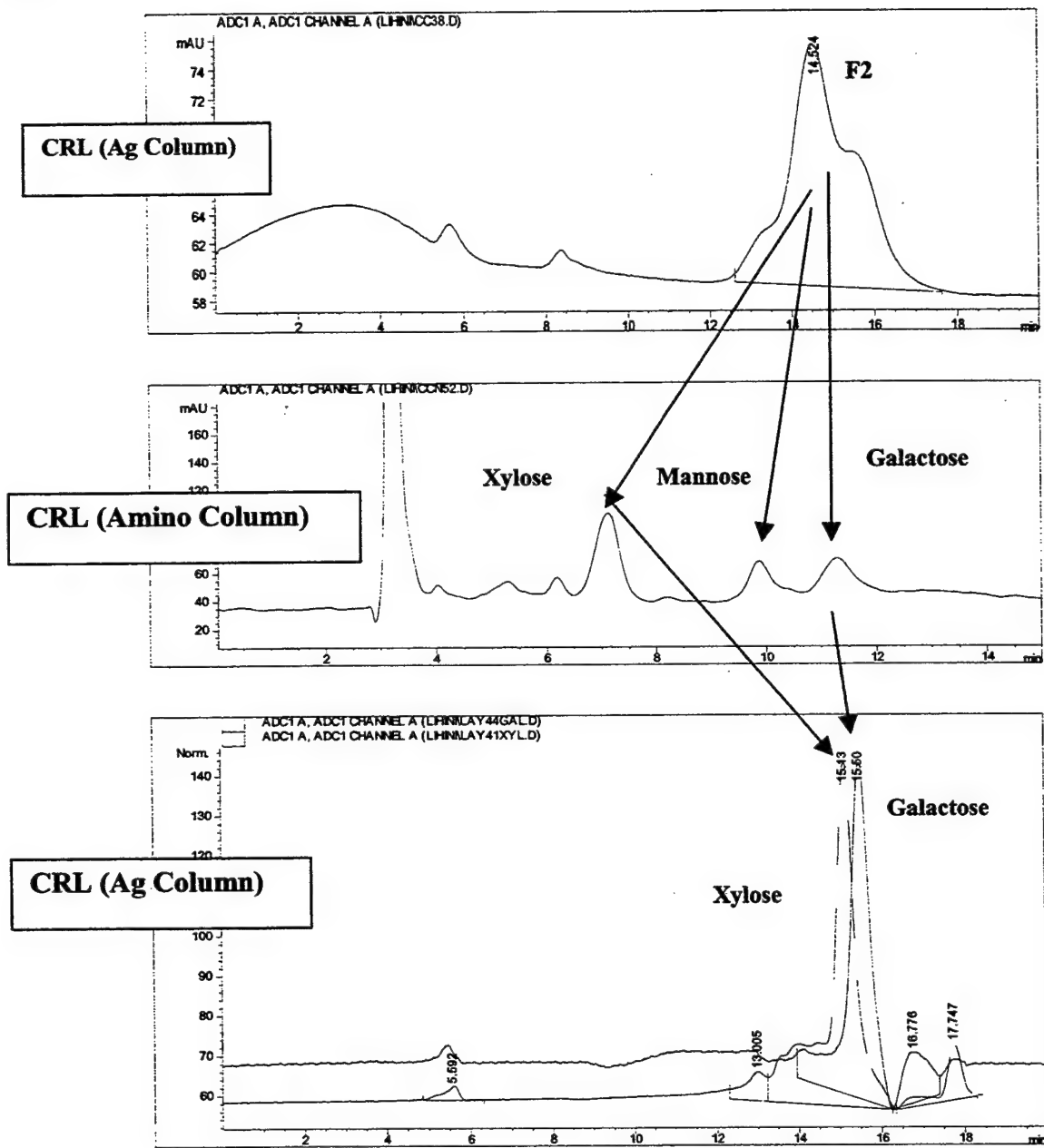


**Figure 4.6 HPLC of CRL on the Ag column, during the initial separation (A) and the second separation (B)**

A



**B**



C

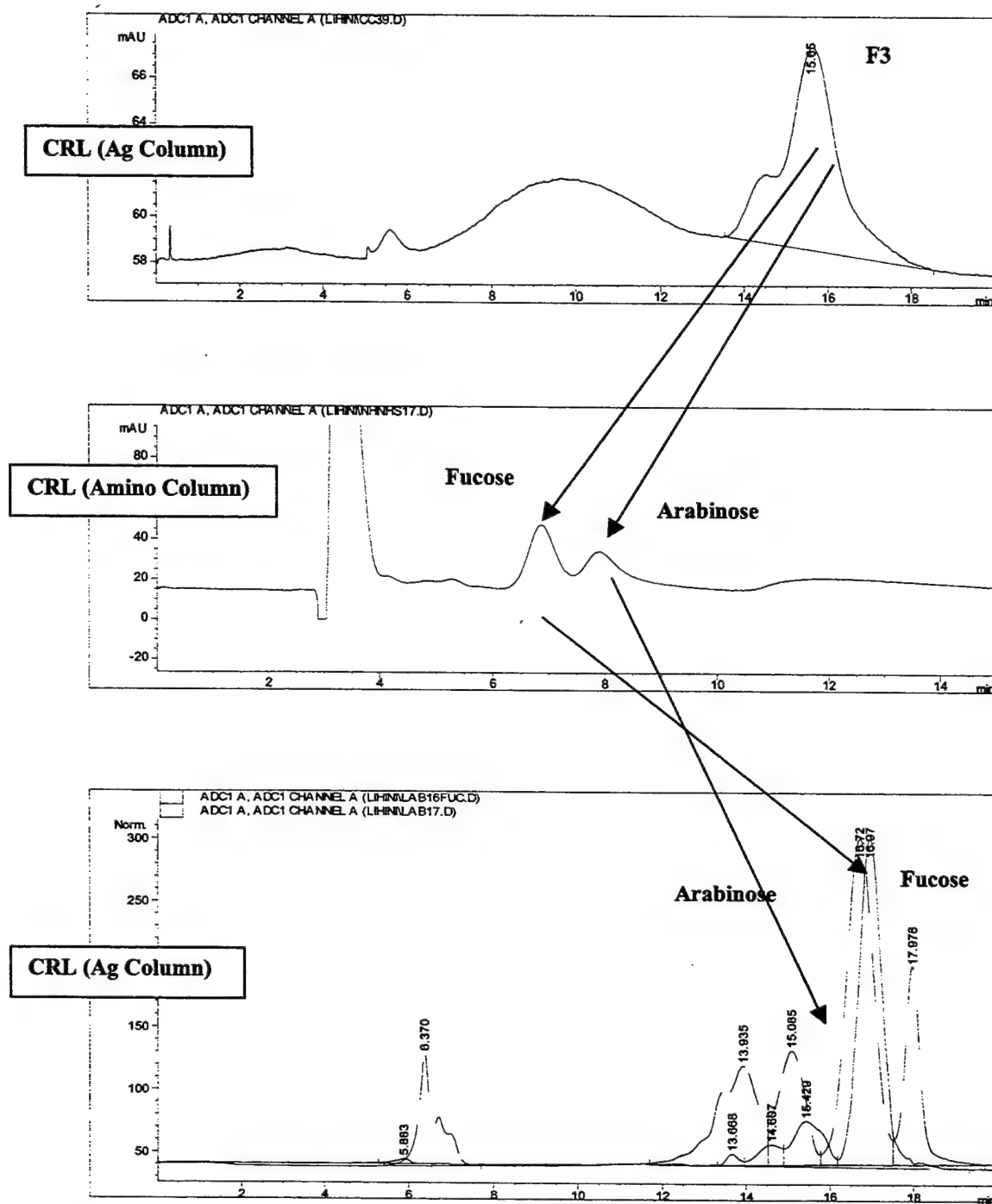


**Figure 4.7** The separation of individual monosaccharides from unhydrolyzed HMW DOM using a combination of cation exchange and reverse phase HPLC. (A) Separation of glucose and rhamnose; (B) separation of mannose, xylose and galactose; (C) separation of fucose and arabinose.

#### 4.3.1 Radiocarbon Analyses

Shown in Table 4.3 are the radiocarbon results for total HMW DOM and the monosaccharide fraction of HMW DOM isolated from each sample. The  $\Delta^{14}\text{C}$  values for the DIC and DOC in both the Atlantic and Pacific Ocean were obtained from Dr. James Bauer (unpublished (Atlantic) and Bauer et al. 1998). The individual monosaccharides isolated from the two Atlantic Ocean surface samples, CRL and MAB961, had modern  $\Delta^{14}\text{C}$  values (between 0 and 116 ‰ for CRL and between 49 and 92 ‰ for MAB961). In both cases,  $\Delta^{14}\text{C}$  values of the individual monosaccharides and DIC (67.3 and 59 ‰, respectively) are in good agreement. The  $\Delta^{14}\text{C}$  values of the monosaccharides isolated from CRL were also in good agreement with the  $\Delta^{14}\text{C}$  value of HMW DOM. The HMW DOM fraction is considerably enriched in  $\Delta^{14}\text{C}$  at this site (95 ‰) and, due to the proximity of this station to shore, may reflect a terrestrial DOM source. The monosaccharides isolated from MAB961 were enriched in  $\Delta^{14}\text{C}$  compared to the total HMW DOM fraction (-10 ‰) by approximately 60 ‰. The HMW DOM and the total DOM at this site are also enriched in  $^{14}\text{C}$  compared to open ocean values (typically -200 ‰) and likely reflects the presence of some terrestrially derived DOM (from the Delaware River and the Chesapeake Bay).

The results from the MAB profile (MAB966 (300 m) and MAB967 (750 m)) indicate that the sugars in HMW DOM at both these depths (-120 and -59 ‰, respectively) are younger than the total HMW DOM fraction (-375 and -255 ‰, respectively), but older than the DIC (-32 and -33 ‰ respectively). HMW DOM is enriched in  $^{14}\text{C}$  compared to DOM at both these depths, indicating that HMW DOM

<b>CRL</b>	<b>Weight</b>	<b><math>\Delta^{14}\text{C}</math></b>	<b>Error <math>\Delta^{14}\text{C}</math></b>
DIC		67.3	
Total DOC			
HMW DOC		95	5.2
HMW Sugar Blank		-431.4	10.3
Rhamnose	112.64	116.2	11
Fucose	83.85	1.0	12.2
Xylose+Arabinose+Galactose	88.4	58.0	11.7
Glucose+Mannose	132.8	84.8	10
<b>MAB961</b>	<b>Weight</b>	<b><math>\Delta^{14}\text{C}</math></b>	<b>Error <math>\Delta^{14}\text{C}</math></b>
DIC		59	
Total DOC		-32	
HMW DOC		-10.2	6.2
HMW Sugar Blank			
Rhamnose	68.8	49.4	17.9
Fucose	110	71.9	11.4
Xylose	79.5	92.3	14.6
<b>MAB966</b>	<b>Weight</b>	<b><math>\Delta^{14}\text{C}</math></b>	<b>Error <math>\Delta^{14}\text{C}</math></b>
DIC		-32	
Total DOC		-414	
HMW DOC		-375	4.4
Total Sugars	720	-120.3	4.5
<b>MAB967</b>	<b>Weight</b>	<b><math>\Delta^{14}\text{C}</math></b>	<b>Error <math>\Delta^{14}\text{C}</math></b>
DIC		-33	
Total DOC		-405	
HMW DOC	290	-254.7	5.9
Total Sugars	250	-59	7.7
<b>P961</b>	<b>Weight</b>	<b><math>\Delta^{14}\text{C}</math></b>	<b>Error <math>\Delta^{14}\text{C}</math></b>
DIC		68	
Total DOC		-275	
HMW DOC		-37.6	4.4
HMW Sugar Blank			
Rhamnose	54		
Fucose	128.4	80.3	15.5
Xylose	65.5		
Arabinose	88	33.8	20.1
Galactose	41.7		
<b>P962</b>	<b>Weight</b>	<b><math>\Delta^{14}\text{C}</math></b>	<b>Error <math>\Delta^{14}\text{C}</math></b>
DIC		-234	
Total DOC		-556	
HMW DOC		-351	5.6
HMW Sugar Blank	102.6	-772.2	3.9
Rhamnose+Fucose+Xylose	32	56.5	70.0

Table 4.1.3 The  $\Delta^{14}\text{C}$  values of different carbon fractions at each of the sites examined in this chapter. Refer to the text for descriptions of fm, fm\* and  $\Delta^{14}\text{C}$ .

may be enriched in a young component. As stated earlier, these two samples were collected after separation using a cation exchange column only, with no subsequent purification of the individual monosaccharide fractions. Thus they are likely to contain compounds other than monosaccharides.

The data for the Pacific Ocean profile are also given in Table 4.3 (P961 (surface) and P962 (1600 m)). Both fucose and arabinose, isolated from the surface ocean HWM DOM sample, have modern  $\Delta^{14}\text{C}$  values (33 and 80 ‰) which compare well to the surface DIC (68 ‰), and are enriched over the total DOM and the HMW DOM fraction (-275 and -37 ‰, respectively). In the case of HMW DOM isolated from the deep ocean, the  $\Delta^{14}\text{C}$  value of the rhamnose + fucose+xylose, ( $56.5 \pm 70$  ‰) fraction was enriched over the total DOM, HMW DOM and DIC (-556, -351 and -234 ‰) at this depth. The  $\Delta^{14}\text{C}$  value of these samples did agree well with the values for the individual monosaccharides in the surface ocean and the surface DIC. Consistent with the Atlantic Ocean data, the HMW DOM fraction is enriched in  $\Delta^{14}\text{C}$  compared to the total DOM, indicating that the fraction with a modern  $\Delta^{14}\text{C}$  value (e.g. sugars) may be enriched in the HWM DOM fraction.

In summary, all surface ocean monosaccharide samples showed modern  $\Delta^{14}\text{C}$  values that compare well with the  $\Delta^{14}\text{C}$  value of DIC at each station. Monosaccharides were also enriched in  $^{14}\text{C}$  compared to HMW DOM. In the deep Atlantic Ocean, the monosaccharide fraction was younger than the HMW DOM but older than the DIC at each depth. In the deep Pacific Ocean, on the other hand, the combined monosaccharide fraction was much younger than the HMW DOM and the DIC (at 1600 m) and compares

well to the  $\Delta^{14}\text{C}$  value of surface ocean DIC. For all samples HMW DOM is enriched in  $\Delta^{14}\text{C}$  compared to total DOM.

The similarity in the  $\Delta^{14}\text{C}$  values of the monosaccharides and DIC (modern values), coupled with the fact that the contaminant in our samples is old (-772 prior to the final silver column injection (contaminant from the amino column), and -432.4 after the final purification and isolation), indicates that the data obtained by this method are robust and not an artifact of the analysis.

The errors reported in Table 4.3 are largely due to small sample sizes. In most cases (except P962) the largest error over the entire procedure is associated with the AMS measurement. The sample weights and blanks were well quantified (by combustion) for the surface samples so there was little error associated with this step. The errors in the AMS measurement are usually associated with the counting: (1) either statistical errors associated with the number of counts measured for each target or (2) errors associated with the reproducibility of the of individual analyses for a given target. The deep Pacific Ocean sample was combusted before the contamination from the amino column was detected and as such had a blank of 100  $\mu\text{g}$  of C ( $\Delta^{14}\text{C}$  values of -770). In this case, the largest error for the entire analysis was that associated with quantifying the total amount of carbon contributed by the sugars to the sample. The weight of the sample, determined by integrating HPLC chromatograms, was  $32 \pm 5 \mu\text{g}$  C, giving a  $\Delta^{14}\text{C}$  error of approximately  $\pm 70 \%$ .



## 4.4 Discussion

### 4.4.1 Radiocarbon Results

Structural studies in Chapter 2 identified the presence of APS with a fixed monosaccharide distribution in both the surface and the deep oceans. Up to 60% of the surface water HMW DOC and 20% of the HMW DOC in the deep ocean is estimated to be APS. This decrease in APS concentration with depth, coupled with the data presented in Chapter 3 indicate that APS is produced during primary productivity in the surface ocean. The cycle of APS in the ocean must thus be controlled by production in surface waters, followed by transport to depth by one of the two mechanisms identified in section 4.1 (Figure 4.1), namely, the formation of deep water at high latitudes or the injection of DOM into the deep sea by particle dissolution.

We can use the radiocarbon data compiled in this chapter to determine the importance of these two mechanisms in controlling the cycle of APS. Shown in Figure 4.8 is a compilation of the  $\Delta^{14}\text{C}$  values in different fractions of carbon at Station M, where the Pacific Ocean profile (P961 and P962) used in this study was collected. The figure shows a depth profile of  $\Delta^{14}\text{C}$  values for both DOC and DIC, and the  $\Delta^{14}\text{C}$  values of suspended POC (at 1600 m) and sinking POC (600 m above the bottom) between 1991 and 1992 (Bauer et al., 1998; Druffel et al., 1996). In addition, the figure also shows the  $\Delta^{14}\text{C}$  values determined in this study for total HMW DOC and the HMW sugar fraction (APS) in both the surface ocean and at a depth of 1600 m. Even though the DOC is consistently 250 ‰ older than the DIC, the depth profiles of both DIC and DOC have a similar shape, indicating that the vertical distribution of these two fractions is controlled by the same mechanism.

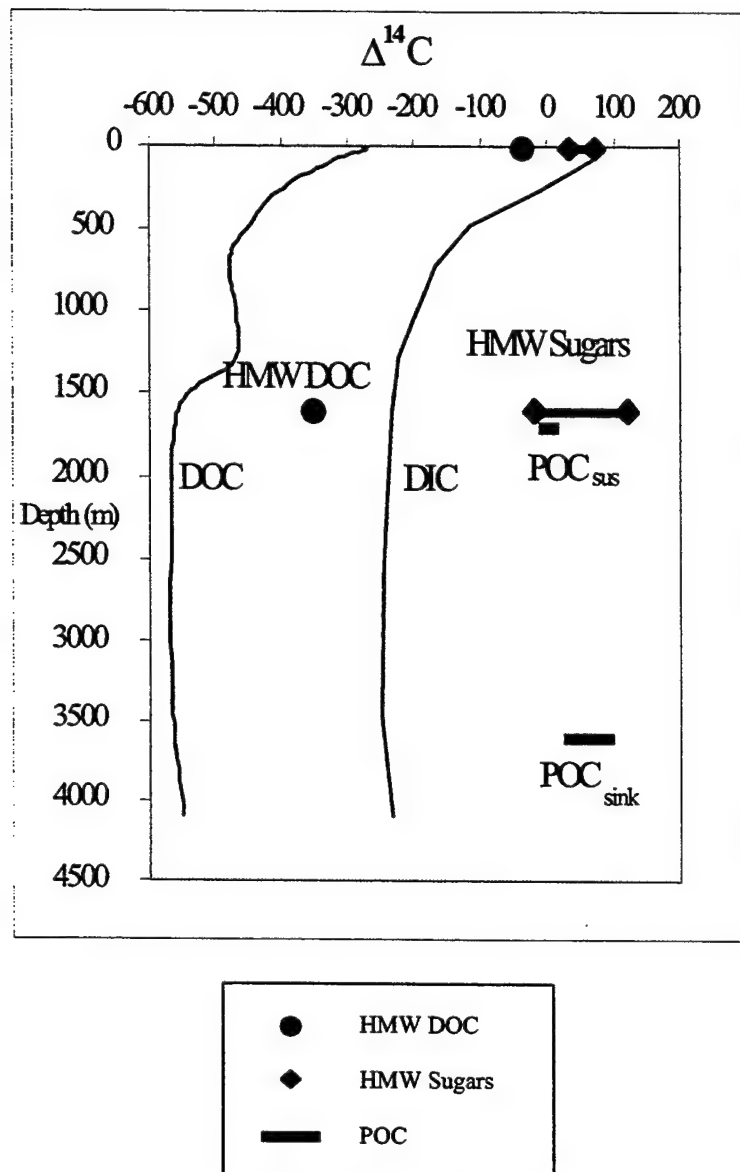


**Figure 4.8** Radiocarbon values for different fractions of carbon in the North East Pacific (Station M). POC<sub>sus</sub> is the  $\Delta^{14}\text{C}$  value of suspended POC, and POC<sub>sink</sub> is the  $\Delta^{14}\text{C}$  value of sinking POC. Depth profiles show DOC and DIC  $\Delta^{14}\text{C}$  values; filled circles are the  $\Delta^{14}\text{C}$  value of total HMW DOC (surface and 1600 m), and filled diamonds are the  $\Delta^{14}\text{C}$  value of the HMW Sugars (surface and 1600 m) DIC, POC and total DOC values were obtained from Druffel et al. 1996 and Bauer et al. 1998.

In both the surface and the deep ocean, HMW DOM is consistently younger (-59 compared to -275 ‰ in the surface oceans, and -351 versus -556 ‰ at 1600 m) than the total DOM. The monosaccharide fraction of HMW DOM, and thus the APS fraction, is

additionally enriched in  $^{14}\text{C}$  (56 ‰ in the deep ocean and between 30-80 ‰ in the surface ocean). Based on the modern  $\Delta^{14}\text{C}$  values of the monosaccharides at 1600 m (compared with DIC and DOM), the mechanisms which transport DIC and total DOM to the deep ocean must be independent of the mechanisms which transport APS to the deep ocean. The  $\Delta^{14}\text{C}$  values of APS (reported as HMW Sugars) at both depths compare well with each other and with the  $\Delta^{14}\text{C}$  values of surface DIC, suspended POC, and sinking POC. Based on the similarity in  $\Delta^{14}\text{C}$  values of APS and the different POC fractions, this data suggests that APS is transported to depth primarily by the dissolution or hydrolysis of POC, and not by the subduction of water masses at the poles.

Druffel et al. (1996) have also observed decreasing  $\Delta^{14}\text{C}$  values for suspended POC with depth (at this station), indicating either the adsorption of old DOC on to particles or the removal of a younger POC component with depth. If the latter case is true then the average age of suspended POC would decrease as the younger POC component is removed and the older component remains. The data for APS presented in this chapter suggests that a new component is indeed stripped from the particulate phase into the dissolved phase, in the deep ocean. This stripping of new APS from the particulate phase may serve to age the suspended POC component with depth.

Past studies on the radiocarbon ages of DOM have focused on the total DOM fraction (Bauer et al., 1998; Druffel et al., 1992; Williams and Druffel, 1987) and have found that  $\Delta^{14}\text{C}$  values in the surface Atlantic and Pacific oceans range from -150‰ to -230‰. The  $\Delta^{14}\text{C}$  values of DOM isolated from the deep ocean range between -400‰ (4000 radiocarbon years), in the Atlantic Ocean to -525‰ (6000 radiocarbon years) in the Pacific Ocean (Druffel et al., 1992; Williams and Druffel, 1987). This 2000 year

inter-basin difference in the radiocarbon age of bulk DOM is similar to the 1500 year deep ocean mixing time, and results from the passive aging of the DOM during deep water mass transport. However, the data collected in our study shows the presence of modern or post-bomb radiocarbon in a specific fraction of DOM (namely APS) isolated from the deep ocean indicating that within the larger cycle of total DOM, smaller, more dynamic cycles exist. Our data is consistent with the recent work of Hansell and Carlson, (1998) which shows variability in the concentration of DOC in the deep ocean (Figure 4.9). The variability in the DOC concentrations at low and middle latitudes is approximately 1-2  $\mu\text{M}$ , which agrees well with the predicted concentration of APS in the deep ocean (20% of HMW DOM, and thus 2-3% of the total DOC) based on the data presented in Chapter 2. Our deep ocean data also indicate that unlike total DOM, which shows inter-basin differences in  $\Delta^{14}\text{C}$  values, APS, delivered by particle dissolution, should have similar  $\Delta^{14}\text{C}$  values in both oceans.

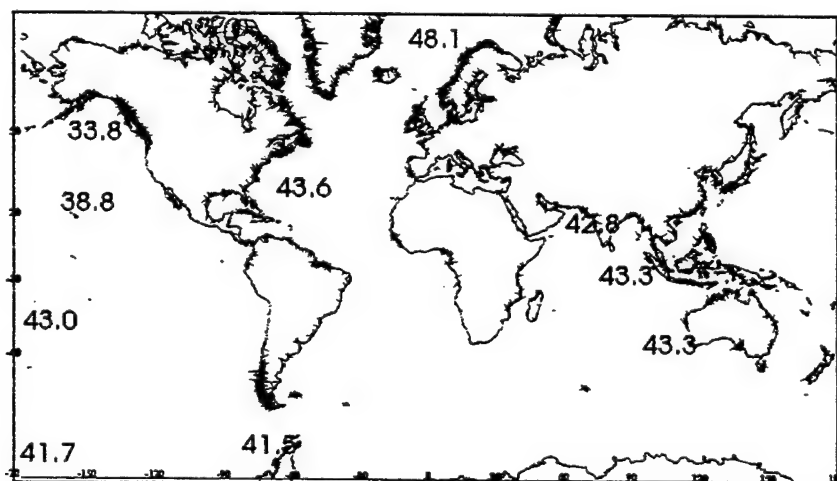


**Figure 4.9** Variations in the concentration of total DOC ( $\mu\text{M}$ ) over the whole ocean (after Hansell and Carlson, 1998).

Several studies exist in the literature indicating the release of DOM into the deep ocean by sinking particles. The diffusion of DOM from rapidly sinking fecal pellets (Jumars et al., 1989) and other particles has been hypothesized as one mechanism for the introduction of labile components from non-living POM to the deep ocean (Ittekkot et al., 1984). Dissolved organic matter may also be produced from particles by attached bacteria, due to loose hydrolysis-uptake coupling (Azam et al., 1983; Cho and Azam, 1988). Investigations of the extracellular hydrolytic activity of attached bacteria show that polymer hydrolysis rates exceed the carbon demand of attached bacteria, suggesting that DOM is being released into the surrounding waters more rapidly than it is being assimilated (Karner and Herndl, 1992; Smith et al., 1992). Studies have also shown elevated growth rates of free bacteria in the presence of colonized marine snow (Herndl, 1988), and a spatial and temporal coupling of deep sea bacterial biomass with surface production (Nagata et al., 1998). This data suggests that bacterial transformation of POM to DOM and ultimately DIC, occurs in the deep sea. Our data shows direct evidence for the production of DOM from POM in the deep ocean. Furthermore, the modern  $\Delta^{14}\text{C}$  value of APS in the deep ocean suggests that this fraction is turning over on short time scales. If APS is indeed 20 % of the HMW DOM in the deep ocean, as indicated by the structural data in Chapter 2, this corresponds to a deep ocean reservoir of approximately 20 Gt C, which is likely to be an important substrate for deep sea bacteria.

Chemical characterization of transparent exopolymer particles (TEP), (which are believed to be an important constituent of marine snow (Alldredge and Gotschalk, 1988; Mopper et al., 1995), POC (Cowie and Hedges, 1984; Skoog and Benner, 1997) and POM gels (Chin et al., 1998) all show the abundance of polysaccharides. Figure 4.10

shows the distribution of individual monosaccharides in TEP and POM compared to seawater HMW DOM. It is clear that these organic carbon fractions contain the same seven neutral monosaccharides. The relative distribution of monosaccharides in HMW DOM and TEP are very similar. If glucose is removed from the distribution, all three fractions show similar monosaccharide distributions. Thus, both possible sources and mechanisms for the rapid delivery of APS into the deep ocean have been identified. The contemporary age of APS is evidence for the occurrence of these processes.

The similarity in the  $\Delta^{14}\text{C}$  values of the individual monosaccharides (30-100‰) and their similarity to surface water DIC confirm previous findings that these monosaccharides are present together in a single polysaccharide, namely APS which is produced in surface waters during photosynthesis.

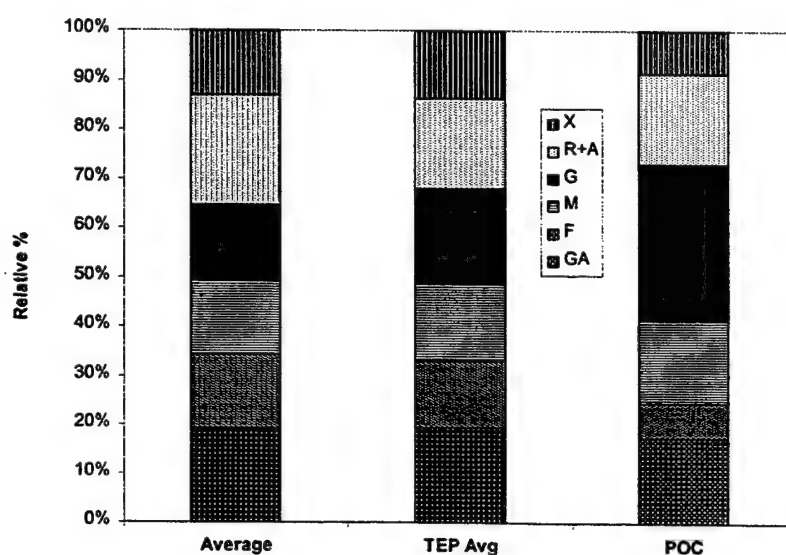


**Figure 4.10** A comparison of the distribution of monosaccharides in HMW DOM (Average), Transparent Exopolymer Particles (Avg TEP) (after Mopper et al., 1995), and sediment trap material (POC) (after Cowie and Hedges, 1984). Monosaccharides are galactose (Ga), fucose (F), mannose (M), glucose (G), rhamnose and arabinose (R+A) and xylose (X)

The monosaccharides separated from the MAB depth profile (-120‰ (MAB966, 300 m) and -59‰ (MAB967, 750 m) had  $\Delta^{14}\text{C}$  values older than the DIC at each depth (-32‰ and -33‰), contrary to the data from the Pacific Ocean sample (P962). However, these MAB samples were only separated on the cation exchange column and showed considerable contamination (up to 60%) from the base line. Unhydrolyzed HMW DOM must be older than the monosaccharide fraction in order to maintain a mass balance of the radiocarbon. Even a small fraction of this old material in the monosaccharide samples could decrease their  $\Delta^{14}\text{C}$  values considerably.

#### 4.4.2 Analytical Methods

The overall method described in this chapter realizes the goal of separating individual monosaccharides from total hydrolyzed HMW DOM for radiocarbon analysis. However, several problems were encountered when developing this method. The cumulative result of these different problems was low monosaccharide recoveries at the end of the analyses shown in Figure 4.2.

Several avenues were explored in an attempt to increase monosaccharide recoveries, including a modification of the hydrolysis and desalting procedures discussed in section 4.2.

Two other hydrolysis methods were compared before the TFA method was chosen. One method used 4M HCl hydrolysis at 100 °C for 4 hours (10 mg of total sample/ 2ml acid). The method of Cowie and Hedges (1984) was also tested, where the HMW DOM samples were hydrolyzed with 12 M  $\text{H}_2\text{SO}_4$  for 2 h at room temperature, then diluted to 1.2 M and hydrolyzed for 3 hours at 100°C. Both the TFA and HCl methods gave comparable yields (7-9% of total carbon in CRL HMW DOM), while the

H<sub>2</sub>SO<sub>4</sub> method gave lower yields (3-5%). Time course studies on the 2M TFA hydrolysis of CRL HMW DOM showed no increase in monosaccharide yields between 40 minutes and 2 h. We also attempted to increase hydrolysis yields by performing consecutive 2 M TFA hydrolyses on HMW DOM. Samples were first hydrolyzed, then neutralized with ammonium hydroxide (NH<sub>4</sub>OH), and hydrolyzed again. There were no detectable increases in monosaccharide yields by either HPLC or <sup>1</sup>HNMR.

Two different cation exchange columns were also tested for the HPLC separation. In addition to the cation exchange column in the Ag form (described in section 4.2), a column using Pb as the counter ion (Supelco (Supelcogel™ Pb, cat # 5-9343, Supelco, Inc, Bellefonte, PA) (referred to hereafter as the Pb column) was also tested. Both columns were sensitive to the cations present in the samples, and while the Pb column gave better separation between monosaccharides, it was also more sensitive to salt concentrations in our samples and deteriorated quickly. Metal ions (Na<sup>+</sup>, Fe<sup>3+</sup>, Ca<sup>2+</sup>) and H<sup>+</sup>, could replace both the Pb and Ag ions, resulting in a mixed ligand-exchange column. This changes the separation characteristics of the column and may also act to swell or shrink the resin. Two methods of desalting (cation and anion exchange) were tested to determine if the column lifetime and separation characteristics of each sample could be enhanced. Monosaccharide recoveries, for a CRL sample, spiked with 0.5 mg of a monosaccharide standard, following hydrolysis, neutralizing and lyophilization were 100±10%, with no detectable changes in the relative distribution of the monosaccharides. During desalting, monosaccharide recoveries were between 70±10% for the anion exchange resin, and 6-7.5% for the cation exchange resin. Due to the high



monosaccharide losses to the cation exchange column, samples were not desalted with this resin.

While desalting with the anion exchange column enhanced the separation of monosaccharides from the unhydrolyzed material, this method introduced high concentrations of  $\text{Cl}^-$  ions into the sample. The presence of  $\text{Cl}^-$  ions in the sample interfered with the separation of monosaccharides in the Ag column over time by stripping the Ag from the column as  $\text{AgCl}$ . In the future, samples should be desalted using an anion exchange column in the hydroxide form.

The low monosaccharide recoveries obtained by this procedure were of concern primarily due the possibility of isotopic fractionation associated with the loss of this material. However, no systematic removal of any particular monosaccharide was observed either during Ag column separation or amino column separation. Following the Ag column separation, the relative distribution of monosaccharides in the samples was similar to the relative distribution of monosaccharides determined by GC. Following the amino column separation, however, changes in the relative distribution of monosaccharides compared to the distribution determined by GC were detected. Figure 4.11 shows the relative distribution of monosaccharides in the three surface samples examined in this study. While the relative distribution of monosaccharides determined by GC and HPLC are different, there is no systematic removal of any particular monosaccharide.

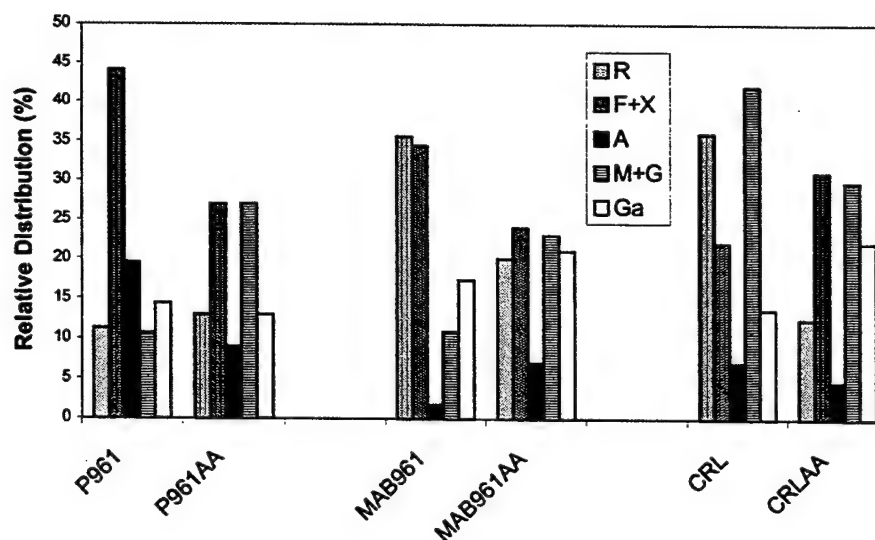


**Figure 4.11** The relative distribution of monosaccharides in HMW DOM injected onto the amino column compared to the relative distribution of monosaccharides in HMW DOM determined by GC (AA).

Furthermore, the comparable ages of the individual monosaccharides and their similarity to the  $\Delta^{14}\text{C}$  value of DIC at each site indicate that there is no isotopic fractionation associated with the losses of monosaccharides during the analysis.

#### 4.5 Conclusions

This chapter describes a robust method for the isolation of individual monosaccharides from hydrolyzed DOM for radiocarbon analysis. The samples processed in this study were not collected specifically for this purpose and due to extensive method development, showed low monosaccharide recoveries. However, none of the steps in this analysis systematically fractionates the monosaccharide distribution. Thus a representative sample of all the monosaccharides can be isolated.

The similarity in the  $\Delta^{14}\text{C}$  values of individual monosaccharides is consistent with the structural data that showed a constant relative distribution of monosaccharides, implying that these monosaccharides are present together within a single polysaccharide. Furthermore, the similarity between the  $\Delta^{14}\text{C}$  values of surface DIC and the monosaccharides isolated from HMW DOM indicates biosynthesis of these polysaccharides from DIC during photosynthesis consistent with the data presented in Chapter 3. The deep ocean data from the Pacific shows for the first time the presence of bomb radiocarbon in DOM isolated from the deep ocean (in the form of APS). The  $^{14}\text{C}$  enrichment of APS relative to DIC (at 1600 m) and the similarity in the  $\Delta^{14}\text{C}$  values of APS and POM suggest that APS is injected into deep ocean by settling particles. The contemporary age of the monosaccharides in the deep ocean further indicates rapid cycling of APS, highlighting its importance as a substrate for deep sea bacteria. Finally, the concentration of APS in the deep ocean is estimated to be 1-2  $\mu\text{M}$  (based on the alditol acetate yields), on the same order of magnitude as the changes in the concentration of DOC in the deep ocean observed by Hansell and Carlson (1998).

#### 4.6 References

- Aldredge A. L. and Gotschalk C. (1988) In situ settling behavior of marine snow. *Limnology and Oceanography* **33**(3), 339-351.
- Azam F., Fenchel T., Field J. G., Gray J. S., Meyer-Reil L. A., and Thingstad F. (1983) The ecological role of water-column microbes in the sea. *Marine Ecology Progress Series* **10**, 257-263.
- Bauer J. E., Druffel E. R. M., Williams P. M., Wolgast D. M., and Griffin S. (1998) Temporal variability in dissolved organic carbon and radiocarbon in the eastern North Pacific Ocean. *Journal of Geophysical Research* **103**(C2), 2867-2881.
- Borch N. H. and Kirchman D. L. (1997) Concentration and composition of dissolved combined neutral sugars (polysaccharides) in seawater determined by HPLC-PAD. *Marine Chemistry* **57**, 85-95.
- Boutton T. (1991) Stable carbon isotope ratio of natural materials: 1. Sample preparation and mass spectrometric analysis. In *Carbon Isotope Techniques* (ed. D. C. Coleman and B. Fry), pp. 155-170.
- Broecker W. M. and Peng T. (1982) *Tracers in The Sea*. Lamont-Doherty Geological Observatory.

- Chin W.-C., Orellana M. V., and Verdugo P. (1998) Spontaneous assembly of marine dissolved organic matter into polymer gels. *Nature* **391**, 568-572.
- Cho B. C. and Azam F. (1988) Major role of bacteria in biogeochemical fluxes in the ocean's interior. *Nature* **332**, 441-443.
- Cowie G. L. and Hedges J. I. (1984) Determination of neutral sugars in plankton, sediments, and wood, by capillary gas chromatography of equilibrated isomeric mixtures. *Analytical Chemistry* **56**, 497-504.
- Druffel E. R. M., Bauer J. E., Williams P. M., Griffin W., and Wolgast D. (1996) Seasonal variability of particulate organic radiocarbon in the northeast Pacific Ocean. *Journal of Geophysical Research* **101**(C9), 20543-20552.
- Druffel E. R. M., Williams P. M., Bauer J. E., and Ertel J. R. (1992) Cycling of dissolved and particulate organic matter in the open ocean. *Journal of Geophysical Research* **97**(10), 15639-15659.
- Hansell D. A. and Carlson C. A. (1998) Deep-ocean gradients in the concentration of dissolved organic carbon. *Nature* **395**, 263-266.

- Herndl G. J. (1988) Ecology of amorphous aggregations (marine snow) in the Northern Adriatic Sea. II. Microbial density and activity in marine snow and its implications to overall pelagic processes. *Marine Ecology Progress Series* **48**, 265-275.
- Ittekkot V., Deuser W. G., and Degens E. T. (1984) Seasonality in the fluxes of sugars, amino acids, and amino sugars to the deep ocean: Sargasso Sea. *Deep Sea Research* **31**(9), 1057-1069.
- Jumars P. A., Penry D. L., Baross J. A., Perry M. J., and Frost B. W. (1989) Closing the microbial loop: Dissolved carbon pathways to heterotrophic bacteria from incomplete ingestion, digestion and adsorption in animals. *Deep Sea Research Part A* **36**, 483-495.
- Kamer M. and Herndl G. J. (1992) Extracellular enzymatic activity and secondary production in free-living and marine snow associated bacteria. *Marine Biology* **113**, 341-347.
- McCarthy M., Hedges J. I., and Benner R. (1996) Major biochemical composition of dissolved high molecular weight organic matter in seawater. *Marine Chemistry* **55**, 282-297.

- Mopper K., Zhou J., Sri Ramana K., Passow U., Dam H. G., and Drapeau D. T. (1995)  
The role of surface active carbohydrates in the flocculation of a diatom bloom in a  
mesocosm. *Deep Sea Research II* **42**(1), 47-73.
- Nagata T., Fukuda H., Fukuda R., and Koike I. (1998) Regional variability of  
bacterioplankton biomass in the deep ocean and its implications for oceanic  
carbon cycling. *American Society of Limnology and Oceanography, Meeting  
Abstracts San Diego, 1998.*
- Santschi P. H., Guo L., Baskaran M., Trumbore S., Southon J., Bianchi T. S., Honeyman  
B., and Cifuentes L. (1995) Isotopic evidence for the contemporary origin of high  
molecular weight organic matter in oceanic environments. *Geochimica et  
Cosmochimica Acta* **59**(3), 625-631.
- Skoog A. and Benner R. (1997) Aldoses in various size fractions of marine organic  
matter: implications for carbon cycling. *Limnology and Oceanography* **42**, 1803-  
1813.
- Smith D. C., Simon M., Alldredge A. L., and Azam F. (1992) Intense hydrolytic enzyme  
activities on marine aggregates and implications for rapid particle dissolution.  
*Nature* **359**, 139-142.
- Stuiver M. and Polach H. A. (1977) Discussion: Reporting of  $^{14}\text{C}$  data. *Radiocarbon* **19**,  
355-363.

Williams P. M. and Druffel E. R. M. (1987) Radiocarbon in dissolved organic matter in the central North Pacific Ocean. *Nature* 330, 246-248.



## **5. Conclusions**

### **5.1 General Conclusions**

Despite its large size and importance to the global carbon cycle, little is known about the composition and cycling of dissolved organic matter (DOM) in the ocean. Our understanding of the oceanic cycle of DOM has been impeded by the inability to isolate sufficient quantities of DOM, without chemical fractionation, for the more sophisticated analytical techniques such as  $^1\text{H}$ NMR spectroscopy. When this thesis work was begun, only 5-10% of the total DOM had been isolated as humic substances by adsorption on to hydrophobic resins (Gagosian and Stuermer, 1977). As discussed in the Chapter 1 the extensive chemical characterization of these XAD isolates coupled with the old average age of DOM determined by radiocarbon analyses (Williams and Druffel, 1987), led to the hypothesis that DOM accumulating in the ocean was formed by the geopolymerization of simple biochemicals.

Due to the advent of tangential flow ultrafiltration, it has been possible isolate DOM based on size rather than chemical characteristics. Using filters with a nominal pore size of 1 nm, it is possible to consistently isolate 20-30% of total DOM (high molecular weight (HMW)) by ultrafiltration (Benner et al., 1992; Carlson and Mayer, 1985). This has allowed us and other investigators (Aluwihare et al., 1997; Benner et al., 1992; McCarthy et al., 1996; McCarthy et al., 1998) to chemically characterize a more representative fraction of DOM. The work presented in this thesis was undertaken with the recognition that some knowledge of the molecular-level composition of DOM was required in order to gain a better understanding of its cycle in the ocean.

Presented in Chapter 2 are the results from the chemical characterization of HMW DOM isolated from several different sites including the Pacific Ocean, the Middle Atlantic Bight, and the Eastern North Atlantic. Chapter 3 describes the isolation and chemical characterization of HMW DOM from the cultures of three species of phytoplankton: *Thalassiosira weissflogii*, *Emiliana huxleyi* and *Phaeocystis*. Chapter 4 addresses the use of radiocarbon analyses to determine the mechanisms that control the vertical distribution of HMW DOM in the ocean. The results of this analysis are as follows:

- (1) *Fifty to sixty percent of the HMW DOM isolated from the surface ocean and 20-30% of the HMW DOM isolated from the deep ocean consist of chemically related, identifiable biochemicals, at all the sites examined.*

Chemical characterization using  $^1\text{H}$ NMR,  $^{13}\text{C}$ NMR,  $^{15}\text{N}$ NMR, monosaccharide analysis, lipid analysis and linkage analysis, showed the presence of compounds with a similar chemical composition at all the sites examined. These compounds were termed acylated polysaccharides (APS), and are composed of a similar ratio of carbohydrate: acetate: lipid carbon ( $80\pm4:10\pm2:9\pm4$ ). APS contains 7 neutral monosaccharides in a fixed ratio. Rhamnose, fucose, xylose, mannose, and glucose all show similar relative abundance ( $14\pm1\%$ ), with arabinose being slightly depleted (6%) and galactose being slightly enriched (21%). Furthermore, the  $^{15}\text{N}$ NMR data in Chapter 2 in combination with the C/N ratios in HMW DOM suggests that APS also contain N-acetylated amino sugars, which constitute approximately 50% of the carbohydrate fraction. Contrary to earlier beliefs that

DOM was uncharacterizable due to its polycondensate nature, this study indicates that the high resolution analytical methods available today can be used successfully to determine the structure of a large fraction of the DOM isolated from the ocean.

- (2) *Two of the three cultured phytoplankton species examined in this study, Thalassiosira weissflogii and Emiliania huxleyi, produced HMW DOM with similar chemical characteristics to HMW DOM isolated from seawater. APS produced in these cultures were degraded more slowly than other polysaccharides present in the exudate at the beginning of the incubation.*

The work in Chapter 3 showed that both *Thalassiosira weissflogii* and *Emiliania huxleyi* produced compounds that are closely related to APS isolated from seawater. The *Phaeocystis* species examined in this study did not produce detectable amounts of APS. Furthermore, degradation of the *T. weissflogii* exudate showed that the component resembling APS was degraded more slowly than other polysaccharides in the exudate suggesting an inherent resistance to bacterial degradation. While the total amount of carbon associated with APS in each of these cultures is likely to vary depending on growth conditions, this particular study implies that APS may comprise 2-3 % of the total organic carbon produced by these algae. Contrary to the geopolymerization model, this study demonstrated that DOM accumulating in seawater might be directly produced by biosynthesis.

- (3) *The  $\Delta^{14}C$  values of the individual monosaccharides confirm that the carbohydrate fraction of HMW DOM (APS) is produced during photosynthesis in the surface*

*ocean. Furthermore, the APS fraction in the deep ocean is of contemporary origin also, indicating delivery of APS to the deep ocean on time scales shorter than the mixing time of the ocean.*

Chapter 4 describes a robust method for the isolation of the monosaccharides that constitute APS from total HMW DOM for radiocarbon analysis. The data show that the individual monosaccharides from each sample have similar  $\Delta^{14}\text{C}$  values ( $50 \pm 30$  ‰) indicating that they were formed recently in surface waters and are likely present together in a single polymer. These values also compare well to the  $\Delta^{14}\text{C}$  of DIC at these same sites confirming that the APS fraction is produced during photosynthesis. The  $\Delta^{14}\text{C}$  values of APS in the deep ocean are also similar to surface water DIC values indicating rapid transport of APS to depth. Thus we hypothesize that APS produced in surface waters are delivered to the deep ocean by settling and subsequent hydrolysis and dissolution of particulate organic matter raining through the water column. This data implies that APS in the deep ocean is turning over on annual to decadal time scales and is the first evidence for the presence of bomb radiocarbon in deep ocean DOM.

Figure 5.1 shows a compilation of the data presented above into a simple model for the cycling of APS in the ocean. This work shows that contrary to the accepted dogma of geopolymerization up to 20% of the DOM accumulating in the ocean on annual to decadal time scales is produced directly by biosynthesis. Furthermore, the radiocarbon results suggest that while a major fraction of DOM is passively distributed throughout the

ocean via ocean circulation, particular fractions of DOM have more dynamic cycles and may be injected into the deep ocean by particle dissolution.

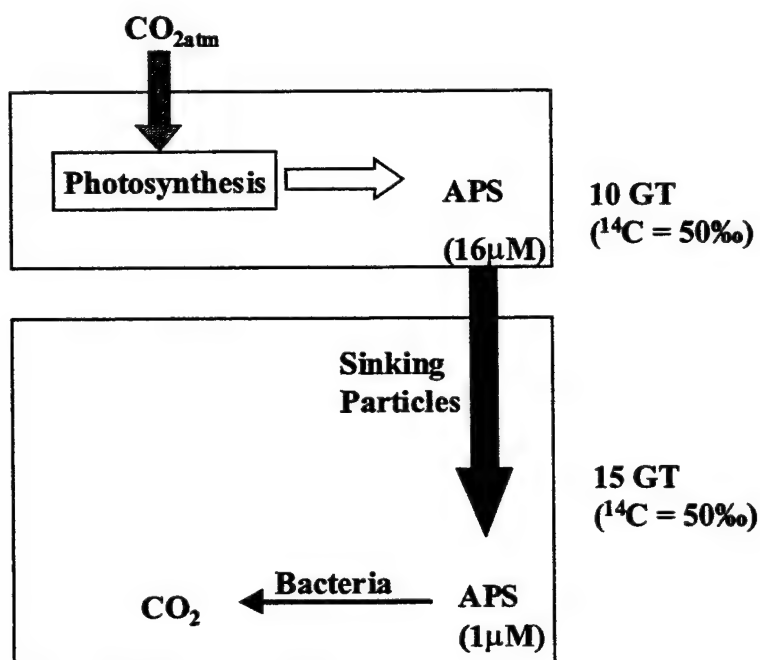


**Figure 5.1** Cycling of APS in the Ocean.

In order to better understand the rates associated with each of the arrows shown in the Figure 5.1 a more comprehensive model (as in Figure 5.2) for the cycling of APS in the surface ocean needs to be constructed .

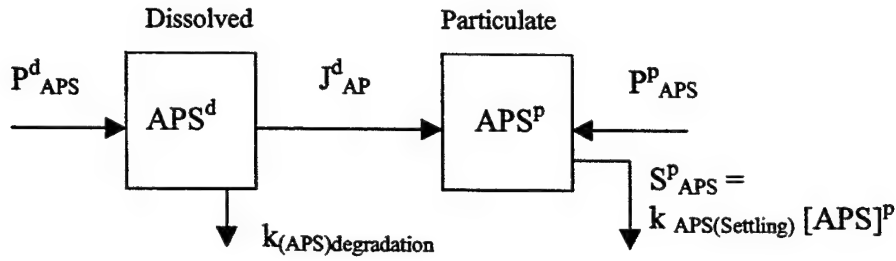


Figure 5.2 The cycling of APS in the Surface Ocean. See text for an explanation of the terms.

Using Figure 5.2, the time dependent change in the inventory of APS in both the surface dissolved phase and the surface particulate phase may be expressed as follows:

$$\left( \frac{\partial [APS]^d_{surf}}{\partial t} \right) = P^d_{APS} - k_{APS(deg\ radiation)} [APS]^d - J^d_{APS} = 0$$

$$\left( \frac{\partial [APS]^p_{surf}}{\partial t} \right) = P^p_{APS} + J^d_{APS} - k_{APS(Settling)} [APS]^p = 0$$

where  $[APS]^d_{surf}$  and  $[APS]^p_{surf}$  are the inventories of dissolved and particulate APS, respectively, in the surface ocean (in Gt).  $P^d_{APS}$  and  $P^p_{APS}$  are the production rates of dissolved and particulate APS, respectively (in Gt C/yr).  $k_{APS(deg\ radiation)}$  and  $k_{APS(settling)}$  are the rate constants for the biodegradation of the dissolved APS and the settling of particulate APS, respectively.  $S^p_{APS}$  is the sinking flux of POC, which is equal to the product of  $k_{APS(settling)}$  and  $[APS]^p_{surf}$ . Combining the two equations we have

$$P^d_{APS} + P^p_{APS} = k_{APS(Settling)} [APS]^p + k_{APS(deg\ radiation)} [APS]^d$$

The production rate ( $P_{\text{APS}}^{\text{d}}$ ) of dissolved APS can be estimated from the culture data presented in Chapter 3. Dissolved APS concentrations in the cultures were approximately 2% of the total POC plus DOC. Extending these values to the field and using a value of 50 Gt C/yr for annual primary productivity in the ocean, the annual production rate of APS (from the culture data) is approximately 1 Gt C/yr. The production rate of particulate APS ( $P_{\text{APS}}^{\text{p}}$ ) can be estimated using the carbohydrate content of phytoplankton. Dissolved APS contains rhamnose, fucose, xylose, mannose, glucose and galactose in roughly equal abundance with arabinose being approximately half as abundant and the other sugars (Chapter 2). Assuming that particulate APS also contains these same ratios of monosaccharides and that all the rhamnose in the phytoplankton cell is present only in APS, the rhamnose content of phytoplankton cells can be used to estimate the total amount of particulate (or phytoplankton associated) APS. Using the values for total POC and the percentage of rhamnose associated with this POC in a laboratory culture of *Skeletonema Costatum* (Biersmith and Benner, 1998), it is possible to estimate that 1.9-3 % of the total POC may be present as APS. The biodegradation rate constant ( $k_{\text{APS}(\text{degradation})}$ ) can be estimated from the *T. weissflogii* degradation experiment discussed in Chapter 3. Since the bacterial cell numbers in the degradation experiment were higher than those observed in the field, the rate constant, 0.042/day (or 15.33/yr) calculated from the culture experiment is likely to be up to 2 orders of magnitude lower in the field. Thus  $k_{\text{APS}(\text{degradation})}$  is taken to be approximately 0.15 /yr. An average POC settling rate constant of 0.05/day (or 18.25/yr), was assumed based on the data of Gustafsson et al. (1997). Sinking POC inventories are estimated to be approximately 0.24-1.3 Gt C based on the data of Martin et al. (1997), and of this APS

is expected to be between 1.9-3% (as above for  $P^p_{APS}$ ) . Each of the numbers used in this model are given below in Table 6.1

Term	Value
$[APS]^d_{surf}$	10 Gt C
$[APS]^p_{surf}$	0.04 Gt C
$P^d_{APS}$	1 Gt C/yr
$P^p_{APS}$	1.5 Gt C/yr
$k_{APS(degradation)}$	0.15 /yr
$k_{APS(settling)}$	18.25/yr

**Table 5.1 Numerical values for each of the terms shown in Figure 5.2.** See text for an explanation of each of the terms and the sources of each of the reported values.

Substituting these values into

$$P^d_{APS} + P^p_{APS} = k_{APS(Settling)} [APS]^p + k_{APS(degradation)} [APS]^d$$

we get

$$1 \text{ Gt C/yr} + 1.5 \text{ Gt C/yr} = 18.33/\text{yr} (0.04 \text{ Gt}) + 0.15/\text{yr} (10 \text{ Gt})$$

These values show surprisingly good agreement indicating that the estimates from the culture data are reasonable. However, many assumptions went into the generating these numbers and in order to be certain of this data more work needs to be done in order to



establish robust production rates for both particulate and dissolved APS and biodegradation rates for dissolved APS in culture.

In the deep ocean the only source of APS is the degradation of POC. Thus at steady state, both the production of dissolved APS from particles and the degradation of dissolved APS must be equal and can be expressed as :

$$k_{APS(\text{Settling})} [APS]^p = k_{APS2(\text{degradation})} [APS]^d_{\text{deep}}$$

where  $k_{APS2(\text{degradation})}$  is the rate constant for the degradation of dissolved APS in the deep ocean and  $[APS]^d_{\text{deep}}$  is the inventory of APS in the deep ocean (from Figure 5.1). Substituting the appropriate values in the equation we can estimate that the degradation rate of constant of APS in the deep ocean is approximately 0.05/yr.

## 5.2 Future Research Directions

Structural identification is likely to be the most powerful tool in understanding the different processes that affect the concentration, distribution and residence time of different fractions of DOM. Microbial degradation rates of DOM, the metal chelating ability of DOM, the light absorbing properties and so on, are all controlled by the chemical structure of DOM. Thus, a comprehensive understanding of any of these processes requires an understanding of the molecular level composition of DOM. While this study has made an initial attempt to do this, much work remains to be done, and many avenues remain unexplored.

For example, 70-80% of total DOM (low molecular weight) remains uncharacterized. If we are to understand the cycle of DOM, a concerted effort must be made to design a method for the isolation of low molecular weight DOM from seawater. Some similarities between the HMW and LMW fraction of DOM have been observed, the C/N ratio of total DOM is similar to HMW DOM, between 15-22. Investigators have also looked at the monosaccharide composition of the LMW fraction (Skoog and Benner 1997). However, little compositional information has been gleaned from these studies, thus much work needs to be done in this area if we are to understand the composition of LMW DOM.

The major challenge that remains from the work done in Chapter 2 is the development of a method to isolate APS from the total HWM DOM fraction. Once this is done, rigorous quantification of the individual components of APS may be performed. The most promising method to do this may still be methylation of the polysaccharide. Perfecting the methylation reaction will also aid in the linkage analysis, which is essential for completely characterizing the polymer. Other possible methods for the isolation of the polysaccharide fraction are gel electrophoresis, ethanol precipitation and affinity chromatography. The source of lipid resonances in the  $^1\text{H}$ NMR needs to be identified, perhaps by repeating the  $\text{BBr}_3$  reaction. In order to establish the presence of N-acetylated sugars (which are an important fraction of the HWM DOM as suggested by the data in Chapter 2), a method to hydrolyze these polymers needs to be developed. Isolation of APS from the total HMW DOM fraction may aid in this hydrolysis. Finally, this chapter briefly addressed the possible presence of unhydrolyzable proteins as the major fraction of nitrogen in the deep ocean, and thus the major fraction of nitrogen in the entire ocean.

Nitrogen-15 NMR should be pursued as the major tool to characterize this fraction. In order to establish the presence of proteins a similar hydrolysis experiment as was carried out for surface water HMW DOM should be repeated for a deep ocean sample. Again, gel electrophoresis may be a good tool for the final isolation of the protein fraction.

Many avenues remain to be studied in Chapter 3. From a physiological point of view, variations in the production of APS according to changes in growth conditions may offer some insight into the function of these compounds. It would also be interesting to test if other *Phaeocystis* species can produce APS, particularly in light of the differences in the quality of the DOM observed in regimes dominated by this species. While the bacterial degradation of the exudates was extensively chemically characterized, much needs to be done in determining the dynamics of the bacterial population during the degradation of DOM. Not only should respiration, bacterial production and bacterial numbers be monitored, but changes in species composition should also be monitored and correlated with the removal of different fractions of DOM. This work can then be used to correlate the vertical and horizontal variations in bacterial population with the chemical quality of the DOM available for degradation in the ocean.

The radiocarbon method presented in Chapter 4 is a powerful tool for elucidating the cycle of DOM in the ocean. However, the method needs some refinement. Some of the carbon losses may be compensated for by collecting bigger samples, and avoiding diafiltration. Furthermore, better desalting protocols should be developed in order to preserve the life of the HPLC column and to avoid losing material to the column. In order to conclusively establish the hypothesis that APS are released into the deep ocean from POM (either due to hydrolysis or dissolution), depth profiles of the  $\Delta^{14}\text{C}$  values in

APS isolated from both the Pacific and the Atlantic Ocean need to be constructed. Further evidence for the release of APS from POC could be obtained by correlating small variations in APS concentration with variations in particle flux. In order to do this however, robust methods for the quantification of APS need to be developed. If the concentration of APS is conclusively established, this can be used in conjunction with the  $\Delta^{14}\text{C}$  values of HMW DOM and APS to determine the average age of the old component of DOM present at each site. It would also be interesting to determine what fraction of the DOM utilized by free living deep sea bacteria is derived from old refractory DOM and young, newly synthesized DOM. An alternative explanation for the presence of modern APS in the deep ocean is the biosynthesis of APS by deep sea bacteria. It is thus important to determine if deep sea bacteria produce sufficient quantities of DOM to maintain the deep sea inventory of APS. Furthermore, exudates of bacteria should be analyzed as in Chapter 3 to determine if bacteria are an additional source of APS.

### 5.3 References for Chapter 5

Aluwihare L. I., Repeta D. J., and Chen R. F. (1997) A major biopolymeric component to dissolved organic carbon in surface seawater. *Nature* **387**, 166-169.

Benner R., Pakulski J. D., McCarthy M., Hedges J. I., and Hatcher P. G. (1992) Bulk chemical characteristics of dissolved organic matter in the ocean. *Science* **255**, 1561-1564.

Biersmith A. and Benner R. (1998) Carbohydrates in phytoplankton and freshly produced dissolved organic matter. *Marine Chemistry* **63**, 131-144.

Carlson D. J. and Mayer L. M. (1985) Molecular weight distribution of dissolved organic materials in seawater as determined by ultrafiltration : A re-examination. *Marine Chemistry* **16**, 155-171.

Gagosian R. B. and Stuermer D. H. (1977) The cycling of biogenic compounds and their diagenetically transformed products in seawater. *Marine Chemistry* **5**, 605-632.

- Gustafsson, O., Gschwend, P. M., and Buesseler, K. O. (1997) Settling removal rates of PCBs into the northwestern Atlantic derived from  $^{138}\text{U}$ - $^{134}\text{Th}$  disequilibria. *Environmental Science and Technology* **31**, 3544-4550.
- Martin, J. H, Knauer, G. A., Karl, D. M. and Broenkow, W. W. (1997) VERTEX: carbon cycling in the northeast Pacific. *Deep-Sea Research* **34(2)**, 267-285.
- McCarthy M. D., Pratum T., Hedges J. I., and Benner R. (1998) Chemical composition of dissolved organic nitrogen in the ocean. *Nature* **390**, 152-153.
- McCarthy M. D., Pratum T., Hedges J. I., and Benner R. (1998) Chemical composition of dissolved organic nitrogen in the ocean. *Nature* **390**, 152-153.
- Skoog, A. and Benner, R. (1997) Aldoses in various size fractions of marine organic matter: implications for carbon cycling . *Limnology and Oceanography* **42**: 1803-1813.
- Williams P. M. and Druffel E. R. M. (1987) Radiocarbon in dissolved organic matter in the central North Pacific Ocean. *Nature* **330**, 246-248.

## Document Library

*Distribution List for Technical Report Exchange—November 1998*

University of California, San Diego  
SIO Library 0175C  
9500 Gilman Drive  
La Jolla, CA 92093-0175

Hancock Library of Biology & Oceanography  
Alan Hancock Laboratory  
University of Southern California  
University Park  
Los Angeles, CA 90089-0371

Gifts & Exchanges  
Library  
Bedford Institute of Oceanography  
P.O. Box 1006  
Dartmouth, NS B2Y 4 A2  
CANADA

NOAA/EDIS Miami Library Center  
4301 Rickenbacker Causeway  
Miami, FL 33149

Research Library  
U.S. Army Corps of Engineers  
Waterways Experiment Station  
3909 Halls Ferry Road  
Vicksburg, MS 39180-6199

Institute of Geophysics  
University of Hawaii  
Library Room 252  
2525 Correa Road  
Honolulu, HI 96822

Marine Resources Information Center  
Building E38-320  
MIT  
Cambridge, MA 02139

Library  
Lamont-Doherty Geological Observatory  
Columbia University  
Palisades, NY 10964

Library  
Serials Department  
Oregon State University  
Corvallis, OR 97331

Pell Marine Science Library  
University of Rhode Island  
Narragansett Bay Campus  
Narragansett, RI 02882

Working Collection  
Texas A&M University  
Dept. of Oceanography  
College Station, TX 77843

Fisheries-Oceanography Library  
151 Oceanography Teaching Bldg.  
University of Washington  
Seattle, WA 98195

Library  
R.S.M.A.S.  
University of Miami  
4600 Rickenbacker Causeway  
Miami, FL 33149

Maury Oceanographic Library  
Naval Oceanographic Office  
Building 1003 South  
1002 Balch Blvd.  
Stennis Space Center, MS 39522-5001

Library  
Institute of Ocean Sciences  
P.O. Box 6000  
Sidney, B.C. V8L 4B2  
CANADA

National Oceanographic Library  
Southampton Oceanography Centre  
European Way  
Southampton SO14 3ZH  
UK

The Librarian  
CSIRO Marine Laboratories  
G.P.O. Box 1538  
Hobart, Tasmania  
AUSTRALIA 7001

Library  
Proudman Oceanographic Laboratory  
Bidston Observatory  
Birkenhead  
Merseyside L43 7 RA  
UK

IFREMER  
Centre de Brest  
Service Documentation—Publications  
BP 70 29280 PLOUZANE  
FRANCE

<b>REPORT DOCUMENTATION PAGE</b>	<b>1. REPORT NO.</b> MIT/WHOI 99-08	<b>2.</b>	<b>3. Recipient's Accession No.</b>
<b>4. Title and Subtitle</b> High Molecular Weight (HMW) Dissolved Organic Matter (DOM) in Seawater: Chemical Structure, Sources and Cycling		<b>5. Report Date</b> June 1999	
<b>7. Author(s)</b> Lihini I. Aluwihare		<b>6.</b>	
<b>9. Performing Organization Name and Address</b> MIT/WHOI Joint Program in Oceanography/Applied Ocean Science & Engineering		<b>8. Performing Organization Rept. No.</b>	
<b>12. Sponsoring Organization Name and Address</b> US Department of Energy, Ocean Margins Program Woods Hole Oceanographic Institution.		<b>10. Project/Task/Work Unit No.</b> MIT/WHOI 99-08	
		<b>11. Contract(C) or Grant(G) No.</b> (C) DE-FG02-92ER61428 (G)	
		<b>13. Type of Report &amp; Period Covered</b> Ph.D. Thesis	
		<b>14.</b>	
<b>15. Supplementary Notes</b> This thesis should be cited as: Lihini I. Aluwihare, 1999. High Molecular Weight (HMW) Dissolved Organic Matter (DOM) in Seawater: Chemical Structure, Sources and Cycling. Ph.D. Thesis. MIT/WHOI, 99-08.			
<b>16. Abstract (Limit: 200 words)</b>  The goal of this thesis was to use high resolution analytical techniques coupled with molecular level analyses to chemically characterize high molecular weight (> 1 k Da (HMW)) dissolved organic matter (DOM) isolated from seawater in an attempt to provide new insights in to the cycling of DOM in the ocean. While a variety of sites spanning different environments (fluvial, coastal and oceanic) and ocean basins were examined, the chemical structure of the isolated HMW DOM varied little at both the polymer and monomer levels. All samples show similar ratios of carbohydrate:acetate:lipid carbon (80±4:10±2:9±4) indicating that these biochemicals are present within a family of related polymers. The carbohydrate fraction shows a characteristic distribution of seven major neutral monosaccharides: rhamnose, fucose, arabinose, xylose, mannose, glucose and galactose; and additionally contains N-acetylated amino sugars as seen by Nuclear Magnetic Resonance Spectroscopy (NMR). This family of compounds, consisting of a specifically linked polysaccharide backbone that is acylated at several positions, has been termed acylated polysaccharides (APS) by our laboratory. APS accounts for 50% of the carbon in HMW DOM isolated from the surface ocean and 20% of the carbon in HMW DOM isolated from the deep ocean.  In order to identify a possible source for APS three species of phytoplankton, <i>Thalassiosira weissflogii</i> , <i>Emiliania huxleyi</i> and <i>Phaeocystis</i> , were cultured in seawater and their HMW DOM exudates examined by a variety of analytical techniques. Both the <i>T. weissflogii</i> and <i>E. huxleyi</i> exudates contain compounds that resemble APS indicating that phytoplankton are indeed a source of APS to the marine environment. Furthermore, the degradation of the <i>T. weissflogii</i> exudate by a natural assemblage of microorganisms indicates that the component resembling APS is more resistant to microbial degradation compared to other polysaccharides present in the culture.  Molecular level analyses show the distribution of monosaccharides to be conservative in surface and deep waters suggesting that APS is present throughout the water column. In order to determine the mechanism by which APS is delivered to the deep ocean the $\Delta^{14}\text{C}$ value of APS in the deep ocean was compared to the $\Delta^{14}\text{C}$ value of the dissolved inorganic carbon (DIC) at the same depth. If the formation of deep water is the dominant mode of transport then both the DIC and APS will have similar $\Delta^{14}\text{C}$ values. However, if APS is injected into the deep ocean from particles or marine snow then the $\Delta^{14}\text{C}$ value of APS will be higher than the DIC at the same depth. Our results indicate that APS in the deep Pacific Ocean carries a modern $\Delta^{14}\text{C}$ value and is substantially enriched in $^{14}\text{C}$ relative to the total HMW DOM and the DIC at that depth. Thus, particle dissolution appears to be the most important pathway for the delivery of APS to the deep ocean.			
<b>17. Document Analysis</b>			
<b>a. Descriptors</b> carbohydrates algal exudates radiocarbon			
<b>b. Identifiers/Open-Ended Terms</b>			
<b>c. COSATI Field/Group</b>			
<b>18. Availability Statement</b> Approved for publication; distribution unlimited.	<b>19. Security Class (This Report)</b> UNCLASSIFIED	<b>21. No. of Pages</b> 224	
	<b>20. Security Class (This Page)</b>	<b>22. Price</b>	